

**Development of Novel Quinoline Analogues as
Mycobacterium tuberculosis DNA Gyrase Inhibitors**

THESIS

Submitted in partial fulfilment
of the requirements for the degree of
DOCTOR OF PHILOSOPHY

by

MEDAPI BRAHMAM

ID No 2012PHXF510H

Under the Supervision of
Prof. P. YOGEE SWARI



BITS Pilani

Pilani | Dubai | Goa | Hyderabad

BIRLA INSTITUTE OF TECHNOLOGY AND SCIENCE, PILANI

2016

BIRLA INSTITUTE OF TECHNOLOGY AND SCIENCE, PILANI

CERTIFICATE

This is to certify that the thesis entitled “**Development of Novel Quinoline Analogues as *Mycobacterium tuberculosis* DNA Gyrase Inhibitors**” and submitted by **MEDAPI BRAHMAM** ID No. **2012PHXF510H** for award of Ph.D. of the Institute embodies original work done by him under my supervision.

Signature of the Supervisor:

Name in capital letters : **P. YOGEE SWARI**

Designation : **Professor**

Date:

Acknowledgement

It is a moment of gratification and pride to look back with a sense of contentment at the long travelled path, to be able to recapture some of the fine moments and to be able to thank the infinite number of people, some of whom were with me from the beginning, some who joined me at some stage during the journey, whose rally round kindness, love and blessings have brought me to this day. I wish to thank each and every one of them with all my heart.

*Foremost, I would like to express my sincere gratitude to my advisor **Prof. P. Yogeeswari** for the continuous support of my Ph.D. study and research, for her patience, motivation, enthusiasm, and immense knowledge. Her guidance helped me in all the time of research and writing of this thesis. I could not have imagined having a better advisor and mentor for my Ph.D. study.*

*I deeply acknowledge and my heartfelt thanks to **Prof. D. Sriram**, for his valuable suggestions, guidance and precious time which he offered me throughout my research.*

*I gratefully acknowledge my DAC member **Dr. A. Sajeli Begum** for her understanding, encouragement and personal attention which have provided good and smooth basis for my Ph.D. tenure.*

*I take this opportunity to thank **Prof. V.S. Rao**, Acting Vice-Chancellor (BITS) and Director (Hyderabad campus), for allowing me to carry out my doctoral research work in the institute.*

*I am thankful to **Prof. S.K. Verma**, Dean, Academic Research Division, BITS-Pilani and **Dr. Vidya Rajesh**, Associate Dean, Academic Research Division, BITS-Pilani, Hyderabad campus for their co-operation and encouragement at every stage of this research work.*

*I would like to express my gratitude to **Dr. Shrikant Y. Charde**, Head of the department, Pharmacy, for providing me with all the necessary laboratory facilities and for having helped me at various stages of my research work.*

I take this opportunity to sincerely acknowledge the Department of Science & Technology (DST), Indian Council of Medical Research (ICMR), Government of India, New Delhi, for providing financial assistance in the form of Fellowship which buttressed me to perform my work comfortably.

*It's my fortune to gratefully acknowledge the support of some special individuals. Words fail me to express my appreciation to all my friends **Jean, Manoj, Bobesh, Madhubabu, Renuka, Shalini, Hasitha, P. Ganesh, S. Ganesh, Mahibalan, Reshma Srilakshmi, Praveen, Suman, Poorna, Gangadhar, Saketh, Srikanth, Venkat, Brinda, Koushik, S. Priyanka, Shailender, Sridevi, Nikhila, Prasanthi, Anup, Omkar and Santosh** for the time they had spent for me and making my stay at campus a memorable one. I take this opportunity to thank one and all for their help directly or indirectly.*

*I express my thanks to our laboratory assistants, **Mr. Uppalaih, Mrs. Saritha, Mr. Srinivas, Mr. Rajesh, Mr. Ramu, also Mrs. Rekha.***

*Most importantly to my wife, **Tulasi.** You have supported me in the darkest times and believed in me even when I did not believe in myself. Your tireless effort enabled me to take the time necessary to complete this work. I've always loved your joyful spirit and this spirit provided the boost that made even the longest hours enjoyable. This would not have been possible without you. No words can express how grateful I am for your love and support and how very much I love and appreciate you.*

*I would like to begin by dedicating this piece of work to **my parents**, whose dreams had come to life with me getting the highest degree in education. I owe my doctorate degree to my parents who kept with their continuous care, support and encouragement my morale high. Thanks are due if I don't dedicate this thesis to all my family members, whose constant and continuous support, love and affection made me reach this height.*

Lastly, and above all, I would like to thank the God Almighty; for all that he has given to me.

Date:

Medapi Brahmam

Abstract

In the present study we focused on achieving promising antimycobacterial cellular potency through developing potential quinoline based *Mycobacterium tuberculosis* (*Mtb*) DNA gyrase inhibitors. Tuberculosis is one of the world's health burdens of society and it claims more than 2 million deaths annually.

Utilizing the medicinal chemistry tools of structure based drug design and molecular hybridization/scaffold hopping; 5 different classes of inhibitors were identified as potential DNA Gyrase inhibitors as leads. The hits identified were further customized using a combination of molecular docking and chemical synthesis to develop various analogues that displayed considerable *in vitro* enzyme efficacy and bactericidal activity against *Mtb* H₃₇Rv strain. Compound **BB_19** emerged as the most potent Gyr B lead with Gyr B inhibitory IC₅₀ of 0.39 ± 0.14 μM; Supercoiling inhibitory IC₅₀ of 0.29 ± 0.31 μM; *Mtb* MIC of 1.78 μM and selectivity index of more than 25, another compound **BD_53** showed Gyr B inhibitory IC₅₀ of 0.86 ± 0.16 μM; Supercoiling inhibitory IC₅₀ of 0.63 ± 0.15 μM; *Mtb* MIC of 3.3 μM and selectivity index of more than 40. The binding affinity of the potent ligands towards the Gyr B domain was re-ascertained by differential scanning fluorimetry experiments wherein a shift in the melting temperature T_M was monitored. All the tested compounds brought a shift in T_M in the range of 2.9 °C – 3.3 °C compared to the native protein, a repercussion of strong inhibitor binding. Further evaluation of hERG toxicity; a major limitation among the previously reported Gyr B analogues in a zebra fish model indicated these molecules to be completely devoid of cardiotoxicity, a significant achievement within this class. The safety profile of synthesized compounds was evaluated by checking their *in vitro* cytotoxicity against RAW 264.7 cell line (mouse leukemic monocyte macrophage) using MTT assay.

With new anti-TB agents desperately needed, we believe that the present class of quinoline based inhibitors reported in this work would be interesting as potential lead to be worked for rational drug design against *Mtb* from pharmaceutical point of view.

Table of contents

Contents	Page No.
<i>Certificate</i>	<i>i</i>
<i>Acknowledgements</i>	<i>ii</i>
<i>Abstract</i>	<i>iv</i>
<i>List of Tables</i>	<i>v</i>
<i>List of Figures</i>	<i>vi</i>
<i>Abbreviations</i>	<i>xi</i>
Chapter 1 – Introduction	1-8
1.1 <i>Mycobacterium tuberculosis</i> (<i>Mtb</i>) - Etiology of TB	3
1.2 Standard regimen for treating TB	4
1.3 Current TB drug development pipeline	6
Chapter 2 - Literature review	9-25
2.1 Bacterial DNA gyrase inhibitors	10
2.1.2 Fluoroquinolones (FQs)	13
2.1.3 Different classes of fluoroquinolones	14
2.1.4 Drugs acting through the allosteric inhibition of DNA Gyrase (NBTI's)	17
2.1.5 Mycobacterial Gyr B inhibitors	19
2.1.5.1 Aminocoumarins	20
2.1.5.2 Aminopyrazinamide class of Gyr B inhibitors	21
2.1.5.3 Pyrrolamides as DNA Gyr B inhibitors	22
2.1.5.4 Thiazolopyridine and benzimidazole urea based inhibitors	23

Contents	Page No.
Chapter 3 - Objectives and Plan of work	26-28
3.1 Objectives	26
3.2 Plan of work	27
3.2.1 Designing new antimycobacterial inhibitors	27
3.2.2 Synthesis and characterization	27
3.2.3 <i>In vitro</i> DNA gyrase enzyme inhibitory potency	27
3.2.4 <i>In vitro</i> <i>Mtb</i> activity studies	27
3.2.5 Evaluation of protein-inhibitor binding affinity using biophysical characterization by DSF	28
3.2.6 <i>In vitro</i> cytotoxicity screening	28
3.2.7 <i>In vitro</i> zERG channel inhibition screening	28
3.2.8 Docking studies (Comparison docking study of known to synthesized inhibitors)	28
Chapter 4 - Materials and Methods	29-42
4.1 Design of novel Quinoline based <i>Mtb</i> DNA gyrase inhibitors	29
4.2 Chemistry and Method of synthesis	31
4.2.1 Scheme-1: Synthesis of 1-(1-(2-Methylquinolin-4-yl) piperidin-4-yl) -3-phenylurea /thiourea derivatives	32
4.2.2 Scheme-2: Synthesis of 1-(4-substituted phenyl)-3-(6-substituted-(2-methylquinolin-4-yl)amino)phenyl thiourea/urea derivatives	32
4.2.3 Scheme-3: Synthetic protocol for the entitled substituted N-[4-(substituted-9-acridinyl amino] phenyl sulphonamide, urea/thiourea derivatives	33

Contents	Page No.
4.2.4 Scheme-4: Synthesis of phenyl-amino-quinoline derivatives	34
4.2.5 Scheme-5: Substituted 4-((1-quinolin-4-yl)-1H-1,2,3-triazol-4-yl)-2-phenyl thiazole derivatives	35
4.3 Biological screening of synthesized inhibitors	36
4.3.1 <i>Msm</i> DNA Gyr B cloning, protein expression and purification	36
4.3.2 <i>In vitro Msm</i> Gyr B assay for the determination of IC ₅₀	38
4.3.3 <i>In vitro Mtb</i> DNA gyrase supercoiling assay	38
4.3.4 <i>In vitro Mtb</i> LAT (Lysine aminotransferase) assay	39
4.3.5 <i>In vitro Mtb</i> MABA assay for MIC determination	39
4.4 Evaluation of protein-inhibitor binding affinity using biophysical characterization (DSF)	40
4.5 Cell cytotoxicity studies by MTT assay	40
4.6 <i>In vitro</i> zERG channel inhibition screening	41
4.7 Molecular docking studies	42
Chapter 5 - Results and Discussion	43-181
5.1 Development of 1-(1-(2-Methylquinolin-4-yl) piperidin-4-yl) -3-phenylurea /thiourea derivatives as potential <i>Mtb</i> DNA gyrase B inhibitors	43
5.1.1 Chemical synthesis and characterization	45
5.1.2 Experimental protocol followed for synthesis	45
5.1.3 Characterization of synthesized compounds	51
5.1.4 <i>In vitro Msm</i> Gyr B assay, supercoiling assay, antimycobacterial potency and cytotoxicity studies of the synthesized molecules	65

Contents	Page No.
5.1.5 Docking studies	70
5.1.6 Evaluation of protein interaction and stability using biophysical characterization experiment (DSF)	71
5.1.7 Evaluation of zERG channel inhibition in a zebra fish model.	72
5.1.8 Discussion	73
5.1.9 Highlights of the study	83
5.2 Development of 1-(4-((6-substituted-2-methylquinolin-4-yl)amino)phenyl)-3-phenylurea/thiourea derivatives as potential <i>Mtb</i> DNA gyrase B inhibitors	84
5.2.1 Chemical synthesis and characterization	84
5.2.2 Experimental protocol followed for synthesis	85
5.2.3 Characterization of synthesized compounds	87
5.2.4 <i>In vitro</i> <i>Msm</i> Gyr B assay, supercoiling assay, antimycobacterial potency and cytotoxicity studies of the synthesized molecules	93
5.2.5 Evaluation of protein interaction and stability using biophysical characterization experiment (DSF)	96
5.2.6 Evaluation of zERG channel inhibition in a zebra fish model	97
5.2.7 Discussion	98
5.2.8 Highlights of the study	100
5.3 Development of acridine derivatives as selective <i>Mtb</i> DNA gyrase inhibitors	101
5.3.1 Chemical synthesis and characterization	101
5.3.2 Experimental protocol followed for synthesis	102
5.3.3 Characterization of synthesized compounds	106

Contents	Page No.
5.3.4 <i>In vitro</i> supercoiling assay, antimycobacterial potency and cytotoxicity studies of the synthesized molecules	115
5.3.5 Evaluation of zERG channel inhibition in a zebra fish model	118
5.3.6 Discussion	119
5.3.7 Highlights of the study	121
5.4 Development of ethyl 4-((4-Amino/Hydroxyphenyl)amino)quinoline-3-carboxylate derivatives as potential <i>Mtb</i> DNA gyrase B inhibitors	122
5.4.1 Chemical synthesis and characterization	122
5.4.2 Experimental protocol followed for synthesis	123
5.4.3 Characterization of synthesized compounds	128
5.4.4 <i>In vitro Msm</i> Gyr B assay, supercoiling assay, antimycobacterial potency and cytotoxicity studies of the synthesized molecules	147
5.4.5 Docking studies of synthesized derivatives	151
5.4.6 Evaluation of protein interaction and stability using biophysical characterization experiment (DSF)	152
5.4.7 Discussion	153
5.4.8 Highlights of the study	159
5.5 Development of substituted 4-((1-(3-(substituted) quinolin-4-yl)-1H-1,2,3-triazol-4-yl)methoxy)-2-phenylthiazole derivatives as potential <i>Mtb</i> DNA gyrase B inhibitors	160
5.5.1 Chemical synthesis and characterization	160
5.5.2 Experimental protocol followed for synthesis	161
5.5.3 Characterization of synthesized compounds	164

Contents	Page No.
5.5.4 <i>In vitro</i> Msm Gyr B assay, supercoiling assay, antimycobacterial potency, <i>Mtb</i> LAT assay and cytotoxicity studies of the synthesized molecules	174
5.5.5 Docking studies of selected LAT inhibitors	176
5.5.6 Evaluation of protein interaction and stability using biophysical characterization experiment (DSF)	178
5.5.7 Discussion	179
5.5.8 Highlights of the study	181
Chapter 6 - Summary and Conclusion	182-184
Future perspectives	185
References	186-195
Appendix	196-200
List of publications, Indian Patents and Presentations	196-198
Biography of the candidate	199
Biography of the supervisor	200

List of Tables

Table No.	Description	Page No.
Table 1.1	Standard regimens for new TB patients	5
Table 1.2	Dosing frequencies for new TB patients	5
Table 1.3	WHO recommended regimen for drug-susceptible TB	5
Table 5.1	Physicochemical properties of synthesized compounds BA_06 – BA_29 and BA_30 – BA_53	48-50
Table 5.2	<i>In vitro</i> biological evaluation of the synthesized derivatives BA_06 – BA_29 and BA_30 – BA_53	66-69
Table 5.3	Physicochemical properties of synthesized compounds BB_02 – BB_21	86-87
Table 5.4	<i>In vitro</i> biological evaluation of the synthesized derivatives BB_02 – BB_11 and BB_12 – BB_21 .	94-95
Table 5.5	Physicochemical properties of synthesized acridine derivatives BC_04-39	104-106
Table 5.6	<i>In vitro</i> biological evaluation of the synthesized derivatives BC_04 – BC_15 and BC_16 – BB_39 .	115-117
Table 5.7	Physicochemical properties of synthesized derivatives BD_12-57	127-128
Table 5.8	Biological evaluation of synthesized derivatives BD_12-57	148-149
Table 5.9	Physicochemical properties of synthesized derivatives BE_06- BE_29	163-164
Table 5.10	Biological screening of synthesized derivatives BE_06-BE_29	175-176

List of Figures

Figure No.	Description	Page No.
Figure 1.1	The various stages of <i>Mtb</i> infection in humans	3
Figure 1.2	Mechanism of action of currently prescribed anti-mycobacterial drugs	4
Figure 1.3	Current global pipeline of TB drug development	7
Figure 1.4	Mechanism of action of new anti-tubercular drugs in development	8
Figure 2.1	The picture depicts how the DNA gyrase enzyme introduces negative supercoiling in DNA	11
Figure 2.2	The catalytic cycle of topoisomerase II	11
Figure 2.3	Represents the bacterial type II & IV topoisomerases function	12
Figure 2.4	Structural activity relationships (SAR) of fluoroquinolones	14
Figure 2.5	The MIC data for fluoroquinolones commonly used in treatment of TB	16
Figure 2.6	Mechanism of action of FQ drugs and NBTIs	18
Figure 2.7	The various reported novel bacterial topoisomerase inhibitors	19
Figure 2.8	Structure of novobiocin	21
Figure 2.9	SAR of aminopyrazinamide based mycobacterial Gyr B inhibitors	22
Figure 2.10	General structure and SAR of pyrrolamide Gyr B inhibitors	23
Figure 2.11	SAR of thiazolopyridine and benzimidazole inhibitors targeting Gyr B inhibitors	24
Figure 2.12	The various reported Gyr B inhibitors	25
Figure 4.1	Scheme-1, New inhibitor designed through molecular hybridization approach.	30
Figure 4.2	Scheme-2 & Scheme-3, further modifications of constructed hybrid/inhibitor through molecular hopping	30
Figure 4.3	Scheme-4, Design logic, Scaffold modification and	31

Figure No.	Description	Page No.
	derivatization of reported DNA Gyr B inhibitor	
Figure 4.4	Scheme-5, Design logic and Scaffold modification and derivatization based on reported antimycobacterials	31
Figure 4.5	Synthetic scheme utilized for synthesis of 1-(1-(2-methylquinolin-4-yl) piperidin-4-yl) -3-phenylurea /thiourea derivatives	32
Figure 4.6	Synthetic scheme utilized for synthesis of 1-(4-substituted phenyl)-3-(6-substituted-(2-methylquinolin-4-yl)amino)phenyl thiourea/urea derivatives	33
Figure 4.7	The protocol utilized for the synthesis of compounds, scheme-3	33
Figure 4.8	The two synthons utilized for the synthesis of phenyl-amino-quinoline derivatives	34
Figure 4.9	Synthetic protocol utilized to achieve the phenyl amine intermediates	34
Figure 4.10	Synthetic procedure utilized for the preparation of entitled phenyl-amino-quinoline derivatives	35
Figure 4.11	Synthetic protocol for the preparation of intermediates	35
Figure 4.12	Synthetic protocol utilized to achieve the titled substituted 4-((1-quinolin-4-yl)-1H-1,2,3-triazol-4-yl)-2-phenyl thiazole derivatives	36
Figure 5.1	Design strategy used for the development of novel quinoline based DNA gyrase B inhibitor	44
Figure 5.2	ATPase activity of <i>Msm</i> DNA gyrase B protein as a function of substrate (ATP) concentration at a constant enzyme concentration (15 μ M)	69
Figure 5.3	Dose response curve of compound BA_38 with <i>Msm</i> DNA Gyr B ATPase assay at six various concentrations	69
Figure 5.4	Picture depicting the supercoiling assay of most active compound BA_38 at four different concentrations	70
Figure 5.5	Interaction profile picture of ligand 6-(3,4-dimethylphenyl)-3-[[4-[3-(4-methylpiperazin-yl)propoxy]phenyl]amino]pyrazine-2-	71

Figure No.	Description	Page No.
	carboxamide in the active site of <i>Msm</i> Gyr B protein	
Figure 5.6	DSF experiment for compound BA_38 showing an increase in thermal stability between the native <i>Msm</i> DNA Gyr B protein (red) and <i>Msm</i> DNA Gyr B protein-compound BA_38 complex (blue)	72
Figure 5.7a	Mean (\pm S.E.M.) of the heart rates of atria and ventricles of Compounds BA_38 & BA_40 treatment groups.	73
Figure 5.7b	Mean (\pm S.E.M.) score of atrio ventricular ratio of Compounds BA_38 & BA_40 treatment groups	73
Figure 5.8	The interaction profile pictures of compounds BA_15 and BA_17 at the active pocket of Gyr B of <i>Msm</i>	74
Figure 5.9	The interaction profile pictures of compounds BA_19 and BA_21 at the active pocket of Gyr B of <i>Msm</i>	75
Figure 5.10	The interaction profile pictures of compounds BA_20 at the active pocket of Gyr B of <i>Msm</i>	76
Figure 5.11	The interaction profile pictures of compounds BA_29 posing out of the active pocket of Gyr B of <i>Msm</i>	77
Figure 5.12	The interaction profile pictures of compounds BA_33 and BA_34 at the active pocket of Gyr B of <i>Msm</i>	78
Figure 5.13	The hydrophobic interactions in interaction profile picture of compound BA_31	79
Figure 5.14	The interaction profile pictures of compounds BA_36 and BA_39 at the active pocket of Gyr B of <i>Msm</i>	79
Figure 5.15	The interaction profile pictures of the most active compounds BA_38 at the active pocket of Gyr B of <i>Msm</i>	80
Figure 5.16	The interaction profile pictures of compounds BA_50 and BA_53 at the active pocket of Gyr B of <i>Msm</i>	81
Figure 5.17	The interaction profile pictures of compounds BA_49 and BA_51 at the active pocket of Gyr B of <i>Msm</i>	81
Figure 5.18	Structure and activity of most active compound BA_38	83
Figure 5.19	Scheme-2, further modifications of constructed hybrid/inhibitor	84

Figure No.	Description	Page No.
	through molecular hopping	
Figure 5.20	Dose response curve of compound BA_19 with <i>Msm</i> DNA Gyr B ATPase assay at six various concentrations	95
Figure 5.21	Picture depicting the supercoiling assay of most active compound BB_19 at five different concentrations	96
Figure 5.22	DSF experiment for compound BB_19 showing an increase in thermal stability between the native <i>Msm</i> DNA Gyr B protein (red) and <i>Msm</i> DNA Gyr B protein-compound BB_19 complex (green).	97
Figure 5.23a	The Mean (\pm S.E.M.) of the heart rates of atria and ventricles of most potent compound BB_19	98
Figure 5.23b	Mean (\pm S. E. M.) score of atrio ventricular ratio of most potent compound BB_19	98
Figure 5.24	Structure and activity of most active compound BB_19	100
Figure 5.25	Scheme-3, further modifications of constructed hybrid/inhibitor through molecular hopping	101
Figure 5.26	General structures of synthesized derivatives BC_04-BC_39	104
Figure 5.27	Picture depicting the supercoiling assay of compound BC_05.	118
Figure 5.28a	Mean (\pm S.E.M.) of the heart rates of atria and ventricles of most potent Compound BC_05 treatment groups	118
Figure 5.28b	Mean (\pm S.E.M.) score of atrio ventricular ratio of most potent Compound BC_05 treatment groups	119
Figure 5.29	Structure of m-Amsacrine, most active compound BC_05	120
Figure 5.30	The design process of lead optimization with substituents at the respective positions, Scheme-4	122
Figure 5.31	General structures of synthesized derivatives BD_12-57	126
Figure 5.32	ATPase activity of <i>Msm</i> DNA Gyr B protein as a function of substrate (ATP) concentration at a constant enzyme concentration	150
Figure 5.33	Percentage inhibition of <i>Msm</i> Gyr B by compound BD_53 at various concentrations	150

Figure No.	Description	Page No.
Figure 5.34	DNA supercoiling assay picture of compound BD_53	150
Figure 5.35	Interaction profile picture of ligand 6-(3,4-dimethylphenyl)-3-[[4-[3-(4-methylpiperazin-yl)propoxy]phenyl]amino]pyrazine-2-carboxamide in the active site of <i>Msm</i> Gyr B protein	152
Figure 5.36	Differential scanning fluorimetry curve for Gyr B protein complexed with compound BD_53	153
Figure 5.37	Interaction profile of compound BD_53 (pink sticks) at the ATPase domain of <i>Msm</i> Gyr B	155
Figure 5.38	Interaction patterns of (a) compound BD_23 and (b) compound BD_28 at <i>Msm</i> Gyr B ATPase domain	156
Figure 5.39	Interaction profile of (a) compound BD_23 and (b) compound BD_15 at <i>Msm</i> Gyr B ATPase domain active site	157
Figure 5.40	Interaction profile of (a) compound BD_28 and (b) compound BD_12 at <i>M. smegmatis</i> Gyr B ATPase domain active site.	158
Figure 5.41	Structure and activity of most active compound BD_53	159
Figure 5.42	Scheme-5, Design logic and Scaffold modification and derivatization based on reported antimycobacterials	160
Figure 5.43	Dose response curve of compound BE_18 with <i>Mtb</i> LAT assay at six various concentrations	176
Figure 5.44	Kinetic parameters of lysine and α -ketoglutarate	176
Figure 5.45	The interaction profile picture of reference ligand lysine in active site of LAT (lysine aminotransferase)	177
Figure 5.46	Interaction profile picture of Compound BE_18 in <i>Mtb</i> LAT protein	178
Figure 5.47	Interaction profile picture of Compound BE_22 in <i>Mtb</i> LAT protein	178
Figure 5.48	Differential scanning fluorimetry curve for <i>Mtb</i> LAT protein complexed with compound BE_18	179
Figure 5.49	Most active compound against <i>Mtb</i> LAT inhibition BE_18	181

List of Abbreviations

μg	:	Microgram
μL	:	Microlitre
μM	:	Micromolar
^{13}C NMR	:	Carbon Nuclear Magnetic Resonance
^1H NMR	:	Proton Nuclear Magnetic Resonance
3D	:	Three Dimensional
ADMET	:	Absorption, Distribution, Metabolism, Elimination and Toxicity
ADPNP	:	5'Adenylyl β, γ Imido Diphosphate
Anhy.	:	Anhydrous
Anova	:	Analysis of Variance
ATP	:	Adenosine Triphosphate
AZ	:	AstraZeneca
BMS	:	Bristol-Myers Squibb
(BOC) $_2$ O	:	Di-tert-butyl dicarbonate
BSA	:	Bovine serum albumin
CDCl_3	:	Chloroform deuterated
CoA	:	Coenzyme A
Cu	:	Copper
D	:	Doublet
DCM	:	Dichloromethane
Dd	:	Doublet of doublet
DIPEA	:	Diisopropylethylamine
DMF	:	<i>N,N</i> -Dimethylformamide
DMSO	:	Dimethyl sulfoxide
DMSO- d_6	:	Dimethyl sulphoxide deuterated

DNA	:	Deoxyribonucleic acid
DOTS	:	Directly Observed Treatment, Short course
DSF	:	Differential Scanning fluorimetry
DTT	:	1, 4 Dithiothreitol
E	:	Ethambutol
EAA	:	Ethyl acetoacetate
EDTA	:	Ethylene diamine tetra acetic acid
EMA	:	European Medical Agency
ESI	:	Electron Spray Ionization
Et ₃ N	:	Triethylamine
EtOH	:	Ethanol
FQ	:	Fluoroquinolone
GLP	:	Good Lab Practices
GSK	:	Glaxo Smith Kline
H	:	Isoniazid
HEPES	:	4-(2-Hydroxyethyl)-1-Piperazineethanesulfonic acid
hERG	:	human Ether-a-go-go-Related Gene
HIV	:	Human Immuno Deficiency Virus
HPLC	:	High Pressure Liquid Chromatography
IC ₅₀	:	Half Maximal Inhibitory Concentration
IPTG	:	Isopropyl-β-D-thiogalactopyranoside
<i>J</i>	:	Coupling constant
KCl	:	Potassium chloride
K _i	:	Inhibitor constant
KOH	:	Potassium hydroxide
LB	:	Luria Broth

LCMS	:	Liquid chromatography–Mass Spectrometry
LHS	:	Left Hand Side
M	:	Multiplet
M.p	:	Melting point
MDR-TB	:	Multidrug-Resistant Tuberculosis
MeOH	:	Methanol
mg	:	Milligram
MgCl ₂	:	Magnesium chloride
MHz	:	Mega hertz
MIC	:	Minimum Inhibitory Concentration
mL	:	Milliliter
Mmol	:	Millimole
<i>Msm</i>	:	<i>Mycobacterium smegmatis</i>
<i>Mtb</i>	:	<i>Mycobacterium tuberculosis</i>
MTT	:	(4,5-Dimethylthiazol-2-yl)-2,5-diphenyltetrazolium bromide
MW	:	Microwave
NaCl	:	Sodium chloride
NADH	:	Nicotinamide Adenine Dinucleotide
NBTIs	:	Novel Bacterial Topoisomerase Inhibitors
NIH	:	National Institutes of Health
nM	:	Nanomolar
P	:	Para
PDB	:	Protein Data Bank
PMSF	:	Phenylmethylsulfonyl fluoride
Ppm	:	Parts per million
PTSA	:	p-Toluene sulfonic acid

R	:	Rifampicin
RNA	:	Ribonucleic acid
Rpm	:	Rotations per minute
RPMI	:	Roswell Park Memorial Institute
Rt	:	Room temperature
S	:	Singlet
SAR	:	Structure Activity Relationship
SDS-PAGE	:	Sodium Dodecyl Sulphate- Polyacrylamide Gel Electrophoresis
T	:	Triplet
TAE	:	Trisbase, Acetic acid, EDTA mixture
TB	:	Tuberculosis
TFA	:	Trifluoroacetic acid
THF	:	Tetrahydrofuran
TLC	:	Thin-layer chromatography
T _m	:	Melting temperature
TMS	:	Trimethylsilane
Toprim	:	Topoisomerase-primase
Tox	:	Toxicology
UV	:	Ultraviolet
WHO	:	World Health Organization
XDR-TB	:	Extensively Drug-Resistant Tuberculosis
XP	:	Extra Precision
Z	:	Pyrazinamide
zERG	:	Zebrafish Ether-a-go-go-Related Gene
δ	:	Chemical shift

Tuberculosis (TB) is one of the most common infectious diseases known to man. One of the hallmarks of TB is its persistent phase of infection. Tuberculosis (TB) is a chronic bacterial airborne infection in humans caused by *Mycobacterium tuberculosis* (*Mtb*), a gram positive bacterium. It divides at an extremely slow rate and transmitted as highly infectious aerosol. This is the most common infectious diseases in the present today world than any other time in human history. In the year 1982, Robert Koch had identified *Mtb* as the causative agent for TB and he had stated that “the importance of a disease for mankind is measured from the number of fatalities which are due to it, then tuberculosis must be considered much more important than those most feared infectious diseases, plague, cholera, and the like” and statistics have shown that 1/7 of all humans die of tuberculosis. The initial fate of exposure to *Mtb* aerosols depends on the host’s innate immune response that may eliminate the organism immediately to infected individuals developing active primary TB (Flynn J. L., *et al.*, 2001). The initial acute infection is controlled by the immunocompetent host’s and the living bacteria are confined in a peculiar localized pulmonary structure called granuloma. There the bacteria persist as in a latent non-virulent form for a long time and it gets reactivated whenever the host’s immunosuppression situation occurs (Ferraris D. M., *et al.*, 2011).

Still TB continues to claim about 2 million deaths per each year (WHO report, 2015) and results in huge mortality with a huge economic burden on undeveloped countries. The standard regimen recommended by World Health Organisation (WHO) containing four drugs administered for six months (Zumla A., *et al.*, 2013) to treat drug sensitive TB. The prolonged TB treatment results in poor patient compliance and severe side effects arising from some of the recommended drugs. During the past years most of the drugs developed for TB were ineffective due to the emergence and spread of resistant *Mtb* strains to these front line drugs resulting in multidrug resistant (MDR), extremely drug resistance (XDR) and totally drug resistant (TDR) strains of *Mtb*. MDR *Mtb* is the one at least resistant to isoniazid and one of the antibiotics like rifampicin is called as multi drug resistance strain. XDR *Mtb* is the MDR strain which is resistant to fluoroquinolone and an injectable aminoglycoside is termed as an

extremely drug resistant strain. The strain of *Mtb* which is resistant to all first line and second line licenced anti-tubercular drugs is defined as totally drug resistant stain (TDR *Mtb*) (Sharma S. K., *et al.*, 2013). The global emergence of these MDR, XDR and TDR TB strains makes to fail greatly the control and eradication of TB.

According to WHO recommended regimen a combination of 6-8 drugs for a period of 1-2 years (WHO report 2013) for the patients infected with MDR or XDR strains of *Mtb*. It has been estimated that 4% of new cases and 20% of already treated cases were fall under the MDR or XDR-TB category. Moreover, 95% of new TB and deaths have been reported by developing countries only. About 60% of infections have been reported in Asian countries like India, china and the Russian federation (Bridgen G., *et al.*, 2014). The burden of this dreadful TB disease can be measured in terms of (i) Incidence (ii) Prevalence (iii) Mortality. TB is a major public health crisis in world's second populated country like India. The incidence of new TB cases in India is higher than any other country.

The important factors that have led to the drug resistance acquired by *Mtb* strains includes incomplete and inadequate treatment procedures and it emerges mostly where TB control programmes are ineffective (Black P. A., *et al.*, 2014). It is believed that the prolonged use of many drug regimens for decades and with poor patient compliance also led to the *Mtb* drug resistance. The standard regimen for MDR-TB includes daily injections of less effective second line drugs for a duration of twenty months. It has been estimated that the cost of treating MDR-TB is ~USD 4000 /patient and the cure rate is less (50-60%) when compared with the cure rate of 94-97% patients with drug sensitive TB (Kwon Y. S., *et al.*, 2014). A total of 92 countries have reported at least one XDR-TB case by September 2013 moreover about 9.6% of MDR-TB cases were found to be XDR-TB (WHO MDR-TB fact sheet 2013). The treatment outcome of XDR-TB is dreadful (Brigden G., *et al.*, 2014; WHO report 2014) in case of XDR tuberculosis patients. The distant global picture demands an urgent need to develop new safer, efficacious drugs with novel mechanism of action to treat drug resistant strains of *Mtb*. It is vital to develop new novel drug regimens to minimize the duration of treatment, drug related toxicity and improve patient compliance.

The last decades had witnessed the global concerted efforts of WHO and TB alliance to discover and develop novel therapeutic agents against *Mtb*. In order to initiate a drug discovery and development programme, it is necessary to understand the complex physiology of *Mtb* infection in humans. The key stages of TB infection in humans are depicted in Figure 1.1.

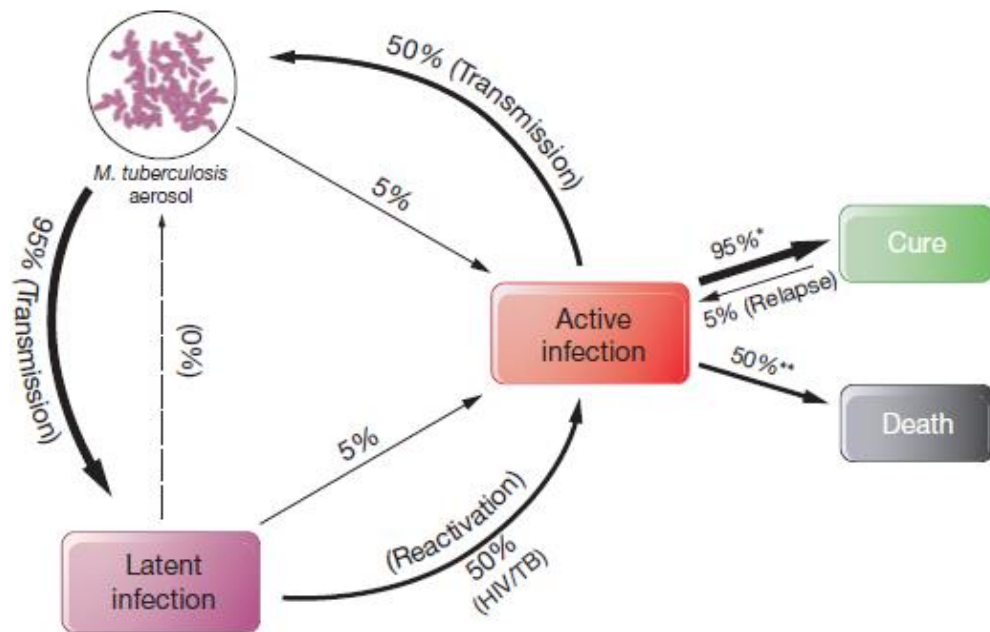


Figure 1.1: The various stages of *Mtb* infection in humans (Koul A., *et al.*, 2011)

Transmission of *Mtb* through the aerosol carrying *Mtb* bacteria results in developing into active infectious TB or non-infectious (latent form) disease. It has been showed that in most of the cases the latently infected people may relapse into active TB, years after their first exposure to *Mtb*. The latent form of TB gets reactivated by the immunosuppression conditions like patients infected with HIV or undergoing chemotherapy. In the case of drug susceptible TB (denoted by an asterisk *), 95% of patients recover by proper treatment whereas 5% relapse during their life time. The high mortality results in the patients with TB left untreated (denoted by double asterisk **).

1.1 *Mycobacterium tuberculosis* (*Mtb*) – Etiology of TB

Mtb is the causative agent for TB. It is found in one third of world's population. Because of its complex cell wall composition resides in host for many years in latent form. Cell wall composed of peptidoglycans and lipids mainly consists of mycolic

acids. These mycolic acids are responsible for its virulence (Rivers E. C., *et al.*, 2008, Forrellad M. A., Klepp L. I., *et al.*, 2013). This contributes chronic nature of the disease, lengthy treatment regimens and makes as formidable obstacle for researchers.

1.2 Standard regimen for treating TB

Current TB treatment capitalizes combination chemotherapy. Multiple drugs are used to increase efficacy that prevent the development of resistant organisms. Based on the mechanism of action present drugs can be classified as i) inhibitors of bacterial protein synthesis (aminoglycosides) ii) electron transport across the bacterial membrane (pyrazinamide) iii) nucleic acid synthesis (4iperidi, quinolones) and iv) cell wall synthesis (isoniazid, ethambutol and cycloserine) (Zhenkun Ma., *et al.*, 2012) as showed in **Figure 1.2**

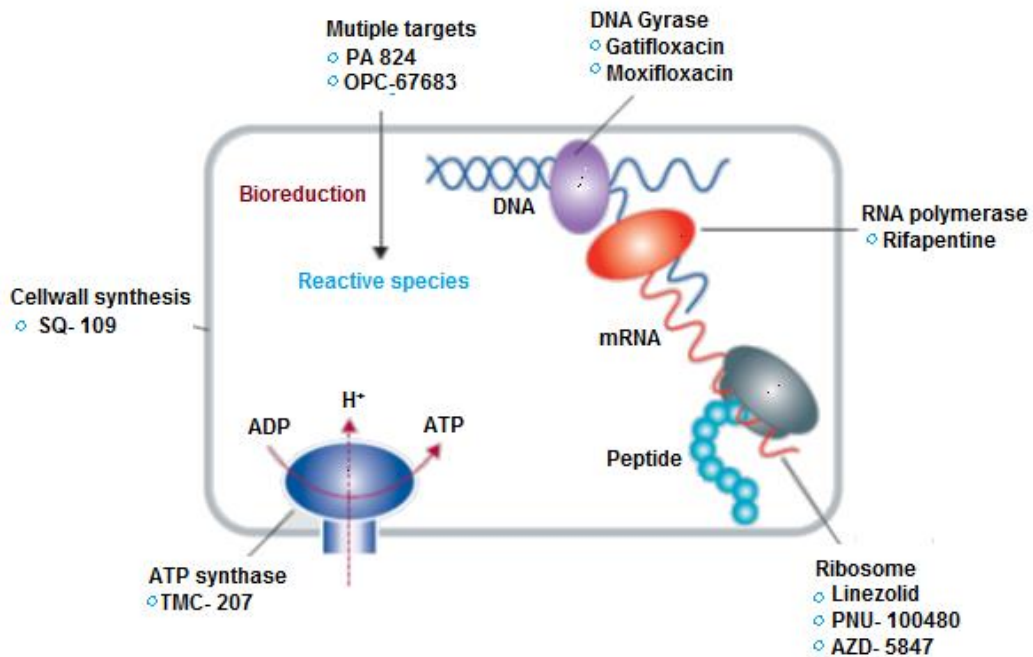


Figure 1.2: Mechanism of action of currently prescribed anti-mycobacterial drugs

Table 1.1 & 1.2 Represents the standard regimen and dosing frequency for new TB patients.

Table 1.1 Standard regimens for new TB patients

Intensive phase	Continuation Phase	Comments
2 months of HRZE	4 months of HR	
2 months of HRZE	4 months of HRE	Applies only in countries with high levels of isoniazid resistance in new TB patients, and where isoniazid drug susceptibility testing in patients is not done before the continuation phase begins

E-Ethambutol, H-Isoniazid, Z-Pyrazinamide, R-Rifampicin.

Table 1.2 Dosing frequencies for new TB patients

Dosing frequency		Comments
Intensive phase	Continuation Phase	
Daily	Daily	Optimal
Daily	3 times per week	Acceptable alternative for any new TB patient receiving directly observed therapy
3 times per week	3 times per week	Acceptable alternative provided that the patient is receiving directly observed therapy and is not living with HIV or living in an HIV-prevalent setting

Table 1.3 WHO recommended regimen for drug-susceptible TB^b

Drug	Daily dose	Adverse effects
Isoniazid (H)	5 mg/kg (max. daily dose 300 mg)	Hepatitis, peripheral neuropathy, lupus-like syndrome
Rifampin I	10 mg/kg (max. daily dose 600 mg)	Orange discoloration of secretions, hepatitis, gastrointestinal upset, fever

Drug	Daily dose	Adverse effects
Pyrazinamide (Z)	25 mg/kg	Hepatitis, arthritis, hyperuricemia
Ethambutol I	15 mg/kg	Optical neuritis

^bFor patients who were drug-susceptible disease, standard regimen recommended by the WHO 2 months intensive phase includes four drug combination (H, R, Z and E), followed by 4 months continuation phase includes H and R. The drugs are administered by mouth as above mentioned dosage (Wong E. B., *et al.*, 2013).

About 5% of TB cases are resistant to one of the above mentioned drug regimen. Such patients pose a greater risk of spreading infection and therefore require a second line or a third line treatment which themselves are not very effective, and treatment duration is more than 18 months. This scenario demands urgency for new, more effective and safe anti-tuberculosis drugs to potentially reduce the treatment duration which is a key to increasing patient compliance to therapy.

1.3 Current TB drug development pipeline

There is a lot of progress has been made in last 40 years and a promising portfolio of new anti-tubercular drugs is on the horizon (**Figure 1.2**). Some have the potential to become the drug candidates of future TB treatment. Bedaquiline, a novel ATP synthase inhibitor and it has been recently licensed by the (U.S FDA) United States Food and Drug Administration under its accelerated approval procedure for treatment of MDR-TB patients, as a part of new combination therapy when other alternatives have failed (Cohen J., *et al.*, 2013). European Medicines Agency (EMA) has recently approved Delamanid, a member of the nitroimidazole which has entered phase III trials for the treatment of MDR-TB.

The most rapid progress in the expansion of anti-tubercular drugs portfolio has been made through re-purposing or re-dosing of known anti-tubercular drugs such as rifamycins (R, rifapentine) and fluoroquinolones (moxifloxacin and gatifloxacin). These drugs have all entered advanced phase 3 studies (Zumla A. I., *et al.*, 2014).

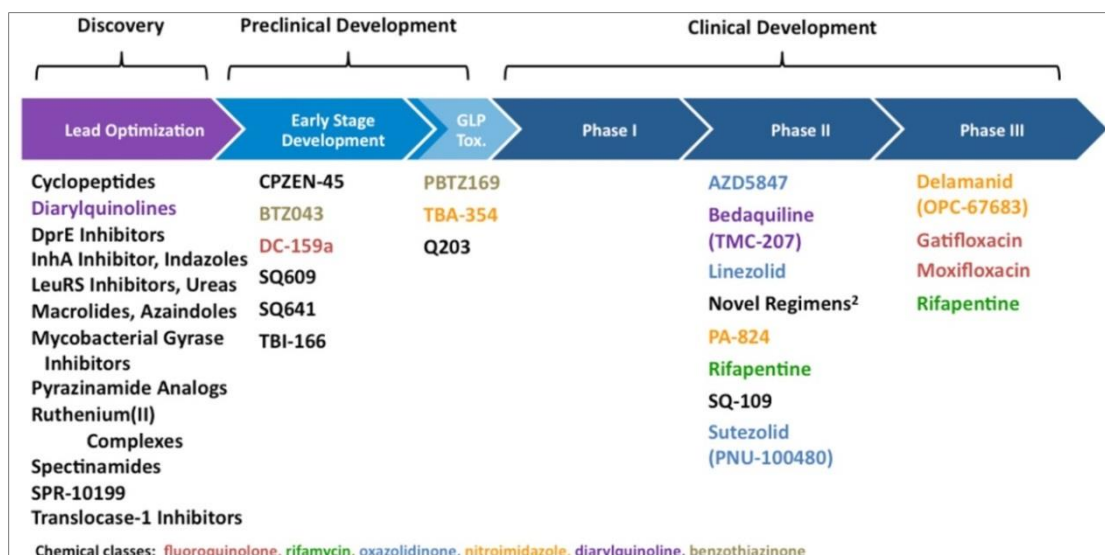


Figure 1.3: Current global pipeline of TB drug development (Source: Stop TB Partnership Working Group on New Drugs)

Abbreviations: GLP, Good laboratory practices; Tox, toxicology studies

The most successful approach was to re-engineer old antibacterial drug classes and improve their antimycobacterial potencies to yield novel drugs (Lechartier B., *et al.*, 2014). Examples of such redesigned scaffolds are the nitroimidazoles (delamanid, PA-824, and TBA-354) and 1,2-ethylenediamine (SQ109). Oxazolidinones such as linezolid were developed for Gram-positive bacterial infections and were later shown to have anti-tubercular activity. Four modified versions of oxazolidinone derivatives (sutezolid, AZD-5847, radezolid, and tedizolid) might have improved activity against *Mtb* and avoid myelosuppression- a problem with linezolid (Sotgiu G., *et al.*, 2012).

Figure 1.4 Promising new antibacterial (especially anti-tubercular) drugs that are now being subjected to *in vitro* and *in vivo* studies are indicated as a **Figure 1.4** as follows.

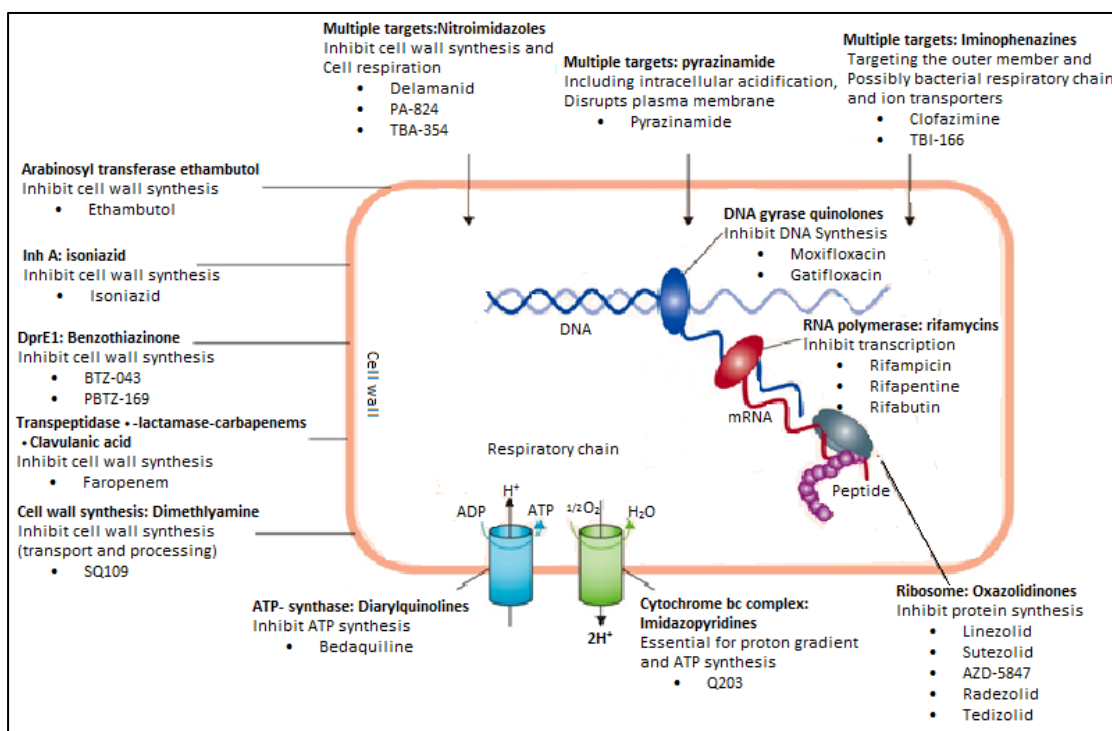


Figure 1.4: Mechanism of action of new anti-tubercular drugs in development (Zumla A. I., *et al.*, 2014)

In search of novel drug targets, more research has to be done to understanding the biology of persistence, the factors involved in tissue liquefaction and granuloma, and the host immune system mechanisms that control latent infection. The outcome of such research will provide improved understanding of the disease. This is a battle that might not be easily won, but with continuous effort and sustained support, it is quite possible for complete eradication of TB.

The search for new TB drugs that can overcome the increasing spread of multi drug resistant tuberculosis and emerging extremely drug resistant tuberculosis can be approached from two directions: the identification and validation of novel targets for the development of novel antibiotics with no pre-existing resistance mechanisms, or exploration of known and clinically validated targets for new chemical series or modification of existing drug classes to eliminate the possibility of cross resistance with existing drugs for which resistances have developed. The rise in drug-resistant *Mtb* and relatively few candidates in drug development pipeline signify the urgent need for novel anti-tubercular agents, ideally with clinical efficiency in MDR, XDR, and TDR isolates.

One such attractive strategy is to inhibit **DNA Gyrase**, the focus of the present study and an ATP-dependent type IIA topoisomerase enzyme.

The advances in biotechnology and cell biology makes easy to sequence the genome of *Mtb* in the year 1998. The availability of *Mtb* genome has boosted efforts towards target-based discovery of antimycobacterial compounds (Cole S. T., *et al.*, 1998). Clinically validated targets of known anti-mycobacterial agents offer great promise in terms of designing novel inhibitors that are likely to be bactericidal under the *in vitro* and *in vivo* growth conditions. Among the extensively studied bacterial targets, DNA gyrase, belonging to the Type II topoisomerase family, has been validated clinically by the fluoroquinolone (FQ) class of drugs (Burman W. J., *et al.*, 2006 and Conde M. B., *et al.*, 2009). The mechanism of action of DNA gyrase is distinct from that of other type II enzymes, and relies crucially on DNA wrapping. The enzyme functions as a tetramer in which two A subunits (encoded by Gyr A) and two B subunits (encoded by Gyr B) bind to the DNA molecule (Orphanides G., *et al.*, 1994). Combination therapy containing moxifloxacin have shown the potential to shorten duration of TB treatment (Diacon A. H., *et al.*, 2011). However, pre-existing resistance to fluoroquinolones (FQs) is likely to restrict the clinical utility of this class of drugs for treating TB in the long run (Duong D. A., *et al.*, 2009). FQs bind to the Gyr A subunit of bacterial DNA gyrase and trap the double strand cleaved DNA-gyrase complex leads to bacterial cell death (Drlica K., *et al.*, 2008). Hence, a novel

inhibitor of DNA gyrase with a unique binding site is likely to have activity against FQ-resistant TB.

2.1 Bacterial DNA gyrase inhibitors

DNA gyrase is a type II topoisomerase enzyme involved in DNA replication and repair. This enzyme is essential for all bacteria and is absent in eukaryotes (Champoux J. J., *et al.*, 2011). DNA gyrase catalyses the crucial steps to maintain the various topological forms of DNA during DNA synthesis/replication. DNA gyrase performs an ATP-dependent reaction to introduce a negative supercoiling into complex circular DNA (Corbett K. D., *et al.*, 2004). This enzyme exists in a hetero tetrameric form, comprising of a Gyr A and a Gyr B sub-unit (A₂B₂). The DNA breakage reunion function resides in the Gyr A subunit, while the GyrB subunit catalyses the ATP- dependent hydrolysis to generate the energy required for enzyme activity. A very similar organization is observed for topoisomerase IV, which is composed of dimers of the Par C and Par E subunits. Interestingly, the *Mtb* genome encodes a functional DNA gyrase, but no topoisomerase IV. DNA gyrase is made of two structural domains, the N-terminal breakage-reunion domain and the carboxy-terminal domain for the Gyr A or Par C subunits and the ATPase domain along with topoisomerase-primase (TOPRIM) domain for the Gyr B or Par E subunits (Mayer C. *et al.*, 2014). The enzyme binds to DNA, and a segment of about 140 base pairs is wrapped around the C-terminal tail domain of the Gyr A protein into a positive supercoil. The bound DNA (the G-segment) is then cleaved in each strand at sites separated by 4 base pairs leaving the active site tyrosines (Tyr22) from the two A subunits covalently attached to the 5'-phosphate groups on the cleaved ends. Another segment of DNA (the T-segment) is transported through this double-stranded break and through the enzyme itself. Upon resealing of the cleaved DNA, the linking number is reduced by two which results in the introduction of negative supercoils, altering the topology of the DNA molecule. The DNA strand-passage reaction is coupled to the hydrolysis of ATP, but exactly how the energy from the ATP hydrolysis is used in the strand passage process is not clear. If ATP is replaced by the non-hydrolyzable analogue, ADPNP (5'-adenylyl β , γ -imidodiphosphate), only limited supercoiling occurs, suggesting that nucleotide binding promotes one round of supercoiling, and ATP hydrolysis is required for recycling the enzyme (Mdluli K., *et*

al., 2007; Champoux J. J., et al., 2001; Drlica K., et al., 1997; Schoeffler A. J., 2005; Reece R., 1991; Roca J., 1995; Critchlow S. E., 1996).

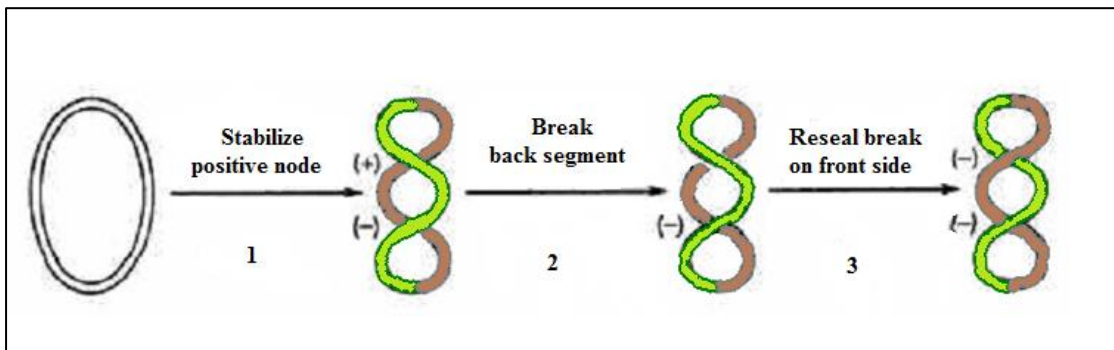


Figure 2.1: The picture depicts how the DNA gyrase enzyme introduces negative supercoiling in DNA

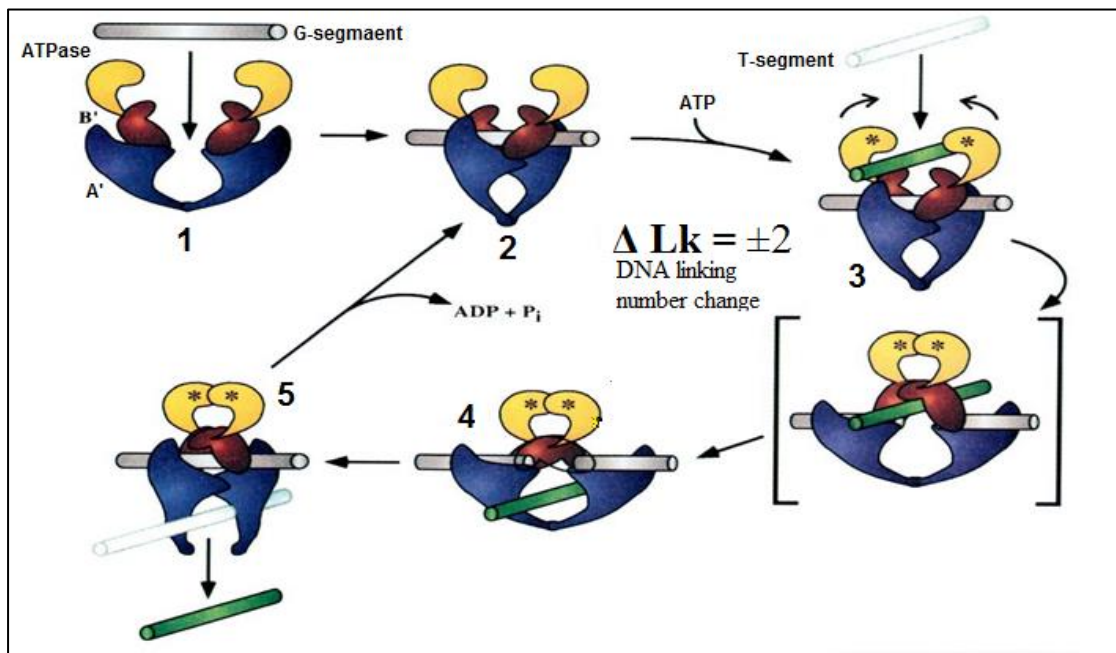


Figure 2.2: The catalytic cycle of topoisomerase II. The individual steps of the catalytic cycle of topoisomerase II are shown. Type IIA topoisomerases create a double-stranded break in one DNA duplex (brown) and pass another DNA duplex (green) through the break before resealing the break, to alter DNA topology (and change the DNA linking number by 2).

In *Mtb*, DNA Gyrase is the sole type II topoisomerase that ensures the regulation of DNA superhelical density. As a result, the *Mtb* enzyme shows a different activity spectrum compared with other DNA gyrases, e.g. it supercoils DNA with efficiency

comparable to that of other DNA gyrases, but shows enhanced relaxation, DNA-cleavage and decatenation activities (Aubry A., *et al.*, 2006).

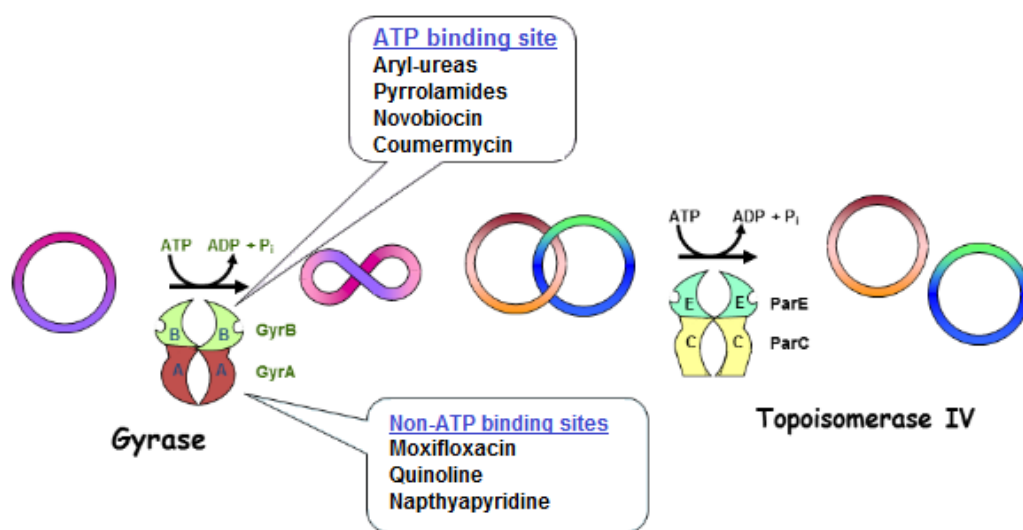


Figure 2.3: Represents the bacterial type II & IV topoisomerases function, DNA gyrase relaxes and introduces supercoiling but topoisomerase IV only relaxes positive supercoiled DNA (Shirude P., Hameed S., *et al.*, 2012)

Many inhibitors for Gyr A have been reported which includes the fluoroquinolones like the moxifloxacin, ciprofloxacin and norfloxacin (Hiasa H., *et al.*, 2003). These inhibitors are more effective and have low IC_{50} and MIC values. While this class of antibacterials has gained a strong position in the treatment and TB therapy, other than fluoroquinolones (FQs), novel bacterial topoisomerases (NBTI's) and aminopiperidines are showed to inhibit DNA breakage-reunion function but the resistance developed by the organisms and undesired side effects hampered the use of quinolones for treatment. On the other hand the Gyr B inhibitors mainly novobiocin, coumermycin and cyclothialidines are highly effective drugs, which target the ATPase activity of the enzyme, by competitive inhibition with the ATP thus abolishing the energy-dependent reactions catalyzed by the DNA gyrase but these drugs were withdrawn from the market due to their hazardous side effects and toxicity, thus creating a gap for the drug discovery field. Thus the focus is placed on the Gyr B subunit which has high scope for the molecular inhibition studies and drug discovery.

Several inhibitors targeting DNA gyrase have been reported to exhibit activity against *Mtb*, a group of inhibitors that target ATP binding site of Gyr B enzyme and block ATP hydrolysis have shown antimycobacterial activity. Examples of this type include aminopyrazinamides (Shirude P., *et al.*, 2013), benimidazole ureas (Chopra S., *et al.*, 2012), thiazolopyridine ureas (Kale M. G., *et al.*, 2013), pyrrolamides (Hameed P. S., *et al.*, 2013) and thiazolopyridone urea (Kale R., *et al.*, 2014) with potent antimycobacterial activity.

Very recently GSK, Vertex pharmaceuticals, AstraZeneca and few others have reported some novel inhibitors of DNA Gyr B with potential antibacterial activity both structurally and mechanistically distinct from FQs (Paul S. C., *et al.*, 2009). These new drugs don't form a stabilized ternary complex but rather form a pre-formed cleavage complex as seen in the *Staphylococcus aureus* (Peter A., *et al.*, 2004). GSK299423 is a NBTI (Novel Bacterial Topoisomerase Inhibitor) derived from a chemical series originating from an unbiased antibacterial screening. GSK299423 shows potent inhibition of supercoiling by DNA gyrase with an IC₅₀ value of 4 nM (Paul S. C., *et al.*, 2010).

2.1.2 Fluoroquinolones (FQs)

FQs are the most successful antibacterial agents targeted to DNA gyrase. FQs were derived from quinine (an alkaloid). Nalidixic acid, the first quinolone derivative was introduced in 1962 by George Lesher *et al* discovered as a by-product of chloroquine synthesis (Marriner G. A., *et al.*, 2011; Lesher G. Y., *et al.*, 1962). Most FQs are being evaluated as potential anti-TB drugs, also for their proven potential to shorten TB treatment duration. Use of FQs is one of the major strategies for TB control. They are the class of antibiotics that have potent antimicrobial activity against a wide range of gram positive and gram negative organisms. The treatment of MDR-TB relies upon a backbone of an injectable agents like kanamycin, capreomycin, or amikacin and a fluoroquinolone namely gatifloxacin, levofloxacin, moxifloxacin, or ofloxacin based on murine model studies (Alvarez-Freites E. J., *et al.*, 2002; Poissy J., *et al.*, 2010; Shandil R. K., *et al.*, 2007). Several members of the FQs class of drugs are currently already used as second line TB drugs for the treatment of MDR-TB. They have high bioavailability in the range of 70-90%, even when given orally.

2.1.3 Different classes of fluoroquinolones

All fluoroquinolone analogues possess majorly 4-quinolone-3-carboxylic acid structure with Fluorine atom at 6th position of quinoline ring. The general structure of quinolones was depicted as shown in figure 2.1.

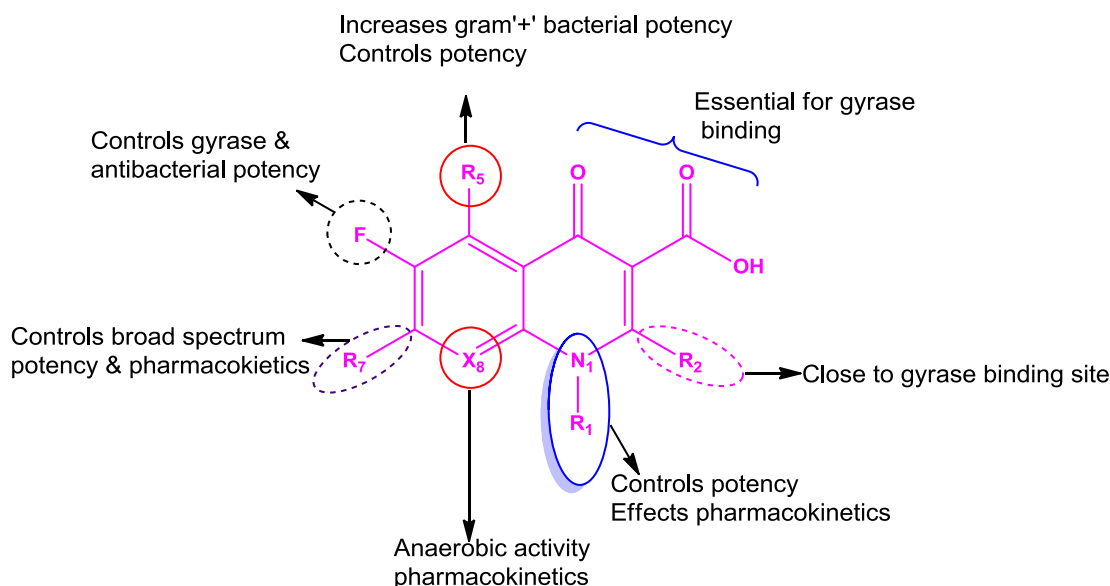


Figure 2.4: Structural activity relationships (SAR) of fluoroquinolones

The C-2 position lies near the DNA gyrase binding site, and thus a sterically undemanding hydrogen atom at R₂ is optimal (Gootz T. D., *et al.*, 1996). The dicarbonyl moiety is required for binding to DNA gyrase and thus is critical for activity. Modifications at C-5 control in-vitro potency with the most active groups being small electron-rich groups such as -NH₂, -OH, and -CH₃ (Domagala J. M., *et al.*, 1994). Additionally, C-5 modifications affect activity against both gram-negative and gram-positive organisms. The fluorine atom at C-6 enhances DNA gyrase inhibition (Mitscher L. A., *et al.*, 2005; Gootz T. D., *et al.*, 1996) and can increase the MIC of the compound 100-fold over that of other substitutions (Domagala J. M., *et al.*, 1994). The most active substituents at C-7 have been five- and six-membered nitrogen heterocycles, with pyrrolidines increasing activity against gram-negative bacteria and piperazines affecting potency against gram-positive organisms. The C-8 position controls absorption and half-life, and optimal modifications for *in vivo* efficacy include groups that create an electron deficient pi system (Bolon M. K., *et al.*, 2009). Several modifications that create an N-1 to C-8 bridge have also been

successful, *i.e.*, ofloxacin and levofloxacin, which both display significant gyrase inhibition (Gootz T. D., *et al.*, 1996).

Gatifloxacin was discovered by Bristol-Myers Squibb (BMS) in the year 1999 for the treatment of respiratory tract infections whereas moxifloxacin developed by Bayer AG was marketed worldwide under the trade name of Avelox. In 1999, moxifloxacin hydrochloride (Avelox) was approved by US FDA for use in US. The structures of different fluoroquinolones and their MIC's against *Mtb* H₃₇Rv strain for the clinically relevant fluoroquinolones range from 0.1 to 5 µM were showed in **Figure 2.5**.

Moxifloxacin and gatifloxacin are fourth-generation FQs inhibit the bacterial enzyme DNA gyrase and topoisomerase IV. But in *Mtb* it is assumed that they target solely DNA gyrase since there is no evidence of topoisomerase IV present in *Mtb*. Other quinolones, such as ciprofloxacin and ofloxacin, have been used as second-line anti-tubercular drugs but moxifloxacin and gatifloxacin are more potent *in vitro* than these older quinolones. Moxifloxacin and gatifloxacin have an extended spectrum of antibacterial activity and provide better inhibition of gram-positive bacteria and favour pharmacokinetic properties. Moxifloxacin and gatifloxacin inhibited *Mtb* DNA gyrase with an IC₅₀ of 4.5 and 3 µg/mL respectively, whereas *Mtb* MIC was found to be 0.05 and 0.12 µg/mL respectively (Villemagne B., *et al.*, 2012).

Moxifloxacin and gatifloxacin are attached with a methoxy group at position 8 and a bulky side chain at 7th position. The C-8 methoxy group has potent activity against DNA gyrase (topoisomerase II) and topoisomerase IV, a capability that allows both these agents to kill resting bacterial cells as well as those that are actively multiplying. That leads to the prevention of the emergence of bacterial resistance to the quinolones. A cyclopropyl group at N-1 and fluorine at C-6 brings an enhanced antibacterial activity. The bulky side-chain and bicyclic side chain at position C-7 of moxifloxacin and gatifloxacin respectively reduces the ability of the bacterial cells efflux pump to flush out the antibiotic, resulting to the increased drug stay in the bacterial cell improves the enhanced activity, expanded spectrum of activity and additional defense against resistance.

Moxifloxacin and gatifloxacin are currently in phase III clinical trials. The potential adverse effects that have been reported for these drugs are dysglycemia with

gatifloxacin and QT prolongation with moxifloxacin (Alvarez-Freites E. J., *et al.*, 2002).

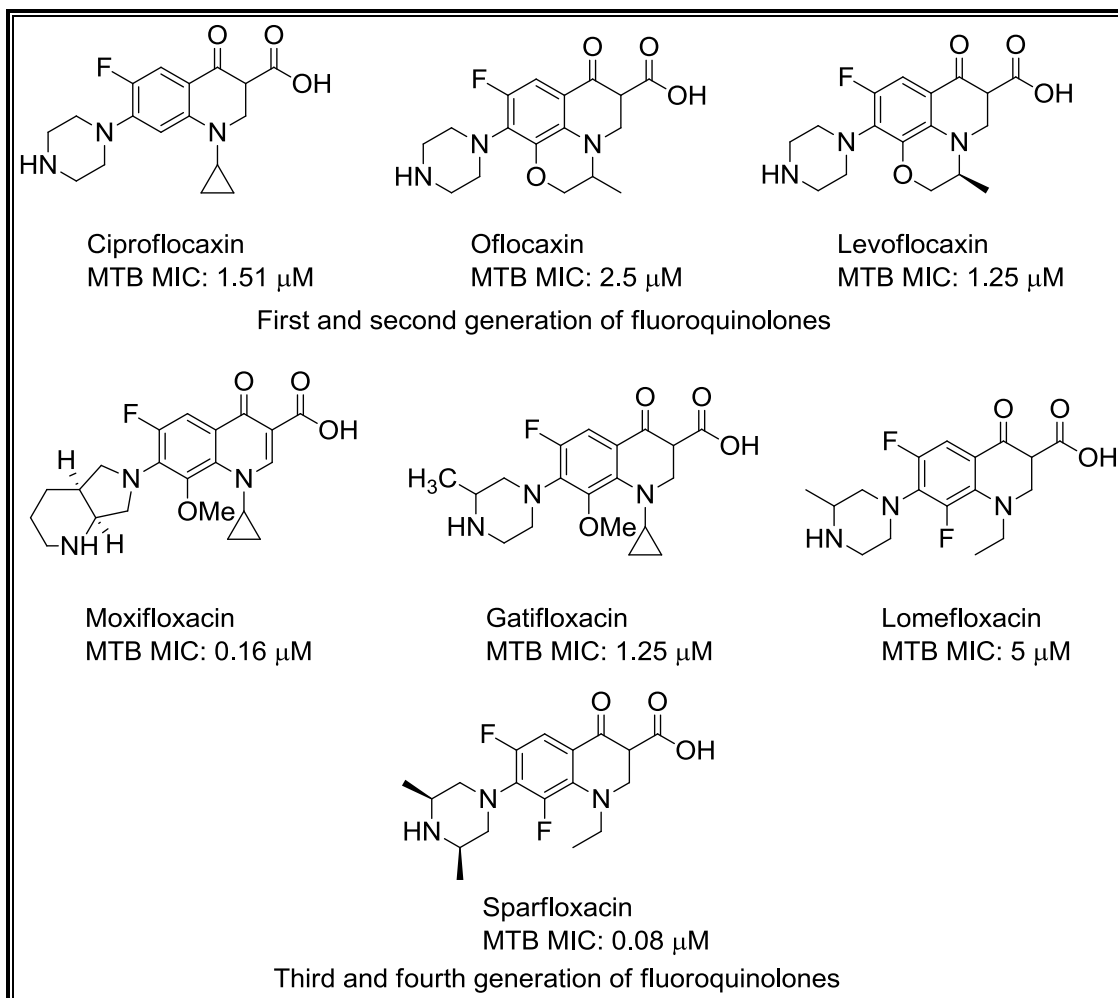


Figure 2.5: The MIC data for fluoroquinolones commonly used in treatment of TB.

Moxifloxacin and gatifloxacin are currently in phase III clinical trials. The potential adverse effects that have been reported for these drugs are dysglycemia with gatifloxacin and QT prolongation with moxifloxacin (Alvarez-Freites E. J., *et al.*, 2002).

The general limitations to fluoroquinolones are i) Alteration of molecular targets i.e. mutations in specified regions of DNA and genes coding for the gyrase and/or topoisomerase leads to clinical resistance. Mutations in Gyr A are those the most frequently found in gram-negative bacteria, and mutations in Par C/Gyr A are generally the most common in Gram-positive bacteria (Black M. T., *et al.*, 2008) ii)

Resistance due to reduced drug accumulation which can probably be due to inability of the drug to cross the bacterial cell wall (permeability barriers) or an efflux pump effective in pumping out hydrophilic quinolones

In addition, the resistance acquired by mycobacteria to the fluoroquinolone class of drugs, severe side effects such as tendonitis and tendon rupture due to collagen damage and QT prolongation by blocking voltage-gated potassium channels.

2.1.4 Drugs acting through the allosteric inhibition of DNA Gyrase (NBTI's)

Novel (non-fluoroquinolone) bacterial type II topoisomerase inhibitors (NBTIs) were reported by GlaxoSmithKline (GSK) and Aventis Pharma AG. These are a unique class of antibacterial DNA Gyrase inhibitors that has gained importance in recent times. These classes of drugs are structurally and mechanistically distinct from fluoroquinolones and acting through a novel mechanism of action and hence there is no impact by target mutations that cause resistance by fluoroquinolones (Bax B. D., *et al.*, 2010).

The promising leads were developed by this approach includes the NXL 101 developed by Aventis Pharma AG, and then by GSK lead GSK299423, found to be 70 times more potent than NXL 101 and 2,000 times more potent than ciprofloxacin for inhibition of *Staphylococcus aureus* DNA Gyrase supercoiling. More interestingly these classes of drugs were not affected by a Gyr A mutation in DNA Gyrase and showed good *in vitro* activity against a spectrum of both Gram-positive and Gram-negative bacteria. The general chemical structures of NBTIs consist of three parts, a linker stacked between a bicyclic aromatic left-hand side (LHS) and a mono or bicyclic right-hand side (RHS). By this approach so many inhibitors were identified for DNA gyrase few of them were showed in **Figure 2.7**.

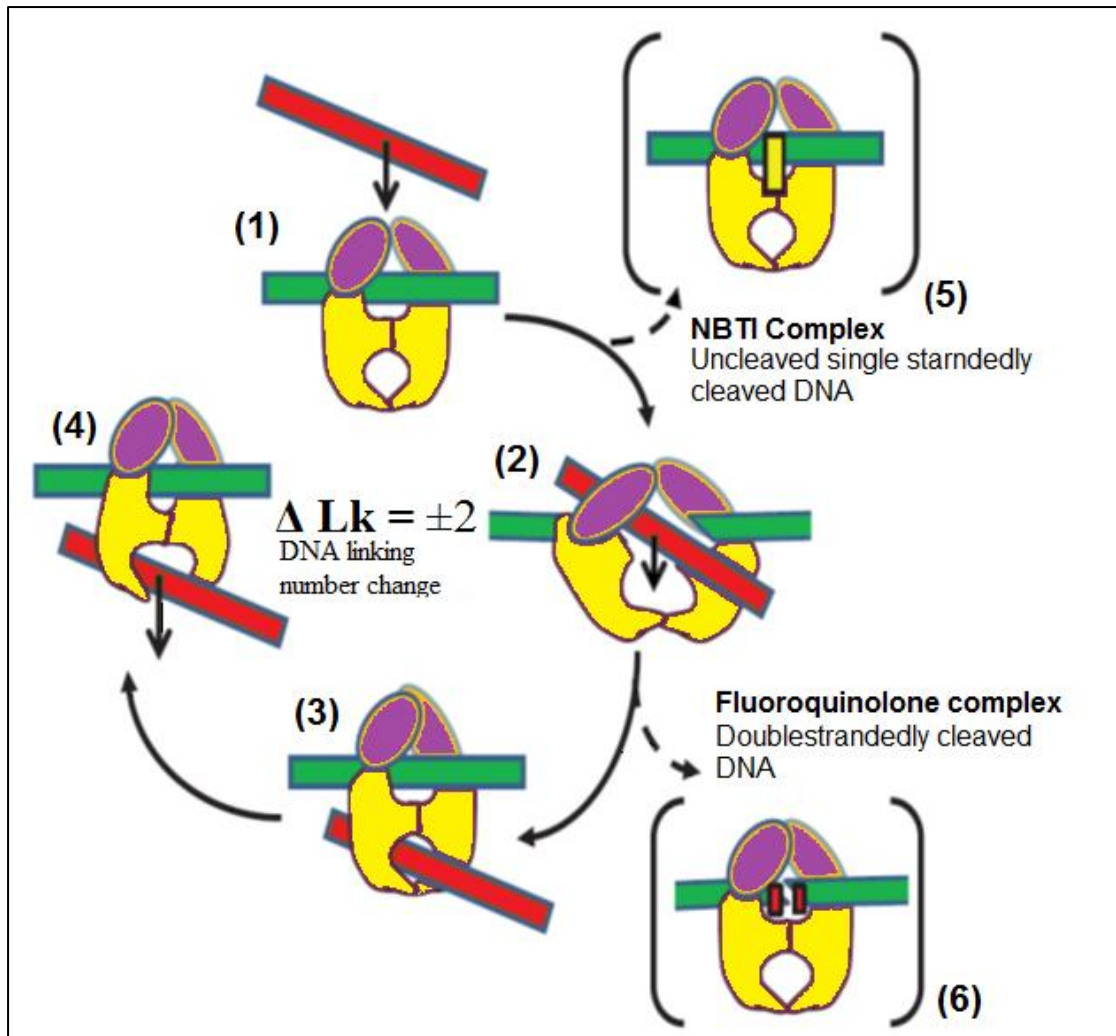


Figure 2.6: Mechanism of action of FQ drugs and NBTIs; Simplified schematic representation of type IIA topoisomerase action (1) to (4), and inhibitor complexes of NBTI (5) and fluoroquinolone (6) antibacterial agents (Bax B. D., *et al.*, 2010).

Type IIA topoisomerases create a double-stranded break in one DNA duplex (green) and pass another DNA duplex (red) through a break before resealing the break (2), to alter DNA topology (and change the DNA linking number by two). NBTI complex – a single NBTI inhibitor molecule (yellow) binds to an uncleaved G-segment of DNA and Gyr A (5). FQ complex- two FQs (red) bind in the cleaved G-segment of DNA (6). Par E/Gyr B = purple subunits; Par C/Gyr A = yellow subunits; green bar = gate or G-segment DNA; red bar = translocated T-segment; black arrows indicate the direction of DNA segment translocation.

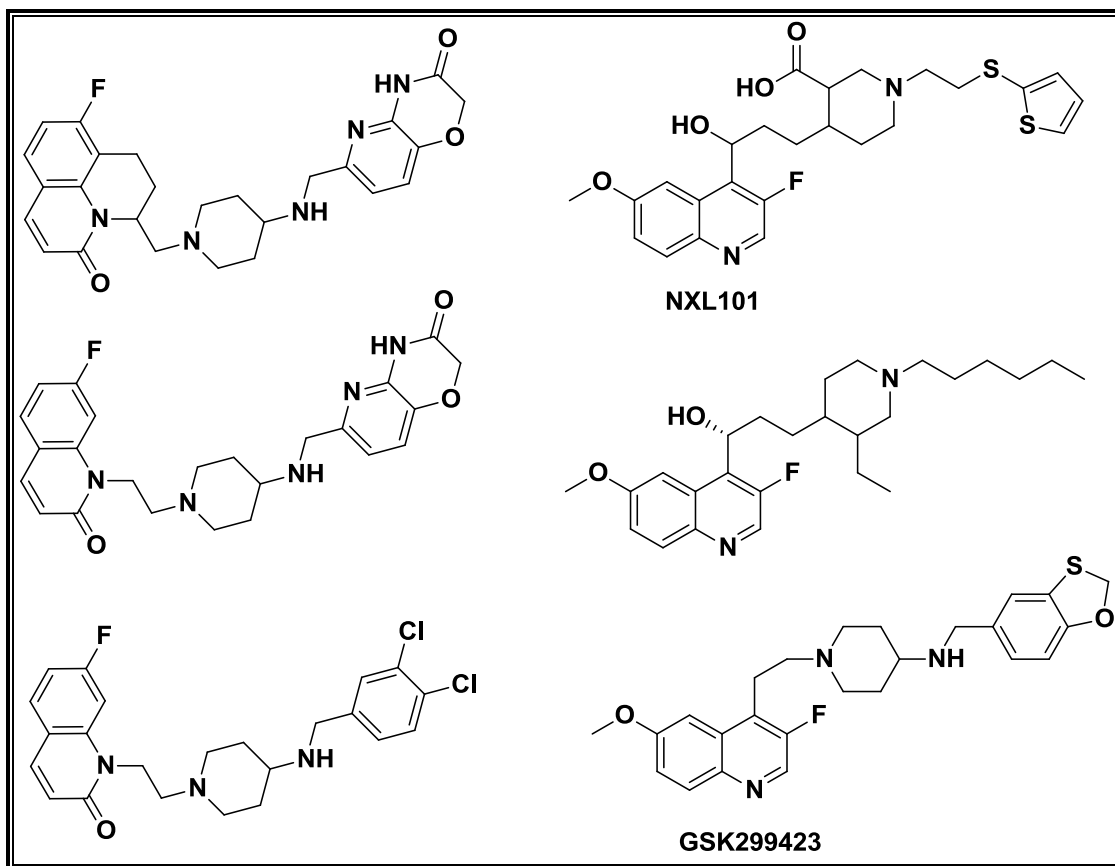


Figure 2.7: The various reported novel bacterial topoisomerase inhibitors

The limitations of NBTIs include the intrinsic factors to achieve an acceptable cardiovascular safety profile of compounds designed through NBTI approach. Their encouraging growth has been significantly slowdown by considerable cardiovascular safety risk arising from their potent human ether-a-go-go-related gene (hERG) inhibition and QTc prolongation *in vivo*.

2.1.5 Mycobacterial Gyr B inhibitors

The Gyr B protein comprises a 43 kDa N-terminal domain (NTD) of DNA gyrase enzyme which contains the ATPase site and dimerizes upon ATP binding. ATP binding and hydrolysis is required for protein-protein interactions and recycling of the enzyme (Brino L., *et al.*, 2000). It has also been shown that to perform as an ATP-operated clamp that binds DNA during the supercoiling process (Tingey A.P., *et al.*, 1996). There is a loop that is thought to close the active site and it contains amino acid residues 98-118. This loop is also implicated in the binding and hydrolysis of ATP, and is composed of a number of conserved residues which are involved in the

catalytic mechanism (Lee M. P., *et al.*, 1994; Li W., *et al.*, 1997; Tamura J. K., *et al.*, 1990).

DNA gyrase B has similar qualities required for an attractive antimycobacterial target. It is an essential gene for bacterial survival and its inhibition results in cell death because there are no viable alternative mechanisms for performing this function. The Gyr B genes, among a variety of *Mtb* isolates have an almost 99.9% homology with almost no changes in sequence, further signifying its broad applicability as a drug target.

Base on literature, there are few different classes of inhibitors are reported for mycobacterial DNA Gyr B domain. These include aminocoumarins, Novobiocin and four synthetic analogues that include the benzimidazole ureas from Vertex and the pyrrolamides, pyrazinamides, thiazolopyridine ureas from AstraZeneca (AZ). A brief description of these classes has been provided below.

2.1.5.1 Aminocoumarins

Aminocoumarins are comes under antibiotic category those inhibit of the DNA gyrase enzyme involved in the cell division in bacteria. Aminocoumarins has common 3-amino-4,7-dihydroxycoumarin ring as the basic skeleton. In comparison with FQs, aminocoumarins are regarded as the ‘Cinderellas’ of the gyrase inhibitors (Heide L., *et al.*, 2009). Novobiocin, clorobiocin and coumermycin A₁ are the class of aminocoumarins isolated from *Streptomyces* bacterial species and many other derivatives were made in different methods include, genetic manipulation, metabolic engineering and mutasynthesis and chemical synthesis. Structurally clorobiocin and novobiocin are differ in the substitution of the methyl group at the 8' position of the coumarin ring with a chlorine atom, and a 5-methyl-pyrrole-2-carboxyl group substitutes the carbamoyl group at the 3' position of the noviose.

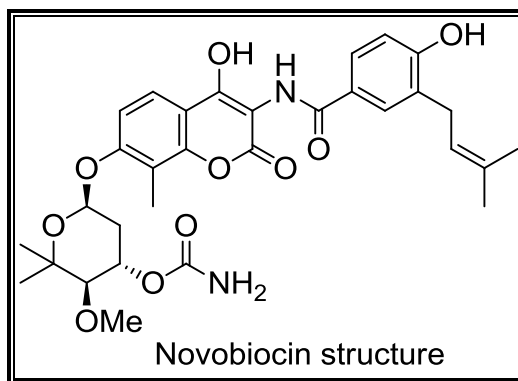


Figure 2.8: Structure of novobiocin

Novobiocin exhibited an MIC of 4 mg/mL against drug sensitive *Mtb* H₃₇Rv strain and MIC's in the range of 0.62 mg/mL – 8 mg/mL against various drug resistant strains of *Mtb* (Chopra S., *et al.*, 2012). Simocyclinones are another variety of aminocoumarin moiety with an additional angucyclinone polyketide group. Both aminocoumarins and simocyclinones are different from quinolone group those target gyrase but bind at different subunits of DNA gyrase enzyme.

Though aminocoumarins are potent inhibitors of DNA gyrase *in vitro*, their poor activity against gram-negative bacteria, solubility and cell safety profile prevent them from being clinically successful drugs. So their further structural exploration is still needed.

2.1.5.2 Aminopyrazinamide class of Gyr B inhibitors

AstraZeneca identified aminopyrazinamides through high throughput screen of their compound library against *Msm* Gyr B ATPase of gyrase enzyme (Shirude P. S., *et al.*, 2013). They co crystallized aminopyrazinamide with *Msm* Gyr B protein. The crystal structure of *Msm* Gyr B in complex with one of the aminopyrazinamides revealed three important locations namely pocket I, pocket II and the hydrophobic pocket III are critical for showing antibacterial potency.

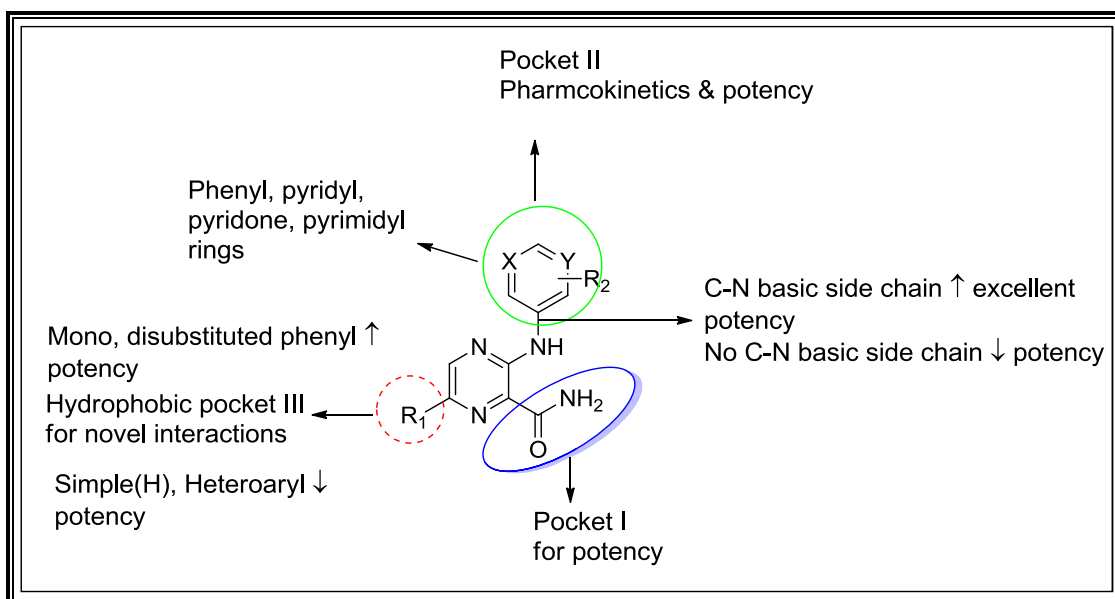


Figure 2.9: SAR of aminopyrazinamide based mycobacterial Gyr B inhibitors

Compounds in the series have demonstrated excellent mycobacterial kill against both replicating and non-replicating *Mtb* and have potent intracellular activity against *Mtb* residing within macrophages. The initial pharmacokinetic profiling of aminopyrazinamide class not encouraging but there is a desperate need for new anti-TB agents; the aminopyrazinamide class has the potential for further optimization to get new safer, effective antitubercular agents. Still there is lot of scope to discover new Gyr B leads.

2.1.5.3 Pyrrolamides as DNA Gyr B inhibitors

Pyrrolamide class of antimycobacterial agents were identified by AstraZeneca in search of new antibacterial collection programme against *Msm* Gyr B ATPase domain. Pyrrolamides had shown promising antibacterial Gyr B inhibitory potency were taken up for further the study, encouragingly most of the molecules tested were showed promising Gyr B IC₅₀ potency with good MIC.

The basic structural framework of the molecules belonging to this class consists of an aminopiperidine linker stacked between a substituted thiazole core on the RHS and a pyrrolamide analogue on the LHS quite similar to NBTIs. The structure of pyrrolamide was shown in **Figure 2.10**

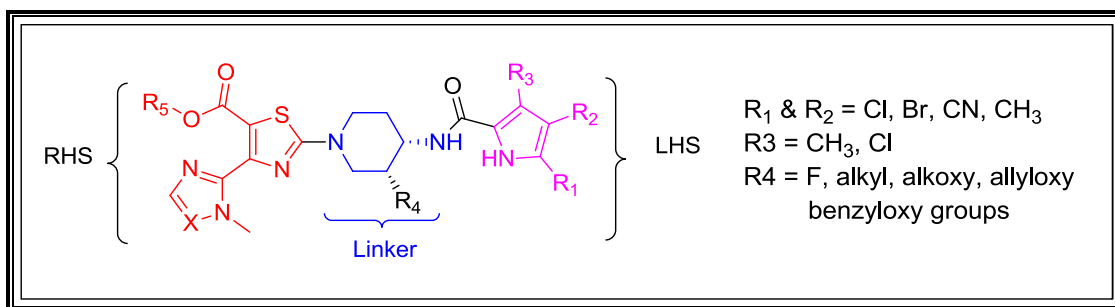


Figure 2.10: General structure and SAR of pyrrolamide Gyr B inhibitors

The most potent compound in this series showed Gyr B inhibitory IC₅₀ of 5 nM, inhibited super coiling activity of DNA Gyrase with an IC₅₀ < 5 nM, an MIC of 0.03 µg/mL against *Mtb* H₃₇Rv and an MIC₉₀ < 0.25 µg/mL against drug resistant, clinical isolates of *Mtb*. In overall we can conclude that the reported pyrrolamide class of Gyr B inhibitors offer an attractive lead for development of novel mycobacterial agents against both drug sensitive and drug resistant TB.

2.1.5.4 Thiazolopyridine and benzimidazole urea based inhibitors

AstraZeneca compound collection programme for gyrase inhibitors, thiazolopyridine ureas are one of such class, prepared from a scaffold hopping efforts using benzimidazole ureas as initial starting point.

The thiazolopyridine ureas represent a novel class of potent anti-tubercular agents acting through the inhibition of DNA Gyr B ATPase activity. These compounds were efficacious in a murine model of tuberculosis as well. The series has sufficient lead-like properties and has structural advantages for further optimization. These compounds have the potential to treat drug-susceptible as well as drug-resistant TB, including quinolone-resistant TB, because they target a different activity of DNA Gyrase.

Coming to benzimidazole ureas, these are a new class of inhibitors with dual targeting agents identified by Vertex pharmaceuticals through a high-throughput ATPase assay screening against the Gyr B subunit of gyrase enzyme. Benzimidazole ureas also showed potent inhibition similar to pyrrolamide derivatives for the mycobacterial gyrase domain with Gyr B inhibitory IC₅₀ in nanomolar range. The study also showed

that the molecule belonging to benzimidazole class of drugs were effective against fluoroquinolone resistant *Mtb* strains and their efficacy also good in murine models of TB.

With respect to the structure activity relationship study; as observed in the case of benzimidazole urea based inhibitors, smaller alkyl chain at the R₄ position (**Figure 2.11**) was found to be favourable for activity.

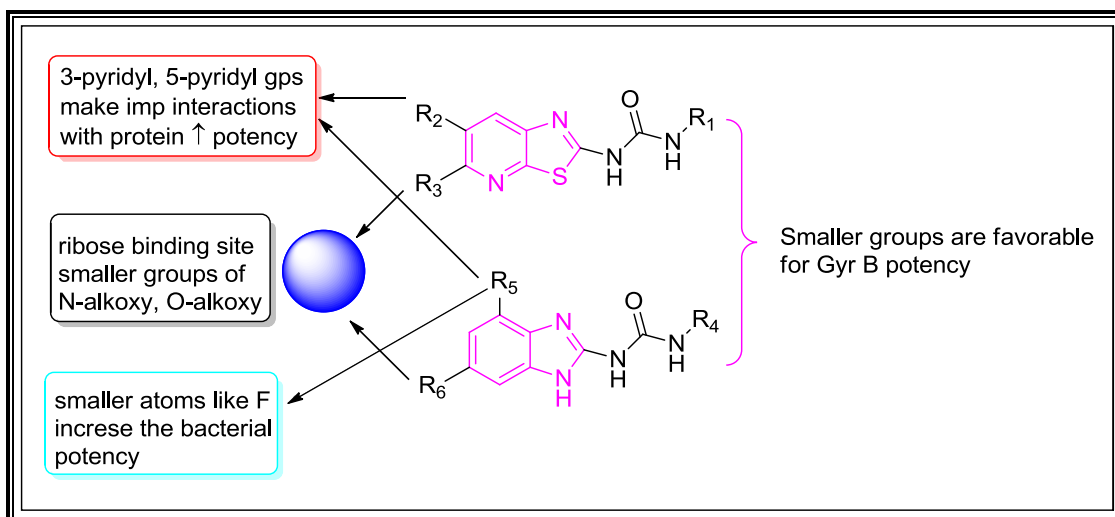


Figure 2.11: SAR of thiazolopyridine and benzimidazole inhibitors targeting Gyr B inhibitors

With recent data suggesting that incorporating fluoroquinolones in first-line anti-TB drugs may shorten the required length of drug treatments, it is important to begin the development of backup drugs to replace fluoroquinolones when resistance for that class of drugs becomes prevalent. The data generated with the above class of drugs suggest that drugs targeting Gyr B may be a viable alternative to include in first-line anti-TB drugs.

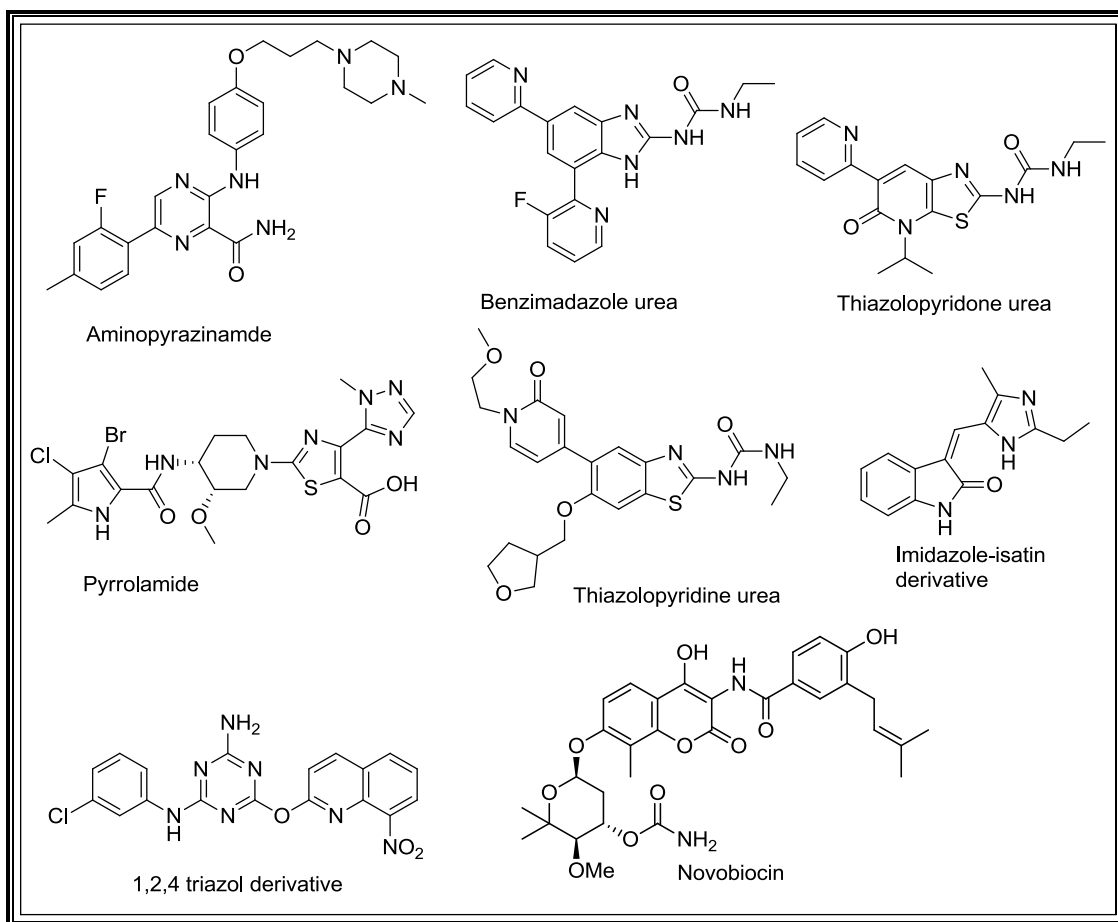


Figure 2.12: The various reported Gyr B inhibitors

The search for new TB drugs remains a challenging but it is necessary. Although a number of classes of compounds have been reported against *Mtb* because of improper treatment and new resistant strains of *Mtb* makes public health in serious. Therefore, the urgency and the growing need for the new class of chemical compounds are well accepted. Based on extensive literature, the quest for new anti TB drugs has to be discovered, in this process our inputs were majorly focused on development of novel quinoline analogues that inhibit drug sensitive as well as drug resistant strains of *Mtb* using molecular hopping techniques may reduce the treatment duration.

3.1 Objectives

TB is become one of the global pandemics and the emergence of various drug resistant strains of *Mtb* as well as its complications in different disease conditions makes the worst situations for the treatment of TB. These situations necessitate designing newer, more effective and safer anti-tubercular agents for the better treatment of TB. Based on a thorough literature review available it signifies the importance of DNA gyrase enzyme as a drug target for TB and it plays a vital role in viability of most bacteria including *Mtb*. The Gyr B portion of *Mtb* was less exploited thus present study focus on developing promising mycobacterial cellular potency achieving through *Mtb* DNA gyrase inhibitors.

The main objectives of the proposed work are:

1. To design novel *Mtb* DNA gyrase inhibitors based on reported anti-tubercular leads.
2. To synthesize and characterize the designed compounds using various synthetic and analytical techniques.
3. To evaluate the inhibitory potency of the synthesized compounds by *in vitro* *Mtb* DNA Gyr B and supercoiling assay.
4. To undertake *in vitro* antimycobacterial screening of the synthesized compounds against *Mtb*.
5. To evaluate the protein inhibition and stability of synthesized inhibitors using biophysical characterization technique.
6. To perform the *in vitro* cytotoxicity studies of the synthesized compounds
7. To evaluate the *in vitro* zERG channel inhibition assay, and
8. Docking studies (Comparison docking study of known to synthesized inhibitors)

3.2 Plan of Work

The plan of work was classified into the following categories

3.2.1 Designing new antimycobacterial inhibitors

For designing the new antitubercular agents we approached in two different methods

- i) *Molecular hybridization/Scaffold hopping* method: Which is medicinal chemistry approach in this method by fusing one or more pharmacophoric units from the reported molecular structure of inhibitors/ligands/prototypes showing potency towards DNA gyrase enzyme?
- ii) *Molecular derivatization* method: In this method we will take up the already reported DNA gyrase inhibitors and further possible new derivatives will be synthesized to increase the potency, efficacy and to develop strong SAR through derivatization method.

3.2.2 Synthesis and characterization

The designed molecules were further synthesized in our laboratory utilizing previously reported methodology available in literature for structurally similar molecules. All reactions were monitored using thin layer chromatography and LCMS. The synthesized compounds were fully characterized using modern analytical techniques. LCMS, ^1H NMR and ^{13}C NMR were recorded and analysed to confirm the structure of the compounds. Purity of the compounds was evaluated by HPLC, Elemental analysis.

3.2.3. *In vitro* DNA gyrase enzyme inhibitory potency

The synthesized compounds were evaluated *in vitro* for their *Msm* DNA Gyr B inhibitory potency and *Mtb* DNA Gyrase supercoiling assay.

3.2.4. *In vitro* *Mtb* activity studies

All the synthesized compounds were further screened for their *in vitro* antimycobacterial activity against *Mtb* H₃₇Rv (ATCC27294) by using micro plate alamar blue assay (MABA) method.

3.2.5 Evaluation of protein-inhibitor binding affinity using biophysical characterization by DSF

Binding affinity of the potent Gyr B analogues was evaluated by differential scanning fluorimetry (DSF) experiment to estimate the thermal stability of the protein-ligand/inhibitor complex.

3.2.6 *In vitro* cytotoxicity screening

The synthesized compounds were also screened for their *in-vitro* cytotoxicity against RAW 264.7 cell line (mouse leukemic monocyte macrophage) using 3-(4,5-dimethylthiazol-2-yl)-2,5-diphenyltetrazolium bromide (MTT) assay.

3.2.7 *In vitro* zERG channel inhibition screening

Since most of the previously reported aminopiperidine based DNA gyrase inhibitors showed hERG toxicity, the more potent Gyr B leads were also evaluated for hERG channel inhibition by assessing arrhythmogenic potential on Zebrafish ether-a-go-go-related gene (zERG) which is orthologous to the human ether-a-go-go-related gene (hERG).

3.2.8 Docking studies (Comparison docking study of known to synthesized inhibitors)

Synthesized compounds subjected to docking studies to develop SAR (Structure activity studies) using commercially available computational software's like. The synthesized compounds which were active in Gyr B as well as in supercoiling assay were docked onto the active pocket of the Gyr B ATPase domain of *Mycobacterium smegmatis* (*Msm*) retrieved from protein data bank.

4.1 Design of novel Quinoline based *Mtb* DNA gyrase inhibitors

For designing the new antitubercular agents we had approached in two different methods i) *Molecular hybridization/Scaffold hopping* method: It is medicinal chemistry approach in this method by fusing one or more pharmacophoric units from the reported molecular structure of inhibitors/ligands/prototypes showing potency towards DNA gyrase enzyme. The newly designed architecture can lead to compounds having improved affinity and efficacy than the parent compounds with reduced side effects, besides carrying the desired characteristics of the original template. In this protocol, using the previously reported N-linked aminopiperidine/1,2,3 Triazole/*p*-Phenylenediamine based gyrase inhibitors as a template we reengineered novel inhibitors; by introducing subunits that has previously demonstrated to have inhibitory effect on Gyr B domain, as left and right hand core of the aminopioperidine and other linkers followed by ii) *Molecular derivatization method*: In this method we will take up the already reported DNA gyrase inhibitors and further possible new derivatives will be synthesized to increase the potency, efficacy and to develop strong SAR through derivatization method. Together five novel inhibitors were achieved through molecular hopping method, the design strategies were shown as below.

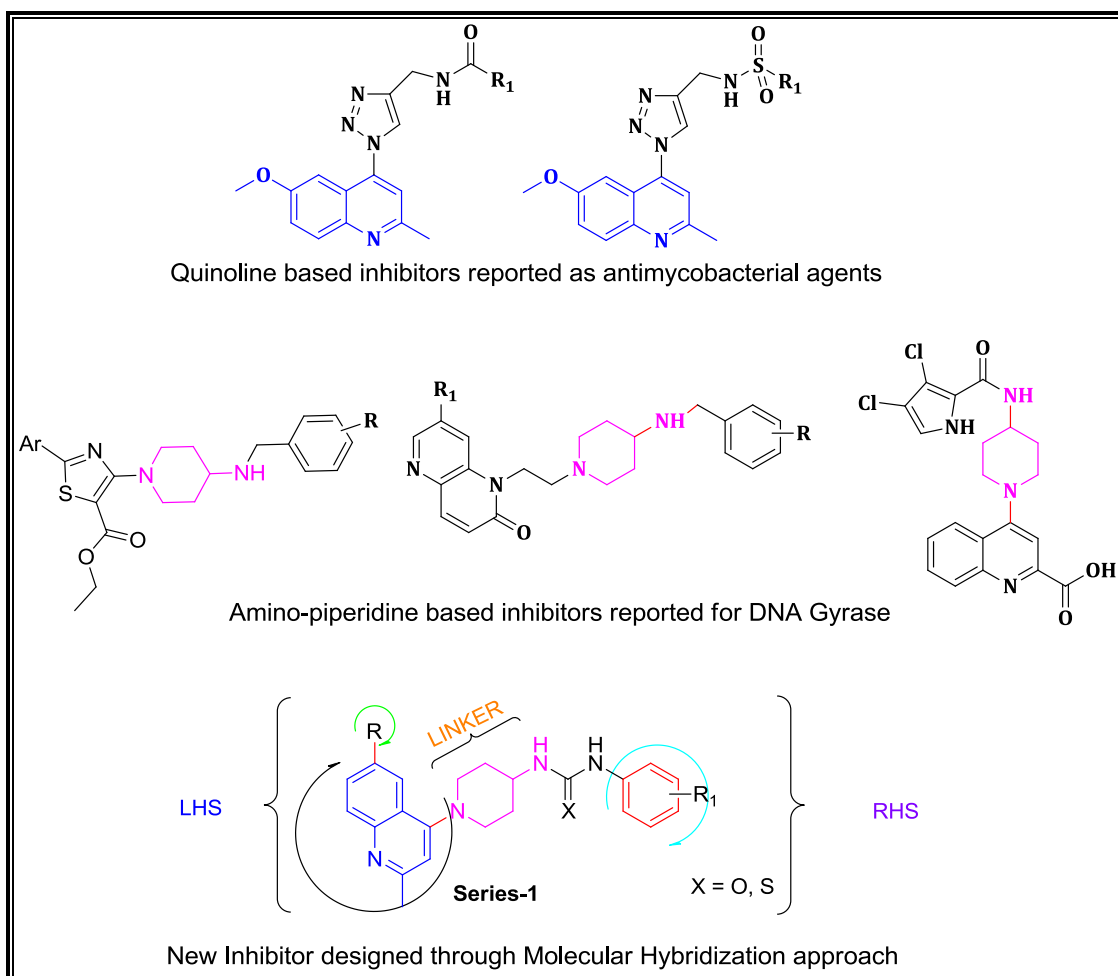


Figure 4.1: Scheme-1, New inhibitor designed through molecular hybridization approach.

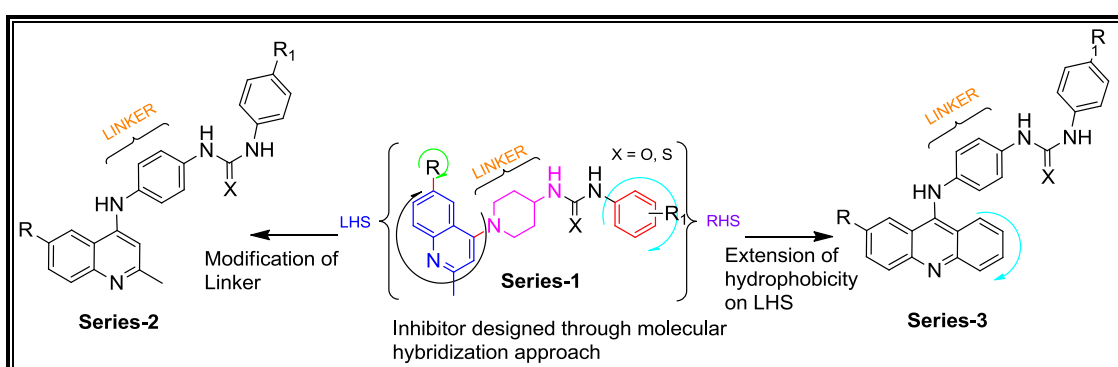


Figure 4.2: Scheme-2 & Scheme-3, further modifications of constructed hybrid/inhibitor through molecular hopping.

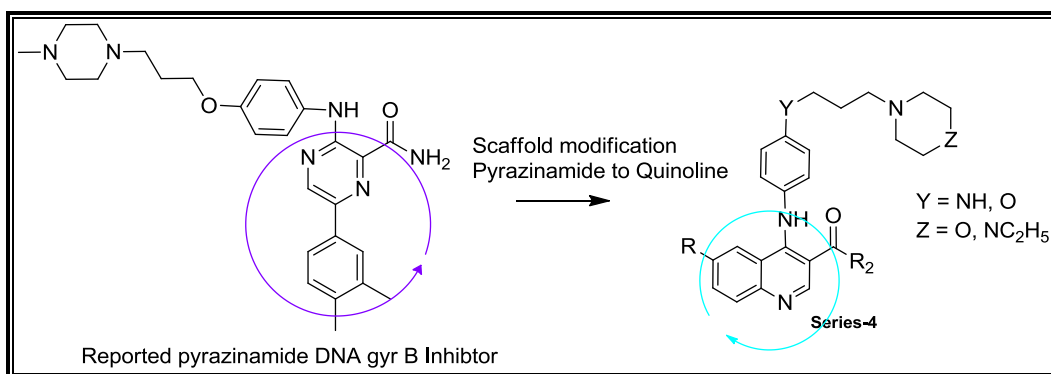


Figure 4.3: Scheme-4, Design logic, Scaffold modification and derivatization of reported DNA Gyr B inhibitor

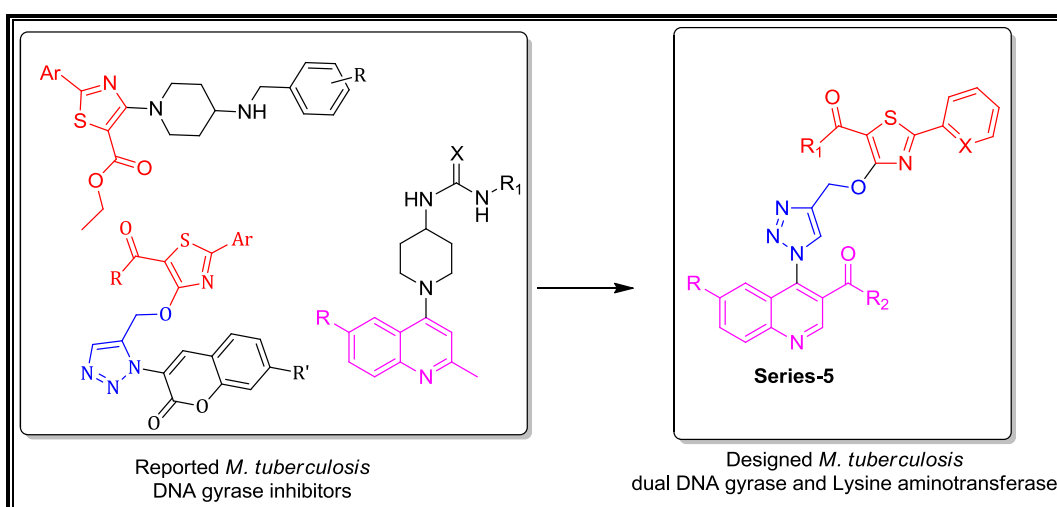


Figure 4.4: Scheme-5, Design logic and Scaffold modification and derivatization based on reported antimycobacterials

4.2 Chemistry and Method of synthesis

All commercially available chemicals and solvents were used without further purification. Melting points of the synthesized compounds were determined by Buchi B-540 open capillary instrument and were uncorrected. The homogeneity of the compounds was monitored by TLC (Thin layer chromatography) on silica gel 40 F254 coated on alumina plates, visualized by UV or iodine chamber and KMnO_4 treatment. All ^1H and ^{13}C NMR spectra were recorded on a Bruker AM-300 (300.12 MHz, 75.12 MHz) NMR spectrometer and Bruker BioSpin Corp, Germany respectively. Molecular weights of the synthesized compounds were checked by SHIMADZU LCMS-2020 series in ESI mode. Chemical shifts are reported in ppm (δ) with reference to the internal standard TMS. The signals were designated as follows:

s, singlet; d, doublet; dd, doublet of doublets; t, triplet; m, multiplet. Elemental analyses were carried out on Elementar Vario MICRO CUBE CHN Analyser. Purity of compounds were analysed by SHIMADZU HPLC system.

4.2.1 Scheme-1: Synthesis of 1-(1-(2-Methylquinolin-4-yl) 32iperidine-4-yl) -3-phenylurea /thiourea derivatives

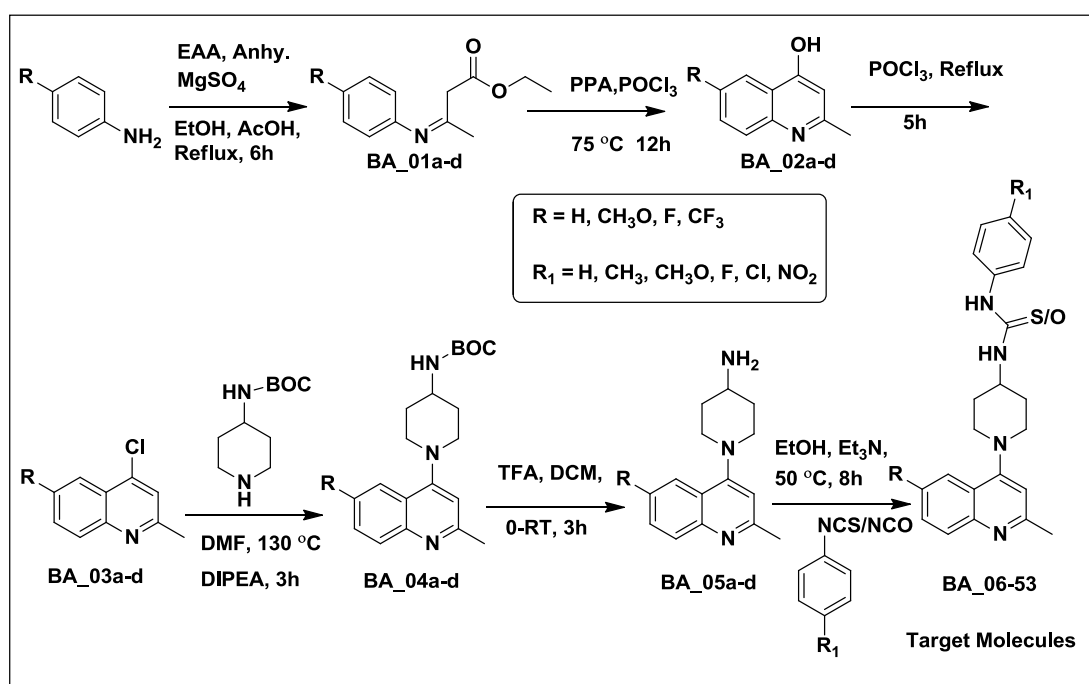


Figure 4.5: Synthetic scheme utilized for synthesis of 1-(1-(2-methylquinolin-4-yl) 32iperidine-4-yl) -3-phenylurea /thiourea derivatives

4.2.2 Scheme-2: Synthesis of 1-(4-substituted phenyl)-3-(6-substituted-(2-methylquinolin-4-yl)amino)phenyl thiourea/urea derivatives

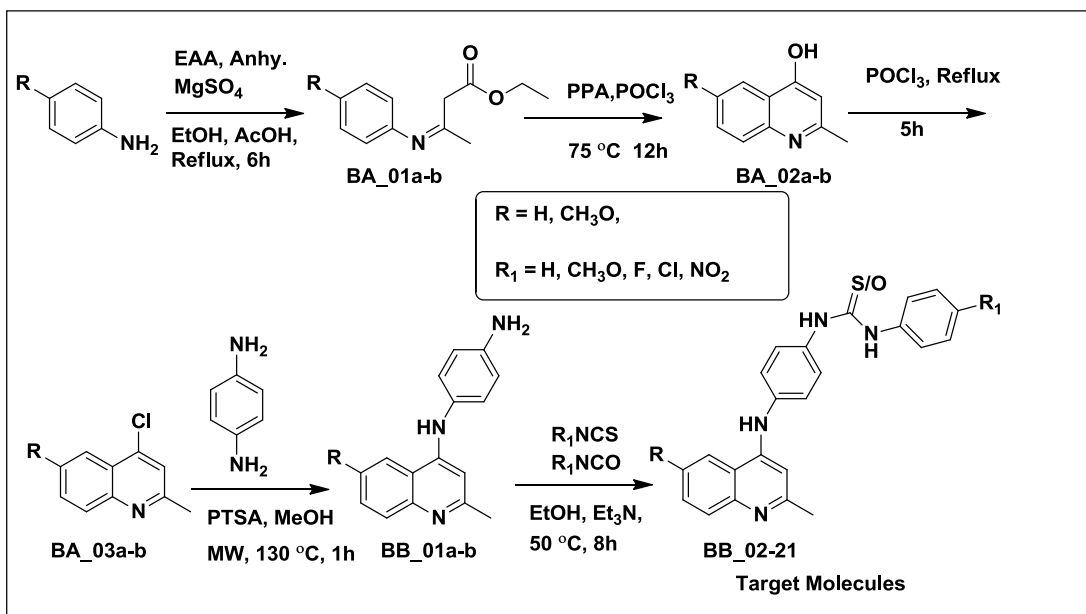


Figure 4.6: Synthetic scheme utilized for synthesis of 1-(4-substituted phenyl)-3-(6-substituted-(2-methylquinolin-4-yl)amino)phenyl thiourea/urea derivatives

4.2.3 Scheme-3: Synthetic protocol for the entitled substituted N-[4-(substituted-9-acridinyl amino) phenyl sulphonamide, urea/thiourea derivatives

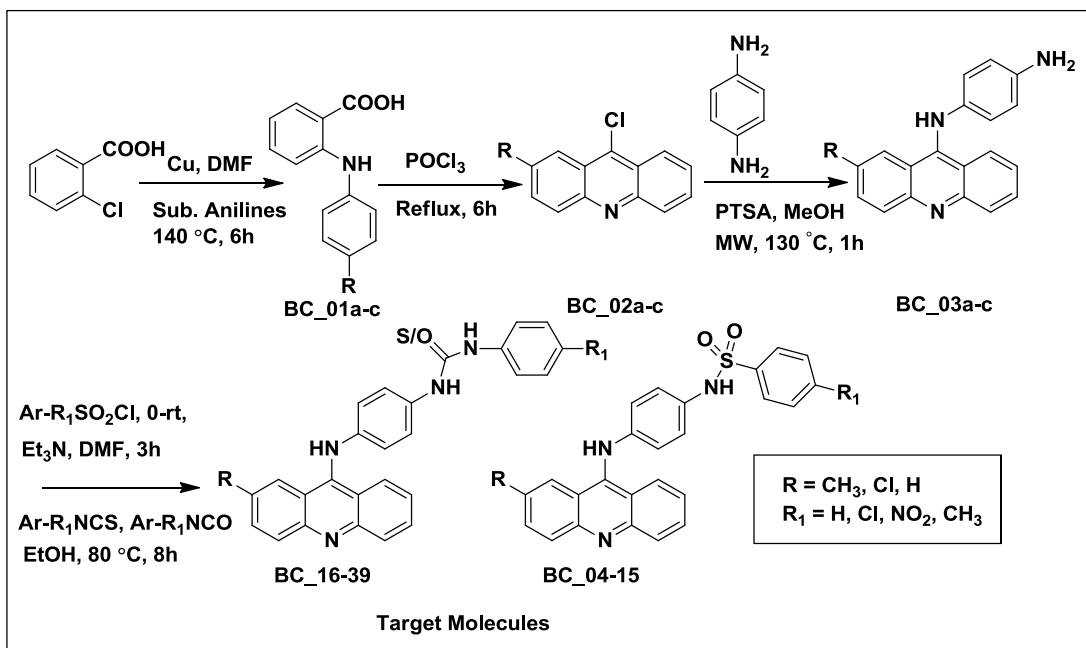


Figure 4.7: The protocol utilized for the synthesis of compounds, scheme-3

4.2.4 Scheme-4: Synthesis of phenyl-amino-quinoline derivatives

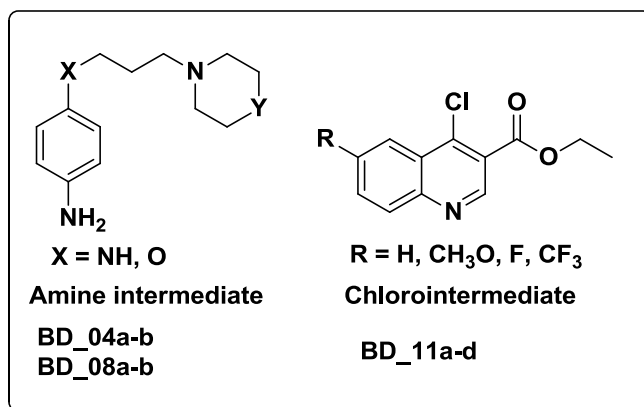


Figure 4.8: The two synthons utilized for the synthesis of phenyl-amino-quinoline derivatives

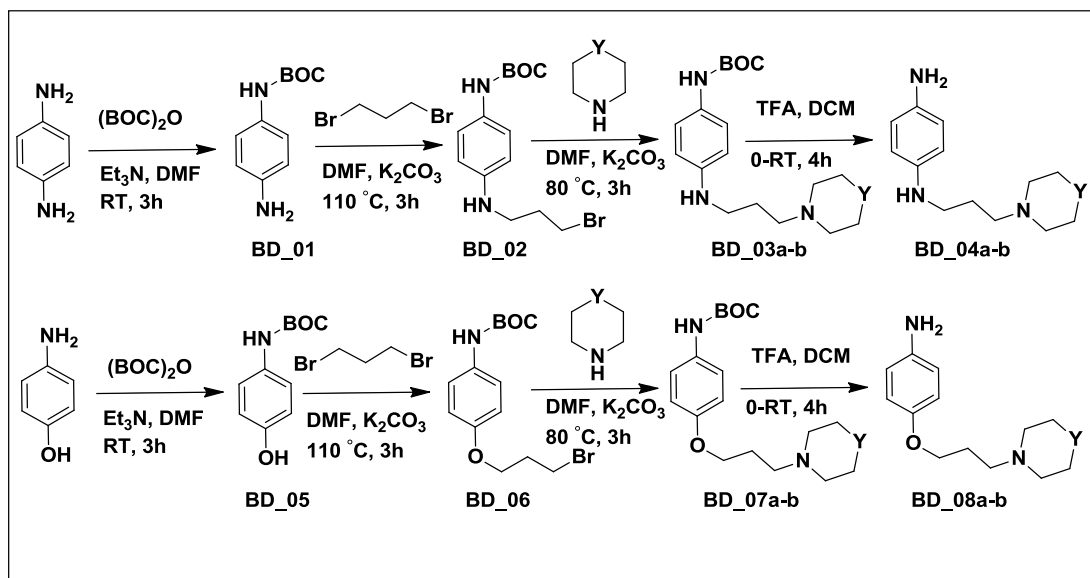


Figure 4.9: Synthetic protocol utilized to achieve the phenyl amine intermediates

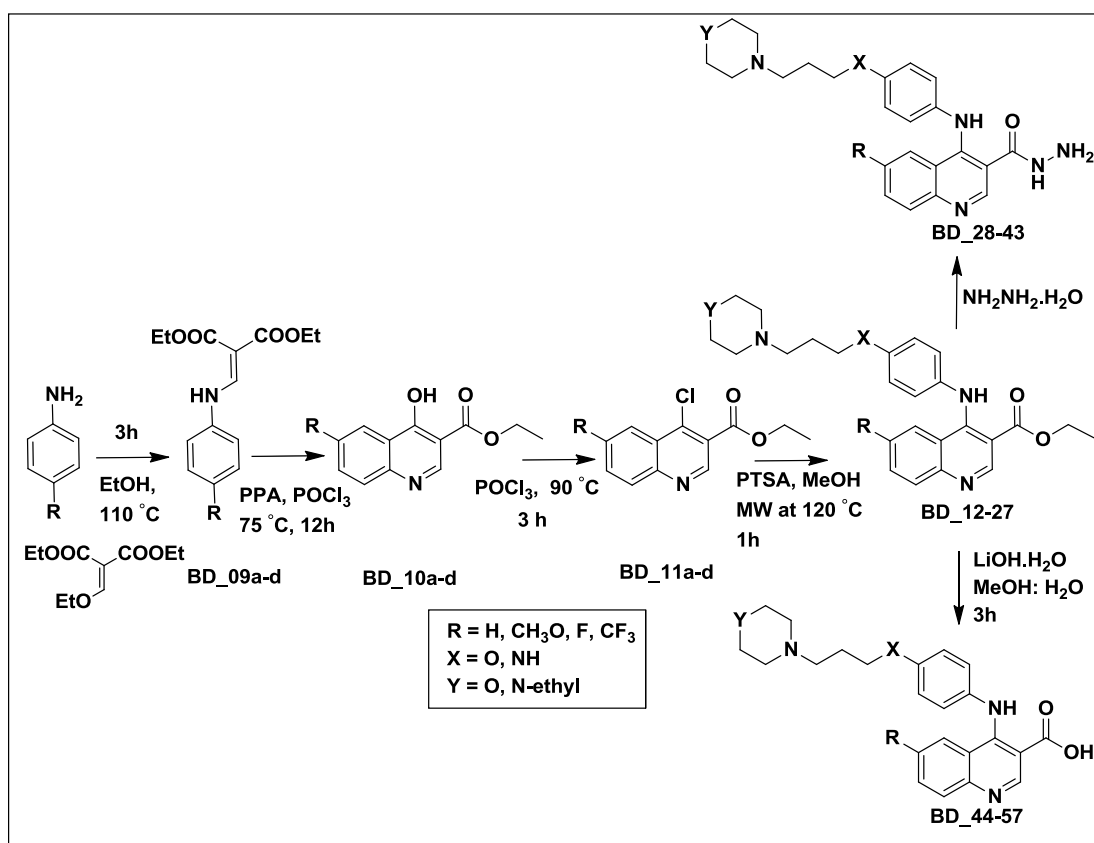


Figure 4.10: Synthetic procedure utilized for the preparation of entitied phenyl-amino-quinoline derivatives

4.2.5 Scheme-5: Synthesis of substituted 4-((1-quinolin-4-yl)-1H-1,2,3-triazol-4-yl)-2-phenyl thiazole derivatives

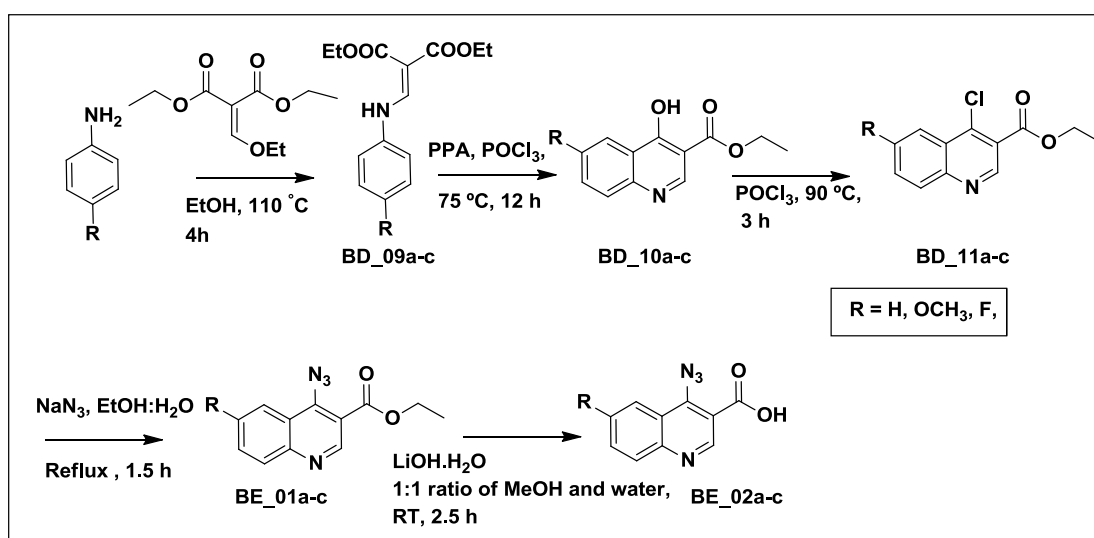


Figure 4.11: Synthetic protocol for the preparation of intermediates

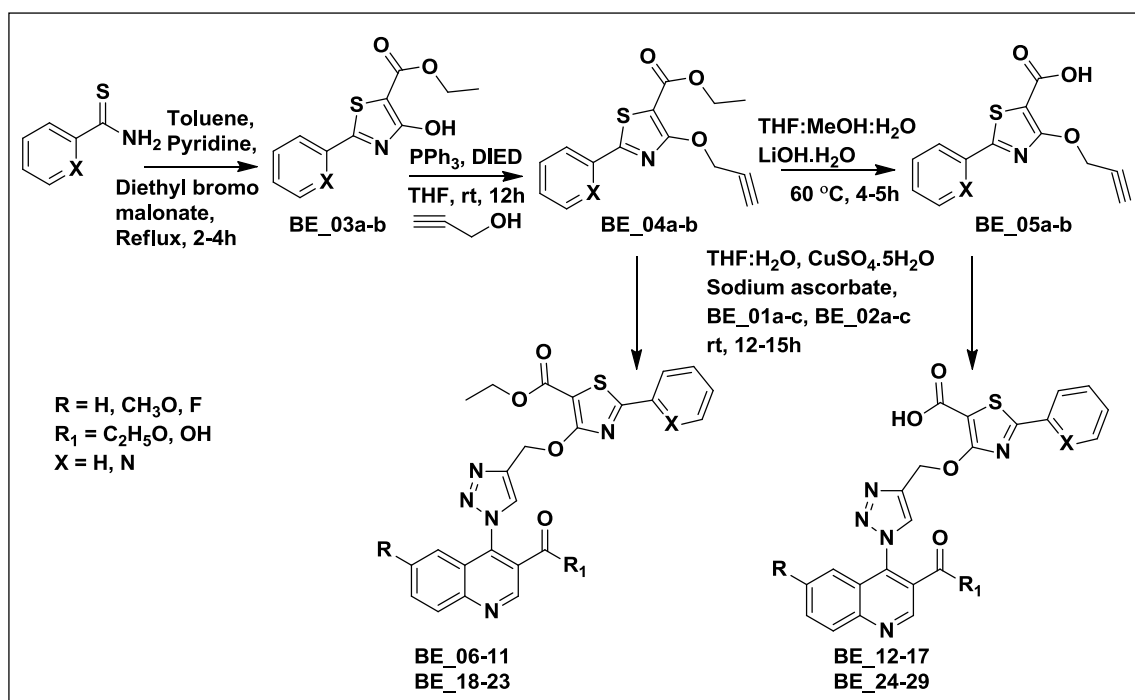


Figure 4.12: Synthetic protocol utilized to achieve the titled substituted 4-((1-quinolin-4-yl)-1H-1,2,3-triazol-4-yl)-2-phenyl thiazole derivatives

4.3 Biological screening of synthesized inhibitors

4.3.1 *Mycobacterium smegmatis* (*Msm*) DNA Gyr B cloning, protein expression and purification

The vectors used for cloning and expression were from Qiagen, while the primers were from Sigma-aldrich and all the enzymes unless otherwise mentioned were from New England Biolabs. Cloning of *Msm* DNA Gyr B was performed by amplifying the gene from mc2155 host strains genomic DNA using the specific forward and reverse primers and the desired restriction enzymes 5' CACCCATATGGTGGCTGCCAAGAACA 3' (NdeI), and 5' AGCTAAGCTTTTAAACATCCAGGAAGCGAA 3' (Hind III) respectively for about 35 cycles reaction (Jeankumar V. U., *et al.*, 2013). The digested products were ligated at the same site of the pQE2 vector, downstream of the T5 promoter with an N-terminal His tag, the clone was later authenticated by sequencing using a DNA sequencer. Final clones after confirmation were transformed into BL21 (DE3) pLysS cells of *E. coli* as they possess a better compatibility. Transformants were grown in

Luria Bertani (LB) broth (Himedia) at 37 °C shaking (rpm 140), in the presence of an antibiotic ampicillin (100 µg/mL) (Sigma-aldrich) until the starting optical density of 0.1 reached the value of 0.4–0.6 when measured in a cuvette. The protein expression was induced with 0.2 mM IPTG (Himedia) in the growing culture and further grown overnight for induction of the protein, at 18 °C. Further, on the following day cells were harvested by centrifugation at 5500 rpm (4 °C, 15 minutes) and suspended in lysis buffer containing 20 mM Tris-HCl (pH 7.4), 0.1 M NaCl, 2 mM KCl, 1.3 mM K₂HPO₄, 10 mM Na₂HPO₄, 5% Glycerol, 1 mM DTT, 1:200 µL protease inhibitor cocktail (Sigma-aldrich). The mixture was subjected to sonication (amplitude 35%, 1 s on 2 s off for 6 minutes) and was centrifuged at 12000 rpm (4 °C, 20 minutes). To the supernatant, pre-equilibrated Ni-NTA beads (GE) were mixed and swirled for an hour in cold room, centrifuged at 500 rpm for 5 minutes at 4 °C twice, later the pellets were redissolved in lysis buffer and loaded onto the Bio-Rad column, each loaded fraction was washed with 50 mL Tris-HCl (pH ~ 7.4), 500 mM NaCl, 2 mM KCl, 1.3 mM K₂HPO₄, 10 mM Na₂HPO₄, 5% Glycerol, 1 mM DTT. Protein was eluted with 25 mM Tris-HCl (pH 8), 140 mM NaCl, 5% Glycerol, 1 mM DTT, and 1 mM PMSF. Initial wash was done with elution buffer without imidazole. Subsequently, elution was carried out with various imidazole concentration gradients from 5 mM to 500 mM. Samples were collected in autoclaved 2 mL eppendorf tubes. Dialysis was performed 4 times overnight, against (25mM Tris-HCl pH ~ 7.4, 140 mM NaCl, 2 mM dithiothreitol, 15% glycerol, 1 mM EDTA), and dialyzed protein was concentrated at (4,500 rpm, 4 °C) to a final concentration of 2 mg/mL. The purity of the protein was analysed by SDS-PAGE. A 25 µL volume of the dialyzed protein was applied on the polyacrylamide gel (1 mm, 10%), and 10 µL of a commercially available pre-stained multi-coloured protein molecular weight marker (Genetix) was added. The electrophoresis was run in 1X TBE buffer (Tris-HCl pH ~ 7.5, 1 mM boric acid, 1 mM EDTA) for a period of 90 minutes at a constant voltage. Later the gel was transferred to a solution of coomassie Brilliant Blue dye mixed with 20% acetic acid. After 20 minutes of shaking in an orbital shaker, it was destained several times with 10% acetic acid in 30% methanol and 60% of water until the staining is lost and transparency of the gel was achieved. Subsequently, the purity of the protein was determined to be >85% as only single bands corresponding to its molecular weight 72 kDa was observed.

4.3.2 *In vitro* Msm Gyr B assay for the determination of IC₅₀

The *in vitro* ATPase assay was performed by *Msm* DNA Gyr B subunit. As the assay does not involve any substrate it is called as DNA independent assay. Gyr B being a catalytic domain undergoes the ATPase assay, resulting in hydrolysis of ATP and in energy generation. This assay was performed similar to previously reported method. It was performed in 30 μ L reaction volume for 100 minutes at 25°C in reaction buffer containing 60 mM HEPES-KOH (pH ~ 7.7), 200 mM KCl, 250 mM potassium glutamate, 2 mM MgCl₂, 1 mM DTT, 2% Glycerol, 4% DMSO, 0.001% BriJ-35, 0.65 mM ATP, 40 nM Gyr B. The protein undergoes the ATPase assay, resulting in hydrolysis of ATP. The assay was performed in 96 well flat-bottomed plates (polystyrene untreated). Desired drug concentrations of the compounds were aliquoted in the assay well, followed by 6 μ L of 5X assay buffer mixed with substrate along with 1 μ L of enzyme and the reaction volume was made to 30 μ L. The contents were added and incubated in the above sequential order as it was of importance for the binding and interaction of the protein consequently the enzyme reaction was initiated by adding 14 μ L of MgCl₂ solution. The reaction was allowed to proceed for about 100 minutes at room temperature without shaking. Subsequently, the reaction was quenched by adding 20 μ L malachite green reagent (Bioassay systems, USA). Inorganic phosphates (Pi) released during the reaction were read at 620 nm after 20 minutes incubation.

4.3.3 *In vitro* Mtb DNA gyrase supercoiling assay

DNA supercoiling assay was performed using gyrase of *Mtb* DNA gyrase. The assay was performed using the commercially available kit (DNA gyrase supercoiling assay kit: MTS001) from Inspiralis limited, Norwich, UK. The assay was carried out in a 1.5 mL eppendorf tubes at room temperature (Jeankumar V. U., *et al.*, 2013). Usually 1U of *Mtb* DNA gyrase was incubated with 0.5 μ g of relaxed pBR 322 DNA (substrate) in 30 μ L reaction volume at 37 °C, 30 minutes in 40 mM HEPES. KOH (pH ~ 7.6), 10 mM magnesium acetate, 10 mM DTT, 2 mM ATP, 500 mM potassium glutamate, 0.05 mg/mL albumin (BSA). Novobiocin was used as a positive control and 4% DMSO was considered for negative control. DNA gyrase supercoils the relaxed pBR 322 effectively resulting in a denser supercoiled DNA. Subsequently, each reaction was stopped by addition of 30 μ L of stop dye [40% sucrose, 100 mM

Tris-HCl (pH ~ 7.5), 1 mM EDTA and 0.5 mg/mL bromophenol blue], followed by a brisk centrifugation for 45 sec and was run in 1% agarose gel in 1X TAE buffer (40 mM Tris acetate, 2 mM EDTA) (Jeankumar V. U., *et al.*, 2014). Furthermore, concentration of the range of compounds that inhibits 50% of supercoiling activity IC_{50} of the enzyme was determined using densitometer and NIH image through Bio-Rad GelDoc image viewer.

4.3.4 *In vitro* Mtb LAT (Lysine aminotransferase) assay

Mtb LAT enzymatic assay was performed in 100 μ L volume containing 200 mM phosphate buffer (p^H 7.2), 1.5 mM L-Lysine, 1.5 mM α -ketoglutarate, 15 μ M pyridoxal 5-phosphate with various concentration of *Mtb* LAT for 1 hrs at 37 °C. Reactions were terminated by adding 10% trichloroacetic acid in ethanol. The *Mtb* LAT activity was monitored and the end product was detected at an absorbance of 465 nm and 280 nm. To determine the kinetic parameter K_m and V_{max} , either L-Lysine or α -ketoglutarate was varied keeping the other substrate constant at 1 mM. Concentration of LAT enzyme was determined based on the range finding experiments. The reactions were performed same as enzymatic assay described and the K_m and V_{max} were obtained using non-linear regression analysis using GraphPad prism software (Jagtap P. K., *et al.*, 2012).

4.3.5 *In vitro* Mtb MABA assay for MIC determination

MABA assay was performed to check the MIC of the *Mtb* bacteria. In brief, the inoculum was prepared from fresh LJ medium resuspended in 7H9 medium (7H9 broth, 0.1% casitone, 0.5% glycerol, supplemented oleic acid, albumin, dextrose, and catalase – OADC), subsequently, adjusted to a McFarland tube No.1, and diluted 1:20; 100 μ L was used as inoculum. Each drug stock solution was thawed and diluted in 7H9-S at four-fold the final highest concentration tested (Jeankumar V. U., *et al.*, 2013; Jeankumar V. U., *et al.*, 2014). Serial two-fold dilutions of each drug were prepared directly in a sterile 96-well microtiter plate using 100 μ L 7H9-S. A growth control containing no antibiotic and a sterile control were also prepared on each plate. Sterile water was added to all perimeter wells to avoid evaporation during the incubation. The plate was covered, sealed in plastic bags and incubated at 37 °C in normal atmosphere. After 7 days of incubation, 30 μ L of alamar blue solution was

added to each well, and the plate was re-incubated overnight. A change in colour from blue (oxidized state) to pink (reduced) indicated the growth of bacteria, and the MIC was defined as the lowest concentration of drug that prevented this change in colour.

4.4 Evaluation of protein-inhibitor binding affinity using biophysical characterization (DSF)

The most active compounds were further investigated using a biophysical technique, differential scanning fluorimetry (DSF). The ability of the compound to stabilize the *Msm* Gyr B protein was assessed utilizing this technique by measuring fluorescence of the native protein and the protein-ligand complexes in the presence of a fluorescent dye SYPRO-orange whose fluorescence was increased when exposed to non-polar residues of the protein and reached a maximum when the protein denatured as it happened to bind with maximum number of residues in uncoiled state (Pushkar K., *et al.*, 2014). Complex with compound was heated stepwise from 25 to 95 °C in steps of 0.1°C in the presence of the fluorescent dye, whose fluorescence increased as it interacted with protein. A right side positive shift of T_m in comparison to native protein meant higher stabilization of the protein-ligand complex, which was a consequence of the inhibitor binding profile.

4.5 Cell cytotoxicity studies by MTT assay

As the *Mtb* organism targets the macrophage cell lines, the toxicity studies were performed in the RAW cell lines. Cytotoxic safety profiling of all the test compounds was done on RAW 264.7 mouse leukemic monocyte macrophage cell line from ATCC (Jeankumar V. U., *et al.*, 2014). Briefly, RAW 264.7 cells were seeded at 6000 cells per well in a 96-well microtiter plate (NEST) in Roswell Park Memorial Institute (RPMI-1640) media. After 24 h incubation, the cells were washed with PBS and 2-fold dilutions of the drug was made in 200 µL of standard culture media (RPMI + 5% FBS + 1% penicillin and streptomycin) was added, while the final DMSO concentration of the culture was limited to 0.5%. Furthermore, the cells were incubated with a drug concentration of 100 µM at 37 °C in 5% CO₂/95% air for 72 h to analyse the toxicity levels. Untreated cells with 0.5% DMSO were included as controls. The viability of the cells were assessed on the basis of cellular conversion of the dye MTT (3-(4, 5-dimethylthiazol-2-yl)-2,5-diphenyl-2H-tetrazolium bromide)

into formazan crystals using Perkin Elmer Victor X3 Titre 96 plate reader at 590 and 620 nm. Ciprofloxacin (3% inhibition) and novobiocin (9.8% inhibition) were used as standards in this assay. The percentage inhibition was calculated from the following formula:

$$\text{Percentage inhibition} = \frac{100 - \text{mean OD sample}}{\text{mean OD day 0}}$$

4.6 *In vitro* zERG channel inhibition screening

The most potent compounds were evaluated for zERG toxicity inhibition by assessing arrhythmogenic potential on Zebrafish ether-a-go-go-related gene (zERG) which was orthologous to the human ether-a-go-go-related gene (hERG). Zebrafish acquired commercially were maintained as described earlier (Pushkar K., *et al.*, 2014; Rakesh Kumar B., *et al.*, 2013). In brief, zebrafish were maintained in the recirculatory system with 14 h light and 10 h dark cycles, with 28°C as optimum temperature. Breeding, embryo collection and drug exposure was carried out as described previously. Briefly, breeding was carried out using 2 females: 3 males in a separate breeding cage. Embryos were collected into petridishes containing E3 medium and incubated at 28°C temperature. Three day post fertilized embryos were used for screening cardiotoxic potential of test drugs. The embryos were segregated and washed and distributed in 24-well plate i.e. six embryos with 250 µL of 0.1% DMSO per well. Stock solution of the drug was prepared in 100% DMSO and the 2X working concentrations were prepared accordingly by serial dilutions. Each well was then added with 250 µL of 2X working concentration and embryos were allowed to incubate at the optimum temperature for 4 h. After 4 h of incubation, the respective drug concentration exposed embryos were treated with tricaine and the heart rate was measured. The time taken for 30 atrial and ventricular beats was measured for each embryo, from which number of heart beats per minute was calculated by using the formula $1800/X = \text{beats /minute}$ (where X = time in seconds) (Ram Shankar U., *et al.*, 2010). The most active compounds were exposed from 1 µM to 30 µM concentrations with 0.1% DMSO as vehicle. All the statistical analysis was done using GraphPad Prism® software applying one way ANOVA and Dunnet's post test.

4.7 Molecular docking studies

All computations were carried out on an Intel Core 2 Duo 63 E7400 2.80 GHz capacity processor with memory of 2 GB RAM 64 running with the RHEL 5.2 operating system. The synthesized compounds which were active in Gyr B as well as in supercoiling assay were docked onto the active pocket of the Gyr B ATPase domain of *M. smegmatis* retrieved from protein data bank (PDB ID: 4B6C). The protein was initially processed using the Protein Preparation Wizard of Schrödinger Suite 2012. The optimization of the hydrogen-bonding network and the ligands to be docked were sketched in Maestro panel of Schrödinger and optimized with OPLS force field. The virtual screening options for HTVS (High Throughput Virtual Screening), SP (Standard Precision) and Glide XP (extra precision) docking were all checked to be executed. Glide XP (extra precision) module of Schrödinger 9.3 (Maestro version 9.3, Glide version 5.7, Schrödinger, LLC, New York, NY, 81 2012) was utilized for docking.

Quinoline based analogues gained importance for the development of newer, safer and effective antitubercular agents and recently US FDA approved bedaquiline drug for MDR-TB which consists quinoline as one of the basic pharmacophores. The present study target of interest is to develop novel quinoline based new DNA gyrase inhibitors, DNA gyrase which is well established and validated target to develop new inhibitors. Consequently, inhibitors targeting DNA gyrase would be promising candidates for development of new anti-tubercular agents. Thus in present study we focus on achieving promising mycobacterial cellular potency through developing potential *Mtb* DNA gyrase inhibitors.

5.1 Development of 1-(1-(2-Methylquinolin-4-yl) 4-piperidine-4-yl) -3-phenylurea /thiourea derivatives as potential *Mtb* DNA gyrase B inhibitors

Molecular hybridization/Molecular hopping is a well-known strategy and employed to design novel inhibitors. In this strategy molecular fusion/hybridization of two or more pharmacophoric subunits from the previously reported ligands/prototypes leading to molecular structures of possessing an inhibitory profile/potency against the targeted enzyme/disease was explored (Maia R., *et al.*, 2010; Fraga C. A. M., *et al.*, 2009; Lazar C., *et al.*, 2004). Subsequently, the designed new lead molecule formed with two or more potent moieties resulted in having more chances to improved affinity/specificity towards the target protein, along with increased efficacy than the parent compounds. In this study we utilized chemical structures of previously reported anti-tubercular Quinoline bearing (left hand side-LHS) derivatives and on the other side *Mtb* DNA gyrase inhibitor bearing different aryl systems on right hand side (RHS) resulted in designed new hybrid scaffold through molecular hopping with the linker as shown in **Figure 5.1**.

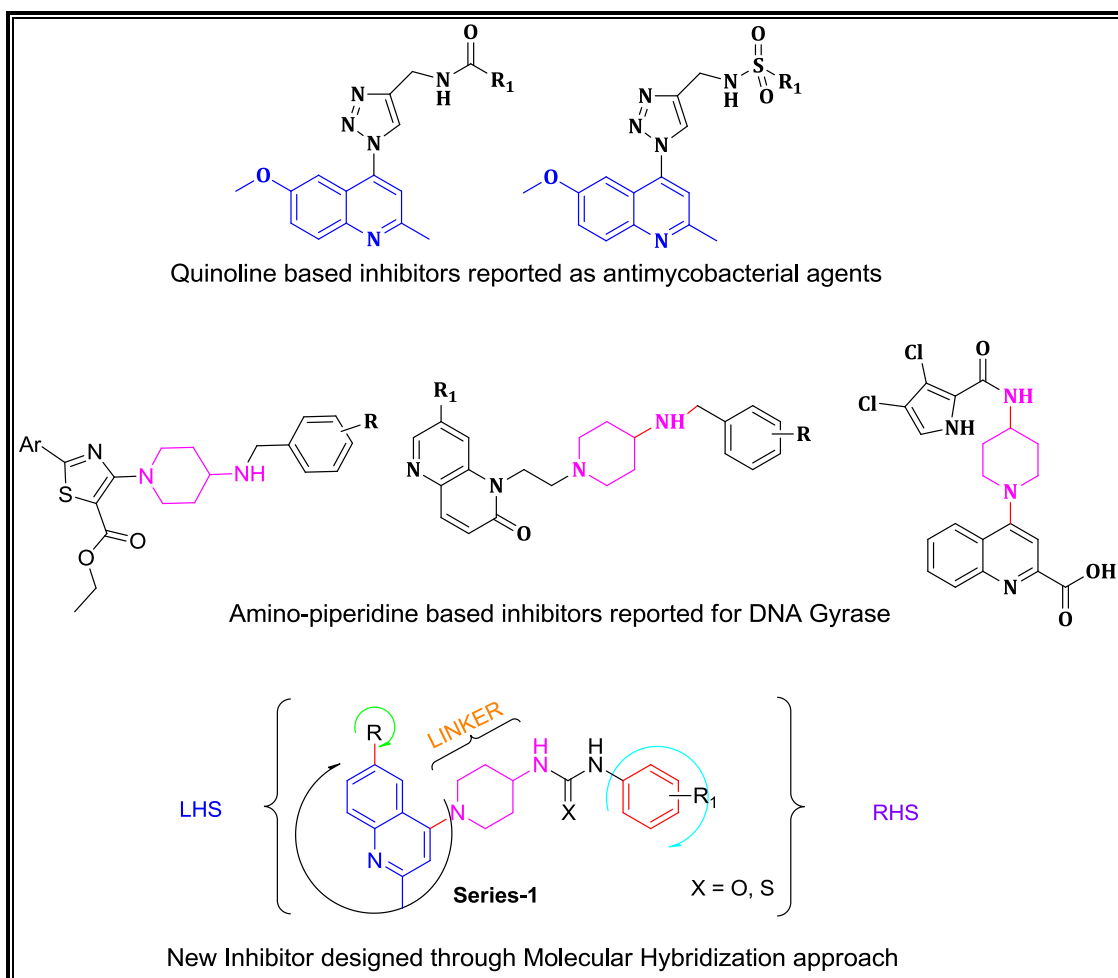


Figure 5.1: Design strategy used for the development of novel quinoline based DNA gyrase B inhibitor

The major aim of designing the hybrid architecture was to develop compounds with improved potency towards the target than the parent lead and lower the side effects. Many scientists have explored hybrid design of newer analogues as potential candidates for biological evaluation. N-linked 4-aminopiperidine derivatives were already reported as DNA gyrase inhibitors (Bax B. D., *et al.*, 2010; Geng B., *et al.*, 2011) and the concept of molecular hybridization was implemented successfully in our previous work with this template (Santhosh Reddy P., *et al.*, 2012; Yempala T., *et al.*, 2012; Jeankumar V. U., *et al.*, 2013). In continuation to our efforts, we further attempted to design novel *Mtb* gyrase inhibitors by hybridizing aminopiperidine linker to quinoline core to give a desired hybrid. Thus designed ligands possessed three pharmacophoric units, an aminopiperidine as a linker stacked between a left quinoline core and a substituted aryl moiety at the right side as shown in **Figure 5.1**. There are

many reports on quinoline based antimycobacterials and hence utilized in this study as a left hand core (Thomas K. D., *et al.*, 2011). Further, the selection of right hand substituent was purely based on the structure-activity relationship (SAR) inputs from a previous GSK report (Barros, D., 40th Union world conference on Lung health, Cancun. 2009) wherein the most potent analogues possessed methoxy, fluoro, nitro, methyl and chloro substituted aryl rings on the right hand side, and hence we retained these analogues as such for derivation of SAR and lead optimization in the present study.

5.1.1 Chemical synthesis and characterization

The synthetic pathway utilized to achieve the target compounds has been delineated in **Figure 4.1**. Synthesis of the target compounds started with conversion of commercially available substituted anilines to Ethyl 3-(phenyl/4-methoxy/4-fluoro/4-trifluoroimino) butanoates (**BA_01a-d**) were synthesized as intermediates by treating with ethylacetoacetate (EAA) in presence of magnesium sulfate in ethanol at 90 °C. The intermediate (**BA_01a-d**) was then converted to corresponding substituted 4-hydroxyquinoline (**BA_02a-d**) by heating it at 75 °C with polyphosphoric acid and phosphorous oxy-chloride (catalytic) for 8h. The required key intermediate *tert*-butyl (6-substituted -2-methylquinolin-4-yl)45iperidine-4-yl) carbamates (**BA_04a-d**) were obtained by heating (**BA_02a-d**) with phosphorous oxy-chloride, followed by heating the chloro derivative (**BA_03a-d**) with *N,N*-diisopropylethylamine (DIPEA) and 4-*N*-Boc aminopiperidine in *N,N*-dimethylformamide (DMF) as solvent at 130 °C for 3h under N₂↑ atmosphere. The final library of 48 compounds (**BA_06-53**) were obtained by sequential Boc-deprotection of intermediate **BA_04a-d** with trifluoroacetic acid to get amine intermediate (**BA_05a-d**) and followed by reacting with different substituted aryl isocyanates/iso-thiocyanates in presence of triethylamine (Et₃N) in ethanol heating at 55 °C for 8h with good yields and purity.

5.1.2 Experimental protocol followed for synthesis

General procedure for synthesis of ethyl 3-(phenyl/4-methoxy/4-fluoro/4-trifluoroimino) butanoate (BA_01a-d): A mixture of corresponding substituted anilines (35 mmol), ethylacetoacetate (38.5 mmol), anhydrous magnesium sulphate (42 mmol) and catalytic amount of acetic acid (0.5-1 mL) in ethanol (EtOH) (250 mL)

was refluxed for 4 h and TLC analysis indicated that the reaction was complete (Thomas K. D., *et al.*, 2010). The reaction mass was filtered and evaporated under reduced pressure to afford a brown liquid which was further purified by flash column chromatography using silica gel (230-400 mesh) with ethyl acetate: hexane as eluent to afford corresponding desired product in good yield. The physicochemical properties of synthesized derivatives are shown in **Table 5.1**.

General procedure for synthesis of unsubstituted/6-methoxy/6-fluoro/6-trifluoro-2-methylquinolin-4-ol (BA_02a-d): Polyphosphoric acid (PPA) (45 mmol) was added to the corresponding step 1 intermediate (BA_01a-d) (30 mmol) and phosphorous oxy-chloride (POCl₃) (8.57 mmol). The mixture was heated to 75 °C for 8 h, and TLC analysis indicated that the reaction was complete (Ram Shankar U., *et al.*, 2010). The reaction mixture was quenched slowly with 10 % sodium hydroxide solution by keeping it in ice bath adjusted to pH~7, and the solid was filtered then dried and washed with diethyl ether (3*20 mL) to afford as an off-white solid.

General procedure for synthesis of 4-Chloro-6-unsustituted/6-methoxy/6-fluoro / 6-trifloromethyl-2-methylquinoline (BA_03a-d): To the corresponding intermediate obtained in step 2 (BA_02a-d) (25 mmol), POCl₃ (125 mmol) was added slowly and refluxed for 3 h at 105 °C (Thomas K. D., *et al.*, 2010). TLC analysis indicated that the reaction was completed. Excess POCl₃ was removed under reduced pressure and the crude reaction mass was quenched into crushed ice then neutralized with saturated sodium bicarbonate solution (100 mL) and extracted with ethyl acetate (3*100 mL). The organic layer was dried under anhydrous sodium sulphate (anhy. Na₂SO₄) filtered and evaporated under reduced pressure to get corresponding desired product as a liquid/solid.

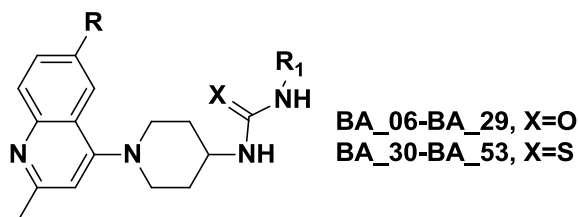
General procedure for synthesis of tert-butyl (1-(unsubstituted/6-methoxy/6-fluoro/6-trifluoromethyl-2-methylquinolin-4-yl) piperidin-4-yl)carbamate (BA_04a-d): 4-*N*-Boc-aminopiperidine (20 mmol) was added to a stirred solution of intermediate (BA_03a-d) (20 mmol) and *N,N*- diisopropyl ethylamine (50 mmol) in *N,N*-dimethyl formamide (DMF) (20 mL) under nitrogen atmosphere which were heated to 130 °C for 2 h. TLC analysis indicated that the reaction was completed. DMF was removed under reduced pressure and to the crude solution crushed ice was added and extracted with (3*60 mL) ethyl acetate. The combined organic layer was

washed with brine (100 mL) and dried over anhy.Na₂SO₄, filtered and evaporated under reduced pressure to get crude solid. The crude solid was further purified by flash column chromatography using silica gel (100-200 mesh) using ethyl acetate: hexane as eluent to afford desired product in good yield.

General procedure for synthesis of 1-(unsubstituted/6-methoxy/6-fluoro/6-trifluoromethyl-2-methylquinolin-4-yl) piperidin-4-amine (BA_05a-d): Trifluoroacetic acid (TFA) (24 mmol) was slowly added to step 4 intermediate (BA_04a-d) (8 mmol) in dichloromethane (DCM) (20 mL) at 0 °C and allowed to stir at room temperature for 2.5 h. TLC analysis indicated that the reaction was completed. Excess TFA was removed under reduced pressure and the crude was diluted with DCM (60 mL). Organic layer was washed with 10% sodium hydroxide solution (2*10 mL) and was dried over anhydrous Na₂SO₄, filtered and evaporated under reduced pressure to get the corresponding desired product which was immediately continued to next step without any purification.



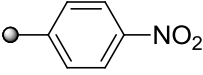
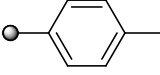
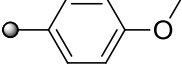
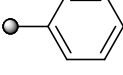
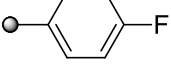
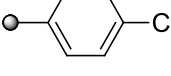
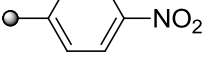
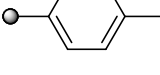
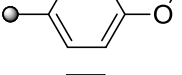
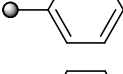
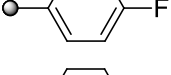
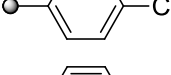
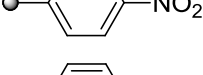
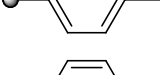
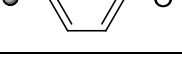
General procedure for preparation of urea/thiourea derivatives of 1-(unsubstituted/6-methoxy/6-fluoro/6-trifluoromethyl-2-methylquinolin-4-yl) piperidin-4-amine (BA_06-BA_053): To a stirred solution of step 5 intermediate (BA_05a-d) (0.6 mmol), tri-ethylamine (0.6 mmol) in ethanol (5 mL), was added the corresponding aryl/hetero aryl isocyanate / isothiocyanate (0.66 mmol) and the resulting reaction mass was heated to 50 °C for 8 h. TLC analysis indicated that the reaction was completed. Ethanol was removed under reduced pressure, and the crude reaction mass was diluted with ethyl acetate (8 mL) and washed with brine (2*4 mL). Organic layer was dried over anhydrous Na₂SO₄, evaporated under reduced pressure to get the corresponding urea/thiourea derivative. The crude residue was further purified by flash column chromatography with silica gel (100-200 mesh) using ethyl acetate: hexane as eluent to get the title compounds. The physicochemical properties of synthesized derivatives as shown in **Table 5.1**

Table 5.1: Physicochemical properties of synthesized compounds **BA_06 – BA_29** and **BA_30 – BA_53**.

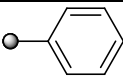
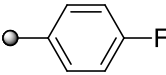
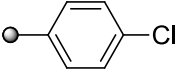
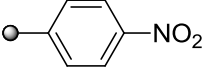
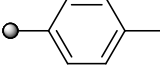
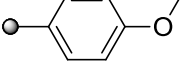
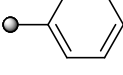
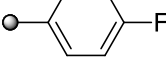
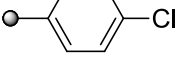
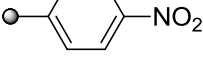
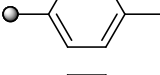
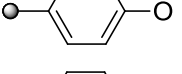
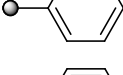
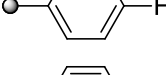
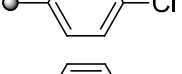
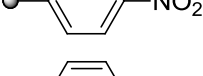
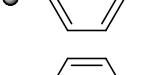
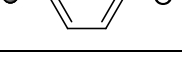


Comp	R	R ₁	Yield (%)	Melting point (°C)	Molecular formula	Molecular weight
BA_06	H		75	196-198	C ₂₂ H ₂₄ N ₄ O	360.20
BA_07	H		70	163-164	C ₂₂ H ₂₃ FN ₄ O	378.19
BA_08	H		71	175-176	C ₂₂ H ₂₃ ClN ₄ O	394.16
BA_09	H		73	166-168	C ₂₂ H ₂₃ N ₅ O ₃	405.18
BA_10	H		70	171-172	C ₂₃ H ₂₆ N ₄ O	374.21
BA_11	H		70	118-120	C ₂₃ H ₂₆ N ₄ O ₂	390.21
BA_12	OCH ₃		72	190-192	C ₂₃ H ₂₆ N ₄ O ₂	390.21
BA_13	OCH ₃		75	215-216	C ₂₃ H ₂₅ FN ₄ O ₂	408.47
BA_14	OCH ₃		79	226-227	C ₂₃ H ₂₅ ClN ₄ O ₂	424.17
BA_15	OCH ₃		69	132-133	C ₂₃ H ₂₅ N ₅ O ₄	435.19
BA_16	OCH ₃		72	236-237	C ₂₄ H ₂₈ N ₄ O ₂	404.22
BA_17	OCH ₃		85	170-172	C ₂₄ H ₂₈ N ₄ O ₃	420.22
BA_18	F		75	215-216	C ₂₂ H ₂₃ FN ₄ O	378.19

Conti....

Comp	R	R ₁	Yield (%)	Melting point (°C)	Molecular formula	Molecular weight
BA_19	F		73	198-199	C ₂₂ H ₂₂ F ₂ N ₄ O	396.18
BA_20	F		79	230-231	C ₂₂ H ₂₂ ClFN ₄ O	412.15
BA_21	F		71	177-178	C ₂₂ H ₂₂ FN ₅ O ₃	423.17
BA_22	F		76	206-207	C ₂₃ H ₂₅ FN ₄ O	392.20
BA_23	F		80	243-245	C ₂₃ H ₂₅ FN ₄ O ₂	408.20
BA_24	CF ₃		75	197-198	C ₂₃ H ₂₃ F ₃ N ₄ O	428.18
BA_25	CF ₃		77	185-186	C ₂₃ H ₂₂ F ₄ N ₄ O	446.17
BA_26	CF ₃		78	207-209	C ₂₃ H ₂₂ ClF ₃ N ₄ O	462.14
BA_27	CF ₃		76	179-180	C ₂₃ H ₂₂ F ₃ N ₅ O ₃	473.17
BA_28	CF ₃		77	203-205	C ₂₄ H ₂₅ F ₃ N ₄ O	442.20
BA_29	CF ₃		73	232-233	C ₂₄ H ₂₅ F ₃ N ₄ O ₂	458.19
BA_30	H		77	186-187	C ₂₂ H ₂₄ N ₄ S	376.17
BA_31	H		71	184-185	C ₂₂ H ₂₃ FN ₄ S	394.16
BA_32	H		78	162-163	C ₂₂ H ₂₃ ClN ₄ S	410.13
BA_33	H		75	154-155	C ₂₂ H ₂₃ N ₅ O ₂ S	421.16
BA_34	H		69	182-183	C ₂₃ H ₂₆ N ₄ S	390.19
BA_35	H		73	135-136	C ₂₃ H ₂₆ N ₄ OS	406.18

Conti....

Comp	R	R ₁	Yield (%)	Melting point (°C)	Molecular formula	Molecular weight
BA_36	OCH ₃		70	197-198	C ₂₃ H ₂₆ N ₄ OS	406.18
BA_37	OCH ₃		72	201-202	C ₂₃ H ₂₅ FN ₄ OS	424.17
BA_38	OCH ₃		78	133-134	C ₂₃ H ₂₅ ClN ₄ OS	440.14
BA_39	OCH ₃		71	179-180	C ₂₃ H ₂₅ N ₅ O ₃ S	451.17
BA_40	OCH ₃		70	185-186	C ₂₄ H ₂₈ N ₄ OS	420.20
BA_41	OCH ₃		75	184-185	C ₂₄ H ₂₈ N ₄ O ₂ S	436.19
BA_42	F		80	178-179	C ₂₂ H ₂₃ FN ₄ S	394.16
BA_43	F		70	228-229	C ₂₂ H ₂₂ F ₂ N ₄ S	412.15
BA_44	F		83	208-209	C ₂₂ H ₂₂ ClFN ₄ S	428.12
BA_45	F		75	146-147	C ₂₂ H ₂₂ FN ₅ O ₂ S	439.15
BA_46	F		73	123-124	C ₂₃ H ₂₅ FN ₄ S	408.18
BA_47	F		78	-	C ₂₃ H ₂₅ FN ₄ OS	424.17
BA_48	CF ₃		73	202-203	C ₂₃ H ₂₃ F ₃ N ₄ S	444.16
BA_49	CF ₃		73	196-198	C ₂₃ H ₂₂ F ₄ N ₄ S	462.15
BA_50	CF ₃		73	146-147	C ₂₃ H ₂₂ ClF ₃ N ₄ S	478.12
BA_51	CF ₃		73	187-188	C ₂₃ H ₂₂ F ₃ N ₅ O ₂ S	489.14
BA_52	CF ₃		73	192-194	C ₂₄ H ₂₅ F ₃ N ₄ S	458.18
BA_53	CF ₃		75	238-239	C ₂₄ H ₂₅ F ₃ N ₄ OS	474.17

5.1.3 Characterization of synthesized compounds

Ethyl 3-(phenylimino) butanoate (BA_01a): Brown liquid; Yield 77%; ESI-MS was found at m/z 206.21 (M+H)⁺. ¹H NMR (CDCl₃-300 MHz) δ_{H} . 7.45-6.98 (m, 5H), 4.64 (s, 2H), 4.14 (q, $J = 7.1$ Hz, 2H), 1.92 (s, 3H), 1.29 (t, $J = 7.2$ Hz, 3H).

Ethyl 3-((4-methoxyphenyl)imino)butanoate (BA_01b): Brown liquid; Yield 76%; ESI-MS was found at m/z 236.19 (M+H)⁺. ¹H NMR (CDCl₃-300 MHz) δ_{H} . 7.08-7.05 (d, $J = 8.4$ Hz, 2H), 6.88 (d, $J = 8.5$ Hz, 2H), 4.67 (s, 2H), 4.12 (q, $J = 7.3$ Hz, 2H), 3.80 (s, 3H), 1.9 (s, 3H), 1.29 (t, $J = 7.3$ Hz, 3H).

Ethyl 3-((4-fluorophenyl)imino)butanoate (BA_01c): Brown liquid; Yield 75%; ESI-MS was found at m/z 222.35 (M-H)⁻. ¹H NMR (CDCl₃-300 MHz) δ_{H} . 7.35 (d, $J = 8.5$ Hz, 2H), 6.87 (d, $J = 8.6$ Hz, 2H), 4.63 (s, 2H), 4.13 (q, $J = 7.3$ Hz, 2H), 1.89 (s, 3H), 1.28 (t, $J = 7.4$ Hz, 3H).

Ethyl 3-((4-(trifluoromethyl)phenyl)imino)butanoate (BA_01d): Brown liquid; Yield 79%; ESI-MS was found at m/z 274.77 (M+H)⁺. ¹H NMR (CDCl₃ - 300 MHz) δ_{H} . 7.69 (d, $J = 8.5$ Hz, 2H), 7.26 (d, $J = 8.6$ Hz, 2H), 4.64 (s, 2H), 4.14 (q, $J = 7.2$ Hz, 2H), 1.94 (s, 3H), 1.28 (t, $J = 7.4$ Hz, 3H).

2-Methylquinolin-4-ol (BA_02a): Off-white solid; Yield 72%, m.p. 198-199 °C; ESI-MS was found at m/z 160.21 (M+H)⁺. ¹H NMR (DMSO-d₆- 300 MHz) δ_{H} . 11.21 (brs, 1H), 7.67-7.48 (m, 4H), 5.88 (s, 1H), 2.35 (s, 3H).

6-Methoxy-2-methylquinolin-4-ol (BA_02b): Off-white solid; Yield 68%, m.p. 298-299 °C; ESI-MS was found at m/z 190.32 (M+H)⁺. ¹H NMR (DMSO-d₆- 300 MHz) δ_{H} . 11.42 (brs, 1H), 7.47-7.43 (m, 2H), 7.01-6.98 (m, 1H), 5.87 (s, 1H), 3.84 (s, 3H), 2.31 (s, 3H).

6-Fluoro-2-methylquinolin-4-ol (BA_02c): Off-white solid; Yield 70%, m.p. 273-274 °C; ESI-MS was found at m/z 178.20 (M+H)⁺. ¹H NMR (DMSO-d₆- 300 MHz) δ_{H} . 11.26 (brs, 1H), 7.48-7.44 (m, 2H), 7.03-6.99 (m, 1H), 5.86 (s, 1H), 2.37 (s, 3H).

2-Methyl-6-(trifluoromethyl)quinolin-4-ol (BA_02d): Off-white solid, Yield 73%, m.p. 269-270 °C; ESI-MS was found at m/z 228.18 (M+H)⁺. ¹H NMR (DMSO-d₆- 300 MHz) δ_{H} . 11.45 (brs, 1H), 7.58-7.52 (m, 2H), 7.03-6.99 (m, 1H), 5.87 (s, 1H), 2.33 (s, 3H).

4-Chloro-2-methylquinoline (BA_03a): Brown liquid, Yield 68%; ESI-MS was found at m/z 177.16 (M+H)⁺. ¹H NMR (CDCl₃-300 MHz) δ_{H} . 7.90-7.45 (m, 4H), 7.66 (s, 1H), 2.61 (s, 3H).

4-Chloro-6-methoxy-2-methylquinoline (BA_03b): Off-white solid, Yield 67%, m.p. 100-101 °C; ESI-MS was found at m/z 208.64 (M+H)⁺. ¹H NMR (CDCl₃-300 MHz) δ_{H} . 7.90 (d, 1H, $J = 8.9$ Hz), 7.66 (s, 1H), 7.45 (dd, 1H, $J = 8.9$ Hz), 7.39 (d, 1H, $J = 2.7$ Hz), 3.94 (s, 3H), 2.65 (s, 3H).

4-Chloro-6-fluoro-2-methylquinoline (BA_03c): Pale yellow solid, Yield 70%, m.p. 105-107 °C; ESI-MS was found at m/z 196.52 (M+H)⁺. ¹H NMR (CDCl₃-300 MHz) δ_{H} . 7.89 (d, 1H, $J = 8.8$ Hz), 7.65 (s, 1H), 7.46 (dd, 1H, $J = 8.6$ Hz), 7.41 (d, 1H, $J = 2.6$ Hz), 2.63 (s, 3H).

4-Chloro-2-methyl-6-trifluoromethylquinoline (BA_03d): Brown solid, Yield 69%, m.p. 120-122 °C; ESI-MS was found at m/z 246.63(M+H)⁺. ¹H NMR (CDCl₃-300 MHz) δ_{H} . 8.12 (d, 1H, $J = 2.6$ Hz), 7.85 (dd, 1H, $J = 8.8$ Hz), 7.78 (d, 1H, $J = 2.7$ Hz), 7.66 (s, 1H), 2.61 (s, 3H).

***Tert*-Butyl (1-(2-methylquinolin-4-yl) piperidin-4-yl) carbamate (BA_04a):** Pale yellow solid; Yield 70%; m.p.113-114 °C; ESI-MS was found at m/z 342.42 (M+H)⁺. ¹H NMR (CDCl₃-300 MHz) δ_{H} . 7.90-7.67 (m, 4H, Ar-H), 6.68 (s, 1H, Ar-H), 3.74-3.63 (m, 4H, NCH₂), 2.61 (s, 3H, CH₃), 2.56-2.52 (m, 1H, CH), 2.16-2.08 (m, 2H, CH₂), 1.83-1.77 (m, 2H, CH₂), 1.40 (s, 9H, CH₃).

***Tert*-Butyl (1-(6-methoxy-2-methylquinolin-4-yl)piperidin-4-yl)carbamate (BA_04b):** Off-white solid; Yield 67%; m.p. 110-112 °C ; ESI-MS was found at m/z 372.46 (M+H)⁺. ¹H NMR (CDCl₃-300 MHz) δ_{H} . 7.92 (d, $J = 2.7$ Hz, 1H), 7.84 (d, $J = 8.6$ Hz, 1H), 7.67 (s, 1H), 7.33 (dd, $J = 2.8, 8.7$ Hz, 1H), 3.94 (s, 3H), 3.74-3.63 (m, 4H), 2.60 (s, 3H), 2.55-2.50 (m, 1H), 2.14-2.06 (m, 2H), 1.85-1.78 (m, 2H), 1.42 (s, 9H).

***Tert*-Butyl (1-(6-fluoro-2-methylquinolin-4-yl) piperidin-4-yl) carbamate (BA_04c):** Pale yellow solid; Yield: 68%; m.p. 120-121 °C; ESI-MS was found at m/z 360.43 (M+H)⁺. ¹H NMR (CDCl₃-300 MHz) δ_{H} . 7.89 (d, $J = 8.5$ Hz, 1H), 7.64 (s, 1H), 7.45 (d, $J = 2.6$ Hz, 1H), 7.34 (dd, $J = 2.7, 8.9$ Hz, 1H), 3.76-3.65 (m, 4H), 2.59 (s, 3H), 2.55-2.50 (m, 1H), 2.15-2.07 (m, 2H), 1.82-1.75 (m, 2H), 1.41 (s, 9H).

Tert-Butyl (1-(2-methyl-6-(trifluoromethyl) quinolin-4-yl) piperidin-4-yl)carbamate (BA_04d): Pale yellow solid; Yield 70%; m.p. 127-129 °C; ESI-MS was found at m/z 410.43 (M+H)⁺. ¹H NMR (CDCl₃-300 MHz) δ_H. 8.35-8.31 (d, *J* = 2.6 Hz, 1H), 8.19-8.15 (dd, *J* = 2.9, 9.0 Hz, 1H), 8.12-8.09 (d, *J* = 8.8Hz), 6.89 (s, 1H), 3.78-3.67 (m, 4H), 2.58 (s, 3H), 2.56-2.51 (m, 1H), 2.17-2.08 (m, 2H), 1.84-1.76 (m, 2H), 1.43 (s, 9H).

1-(1-(2-Methylquinolin-4-yl) piperidin-4-yl)-3-phenylurea (BA_06): Off-white solid; Yield: 75%, m.p. 196-198 °C; ¹H NMR (DMSO-d₆): δ_H. 1.60-2.23 (m, 4H), 2.54 (s, 3H), 2.77-3.36 (m, 4H), 3.61 (m, 1H), 6.68 (s, 1H), 7.19-7.89 (m, 8H), 8.25-8.31 (m, 1H), 8.92 (s, 1H), 10.56 (s, 1H). ¹³C NMR (DMSO-d₆): δ_C. 160.1, 159.4, 155.3, 151.7, 139.9, 131.6, 130.1, 129.3, 128.9(2C), 128.3, 126.7, 126.0, 121.6(2C), 112.9, 49.9, 46.8(2C), 30.4(2C), 20.8. EI-MS m/z (Calcd. for C₂₂H₂₄N₄O: 360.20); Found: 359.04 (M-H)⁻. Anal Calcd. for C₂₂H₂₄N₄O: C, 73.31; H, 6.71; N, 15.54; Found: C, 73.36; H, 6.68; N, 15.57.

1-(4-Fluorophenyl)-3-(1-(2-methylquinolin-4-yl)piperidin-4-yl)urea (BA_07): Off-white solid; Yield: 70%, m.p. 163-164 °C; ¹H NMR (DMSO-d₆): δ_H. 1.60-1.85 (m, 2H), 2.08-2.16 (m, 2H), 2.53 (s, 3H), 2.72-3.62 (m, 5H), 6.66 (m, 1H), 7.22-7.89 (m, 6H), 8.18-8.27 (m, 2H), 8.79 (s, 1H), 10.48 (s, 1H). ¹³C NMR (DMSO-d₆): δ_C. 163.4, 159.9, 159.1, 154.9, 151.7, 135.8, 131.2, 129.9, 128.4, 126.6, 126.0(2C), 119.9, 116.2(2C), 112.6, 49.8(2C), 47.3, 29.7(2C), 21.1. EI-MS m/z (Calcd. for C₂₂H₂₃FN₄O: 378.19); Found: 379.41 (M+H)⁺. Anal Calcd. for C₂₂H₂₃FN₄O: C, 69.82; H, 6.13; N, 14.80; Found: C, 69.75; H, 6.18; N, 14.82.

1-(4-Chlorophenyl)-3-(1-(2-methylquinolin-4-yl)piperidin-4-yl)urea (BA_08): Off-white solid; Yield: 71%, m.p. 175-176 °C; ¹H NMR (DMSO-d₆): δ_H. 1.59-2.23 (m, 4H), 2.53 (s, 3H), 2.73-3.30 (m, 5H), 6.65 (s, 1H), 7.47-7.91 (m, 7H), 8.23 (m, 1H), 8.77 (s, 1H), 10.43 (s, 1H). ¹³C NMR (DMSO-d₆): δ_C. 160.5, 159.7, 154.9, 151.5, 138.2, 133.9, 131.1, 130.5, 129.3(2C), 128.5, 126.4, 125.7(2C), 121.9, 111.8, 53.5, 51.7(2C), 31.9(2C), 20.3. EI-MS m/z (Calcd. for C₂₂H₂₃ClN₄O: 394.16); Found: 395.56 (M+H)⁺. Anal. Calcd. for C₂₂H₂₃ClN₄O: C, 66.91; H, 5.87; N, 14.19; Found: C, 66.95; H, 5.84; N, 14.21.

1-(1-(2-Methylquinolin-4-yl)piperidin-4-yl)-3-(4-nitrophenyl)urea (BA_09): Pale yellow solid; Yield: 73%, m.p. 166-168 °C; ¹H NMR (DMSO-d₆): δ_H. 1.60-2.24 (m,

4H), 2.54 (s, 3H), 2.79-3.62 (m, 5H), 6.64 (s, 1H), 7.55-7.89 (m, 5H), 8.18-8.27 (m, 3H), 8.86 (s, 1H), 10.57 (s, 1H). ^{13}C NMR (DMSO- d_6): δ_{C} . 159.5, 158.3, 154.3, 151.7, 146.3, 144.1, 130.9, 130.3, 128.5, 126.2(2C), 124.8(2C), 120.6(2C), 112.8, 51.5(2C), 49.8, 29.6(2C), 20.5. EI-MS m/z (Calcd. for $\text{C}_{22}\text{H}_{23}\text{N}_5\text{O}_3$: 405.18); Found: 406.29 (M+H) $^+$. Anal Calcd. for $\text{C}_{22}\text{H}_{23}\text{N}_5\text{O}_3$: C, 65.17; H, 5.72; N, 17.27; Found: C, 65.22; H, 5.69; N, 17.23.

1-(1-(2-Methylquinolin-4-yl) piperidin-4-yl)-3-p-tolylurea (BA_10): Off-white solid; Yield: 70%, m.p. 171-172 °C; ^1H NMR (DMSO- d_6): δ_{H} . 1.61-2.23 (m, 4H), 2.34 (s, 3H), 2.53 (s, 3H), 2.69-3.37 (m, 5H), 6.67 (s, 1H), 7.21-7.90 (m, 7H), 8.27 (m, 1H), 8.86 (s, 1H), 10.51 (s, 1H). ^{13}C NMR (DMSO- d_6): δ_{C} . 159.4, 158.4, 155.3, 151.6, 137.5(2C), 131.1, 129.7, 129.3(2C), 127.6, 125.8(2C), 122.1(2C), 112.5, 50.2(2C), 49.9, 29.9(2C), 21.8, 21.1. EI-MS m/z (Calcd. for $\text{C}_{23}\text{H}_{26}\text{N}_4\text{O}$: 374.21); Found: 373.11 (M-H) $^-$. Anal Calcd. for $\text{C}_{23}\text{H}_{26}\text{N}_4\text{O}$: C, 73.77; H, 7.00; N, 14.96; Found: C, 73.81; H, 6.97; N, 14.99.

1-(4-Methoxyphenyl)-3-(1-(2-methylquinolin-4-yl)piperidin-4-yl)urea (BA_11): Off-white solid; Yield: 70%, m.p. 118-120 °C; ^1H NMR (DMSO- d_6): δ_{H} . 1.60-1.85 (m, 4H), 2.53 (s, 3H), 2.71-3.56 (m, 5H), 3.83 (s, 3H), 6.59 (s, 1H), 7.01 (m, 2H), 7.51-7.89 (m, 5H), 8.18 (m, 1H), 9.21 (s, 1H), 10.51 (s, 1H). ^{13}C NMR (DMSO- d_6): δ_{C} . 159.2, 158.7(2C), 154.8, 151.5, 132.3, 130.7, 129.9, 128.4, 125.9(2C), 119.8(2C), 114.9(2C), 112.5, 55.1, 51.7(2C), 50.9, 29.5(2C), 19.8. EI-MS m/z (Calcd. for $\text{C}_{23}\text{H}_{26}\text{N}_4\text{O}_2$: 390.21); Found: 391.45 (M+H) $^+$. Anal. Calcd. for $\text{C}_{23}\text{H}_{26}\text{N}_4\text{O}_2$: C, 70.75; H, 6.71; N, 14.35; Found: C, 70.69; H, 6.73; N, 14.31.

1-(1-(6-Methoxy-2-methylquinolin-4-yl) piperidin-4-yl)-3-phenylurea (BA_12): Off-white solid; Yield: 72%, m.p. 190-192 °C; ^1H NMR (DMSO- d_6): δ_{H} . 1.60-2.27 (m, 4H), 2.54 (s, 3H), 2.82-3.37 (m, 5H), 3.84 (s, 3H), 6.68 (s, 1H), 7.20-7.76 (m, 8H), 8.88 (s, 1H), 10.08 (s, 1H). ^{13}C NMR (DMSO- d_6): δ_{C} . 158.9, 158.4, 156.6, 154.9, 147.1, 139.8, 131.5, 129.5, 129.0(2C), 127.2, 123.5, 122.6(2C), 112.9, 105.7, 56.8, 50.5(2C), 49.6, 29.8(2C), 20.6. EI-MS m/z (Calcd. for $\text{C}_{23}\text{H}_{26}\text{N}_4\text{O}_2$: 390.21); Found: 391.39 (M+H) $^+$. Anal Calcd. for $\text{C}_{23}\text{H}_{26}\text{N}_4\text{O}_2$: C, 70.75; H, 6.71; N, 14.35; Found: C, 70.79; H, 6.67; N, 14.38.

1-(4-Fluorophenyl)-3-(1-(6-methoxy-2-methylquinolin-4-yl)piperidin-4-yl)urea (BA_13): Pale yellow solid; Yield: 75%, m.p. 215-216 °C; ^1H NMR (DMSO- d_6): δ_{H} .

1.79-1.83 (m, 2H), 2.14-2.19 (m, 2H), 2.55 (s, 3H), 3.52-3.62 (m, 5H), 3.87 (s, 3H), 6.67 (s, 1H), 7.18-7.23 (m, 2H), 7.25-7.29 (m, 1H), 7.38-7.42 (m, 1H), 7.62-7.70 (m, 2H), 7.71 (d, $J = 9\text{Hz}$, 1H), 10.01 (s, 1H), 10.10 (s, 1H). ^{13}C NMR (DMSO- d_6): δ_{C} . 162.5, 158.1(2C), 157.9, 155.6, 146.3, 135.1, 132.3, 131.5, 126.8, 123.3, 119.2(2C), 115.2(2C), 105.6, 55.4, 51.8(2C), 50.6, 30.3(2C), 20.7. EI-MS m/z (Calcd. for $\text{C}_{23}\text{H}_{25}\text{FN}_4\text{O}_2$: 408.47); Found: 409.54 (M+H) $^+$. Anal. Calcd. for $\text{C}_{23}\text{H}_{25}\text{FN}_4\text{O}_2$: C, 67.63; H, 6.17; N, 13.72; Found: C, 67.59; H, 6.21; N, 13.79.

1-(4-Chlorophenyl)-3-(1-(6-methoxy-2-methylquinolin-4-yl)piperidin-4-yl)urea

(BA_14): Off-white solid; Yield: 79%, m.p. 226-227 °C; ^1H NMR (DMSO- d_6): δ_{H} . 1.61-2.25 (m, 4H), 2.53 (s, 3H), 2.78-3.48 (m, 5H), 3.83 (s, 3H), 6.68 (m, 1H), 7.48-7.80 (m, 7H), 10.41 (s, 1H), 10.51 (s, 1H). ^{13}C NMR (DMSO- d_6): δ_{C} . 158.8(2C), 155.0, 153.7, 147.5, 138.6, 134.1, 131.8, 129.2(2C), 127.7, 123.2, 120.6(2C), 112.8, 105.5, 55.1, 51.0(2C), 49.9, 30.1(2C), 20.8. EI-MS m/z (Calcd. for $\text{C}_{23}\text{H}_{25}\text{ClN}_4\text{O}_2$: 424.17); Found: 425.63 (M+H) $^+$. Anal. Calcd. for $\text{C}_{23}\text{H}_{25}\text{ClN}_4\text{O}_2$: C, 65.01; H, 5.93; N, 13.19; Found: C, 64.97; H, 5.95; N, 13.21.

1-(1-(6-Methoxy-2-methylquinolin-4-yl)piperidin-4-yl)-3-(4-nitrophenyl)urea

(BA_15): Pale yellow solid; Yield: 69%, m.p. 132-133 °C; ^1H NMR (DMSO- d_6): δ_{H} . 1.61-2.29 (m, 4H), 2.53 (s, 3H), 2.80-3.63 (m, 5H), 3.83 (s, 3H), 6.65 (s, 1H), 7.30-7.85 (m, 5H), 8.26 (d, $J = 7.8\text{Hz}$, 2H), 10.21 (s, 1H), 10.39 (s, 1H). ^{13}C NMR (DMSO- d_6): δ_{C} . 158.7, 158.3, 156.5, 154.9, 147.1, 146.5, 143.9, 131.5, 127.2, 124.7(2C), 123.4, 120.6(2C), 112.8, 104.7, 56.7, 49.5(2C), 48.7, 29.7(2C), 20.5. EI-MS m/z (Calcd. for $\text{C}_{23}\text{H}_{25}\text{N}_5\text{O}_4$: 435.19); Found: 434.12 (M-H) $^-$. Anal. Calcd. for $\text{C}_{23}\text{H}_{25}\text{N}_5\text{O}_4$: C, 63.44; H, 5.79; N, 16.08; Found: C, 63.39; H, 5.83; N, 16.15.

1-(1-(6-Methoxy-2-methylquinolin-4-yl)piperidin-4-yl)-3-p-tolylurea (BA_16):

Off-white solid; Yield: 72%, m.p. 236-237 °C; ^1H NMR (DMSO- d_6): δ_{H} . 1.60-2.27 (m, 4H), 2.34 (s, 3H), 2.53 (s, 3H), 2.75-3.58 (m, 5H), 3.83 (s, 3H), 6.68 (s, 1H), 7.23-7.74 (m, 7H), 9.98 (s, 1H), 10.23 (s, 1H). ^{13}C NMR (DMSO- d_6): δ_{C} . 159.1, 158.4, 156.3, 155.1, 147.4, 136.6(2C), 131.2, 129.5(2C), 127.5, 122.9, 122.1(2C), 112.7, 105.8, 56.9, 49.7(2C), 48.7, 29.8(2C), 21.6, 20.9. EI-MS m/z (Calcd. for $\text{C}_{24}\text{H}_{28}\text{N}_4\text{O}_2$: 404.22); Found: 405.38 (M+H) $^+$. Anal. Calcd. for $\text{C}_{24}\text{H}_{28}\text{N}_4\text{O}_2$: C, 71.26; H, 6.98; N, 13.85; Found: C, 71.29; H, 6.95; N, 13.81.

1-(1-(6-Methoxy-2-methylquinolin-4-yl)piperidin-4-yl)-3-(4-methoxyphenyl)urea (BA_17): Off-white solid; Yield: 85%, m.p. 170-172 °C; ¹H NMR (DMSO-d₆): δ_H. 1.60-2.26 (m, 4H), 2.53 (s, 3H), 2.89-3.59 (m, 5H), 3.83 (s, 6H), 6.97 (s, 1H), 7.02-7.71 (m, 7H), 9.97 (s, 1H), 10.12 (s, 1H). ¹³C NMR (DMSO-d₆): δ_C. 159.5, 158.9, 158.2, 156.6, 154.8, 146.9, 132.5, 131.5, 126.9, 122.9, 120.5(2C), 115.0(2C), 112.6, 105.8, 55.1(2C), 49.4(2C), 47.1, 29.9(2C), 20.5. EI-MS m/z (Calcd. for C₂₄H₂₈N₄O₃: 420.22); Found: 421.64 (M+H)⁺. Anal Calcd. for C₂₄H₂₈N₄O₃: C, 68.55; H, 6.71; N, 13.32; Found: C, 68.51; H, 6.68; N, 13.35.

1-(1-(6-Fluoro-2-methylquinolin-4-yl)piperidin-4-yl)-3-phenylurea (BA_18): Off-white solid; Yield: 75%, m.p. 215-216 °C; ¹H NMR (DMSO-d₆): δ_H. 1.60-2.39 (m, 4H), 2.54 (s, 3H), 2.76-3.58 (m, 5H), 6.67 (s, 1H), 7.19-7.88 (m, 8H), 10.12 (s, 1H), 10.31 (s, 1H). ¹³C NMR (DMSO-d₆): δ_C. 159.9(2C), 158.5, 155.4, 148.3, 139.7, 130.6, 129.3, 128.9(2C), 127.4, 122.7, 122.0(2C), 113.5, 106.3, 50.7(2C), 48.9, 29.6(2C), 20.5. EI-MS m/z (Calcd. for C₂₂H₂₃FN₄O: 378.19); Found: 379.41 (M+H)⁺. Anal Calcd. for C₂₂H₂₃FN₄O: C, 69.82; H, 6.13; N, 14.80; Found: C, 69.85; H, 6.09; N, 14.75.

1-(1-(6-Fluoro-2-methylquinolin-4-yl)piperidin-4-yl)-3-(4-fluorophenyl)urea (BA_19): Off-white solid; Yield: 73%, m.p. 198-199 °C; ¹H NMR (DMSO-d₆): δ_H. 1.59-2.29 (m, 4H), 2.53 (s, 3H), 2.79-3.61 (m, 5H), 6.68 (s, 1H), 7.25-7.87 (m, 7H), 10.12 (s, 1H), 10.22 (s, 1H). ¹³C NMR (DMSO-d₆): δ_C. 163.6, 159.3, 158.6(2C), 154.7, 148.1, 135.9, 130.5, 127.3, 122.4, 118.6(2C), 116.4(2C), 113.7, 106.9, 51.6(2C), 49.8, 29.5(2C), 21.1. EI-MS m/z (Calcd. for C₂₂H₂₂F₂N₄O: 396.18); Found: 397.43 (M+H)⁺. Anal Calcd. for C₂₂H₂₂F₂N₄O: C, 66.65; H, 5.59; N, 14.13; Found: C, 66.59; H, 5.63; N, 14.11.

1-(4-Chlorophenyl)-3-(1-(6-fluoro-2-methylquinolin-4-yl)piperidin-4-yl)urea (BA_20): Off-white solid; Yield: 79%, m.p. 230-231 °C; ¹H NMR (DMSO-d₆): δ_H. 1.61-2.36 (m, 4H), 2.53 (s, 3H), 2.85-3.67 (m, 5H), 6.69 (s, 1H), 7.29-7.87 (m, 7H), 9.98 (s, 1H), 10.21 (s, 1H). ¹³C NMR (DMSO-d₆): δ_C. 159.5(2C), 158.6, 154.8, 148.7, 138.1, 133.9, 130.5, 129.5(2C), 127.2, 122.4, 121.6(2C), 113.2, 106.7, 50.9(2C), 49.8, 29.7(2C), 19.7. EI-MS m/z (Calcd. for C₂₂H₂₂ClFN₄O: 412.15); Found: 413.71 (M+H)⁺. Anal Calcd. for C₂₂H₂₂ClFN₄O: C, 64.00; H, 5.37; N, 13.57; Found: C, 63.96; H, 5.41; N, 13.52.

1-(1-(6-Fluoro-2-methylquinolin-4-yl)piperidin-4-yl)-3-(4-nitrophenyl)urea

(BA_21): Yellow solid; Yield: 71%, m.p. 177-178 °C; ¹H NMR (DMSO-d₆): δ_H. 1.60-2.39 (m, 4H), 2.53 (s, 3H), 2.79-3.67 (m, 5H), 6.68 (s, 1H), 7.29-7.39 (m, 2H), 7.82-7.87 (m, 3H), 8.29 (d, *J* = 7.9Hz, 2H), 9.98 (s, 1H), 10.24 (s, 1H). ¹³C NMR (DMSO-d₆): δ_C. 159.7, 159.0(2C), 155.1, 148.3, 146.5, 144.4, 130.8, 127.2, 124.9(2C), 122.3, 119.3(2C), 113.5, 106.7, 49.9(2C), 47.1, 29.6(2C), 20.9. EI-MS *m/z* (Calcd. for C₂₂H₂₂FN₅O₃: 423.17); Found: 424.45 (M+H)⁺. Anal Calcd. for C₂₂H₂₂FN₅O₃: C, 62.40; H, 5.24; N, 16.54; Found: C, 62.44; H, 5.19; N, 16.48.

1-(1-(6-Fluoro-2-methylquinolin-4-yl)piperidin-4-yl)-3-p-tolylurea (BA_22): Off-white solid; Yield: 76%, m.p. 206-207 °C; ¹H NMR (DMSO-d₆): δ_H. 1.61-2.39 (m, 4H), 2.34 (s, 3H), 2.52 (s, 3H), 2.71-3.67 (m, 5H), 6.68 (s, 1H), 7.23-7.89 (m, 7H), 10.20 (s, 1H), 10.23 (s, 1H). ¹³C NMR (DMSO-d₆): δ_C. 158.7(2C), 154.9, 148.8, 137.8, 136.9(2C), 130.7, 129.8(2C), 127.4, 122.5, 121.8(2C), 113.5, 105.8, 49.5(2C), 46.7, 29.9(2C), 22.0, 20.6. EI-MS *m/z* (Calcd. for C₂₃H₂₅FN₄O: 392.20); Found: 393.39 (M+H)⁺. Anal Calcd. for C₂₃H₂₅FN₄O: C, 70.39; H, 6.42; N, 14.28; Found: C, 70.41; H, 6.39; N, 14.33.

1-(1-(6-Fluoro-2-methylquinolin-4-yl)piperidin-4-yl)-3-(4-methoxyphenyl)urea

(BA_23): Pale brown solid; Yield: 80%, m.p. 243-245 °C; ¹H NMR (DMSO-d₆): δ_H. 1.59-2.32 (m, 4H), 2.52 (s, 3H), 2.78-3.65 (m, 5H), 3.83 (s, 3H), 6.63 (s, 1H), 7.10-7.89 (m, 7H), 10.11 (s, 1H), 10.23 (s, 1H). ¹³C NMR (DMSO-d₆): δ_C. 160.1, 159.7(2C), 158.5, 155.1, 148.5, 132.6, 130.8, 127.2, 122.5, 120.4(2C), 114.9(2C), 113.7, 106.8, 56.6, 49.5(2C), 45.8, 30.1(2C), 20.7. EI-MS *m/z* (Calcd. for C₂₃H₂₅FN₄O₂: 408.20); Found: 407.05 (M-H)⁻. Anal Calcd. for C₂₃H₂₅FN₄O₂: C, 67.63; H, 6.17; N, 13.72; Found: C, 67.65; H, 6.14; N, 13.75.

1-(1-(2-Methyl-6-(trifluoromethyl)quinolin-4-yl)piperidin-4-yl)-3-phenylurea

(BA_24): Off-white solid; Yield: 75%, m.p. 197-198 °C; ¹H NMR (DMSO-d₆): δ_H. 1.61-2.36 (m, 4H), 2.52 (s, 3H), 2.82-3.66 (m, 5H), 6.88 (s, 1H), 7.19-7.66 (m, 5H), 8.15-8.34 (m, 3H), 10.01 (s, 1H, Ar-H), 10.23 (s, 1H, Ar-NH). ¹³C NMR (DMSO-d₆): δ_C. 162.5, 159.3, 154.7, 152.5, 140.1, 131.6, 129.4, 128.9(2C), 125.8, 125.3, 124.8(2C), 122.5, 121.9(2C), 112.7, 49.6(2C), 46.8, 29.5(2C), 21.1. EI-MS *m/z* (Calcd. for C₂₃H₂₃F₃N₄O: 428.18); Found: 429.23 (M+H)⁺. Anal Calcd. for C₂₃H₂₃F₃N₄O: C, 64.48; H, 5.41; N, 13.08; Found: C, 64.52; H, 5.38; N, 13.05.

1-(4-Fluorophenyl)-3-(1-(2-methyl-6-(trifluoromethyl)quinolin-4-yl)piperidin-4-yl)urea (BA_25): Off-white solid; Yield: 77%, m.p. 185-186 °C; ¹H NMR (DMSO-d₆): δ_H. 1.60-2.39 (m, 4H), 2.53 (s, 3H), 2.83-3.67 (m, 5H), 6.68 (s, 1H), 7.22-7.63 (m, 4H), 8.15-8.37 (m, 3H), 10.01 (s, 1H), 10.24 (s, 1H). ¹³C NMR (DMSO-d₆): δ_C. 163.5, 162.1, 160.4, 154.7, 152.9, 135.5, 131.7, 128.4, 126.6, 125.8(2C), 122.7, 119.9(2C), 116.3(2C), 113.6, 48.7(2C), 46.6, 28.5(2C), 20.8. EI-MS m/z (Calcd. for C₂₃H₂₂F₄N₄O: 446.17); Found: 447.39 (M+H)⁺. Anal Calcd. for C₂₃H₂₂F₄N₄O: C, 61.88; H, 4.97; N, 12.55; Found: C, 61.92; H, 5.03; N, 12.51.

1-(4-Chlorophenyl)-3-(1-(2-methyl-6-(trifluoromethyl)quinolin-4-yl)piperidin-4-yl)urea (BA_26): Off-white solid; Yield: 78%, m.p. 207-209 °C; ¹H NMR (DMSO-d₆): δ_H. 1.60-2.39 (m, 4H), 2.56 (s, 3H), 2.87-3.74 (m, 5H), 6.88 (s, 1H), 7.47-7.79 (m, 4H), 8.15-8.37 (m, 3H), 10.03 (s, 1H), 10.31 (s, 1H). ¹³C NMR (DMSO-d₆): δ_C. 162.8, 160.6, 154.9, 152.5, 137.8, 133.7, 132.1, 129.4(2C), 126.4, 125.7, 124.6(2C), 122.8, 121.5(2C), 113.7, 49.9(2C), 46.7, 29.1(2C), 20.1. EI-MS m/z (Calcd. for C₂₃H₂₂ClF₃N₄O: 462.14); Found: 463.52 (M+H)⁺. Anal Calcd. for C₂₃H₂₂ClF₃N₄O: C, 59.68; H, 4.79; N, 12.10; Found: C, 59.65; H, 4.81; N, 12.08.

1-(1-(2-Methyl-6-(trifluoromethyl)quinolin-4-yl)piperidin-4-yl)-3-(4-nitrophenyl)urea (BA_27): Yellow solid; Yield: 76%, m.p. 179-180 °C; ¹H NMR (DMSO-d₆): δ_H. 1.61-2.39 (m, 4H), 2.52 (s, 3H), 2.68-3.69 (m, 5H), 6.88 (s, 1H), 7.82 (d, *J* = 7.9 Hz, 2H), 8.15-8.34 (m, 5H), 9.98 (s, 1H), 10.25 (s, 1H). ¹³C NMR (DMSO-d₆): δ_C. 162.5, 159.3, 154.9, 152.7, 146.1, 143.8, 132.4, 127.6, 126.2, 125.5, 124.9, 124.5(2C), 122.7, 120.4(2C), 113.6, 49.7(2C), 46.5, 28.7(2C), 19.6. EI-MS m/z (Calcd. for C₂₃H₂₂F₃N₅O₃: 473.17); Found: 474.23 (M+H)⁺. Anal Calcd. for C₂₃H₂₂F₃N₅O₃: C, 58.35; H, 4.68; N, 14.79; Found: C, 58.31; H, 4.63; N, 14.75.

1-(1-(2-Methyl-6-(trifluoromethyl)quinolin-4-yl)piperidin-4-yl)-3-p-tolylurea (BA_28): Off-white solid; Yield: 77%, m.p. 203-205 °C; ¹H NMR (DMSO-d₆): δ_H. 1.60-2.29 (m, 4H), 2.33 (s, 3H), 2.54 (s, 3H), 2.79-3.64 (m, 5H), 6.86 (s, 1H), 7.21-7.76 (m, 4H), 8.13-8.37 (m, 3H), 9.98 (s, 1H), 10.23 (s, 1H). ¹³C NMR (DMSO-d₆): δ_C. 162.8, 160.2, 155.1, 152.5, 136.9(2C), 130.2(2C), 127.6, 125.9, 125.3, 124.8(2C), 123.1, 121.9(2C), 113.7, 53.5(2C), 50.7, 30.2(2C), 21.6, 20.8. EI-MS m/z (Calcd. for C₂₄H₂₅F₃N₄O: 442.20); Found: 443.25 (M+H)⁺. Anal Calcd. for C₂₄H₂₅F₃N₄O: C, 65.15; H, 5.69; N, 12.66; Found: C, 65.19; H, 5.73; N, 12.61.

1-(4-Methoxyphenyl)-3-(1-(2-methyl-6-(trifluoromethyl)quinolin-4-yl)piperidin-4-yl)urea (BA_29): Off-white solid; Yield: 73%, m.p. 232-233 °C; ¹H NMR (DMSO-d₆): δ_H. 1.60-2.29 (m, 4H), 2.57 (s, 3H), 2.72-3.67 (m, 5H), 3.83 (s, 3H), 6.53 (s, 1H), 6.98-7.56 (m, 4H), 8.15-8.39 (m, 3H), 9.97 (s, 1H), 10.23 (s, 1H). ¹³C NMR (DMSO-d₆): δ_C. 162.9, 160.5, 159.3, 154.8, 152.7, 132.5, 131.9, 128.1, 126.3, 125.8(2C) 122.9, 119.1(2C), 115.4(2C), 113.7, 56.2, 49.9(2C), 46.6, 30.1(2C), 20.9. EI-MS m/z (Calcd. for C₂₄H₂₅F₃N₄O₂: 458.19); Found: 457.13 (M-H)⁻. Anal Calcd. for C₂₄H₂₅F₃N₄O₂: C, 62.87; H, 5.50; N, 12.22; Found: C, 62.83; H, 5.52; N, 12.25.

1-(1-(2-Methylquinolin-4-yl)piperidin-4-yl)-3-phenylthiourea (BA_30): Off-white solid; Yield: 77%, m.p. 186-187 °C; ¹H NMR (DMSO-d₆): δ_H. 1.60-2.04 (m, 4H), 2.53 (s, 3H), 2.65-3.45 (m, 5H), 5.10 (s, 1H), 6.66-7.31 (m, 4H), 7.57-7.77 (m, 4H), 7.90-8.18 (m, 2H), 10.11 (s, 1H). ¹³C NMR (DMSO-d₆): δ_C. 178.5, 161.3, 159.2, 150.5, 138.9, 130.2, 129.7, 129.0(2C), 128.7(2C), 127.6, 126.3, 125.9, 125.3(2C), 111.4, 54.6, 52.1(2C), 30.6(2C), 20.4. EI-MS m/z (Calcd. for C₂₂H₂₄N₄S: 376.17); Found: 377.52 (M+H)⁺. Anal Calcd. for C₂₂H₂₄N₄S: C, 70.18; H, 6.42; N, 14.88; Found: C, 70.12; H, 6.35; N, 14.95.

1-(4-Fluorophenyl)-3-(1-(2-methylquinolin-4-yl)piperidin-4-yl)thiourea (BA_31): Off-white solid; Yield: 71%, m.p. 184-185 °C; ¹H NMR (DMSO-d₆): δ_H. 1.76-2.02 (m, 2H), 2.09-2.17 (m, 2H), 2.53 (s, 3H), 2.90-3.36 (m, 5H), 5.20 (s, 1H), 6.45 (d, *J* = 8.8 Hz, 2H), 6.68 (s, 1H), 6.98 (d, *J* = 8.6 Hz, 2H), 7.56-8.19 (m, 4H), 10.01 (s, 1H). ¹³C NMR (DMSO-d₆): δ_C. 177.5, 163.3, 159.5, 158.6, 150.5, 134.2, 131.0(2C), 129.5, 127.8, 126.1, 125.6(2c), 115.7(2C), 111.2, 51.4(2C), 50.5, 30.2(2C), 20.6. EI-MS m/z (Calcd. for C₂₂H₂₃FN₄S: 394.16); Found: 395.51 (M+H)⁺. Anal Calcd. for C₂₂H₂₃FN₄S: C, 66.98; H, 5.88; N, 14.20; Found: C, 67.05; H, 5.75; N, 14.28.

1-(4-Chlorophenyl)-3-(1-(2-methylquinolin-4-yl)piperidin-4-yl)thiourea (BA_32): Off-white solid; Yield: 78%, m.p. 162-163 °C; ¹H NMR (DMSO-d₆): δ_H. 1.62-2.20 (m, 4H), 2.53 (s, 3H), 2.63-3.42 (m, 5H), 6.56 (s, 1H), 6.68 (d, *J* = 8.0, 2H), 7.24-7.32 (m, 3H), 7.55-8.18 (m, 4H), 9.98 (s, 1H). ¹³C NMR (DMSO-d₆): δ_C. 177.8, 159.4, 158.7, 151.1, 136.9, 133.6, 131.1(2C), 129.8, 129.6(2C), 129.2, 127.9, 125.8(2C), 112.4, 54.7, 50.8(2C), 30.4(2C), 20.1. EI-MS m/z (Calcd. for C₂₂H₂₃ClN₄S: 410.13); Found: 411.25 (M+H)⁺. Anal Calcd. for C₂₂H₂₃ClN₄S: C, 64.30; H, 5.64; N, 13.63; Found: C, 64.23; H, 5.69; N, 13.48.

1-(1-(2-Methylquinolin-4-yl)piperidin-4-yl)-3-(4-nitrophenyl)thiourea (BA_33): Pale yellow solid; Yield: 75%, m.p. 154-155 °C; ¹H NMR (DMSO-d₆): δ_H. 1.64-2.06 (m, 4H), 2.59 (s, 3H), 2.64-3.41 (m, 5H), 5.23 (s, 1H) 6.63-6.69 (m, 3H), 7.56-8.02 (m, 4H), 8.13 (d, *J* = 7.9 Hz, 2H), 10.22 (s, 1H). ¹³C NMR (DMSO-d₆): δ_C. 177.8, 159.5, 158.8, 150.7, 145.1, 143.7, 129.9, 129.1, 128.3, 126.5, 125.6, 124.8(2C), 124.1(2C), 111.6, 51.4, 50.2(2C), 30.3(2C), 20.1. EI-MS *m/z* (Calcd. for C₂₂H₂₃N₅O₂S: 421.16); Found: 422.51 (M+H)⁺. Anal Calcd. for C₂₂H₂₃N₅O₂S: C, 62.69; H, 5.50; N, 16.61; Found: C, 62.57; H, 5.53; N, 16.64.

1-(1-(2-Methylquinolin-4-yl)piperidin-4-yl)-3-p-tolylthiourea (BA_34): Off-white solid; Yield: 69%, m.p. 182-183 °C; ¹H NMR (DMSO-d₆): δ_H. 1.60-2.16 (m, 4H), 2.35 (s, 3H), 2.53 (s, 3H), 2.63-3.43 (m, 5H), 4.43 (brs, 1H), 6.40-6.98 (m, 5H), 7.57-8.19 (m, 4H), 9.98 (s, 1H). ¹³C NMR (DMSO-d₆): δ_C. 177.3, 161.7, 158.3, 151.3, 138.1, 135.2, 131.2, 129.6, 129.0(2C), 127.7, 126.3(2C), 125.8(2C), 112.4, 54.6, 51.3(2C), 31.7(2C), 22.1, 21.4. EI-MS *m/z* (Calcd. for C₂₃H₂₆N₄S: 390.19); Found: 391.21 (M+H)⁺. Anal Calcd. for C₂₃H₂₆N₄S: C, 70.73; H, 6.71; N, 14.35; Found: C, 70.79; H, 6.67; N, 14.39.

1-(4-Methoxyphenyl)-3-(1-(2-methylquinolin-4-yl)piperidin-4-yl)thiourea (BA_35): Off-white solid; Yield: 73%, m.p. 135-136 °C; ¹H NMR (DMSO-d₆): δ_H. 1.65-2.03 (m, 4H), 2.55 (s, 3H), 2.66-3.45 (m, 5H), 3.83 (s, 3H), 4.47 (brs, 1H), 6.34-6.77 (m, 5H), 7.34-8.21 (m, 4H), 10.11 (s, 1H). ¹³C NMR (DMSO-d₆): δ_C. 177.5, 159.9(2C), 158.1, 150.2, 131.3, 130.3, 129.5, 128.1, 127.5(2C), 126.1, 125.6, 114.3(2C), 111.7, 55.7, 51.7, 50.4(2C), 30.0(2C), 19.8. EI-MS *m/z* (Calcd. for C₂₃H₂₆N₄OS: 406.18); Found: 405.05 (M-H)⁻. Anal Calcd. for C₂₃H₂₆N₄OS: C, 67.95; H, 6.45; N, 13.78; Found: C, 68.12; H, 6.32; N, 13.71.

1-(1-(6-Methoxy-2-methylquinolin-4-yl)piperidin-4-yl)-3-phenylthiourea (BA_36): Off-white solid; Yield: 70%, m.p. 197-198 °C; ¹H NMR (DMSO-d₆): δ_H. 1.72-1.79 (m, 2H), 2.16-2.20 (m, 2H), 2.51 (s, 3H), 2.68 (m, 1H), 3.57-3.64 (m, 4H), 3.88 (s, 3H), 5.19 (s, 1H), 6.45-6.60 (m, 5H), 6.67 (s, 1H), 7.22-7.26 (m, 1H), 7.28-7.33 (m, 1H), 7.76 (d, *J* = 7.8Hz, 1H), 10.02 (s, 1H). ¹³C NMR (DMSO-d₆): δ_C. 178.5, 158.1, 157.8(2C), 147.4, 139.3, 131.8, 129.4(2C), 128.1, 127.3, 126.9(2C), 123.5, 112.7, 104.2, 55.8, 51.4, 50.2(2C), 30.2(2C), 20.5. EI-MS *m/z* (Calcd. for

C₂₃H₂₆N₄OS: 406.18); Found: 405.09 (M-H)⁻. Anal Calcd. for C₂₃H₂₆N₄OS: C, 67.95; H, 6.45; N, 13.78 ; Found: C, 68.03; H, 6.51; N, 13.69.

1-(4-Fluorophenyl)-3-(1-(6-methoxy-2-methylquinolin-4-yl)piperidin-4-yl)

thiourea (BA_37): Pale yellow solid; Yield: 72%, m.p. 201-202 °C; ¹H NMR (DMSO-d₆): δ_H. 1.79-1.83 (m, 2H), 2.14-2.19 (m, 2H), 2.55 (s, 3H), 2.63 (m, 1H), 3.52-3.62 (m, 4H), 3.87 (s, 3H), 5.21 (s, 1H), 6.43-6.52 (m, 2H), 6.67 (s, 1H), 6.98-7.02 (m, 2H), 7.23-7.25 (m, 1H), 7.26-7.32 (m, 1H), 7.78 (d, *J* = 9Hz, 1H), 10.01 (s, 1H). ¹³C NMR (DMSO-d₆): δ_C. 177.8, 164.5, 158.1, 157.9(2C), 155.6, 146.3, 135.1, 132.3(2C), 126.8, 123.3, 115.7(2C), 114.2, 105.6, 55.4, 51.8, 50.6(2C), 30.3(2C), 20.7. EI-MS *m/z* (Calcd. for C₂₃H₂₅FN₄OS: 424.17); Found: 425.54 (M+H)⁺. Anal Calcd. for C₂₃H₂₅FN₄OS: C, 65.07; H, 5.94; N, 13.20; Found: C, 65.13; H, 6.03; N, 13.15.

1-(4-Chlorophenyl)-3-(1-(6-methoxy-2-methylquinolin-4-yl)piperidin-4-yl)

thiourea (BA_38): Off-white solid; Yield: 78%, m.p. 133-134 °C; ¹H NMR (DMSO-d₆): δ_H. 1.77-1.84 (m, 2H), 2.15-2.21 (m, 2H), 2.58 (s, 3H), 2.64 (m, 1H), 3.54-3.66 (m, 4H), 3.86 (s, 3H), 5.19 (s, 1H), 6.47-6.56 (m, 2H), 6.69 (s, 1H), 6.99-7.06 (m, 2H), 7.19-7.23 (m, 1H), 7.27-7.31 (m, 1H), 7.77 (d, *J* = 8.1Hz, 1H), 9.89 (s, 1H). ¹³C NMR (DMSO-d₆): δ_C. 178.8, 158.2, 157.9(2C), 155.3, 147.1, 137.1, 133.9, 132.5, 131.9(2C), 129.0(2C), 122.9, 113.1, 104.9, 55.0, 52.7, 51.3(2C), 30.0(2C), 20.7. EI-MS *m/z* (Calcd. for C₂₃H₂₅ClN₄OS: 440.14); Found: 441.19 (M+H)⁺. Anal Calcd. for C₂₃H₂₅ClN₄OS: C, 62.64; H, 5.71; N, 12.70; Found: C, 62.53; H, 5.76; N, 12.73.

1-(1-(6-Methoxy-2-methylquinolin-4-yl)piperidin-4-yl)-3-(4-nitro phenyl)

thiourea (BA_39): Pale yellow solid; Yield: 71%, m.p. 179-180 °C; ¹H NMR (DMSO-d₆): δ_H. 1.69-1.79 (m, 2H), 2.16-2.27 (m, 2H), 2.51 (m, 1H), 2.55 (s, 3H), 3.38-3.47 (m, 4H), 3.89 (s, 3H), 5.19 (s, 1H), 6.89 (s, 1H), 7.18-7.19 (m, 1H), 7.29-7.33 (m, 1H), 7.78 (d, *J* = 7.6 Hz, 1H), 7.85-8.20 (m, 4H), 10.22 (s, 1H). ¹³C NMR (DMSO-d₆): δ_C. 178.5, 158.3(2C), 157.9, 146.9, 145.7, 144.3, 130.6, 126.8, 124.9(2C), 124.0(2C), 122.9, 113.5, 104.7, 55.2, 52.1, 50.5(2C), 30.7(2C), 20.5. EI-MS *m/z* (Calcd. for C₂₃H₂₅N₅O₃S: 451.17); Found: 450.02 (M-H)⁻. Anal Calcd. for C₂₃H₂₅N₅O₃S: C, 61.18; H, 5.58; N, 15.51; Found: C, 61.25; H, 5.46; N, 15.57.

1-(1-(6-Methoxy-2-methylquinolin-4-yl)piperidin-4-yl)-3-p-tolylthiourea

(BA_40): Off-white solid; Yield: 70%, m.p. 185-186 °C; ¹H NMR (DMSO-d₆): δ_H.

1.62-1.68 (m, 2H), 2.14-2.23 (m, 2H), 2.35 (s, 3H), 2.53 (s, 3H), 3.34-3.41 (m, 5H), 3.82 (s, 3H), 5.17 (s, 1H), 6.37-6.99 (m, 5H), 7.26-7.73 (m, 3H), 10.51 (s, 1H). ¹³C NMR (DMSO-d₆): δ_C. 177.9, 158.1, 157.6(2C), 155.9, 146.7, 138.3, 135.9, 131.8, 129.7(2C), 126.9, 124.7(2C), 112.9, 105.7, 56.5, 51.9, 50.3(2C), 30.2(2C), 21.9, 20.4. EI-MS m/z (Calcd. for C₂₄H₂₈N₄OS: 420.20); Found: 419.08 (M-H)⁻. Anal Calcd. for C₂₄H₂₈N₄OS: C, 68.54; H, 6.71; N, 13.32; Found: C, 68.67; H, 6.75; N, 13.20.

1-(1-(6-Methoxy-2-methylquinolin-4-yl)piperidin-4-yl)-3-(4-methoxy phenyl)thiourea (BA_41): Off-white solid; Yield: 75%, m.p. 184-185 °C; ¹H NMR (DMSO-d₆): δ_H. 1.68-1.73 (m, 2H), 2.12-2.24 (m, 2H), 2.51 (s, 3H), 2.67 (m, 1H), 3.47-3.54 (m, 4H), 3.86 (s, 3H), 3.88 (s, 3H), 5.17 (s, 1H), 6.47-6.56 (m, 2H), 6.70 (s, 1H), 6.89-7.01 (m, 2H), 7.26-7.30 (m, 1H), 7.35-7.39 (m, 1H), 7.78 (d, *J* = 8.0Hz, 1H), 10.00 (s, 1H). ¹³C NMR (DMSO-d₆): δ_C. 177.8, 160.3, 158.5, 158.1(2C), 156.5, 147.7, 130.9(2C), 128.6(2C), 127.2, 114.9(2C), 112.3, 105.7, 56.4(2C), 55.6, 49.2(2C), 31.5(2C), 20.9. EI-MS m/z (Calcd. for C₂₄H₂₈N₄O₂S: 436.19); Found: 437.55 (M+H)⁺. Anal Calcd. for C₂₄H₂₈N₄O₂S: C, 66.03; H, 6.46; N, 12.83; Found: C, 65.97; H, 6.53; N, 12.86.

1-(1-(6-Fluoro-2-methylquinolin-4-yl)piperidin-4-yl)-3-phenylthiourea (BA_42): Off-white solid; Yield: 80%, m.p. 178-179 °C; ¹H NMR (DMSO-d₆): δ_H. 1.61-2.12 (m, 4H), 2.54 (s, 3H), 2.66-3.47 (m, 5H), 5.18 (s, H) 6.66-6.81 (m, 2H), 7.21-7.40 (m, 6H), 7.88 (d, *J* = 6.9 Hz, 1H), 9.98 (s, 1H). ¹³C NMR (DMSO-d₆): δ_C. 178.5, 159.9, 158.2, 158.0, 148.5, 139.1, 130.7, 129.1(2C), 128.7, 127.0, 126.3(2C), 122.4, 112.4, 106.7, 51.7, 50.4(2C), 30.1(2C), 20.5. EI-MS m/z (Calcd. for C₂₂H₂₃FN₄S: 394.16); Found: 395.33 (M+H)⁺. Anal Calcd. for C₂₂H₂₃FN₄S: C, 66.98; H, 5.88; N, 14.20; Found: C, 67.04; H, 5.75; N, 14.25.

1-(1-(6-Fluoro-2-methylquinolin-4-yl)piperidin-4-yl)-3-(4-fluorophenyl)thiourea (BA_43): Off-white solid; Yield: 70%, m.p. 228-229 °C; ¹H NMR (DMSO-d₆): δ_H. 1.63-2.01 (m, 4H), 2.53 (s, 3H), 2.63-3.37 (m, 5H), 6.62-6.99 (m, 6H), 7.20 (d, *J* = 2.2 Hz, 1H), 7.21-7.22 (m, 1H), 7.57 (d, *J* = 9Hz, 1H), 9.93 (s, 1H). ¹³C NMR (DMSO-d₆): δ_C. 177.3, 164.3, 159.7, 158.7(2C), 158.2, 148.5, 134.7, 131.9(2C), 127.1, 121.3, 116.5(2C), 112.9, 107.3, 51.0, 49.7(2C), 30.4(2C), 20.3. EI-MS m/z (Calcd. for C₂₂H₂₂F₂N₄S: 412.15); Found: 413.21 (M+H)⁺. Anal Calcd. for C₂₂H₂₂F₂N₄S: C, 64.06; H, 5.38; N, 13.58; Found: C, 65.99; H, 5.42; N, 13.65.

1-(4-Chlorophenyl)-3-(1-(6-fluoro-2-methylquinolin-4-yl)piperidin-4-yl)thiourea (BA_44): Off-white solid; Yield: 83%, m.p. 208-209 °C; ¹H NMR (DMSO-d₆): δ_H. 1.63-2.01 (m, 4H), 2.55 (s, 3H), 2.66-3.42 (m, 5H), 5.22 (s, 1H) 6.67-6.87 (m, 3H), 7.25 (d, *J* = 8.2 Hz, 2H), 7.28-7.38 (m, 2H), 8.02 (d, *J* = 7.7 Hz, 1H), 10.01 (s, 1H). ¹³C NMR (DMSO-d₆): δ_C. 177.1, 160.1, 159.6, 158.5, 147.9, 137.7, 134.1, 131.7, 130.9(2C), 129.5(2C), 127.3, 122.5, 113.7, 106.9, 51.9, 50.2(2C), 30.4(2C), 19.8. EI-MS m/z (Calcd. for C₂₂H₂₂ClFN₄S: 428.12); Found: 429.09 (M+H)⁺. Anal Calcd. for C₂₂H₂₂ClFN₄S: C, 61.60; H, 5.17; N, 13.06; Found: C, 61.57; H, 5.23; N, 13.17.

1-(1-(6-Fluoro-2-methylquinolin-4-yl)piperidin-4-yl)-3-(4-nitrophenyl)thiourea (BA_45): Off-white solid; Yield: 75%, m.p. 146-147 °C; ¹H NMR (DMSO-d₆): δ_H. 1.60-2.19 (m, 4H), 2.55 (s, 3H), 2.63-3.50 (m, 5H), 5.53 (s, 1H), 6.63-6.68 (m, 3H), 7.35 (m, 2H), 7.88 (d, *J* = 7.6 Hz, 1H), 8.01 (d, *J* = 8.8 Hz, 2H), 10.01 (s, 1H). ¹³C NMR (DMSO-d₆): δ_C. 177.2, 159.8(2C), 158.3, 148.5, 145.4, 144.1, 131.1, 126.4(2C), 124.7(2C), 124.3, 122.3, 113.5, 105.8, 54.4, 51.7(2C), 31.6(2C), 21.2. EI-MS m/z (Calcd. for C₂₂H₂₂FN₅O₂S: 439.15); Found: 440.08 (M+H)⁺. Anal Calcd. for C₂₂H₂₂FN₅O₂S: C, 60.12; H, 5.05; N, 15.93; Found: C, 59.99; H, 5.12; N, 15.86.

1-(1-(6-Fluoro-2-methylquinolin-4-yl)piperidin-4-yl)-3-p-tolylthiourea (BA_46): Off-white solid; Yield: 73%, m.p. 123-124 °C; ¹H NMR (DMSO-d₆): δ_H. 1.61-2.10 (m, 4H), 2.34 (s, 3H), 2.53 (s, 3H), 2.64-3.48 (m, 5H), 5.21 (s, 1H), 6.42-6.97 (m, 5H), 7.29-7.37 (m, 2H), 7.78 (d, *J* = 7.5 Hz, 1H), 9.98 (s, 1H). ¹³C NMR (DMSO-d₆): δ_C. 178.5, 159.6(2C), 158.5, 148.2, 137.7, 135.9, 130.5, 129.5(2C), 127.9, 127.0(2C), 122.3, 113.1, 106.7, 51.9, 53.1(2C), 31.7(2C), 21.7, 20.4. EI-MS m/z (Calcd. for C₂₃H₂₅FN₄S: 408.18); Found: 409.11 (M+H)⁺. Anal Calcd. for C₂₃H₂₅FN₄S: C, 67.62; H, 6.17; N, 13.71; Found C, 67.55; H, 6.09; N, 13.67.

1-(1-(6-Fluoro-2-methylquinolin-4-yl)piperidin-4-yl)-3-(4-methoxyphenyl)thiourea (BA_47): Pale yellow gammy; Yield: 78%; ¹H NMR (DMSO-d₆): δ_H. 1.63-2.03 (m, 4H), 2.56 (s, 3H), 2.62-3.49 (m, 5H), 3.82 (s, 3H), 5.10 (s, 1H), 6.34-6.78 (m, 5H), 7.32-7.87 (m, 3H), 10.01 (s, 1H). ¹³C NMR (DMSO-d₆): δ_C. 178.2, 159.5, 158.7(2C), 157.7, 148.1, 131.3, 130.7, 128.1, 127.1(2C), 122.7, 114.9(2C), 112.0, 106.9, 56.2, 51.9, 50.5(2C), 30.5(2C), 20.3. EI-MS m/z (Calcd. for C₂₃H₂₅FN₄OS: 424.17); Found: 423.11 (M-H)⁻. Anal Calcd. for C₂₃H₂₅FN₄OS: C, 65.07; H, 5.94; N, 13.20; Found: C, 64.97; H, 6.01; N, 13.18.

1-(1-(2-Methyl-6-(trifluoromethyl)quinolin-4-yl)piperidin-4-yl)-3-phenylthiourea (BA_48): Off-white solid; Yield: 73%, m.p. 202-203 °C; ¹H NMR (DMSO-d₆): δ_H. 1.63-1.85 (m, 2H), 2.16-2.22 (m, 2H), 2.54 (s, 3H), 2.84-3.56 (m, 5H), 6.62 (s, 1H), 6.83-7.30 (m, 6H), 8.10-8.35 (m, 3H), 11.21 (s, 1H). ¹³C NMR (DMSO-d₆): δ_C. 178.1, 162.8, 160.5, 152.9, 138.9, 132.0, 129.5, 129.1(2C), 127.9, 126.7, 126.4(2C), 125.1, 124.9, 122.8, 114.0, 55.1, 52.3(2C), 31.3(2C), 20.1. EI-MS m/z (Calcd. for C₂₃H₂₃F₃N₄S: 444.16); Found: 443.02 (M-H)⁻. Anal Calcd. for C, 62.15; H, 5.22; N, 12.60; Found: C, 62.07; H, 5.25; N, 12.54.

1-(4-Fluorophenyl)-3-(1-(2-methyl-6-(trifluoromethyl) quinolin-4-yl)piperidin-4-yl)thiourea (BA_49): Off-white solid; Yield: 73%, m.p. 196-198 °C; ¹H NMR (DMSO-d₆): δ_H. 1.65-1.82 (m, 2H), 2.14-2.21 (m, 2H), 2.52 (s, 3H), 2.85-3.52 (m, 5H), 6.41-6.98 (m, 5H), 7.31 (s, 1H), 8.12-8.33 (m, 3H), 10.51 (s, 1H). ¹³C NMR (DMSO-d₆): δ_C. 178.1, 164.1, 162.5, 160.6, 152.8, 134.9, 131.9, 131.2(2C), 127.9, 126.4, 125.1, 124.9, 122.7, 116.3(2C), 113.9, 54.7, 51.3(2C), 31.0(2C), 20.1. EI-MS m/z (Calcd. for C₂₃H₂₂F₄N₄S: 462.15); Found: 463.35 (M+H)⁺. Anal Calcd. for C₂₃H₂₂F₄N₄S: C, 59.73; H, 4.79; N, 12.11; Found: C, 59.63; H, 4.85; N, 12.17.

1-(4-Chlorophenyl)-3-(1-(2-methyl-6-(trifluoromethyl)quinolin-4-yl)piperidin-4-yl)thiourea (BA_50): Off-white solid; Yield: 73%, m.p. 146-147 °C; ¹H NMR (DMSO-d₆): δ_H. 1.76-1.89 (m, 2H), 2.14-2.20 (m, 2H), 2.53 (s, 3H), 2.82-3.56 (m, 5H), 6.57-6.89 (m, 3H), 7.21-7.35 (m, 3H), 8.14-8.35 (m, 3H), 10.55 (s, 1H). ¹³C NMR (DMSO-d₆): δ_C. 178.5, 162.3, 160.1, 152.7, 136.9, 134.1, 131.9, 131.1(2C), 129.7(2C), 128.0, 126.2, 125.0, 124.6, 122.9, 113.5, 52.1, 50.4(2C), 30.4(2C), 20.5. EI-MS m/z (Calcd. for C₂₃H₂₂ClF₃N₄S: 478.12); Found: 479.35 (M+H)⁺. Anal Calcd. for C₂₃H₂₂ClF₃N₄S: C, 57.68; H, 4.63; N, 11.70; Found: C, 57.75; H, 4.54; N, 11.65.

1-(1-(2-Methyl-6-(trifluoromethyl)quinolin-4-yl)piperidin-4-yl)-3-(4-nitrophenyl)thiourea (BA_51): Off-white solid; Yield: 73%, m.p. 187-187 °C; ¹H NMR (DMSO-d₆): δ_H. 1.63-1.83 (m, 2H), 2.17-2.23 (m, 2H), 2.54 (s, 3H) 2.69-3.77 (m, 5H), 4.98 (brs, 1H), 6.69-7.01 (m, 3H), 8.03-8.35 (m, 5H), 10.40 (s, 1H). ¹³C NMR (DMSO-d₆): δ_C. 178.8, 162.0, 160.2, 152.8, 145.1, 144.5, 131.9, 128.1, 125.7, 125.5, 124.9(2C), 124.5(2C), 123.9(2C), 112.9, 51.5, 49.9(2C), 30.1(2C), 20.3. EI-MS m/z (Calcd. for C₂₃H₂₂F₃N₅O₂S: 489.14); Found: 490.24 (M+H)⁺. Anal Calcd. for C₂₃H₂₂F₃N₅O₂S: C, 56.43; H, 4.53; N, 14.31; Found: C, 56.52; H, 4.46; N, 14.27.

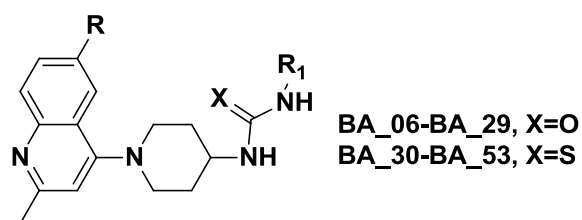
1-(1-(2-Methyl-6-(trifluoromethyl)quinolin-4-yl)piperidin-4-yl)-3-p-tolylthiourea (BA_52): Off-white solid; Yield: 73%, m.p. 192-194 °C; ¹H NMR (DMSO-d₆): δ_H. 1.61-1.88 (m, 2H), 2.17-2.21 (m, 2H), 2.34 (s, 3H), 2.53 (s, 3H), 2.79-3.76 (m, 5H, CH), 5.01 (s, 1H), 6.37-6.97 (m, 5H), 8.12-8.35 (m, 3H), 10.23 (s, 1H). ¹³C NMR (DMSO-d₆): δ_C. 178.5, 162.3, 159.9, 152.5, 137.9, 136.0, 132.2, 129.8(2C), 127.7, 126.1(2C), 125.7, 124.7(2C), 122.5, 113.3, 51.2, 50.1(2C), 30.4(2C), 21.5, 20.1. EI-MS m/z (Calcd. for C₂₄H₂₅F₃N₄S: 458.18); Found: 457.02 (M-H)⁻. Anal Calcd. for C₂₄H₂₅F₃N₄S: C, 62.86; H, 5.50; N, 12.22; Found: C, 62.79; H, 5.56; N, 12.27.

1-(4-Methoxyphenyl)-3-(1-(2-methyl-6-(trifluoromethyl)quinolin-4-yl)piperidin-4-yl)thiourea (BA_53): Off-white solid; Yield: 75%, m.p. 238-239 °C; ¹H NMR (DMSO-d₆): δ_H. 1.61-1.84 (m, 2H), 2.18-2.23 (m, 2H), 2.54 (s, 3H), 2.64-2.79 (m, 5H), 3.83 (s, 3H), 4.89 (s, 1H), 6.33-6.87 (m, 4H), 7.31 (s, 1H), 8.15-8.34 (m, 3H), 10.12 (s, 1H). ¹³C NMR (DMSO-d₆): δ_C. 178.5, 162.5, 159.5(2C), 152.5, 132.4, 131.0(2C), 128.1(2C), 126.4, 125.1, 124.7(2C), 115.6(2C), 113.6, 56.2, 54.6, 51.8(2C), 31.0(2C), 20.4. EI-MS m/z (Calcd. for C₂₄H₂₅F₃N₄OS: 474.17); Found: 475.32 (M+H)⁺. Anal Calcd. for C₂₄H₂₅F₃N₄OS: C, 60.74; H, 5.31; N, 11.81; Found: C, 60.85; H, 5.22; N, 11.99.

5.1.4 *In vitro* Msm Gyr B assay, supercoiling assay, antimycobacterial potency and cytotoxicity studies of the synthesized molecules

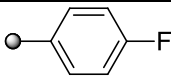
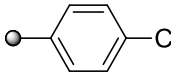
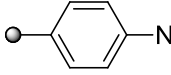
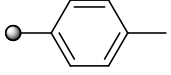
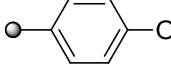
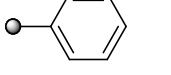
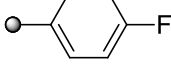
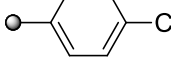
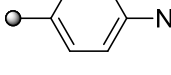
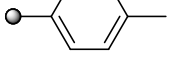
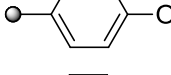
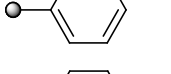
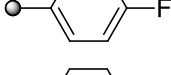
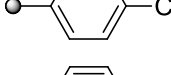
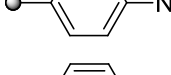
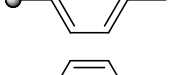
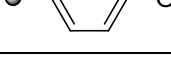
All the synthesized derivatives were evaluated for their *in vitro* Msm Gyr B assay and supercoiling assay for the derivation of SAR and lead optimization. The compounds were further subjected to a whole cell screening against *Mtb* H₃₇Rv strain to understand their bactericidal potency using the agar dilution method and later the safety profile of these molecules were evaluated by checking the *in vitro* cytotoxicity against RAW 264.7 cell line (mouse macrophage) at 50 μM concentration by MTT assay, and the results are shown in **Table 5.2**.

Table 5.2 *In vitro* biological evaluation of the synthesized derivatives **BA_06** – **BA_29** and **BA_30** – **BA_53**

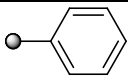
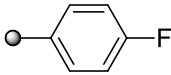

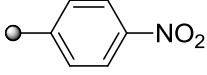
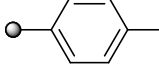
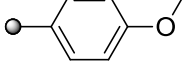
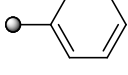
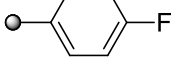
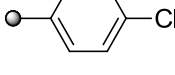
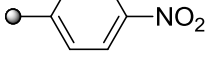
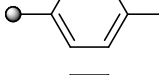
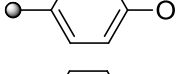
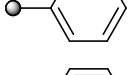
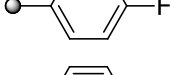
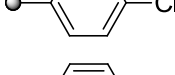
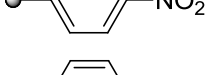
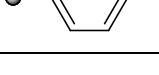


Comp	R	R ₁	<i>Msm</i> Gyr B assay (IC ₅₀)	<i>Mtb</i> Supercoiling assay (IC ₅₀)	<i>Mtb</i> MIC (μM)	Cytotoxicity at 50 μM (% Inhib.)
BA_06	H		17.26±0.87	9.79±0.23	25.84	33.87
BA_07	H		34.88±1.81	19.74±0.27	34.09	49.39
BA_08	H		12.94±1.13	8.2±0.24	7.91	40.07
BA_09	H		16.95±0.59	10.63±0.18	15.41	30.37
BA_10	H		20.48±1.52	14.82±0.32	24.14	51.44
BA_11	H		22.02±1.7	18.54±0.41	32.02	49.54
BA_12	OCH ₃		12.18±0.94	9.32±0.22	32.02	66.47
BA_13	OCH ₃		18.48±0.44	14.8±0.17	25.66	17.31
BA_14	OCH ₃		16.24±1.13	14.33±0.21	17.35	42.40
BA_15	OCH ₃		6.99±0.85	5.33±0.16	14.70	35.01
BA_16	OCH ₃		11.48±0.32	8.63±0.31	15.45	28.17
BA_17	OCH ₃		9.25±0.42	5.86±0.22	12.57	19.58
BA_18	F		20.52±1.26	9.84±0.29	33.03	48.88

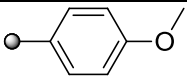
Conti....

Comp	R	R ₁	<i>Msm</i> Gyr B assay (IC ₅₀)	<i>Mtb</i> Supercoiling assay (IC ₅₀)	<i>Mtb</i> MIC (μM)	Cytotoxicity at 50 μM (% Inhib.)
BA_19	F		1.78±0.23	0.78±0.13	3.82	25.39
BA_20	F		48.98±2.66	29.63±0.65	50.78	49.67
BA_21	F		6.83±0.62	2.14±0.18	9.52	47.89
BA_22	F		15.05±0.55	8.83±0.44	15.97	39.73
BA_23	F		10.12±0.85	7.62±0.31	7.65	49.67
BA_24	CF ₃		14.9±0.53	8.3±0.22	29.35	20.13
BA_25	CF ₃		19.77±1.1	11.8±0.31	24.89	39.75
BA_26	CF ₃		33.98±2.3	17.3±0.33	48.53	29.11
BA_27	CF ₃		47.63±2.1	22.3±0.54	52.2	48.24
BA_28	CF ₃		16.6±1.3	9.2±0.2	28.05	16.23
BA_29	CF ₃		41.2±0.96	19.8±0.36	54.26	29.00
BA_30	H		12.7±2.1	9.4±0.2	16.6	11.82
BA_31	H		29.81±1.5	16.72±0.2	36.14	32.93
BA_32	H		12.31±0.92	8.12±0.13	15.21	20.83
BA_33	H		3.77±0.24	1.21±0.2	7.65	31.83
BA_34	H		7.26±0.33	2.66±0.32	15.68	21.63
BA_35	H		19.42±1.91	13.51±0.35	30.22	21.93

Conti....

Comp	R	R ₁	<i>Msm</i> Gyr B assay (IC ₅₀)	<i>Mtb</i> Supercoiling assay (IC ₅₀)	<i>Mtb</i> MIC (μM)	Cytotoxicity at 50 μM (% Inhib.)
BA_36	OCH ₃		2.14±0.15	0.91±0.05	3.81	41.89
BA_37	OCH ₃		8.7±0.22	2.31±0.31	14.72	29.28
BA_38	OCH ₃		0.95±0.12	0.62±0.16	3.47	29.73
BA_39	OCH ₃		2.5±0.26	0.88±0.04	1.72	24.93
BA_40	OCH ₃		11.14±0.39	7.94±0.3	7.28	44.93
BA_41	OCH ₃		10.1±1.26	6.17±0.23	15.84	31.82
BA_42	F		68.22±2.8	39.44±0.43	63.26	37.38
BA_43	F		45.92±1.92	23.54±0.53	63.26	33.93
BA_44	F		41.1±0.98	21.5±0.55	31.68	32.28
BA_45	F		56.15±1.3	25.5±0.4	63.26	40.73
BA_46	F		59.3±0.65	25.41±0.2	67.94	23.93
BA_47	F		39.51±0.87	17.84±0.31	31.68	21.29
BA_48	CF ₃		39.04±1.3	29.4±0.43	35.82	23.28
BA_49	CF ₃		48.5±2.9	22.84±0.77	66.53	50.72
BA_50	CF ₃		16.53±0.91	4.12±0.14	30.68	11.82
BA_51	CF ₃		41.8±0.44	7.54±0.18	51.07	19.80
BA_52	CF ₃		24.68±1.8	5.1±0.22	31.68	19.27

Conti....

Comp	R	R ₁	<i>Msm</i> Gyr B assay (IC ₅₀)	<i>Mtb</i> Supercoiling assay (IC ₅₀)	<i>Mtb</i> MIC (μM)	Cytotoxicity at 50 μM (% Inhib.)
BA_53	CF ₃		32.56±0.52	34.5±0.87	66.88	41.83
		Novobiocin	180±3.9 nM	46±10 nM	>200	NT
		Isoniazid	nd	nd	0.66	NT
		Rifampicin	nd	nd	0.23	NT
		Moxifloxacin	>50	11.2±0.36	1.26	NT

IC₅₀, 50% inhibitory concentration; *Mtb*, *Mycobacterium tuberculosis*; MIC, minimum inhibitory concentration; NT, not tested; nM, nanomolar

Msm Gyr B, *Mycobacterium smegmatis* Gyr B inhibition assay

Mtb DNA gyrase supercoiling enzyme inhibition activity

In vitro activity against *Mtb* H₃₇Rv, Against RAW 264.7 cells

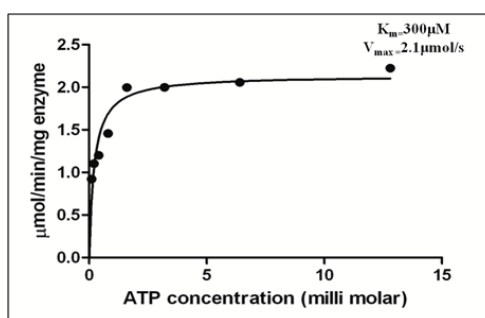


Figure 5.2: ATPase activity of *Msm* DNA gyrase B protein as a function of substrate (ATP) concentration at a constant enzyme concentration (15 μM).

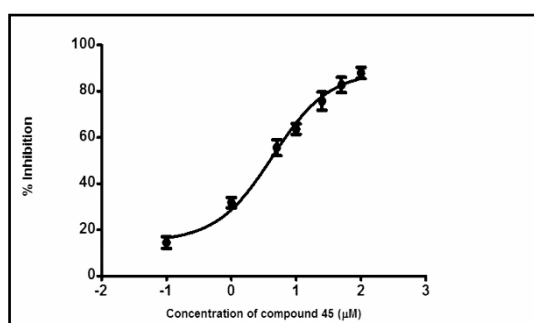


Figure 5.3: Dose response curve of compound BA_38 with *Msm* DNA Gyr B ATPase assay at six various concentrations.

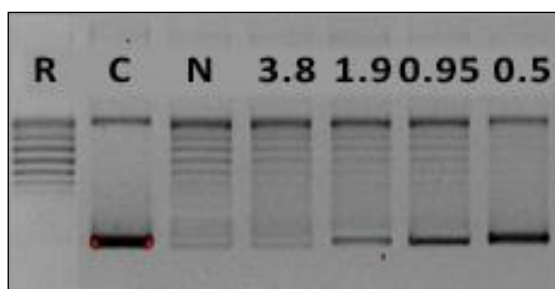


Figure 5.4: Picture depicting the supercoiling assay of most active compound **BA_38** at four different concentrations of 3.8, 1.9, 0.95 and 0.5 μM ; R-Relaxed DNA (substrate + DMSO); C-Control (Relaxed DNA substrate + DNA Gyrase + DMSO); N-Novobiocin.

5.1.5 Docking studies

In order to fully explore the structure–activity relationship associated with the *Msm* Gyr B inhibitors, compounds were docked to the Gyr B ATPase domain of *Msm* retrieved from protein data bank (PDB ID: 4B6C) using extra precision mode (XP) of Glide module. The reference ligand 6-(3,4-dimethylphenyl)-3-[[4-[3-(4-methyl piperazin-yl) propoxy]phenyl]amino]pyrazine-2-carboxamide was further re-docked with the active site residues of the *Msm* protein to validate the active site cavity. The ligand exhibited a Glide score of -6.93 kcal/mole and was placed in the active site cavity with amino acids like Asn52, Ile84, Val99, Val98, Asp97, Pro85, Arg141, Arg82, Glu56, Ala53, Asp79, Ile171, Val99, Val123, Ser126, Val128, and Glu4. Re-docking results showed that the crystal compound exhibited similar interactions as that of the original crystal structure and exhibited RMSD of 0.86Å⁰. The crystal ligand 6-(3,4-dimethylphenyl)-3-[[4-[3-(4-methyl piperazin-yl)propoxy]phenyl]amino] pyrazine-2-carboxamide exhibited two important hydrogen bonding interactions in the active site pocket, one between amino group of the carboxamide moiety and oxygen atom of Asp79 while the other was seen between the nitrogen atom of piperazine and hydrogen atom of guanidine moiety of Arg82. The molecule was stabilized by hydrophobic interaction in the hydrophobic pocket, considered to be important for bringing in specificity observed at the enzyme level as per **Figure 5.5**. In the docking studies, all the active compounds from the synthesized compounds, exhibited good docking score with significant polar and non-polar contacts, hydrogen bond interactions with the relevant amino acids and various hydrophobic interactions.

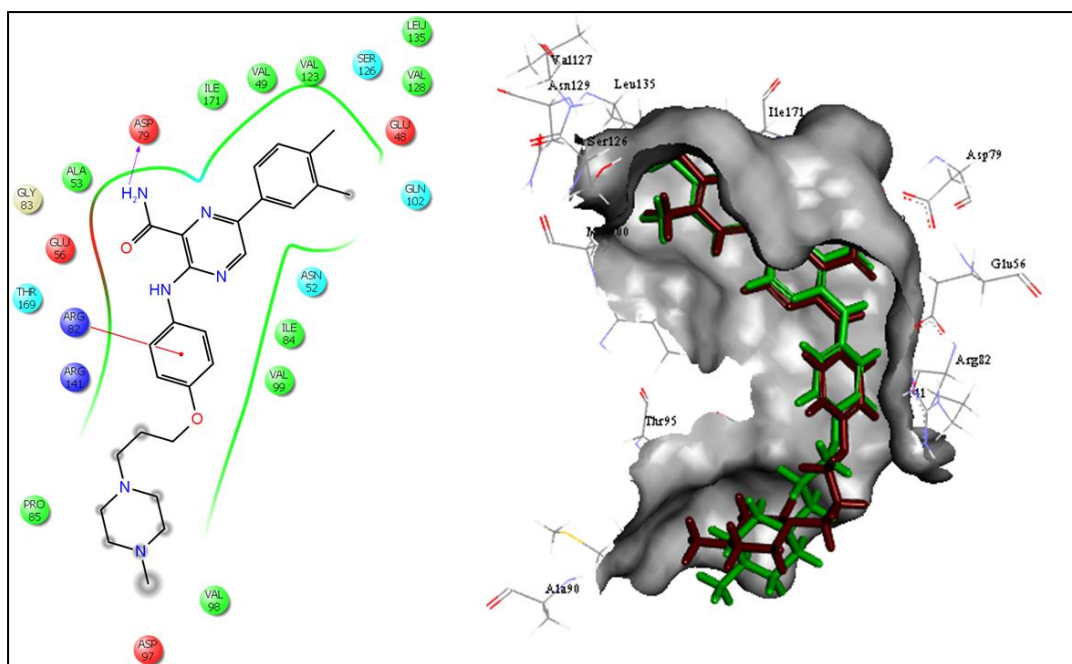


Figure 5.5: Interaction profile picture of ligand 6-(3,4-dimethylphenyl)-3-[[4-[3-(4-methylpiperazin-yl)propoxy]phenyl]amino]pyrazine-2-carboxamide in the active site of *Msm* Gyr B protein.

5.1.6 Evaluation of protein interaction and stability using biophysical characterization experiment (DSF)

The most potent compound from this series of chemical class of molecules was further investigated using a biophysical technique, differential scanning fluorimetry (DSF). The ability of the compounds to stabilize the catalytic domain of the *Msm* Gyr B protein was assessed utilizing the DSF technique by which the thermal stability of the catalytic domain of *Msm* Gyr B native protein and of the protein bound with the ligand was measured. Complex with compound **BA_38** was heated stepwise from 25 to 95 °C in steps of 0.1 °C rise in the presence of a fluorescent dye (sypro orange), whose fluorescence increased as it interacted with hydrophobic residues of the *Msm* Gyr B protein. As the protein was denatured, the amino acid residues became exposed to the dye. A right side positive shift of T_m in comparison to native protein meant higher stabilization of the protein-ligand complex, which was a consequence of the inhibitor binding. In our study, compound **BA_38** showed significant positive T_m shift of 3.1 °C confirming the stability of the protein-ligand complex as shown in **Figure 5.6** which depicts the curves obtained in the DSF experiment for the *Msm* Gyr B protein (red) and protein-compound **BA_38** complex (blue).

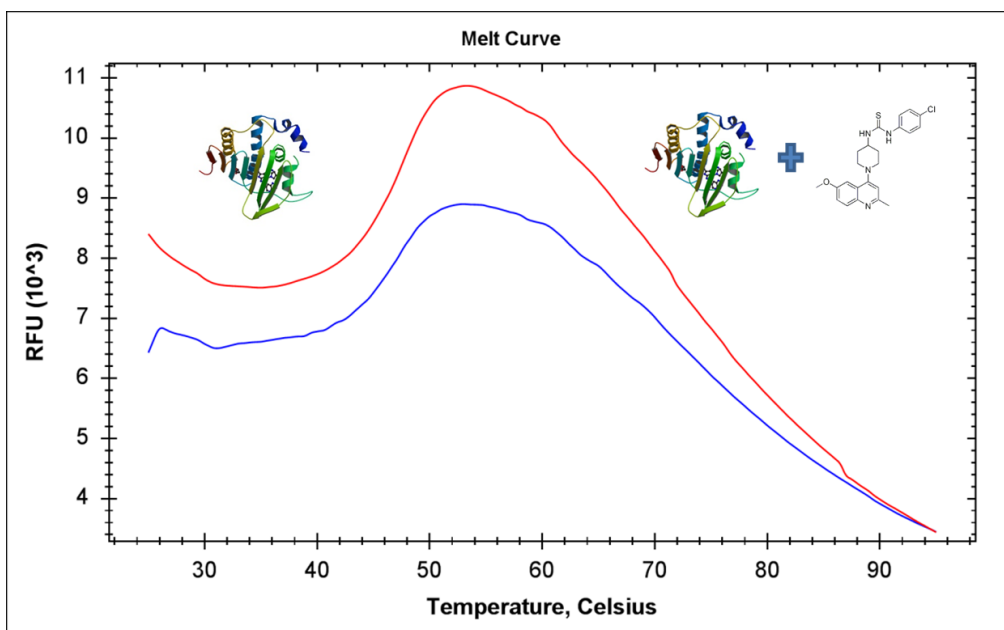


Figure 5.6: DSF experiment for compound **BA_38** showing an increase in thermal stability between the native *Msm* DNA Gyr B protein (red) and *Msm* DNA Gyr B protein-compound **BA_38** complex (blue). The native protein T_m is 45.10 °C and protein with ligand T_m is 48.20 °C, a positive shift of 3.1°C of T_m.

5.1.7 Evaluation of zERG channel inhibition in a zebra fish model.

Since the previously reported *N*-linked aminopiperidine DNA Gyrase inhibitors showed hERG toxicity, to ensure the newly designed molecules did not suffer from similar drawbacks because they possessed a similar architecture. The most potent compound **BA_38** was examined for hERG channel inhibition by assessing arrhythmogenic potential on Zebrafish ether-a-go-go-related gene (zERG) which is orthologous to the human ether-a-go-go-related gene (hERG) the result have been depicted in graphs below (**Figure 5.7a & 5.7b**).

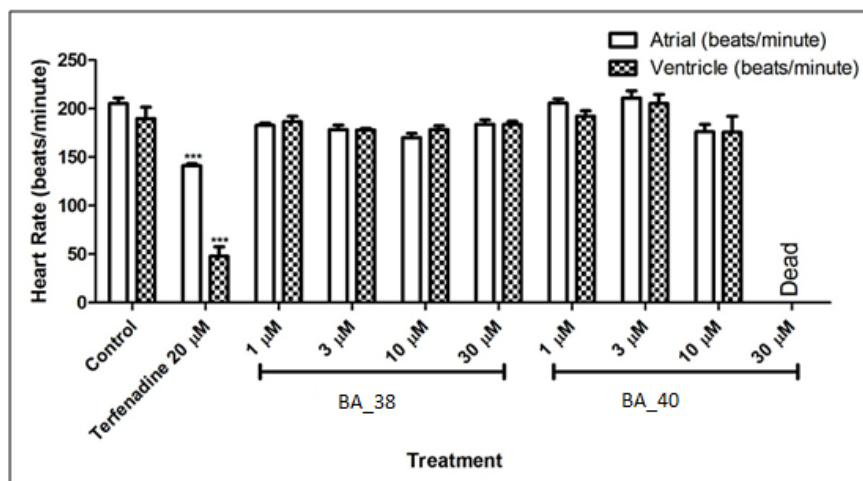


Figure 5.7a: Mean (\pm S.E.M.) of the heart rates of atria and ventricles of Compounds **BA_38** & **BA_40** treatment groups. (* p <0.05, ** p <0.01 and *** p <0.001). Statistical significance was analyzed comparing control group vs. treated groups.

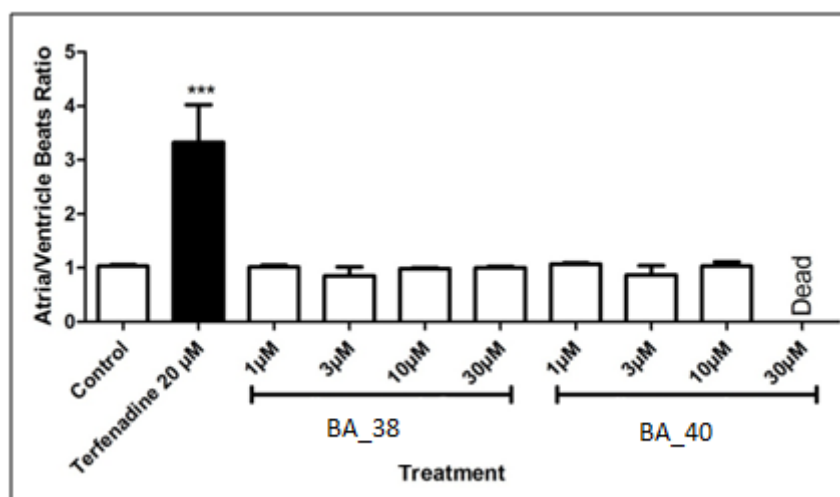


Figure 5.7b: Mean (\pm S.E.M.) score of atrio ventricular ratio of Compounds **BA_38** & **BA_40** treatment groups (* p <0.05, ** p <0.01 and *** p <0.001). Statistical significance was analysed comparing control group vs. all groups.

5.1.8 Discussion

In this series forty eight derivatives were screened for the *Mtb* DNA gyrase supercoiling and the Gyr B inhibitory activity. With respect to structure-activity relationship study, on the left hand core, we attempted phenyl, OCH₃, F and CF₃ groups at R in the sixth position of quinoline nucleus, while the right hand core was substituted with simple/4-F/4-Cl/4-NO₂/4-methyl/4-methoxy phenyl ring. In the first

subset, various substitutions were attempted on the R and R₁ position of quinoline nucleus having oxygen as the X position (**BA_06-29**). The substitutions OCH₃ and F at R position exhibited good activity, while simple phenyl group showed moderate activity and CF₃ was found to be detrimental to activity as compared to other substitutions. These derivatives **BA_06-29** were then evaluated for the Gyr B inhibitory potency using the malachite green assay as described in the materials and methods section. Among the twenty four derivatives evaluated, four compounds showed IC₅₀ less than 10 μM as shown in **Table 5.2**. Among the OCH₃ substituted analogues at R position, the 4-NO₂ of **BA_15** and 4-methoxy phenyl of **BA_17** at R₁ position showed good activity with IC₅₀'s of 6.991±0.85 and 9.255±0.42 μM respectively. A closer look into the interaction profile of these molecules revealed that the NH of quinoline nucleus was involved in a prominent hydrogen bonding interaction with Asp79, analogous to the one observed in the crystal ligand. Compound **BA_15** also showed additional polar contact with Asn52, due to which was found to display good binding with a docking score of -6.74 kcal/mole, similarly compound **BA_17** that showed hydrogen bonds with Asp79 and Glu48. Both the compounds were further stabilized by various hydrophobic interactions with Val125, Val128, Val49, Ile171, Val77, Ala53, Val99, Met100 and Ile84 as shown below in **Figure 5.8**.

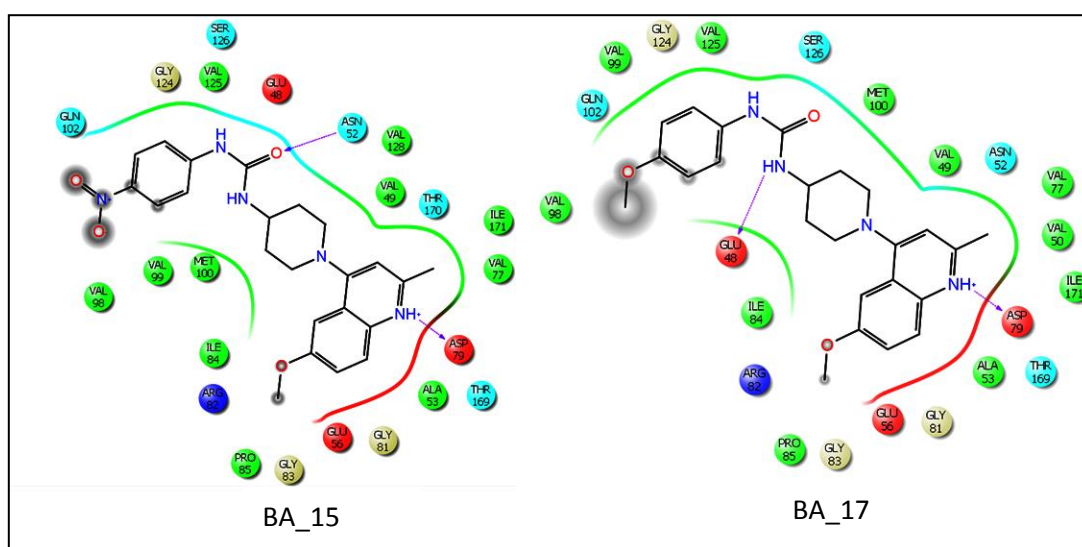


Figure 5.8: The interaction profile pictures of compounds **BA_15** and **BA_17** at the active pocket of Gyr B of *Msm* with respect to the substitutions at R₁ position with 4-nitrophenyl and 4-methoxyphenyl moieties.

The F substituted compounds at R position as in **BA_18-23**, 4-fluoro and 4-nitro phenyl substituted compounds at R₁ (**BA_19** and **BA_21**) turned out to be more promising with IC₅₀'s of 1.78±0.23 and 6.826±0.62 μM respectively. Both the compounds showed good binding with a docking score of -6.12 and -5.99 kcal/mole respectively. The NH group of quinoline nucleus exhibited hydrogen bonding interaction with Asp79, whereas 4-fluoro and 4-nitro groups were exposed to solvent accessible area. Further the compounds were also found to be stabilized by hydrophobic interactions with Val125, Val128, Val49, Ile171, Val77, Ala53, Ile84, Val98, Val99, Met100 and Val123 as shown in **Figure 5.9**.

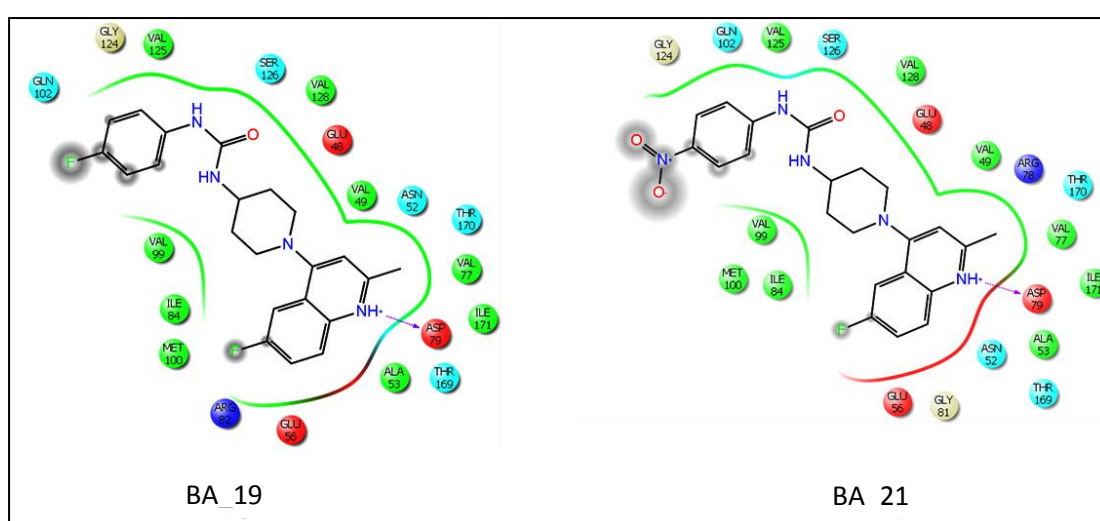


Figure 5.9: The interaction profile pictures of compounds **BA_19** and **BA_21** at the active pocket of Gyr B of *Msm* with respect to the substitutions at R₁ position with 4-tolyl and 4-nitrophenyl moieties with F-substituent at R position.

However it was surprising to note that replacement of F substituent (**BA_19**) with chloro (**BA_20**) on the R₁ position led to a drastic reduction in the activity because the molecule was found to be in a slightly different orientation/pose compared to that of compound **BA_19** thereby losing the hydrogen bonding interaction with Asp79 as presented in **Figure 5.10**.

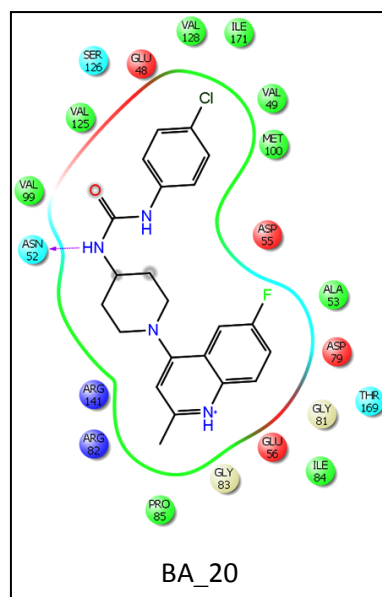


Figure 5.10: The interaction profile pictures of compounds **BA_20** at the active pocket of Gyr B of *Msm* with respect to the substitutions at R₁ position with 4-chlorophenyl with F-substituent at R position.

In the next subset, CF₃ substitution at R position as in **BA_24-29** were found to exhibit moderate activity against *Msm* Gyr B ATPase as well as *Mtb* DNA supercoiling. The simple phenyl and 4-methyl phenyl substitution at R₁ position as in **BA_24** and **BA_28** respectively showed moderate activity when compared with other compounds from this series (IC₅₀'s of 14.9±0.53 and 16.6±1.3 µM in *Msm* Gyr B respectively and 8.3±0.22 and 9.2±0.2 µM respectively in supercoiling assays). Other compounds from this set namely **BA_26**, **BA_27** and **BA_29**, where the R₁ position was substituted with 4-chloro/ nitro and 4-methoxy phenyl were found to be less active with IC₅₀ ≥30 µM. Docking studies revealed that these compounds oriented in a different manner, and a closer look at the interaction pattern of the least active analogues in this class showed that the introduction of 4-chlorophenyl as in compound **BA_26** changed the orientation in the active site of protein and also CF₃ group was found to be placed outside the pocket which could be the reason behind their lesser activity, which was also supported by a low docking score of -4.12 kcal/mole as presented in **Figure 5.11**. The other two compounds substituted with 4-nitro, and 4-methoxy phenyl at R₁ were also not active due to the lack of hydrogen bonding interaction with Asp79 though hydrophobic interactions were present as per **Figure 5.11**.

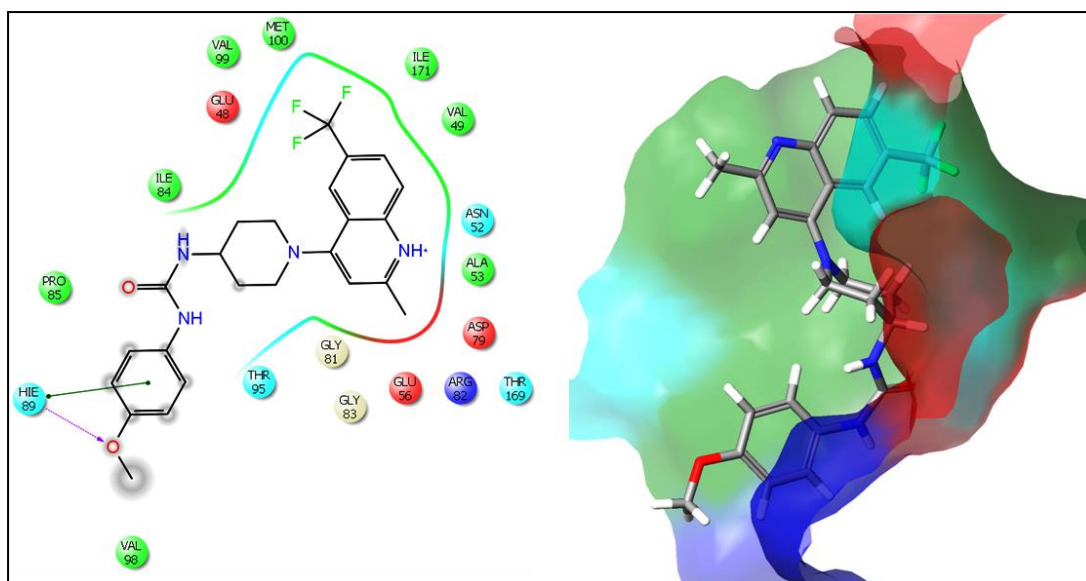


Figure 5.11: The interaction profile pictures of compounds **BA_29** posing out of the active pocket of Gyr B of *Msm* with respect to the substitutions at R₁ position with 4-methoxyphenyl with CF₃-substituent at R position

In the next set of compounds, **BA_30-53**, the effects of similar substituents were explored at R and R₁ positions on left and right sides of quinoline nucleus having S (sulphur) group instead of O (oxygen) at the X position. Among the 24 synthesized compounds, 6 compounds inhibited Gyr B enzyme activity with IC₅₀'s less than 10 μM while compound **BA_38**, 1-(4-chlorophenyl)-3-[1-(6-methoxy-2-methylquinolin-4-yl) piperidin-4-yl] thiourea was found to be the most promising with an Gyr B IC₅₀ of 0.95±0.12 μM which was well correlated with DNA supercoiling IC₅₀ of 0.62±0.16 μM. In this set of compounds simple phenyl and OCH₃ at R position and various simple/4-F/4-Cl/4-NO₂/4-methyl/4-methoxy phenyl ring at R₁ position exhibited good activity, while CF₃ substituted compounds showed moderate activity and F substitution was found to be detrimental to activity. In the first subset, simple phenyl was explored at R position and simple 4-F/4-Cl/4-NO₂/4-methyl/4-methoxy phenyl rings at R₁ position similar to the previous set of compounds (**BA_30-35**). Here, 4-nitro (**BA_33**) and 4-methyl phenyl substituted compounds (**BA_34**) were found to exhibit good activity among the other compounds with IC₅₀s of 3.77±0.24 and 7.26±0.33 μM respectively. The docking analysis of these compounds indicated that the molecules oriented in a similar manner as that of lead compound retaining hydrogen bonding with Asp79 and other significant polar interactions with Glu48 and Asn52 amino acid residues. However their good Gyr B potency could be accounted

due to the hydrophobic interactions which were earlier demonstrated to be crucial for activity and specificity observed at the enzyme level as shown in **Figure 5.12**.

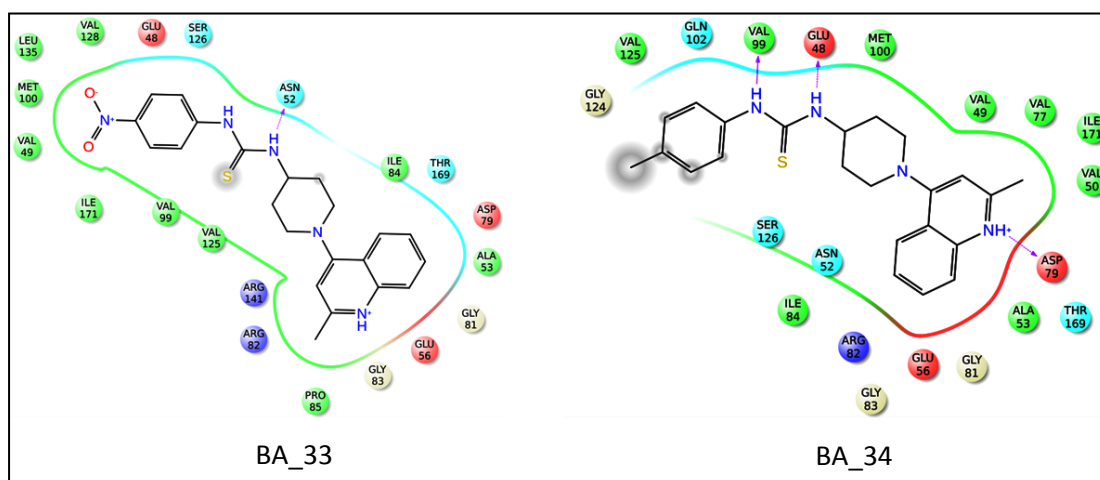


Figure 5.12: The interaction profile pictures of compounds **BA_33** and **BA_34** at the active pocket of Gyr B of *Msm* with respect to the substitutions at R₁ position with 4-nitrophenyl and 4-tolyl without any substituent at R position.

Both the compounds were well inserted into the active site pocket which made these compounds better among all the compounds that showed good binding with the receptor (-6.12 and -6.32 kcal/mole). On the other hand, introduction of 4-fluorophenyl group at R₁ position (**BA_31**) oriented the compound differently, thereby losing key hydrogen bonding interactions which probably resulted in their diminished activity (**Figure 5.13**). The OCH₃ substituted compounds (**BA_36-41**) emerged as the most active compounds as they exhibited activity in the range of 0.95±0.12 to 11.14±0.39 μM in *Msm* Gyr B and 0.62±0.16 to 7.94±0.3 μM in *Mtb* supercoiling assay. The binding analysis of these compounds within the *Msm* protein in the ATP-binding site revealed that the most promising compounds from the series were **BA_36**, **BA_38** and **BA_39** as they showed good binding characteristics with the protein with docking score ranging from -6.87 to -6.33kcal/mole. Also, these compounds were well oriented at the active site cavity of the protein as shown in **Figure 5.14**.

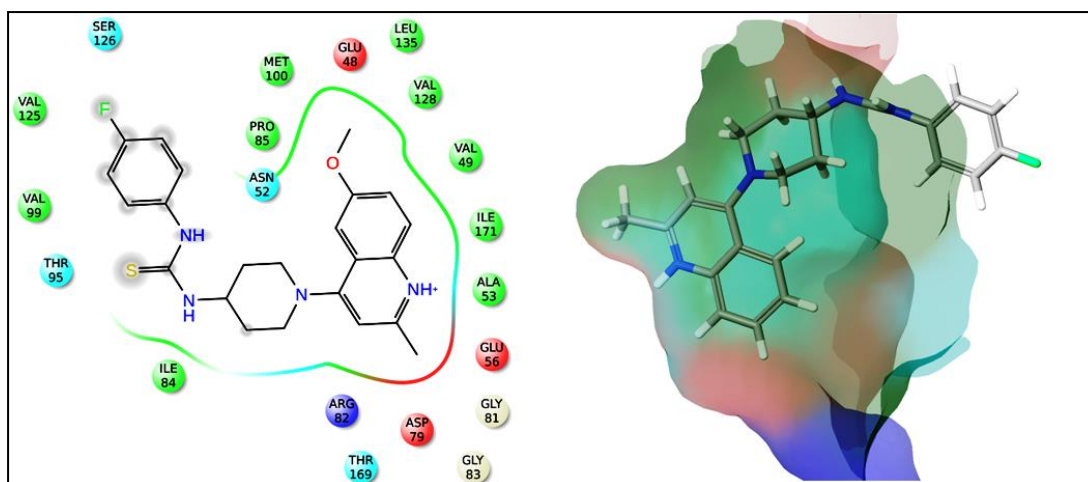


Figure 5.13: The hydrophobic interactions in interaction profile picture of compound **BA_31**.

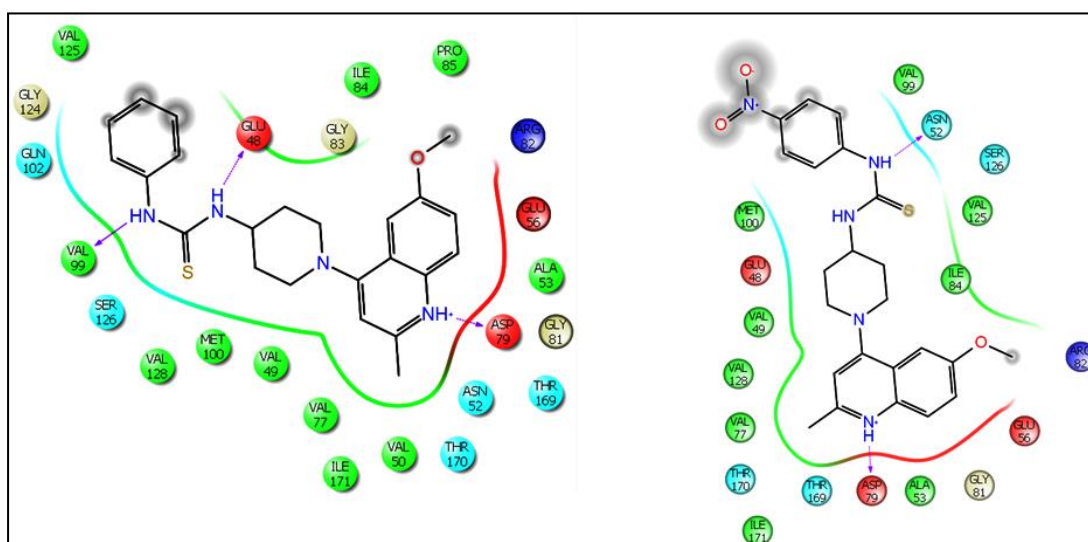


Figure 5.14: The interaction profile pictures of compounds **BA_36** and **BA_39** at the active pocket of Gyr B of *Msm* with respect to the substitutions at R₁ position with phenyl and 4-nitrophenyl with CH₃O substituent at R position.

A closer analysis revealed that all the three active compounds interacted with Asp79 through hydrogen bonding which was important for retaining the bioactivity. Compound **BA_36** was found to show an additional interaction with Glu48, while compound **BA_38** was involved in hydrogen bonding Val99 in addition to Glu48. Furthermore, compound **BA_38** was found to be stabilized by hydrophobic interactions with Ala53, Val128, Val50, Val49, Met100, Ile171 and Val99. Binding pattern of the most active compound **BA_38** is represented in **Figure 5.15**.

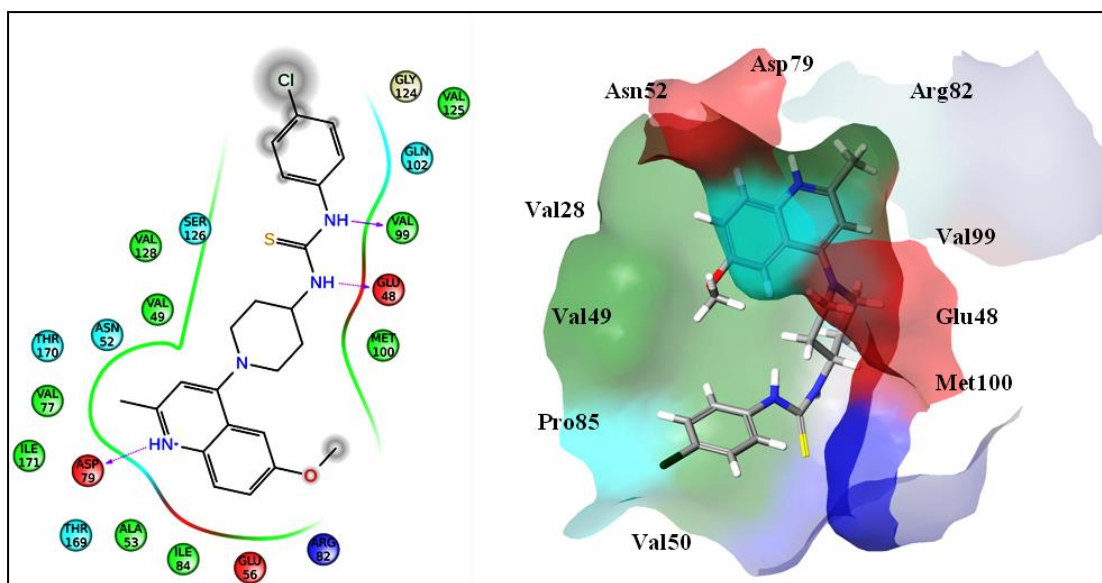


Figure 5.15: The interaction profile pictures of the most active compounds **BA_38** at the active pocket of Gyr B of *Msm*.

The next set of compounds, where R position was substituted with F or CF₃ group (**BA_42-53**) were found to be less active when compared to simple phenyl or OCH₃ substituted compounds. Binding analysis of the least active, F substituted compounds (**BA_42-47**) revealed that all these compounds lacked hydrogen bonding interactions with the protein. This was clearly evident with their lesser docking scores of -4.12 to -3.99 kcal/mol. Similarly among the CF₃ substituted compounds, only 4-methoxy and 4-chloro substitutions were found to exhibit moderate activity (IC₅₀ of 12.56±0.52 and 16.53±0.91 μM) while other compounds did not possess bioactivity. Analysis of this set of compounds revealed that the compounds **BA_50** and **BA_53** were well inserted into active site pocket of *Msm* Gyr B protein and the NH group of quinoline ring was involved in hydrogen bonding interaction with Asp79, while NH of 4-aminopiperidine ring interacted with Glu48 as shown in **Figure 5.16**.

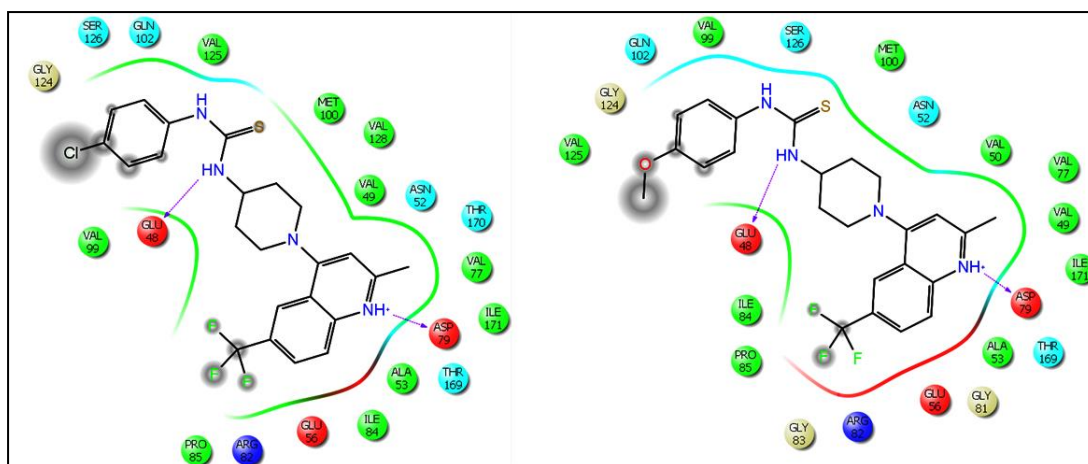


Figure 5.16: The interaction profile pictures of compounds **BA_50** and **BA_53** at the active pocket of Gyr B of *Msm* with respect to the substitutions at R₁ position with 4-chlorophenyl and 4-methoxyphenyl with CF₃ substituent at R position.

Binding analysis of least active compounds revealed that the compounds were oriented differently when compared to active compounds. 4-Fluoro or nitro group at R₁ position was displaced out of the pocket due to which the activity of molecules could have been affected, as shown in **Figure 5.17**.

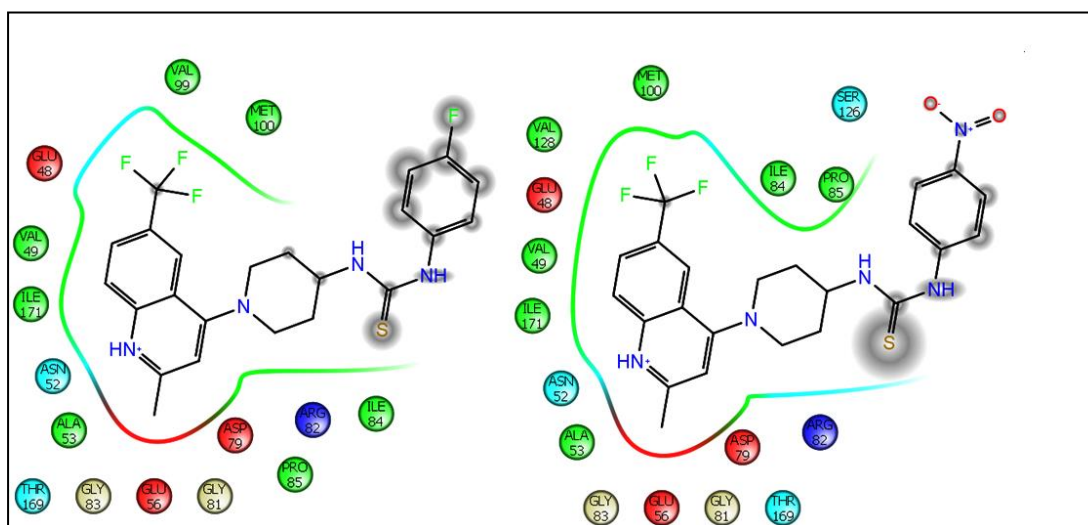


Figure 5.17: The interaction profile pictures of compounds **BA_49** and **BA_51** at the active pocket of Gyr B of *Msm* with respect to the substitutions at R₁ position with 4-nitrophenyl and 4-tolyl without any substituent at R position

Compounds that inhibited ATPase activity of Gyr B protein subsequently were expected to also inhibit DNA supercoiling, as Gyr A and Gyr B domains constituted as holo enzyme DNA gyrase. All the reactions were performed against *Mtb* DNA gyrase enzyme dose dependently at eight concentrations as 100, 50, 25, 12.5, 6.25,

3.125, 1.56 and 0.75 μM , in which the most active compound **BA_38** showed an IC_{50} of $0.62 \pm 0.16 \mu\text{M}$ as illustrated in **Table 5.2, Figure 5.4**. Novobiocin was employed as a standard compound in this assay for comparison. Subsequently, IC_{50} were calculated based on relative quantification using Image lab software, Bio-Rad. Further, the synthesized derivatives were screened for their *in vitro* anti-tubercular activity against *Mtb* H₃₇Rv strain (ATCC 27294) by agar dilution method (Franzbalu G. S., *et al.*, 1998). The minimum inhibitory concentration (MIC) was determined for each compound and was found to be within a range of 0.78 to 50 $\mu\text{g/mL}$, as tested in seven different concentrations in triplicate. Overall, a good correlation was observed between the *Mtb* DNA gyrase supercoiling IC_{50} values and the *in vitro* *Mtb* MICs. However a slight deviation in the *Msm* Gyr B IC_{50} was observed, probably owing to the slight difference in the proteins of the two organisms, as MIC was evaluated on *Mtb* (*M. tuberculosis* H₃₇Rv) and the Gyr B assay was performed on *Msm* protein respectively (Shirude P. S., *et al.*, 2013). Ethambutol, ofloxacin and novobiocin were used as standard compounds. All the synthesized compounds showed good activity against *Mtb* with MIC values ranging from 1.72 to 66.8 μM as shown in **Table 5.2**. Closer observation of MIC values confirmed that these compounds were better in activities than the first-line anti-tubercular drug ethambutol (MIC = 9.84 μM) but were less active when compared to isoniazid and moxifloxacin. The standard compound novobiocin was found to be inactive up to 200 μM concentration. Twenty compounds showed commendable MIC <20 μM among them nine compounds were found to inhibit *Mtb* with MIC <10 μM indicating the importance of fluoro, trifluoromethyl, and nitro functional groups for antimicrobial activity. Again, the compound **BA_38** emerged as the most effective *in vitro* as well with MIC of 3.47 μM against log-phase culture of *Mtb*.

The eukaryotic cell safety profile of the forty eight synthesized compounds was analyzed by testing for *in vitro* cytotoxicity in mouse leukemic monocyte macrophage cell line RAW 264.7 cells at 50 μM concentration using MTT assay (Ferrari M., *et al.*, 1990) All the tested compounds demonstrated a good safety profile with very low inhibitory potential; the inhibitions were within a range of 11.82 to 66.47%. Further, the most active lead molecule **BA_38** exhibited 29.73% inhibition at 50 μM concentration that reflected its safety profile in the eukaryotes. The cytotoxicity results of all the compounds are detailed in **Table 5.2**.

Further, the most potent compound **BA_38** was further examined for zERG channel inhibition by elucidating arrhythmogenic potential on Zebrafish (Chaudhari G. H., *et al.*, 2013). This method has significant advantages over current conventional animal models include ethical issues, low compound requirement and cost of experiment. Compounds **BA_38** and **BA_40** were treated starting from 1 μ M to 30 μ M concentrations with 0.1% DMSO as a vehicle. Both compounds were analyzed for the heart rate variations and AV ratio. The compound **BA_38** was found to be safe when compared to positive control (20 μ M terfenadine), not showing any significant cardiotoxicity until 30 μ M (**Figure 5.7a, 5.7b**). Significant changes in the heart rate as well as AV ratio were also not observed, compared to control group making them relatively safe. But the compound **BA_40** showed lethal at a dose of 30 μ M compared to the control. In our present study with aminopiperidine based *Mtb* DNA gyrase molecules may show cardiotoxicity at 30 μ M.

5.1.9 Highlights of the study

In our continuous efforts to discover novel antimicrobial compounds with anti-gyrase activity, we have described the discovery of novel quinoline derivatives as gyrase inhibitors with potent *Mtb* MIC and inhibitory profiles of the gyrase enzyme with well correlated structural activity relationship and less cytotoxic effect. Among 48 compounds, compound **BA_38** shows supercoiling IC₅₀ of 0.62 \pm 0.16 μ M, *Msm* Gyr B IC₅₀ of 0.95 \pm 0.12 μ M and well correlating MIC of 3.47 μ M against *Mtb*. The compound was also found to be devoid of cytotoxicity against RAW mouse macrophage cell lines and also less cardiotoxic among aminopiperidine class of antimycobacterial agents. Furthermore, we believe that this class of compounds has potential to be as anti-TB drug candidate.

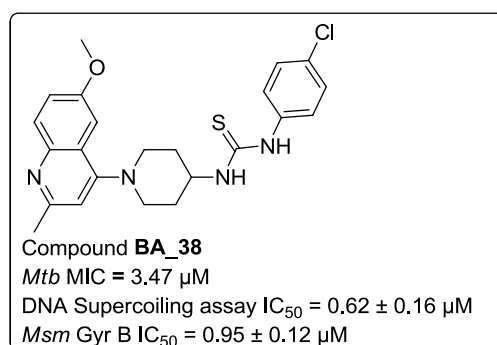


Figure 5.18: Chemical structure and activity of most active compound **BA_38**.

5.2 Development of 1-(4-((6-substituted-2-methylquinolin-4-yl)amino)phenyl)-3-phenylurea/thiourea derivatives as potential *Mtb* DNA gyrase B inhibitors

The design strategy of synthesis of 1-(4-((6-substituted-2-methylquinolin-4-yl)amino)phenyl)-3-phenylurea/thiourea derivatives was based the inhibitor designed in the **Scheme-1** in **Section 5.1, Figure 5.1**, in this a series of 20 new inhibitors were synthesized and tested, the effect of aminopiperidine linker to *p*-phenylenediamine liker on biological activity as well as on the effect of cardiotoxicity carried by the aminopiperidine analogues and to develop the strong SAR based the biological activity and binding mode of inhibitor in the *Mtb* DNA gyrase enzyme. Various substituted quinoline scaffolds were also attempted as the right hand core in the hit expansion step to introduce structural diversification in order to optimize the lead. The designing of the new inhibitor was depicted in the **Figure 5.19** as shown below.

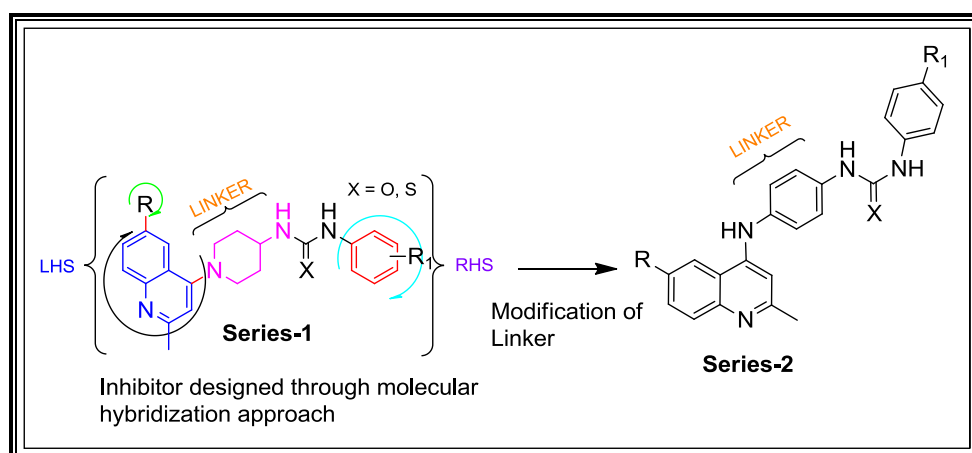


Figure 5.19: Scheme-2, further modifications of constructed hybrid/inhibitor through molecular hopping

5.2.1 Chemical synthesis and characterization

Synthesis of the prosed new *Mtb* DNA gyrase inhibitors was carried in multistep synthesis. The intermediates **BA_03a-b** were prepared in scheme-1 used for further reactions in this second series. 4-Chloro-6-unsustituted / 6-methoxy 2-methyl quinoline **BA_03a-b** were used as starting material. **BA_03a-b** was reacted with *p*-phenylenediamine in methanol at 130 °C for 1 h in microwave conditions using PTSA (*p*-Toluene sulphonic acid. Mono hydrate) as a catalyst to get mixture of products majorly the mono alkylated derivative (**BB_01a-b**) which was column purified and

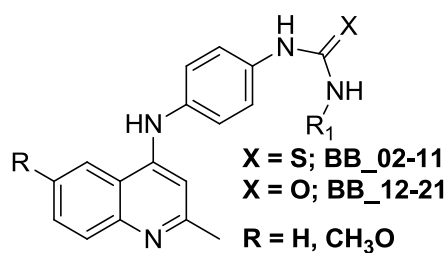
then reacted with various substituted aryl phenyl isocyanates / iso-thiocyanates to get the desired compounds (**BB_02-21**) in good yields. The crude finals were purified by flash column chromatography to get the pure desired compounds.

5.2.2 Experimental protocol followed for synthesis

General procedure for the synthesis of N1-(substituted-2-methylquinolin-4-yl) benzene-1,4-diamine derivatives (BB_01a-b): Intermediate **BA_03a-b** (2g, 0.09mole) , *p*-phenylenediamine (1.35g, 0.012 mole) and PTSA (*p*-Toluene sulphonic acid) monohydrated catalytic 10 mg in 15 mL methanol was irradiated to microwaves for 40 minutes at 130° C (Höglund I. P., *et al.*, 2006) Methanol layer was removed under reduced pressure. The crude was diluted with 50 mL ethyl acetate. The organic layer was washed with 30×2 mL saturated NaHCO₃ solution to get a brown solid which was further purified by giving diethyl ether (50 mL) and dichloromethane (15×2 mL) washings and recrystallized from methanol to afford pale yellow-brown solid (**BB_01a-b**).

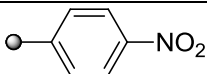

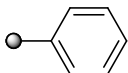
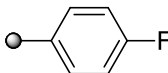

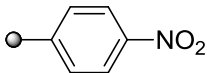
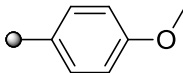
General procedure for the synthesis of 1-(4-((substituted-2-methylquinolin-4-yl) amino) phenyl)-3- substituted phenylurea / thiourea derivatives (BB_02-21): To the corresponding compound (**BB_01a-b**) (0.13g, 0.408 mmol) and **8** (0.15g, 0.537 mmol) were taken in ethanol (3mL) separately to this Et₃N (triethylamine) (1.5 eq) was added. The reaction mixture was cooled to 0° C and corresponding substituted aryl isothiocyanate / isocyanates (1.1 eq) was added and the contents were stirred for 8hr at room temperature. The organic layer was removed under reduced pressure to get crude compound, which was purified by flash column chromatography in 230-400 mesh silica gel using 30-45 % ethyl acetate in n-hexane as eluent to get corresponding thiourea / urea derivatives (**BB_02-BB_21**). The physicochemical properties of synthesized derivatives were shown in **Table 5.3**.

Table 5.3: Physicochemical properties of synthesized compounds **BB_02** – **BB_21**



Comp	R	R ₁	Yield (%)	Melting point (°C)	Molecular formula	Molecular weight
BB_02	H		76	220-221	C ₂₃ H ₁₉ FN ₄ S	402.13
BB_03	H		80	203-204	C ₂₃ H ₁₉ ClN ₄ S	418.20
BB_04	H		73	208-209	C ₂₃ H ₂₀ N ₄ S	384.14
BB_05	H		71	238-239	C ₂₄ H ₂₂ N ₄ OS	414.15
BB_06	H		69	136-137	C ₂₃ H ₁₉ N ₅ O ₂ S	429.13
BB_07	OCH ₃		70	169-170	C ₂₄ H ₂₁ FN ₄ OS	432.14
BB_08	OCH ₃		75	170-171	C ₂₄ H ₂₁ ClN ₄ OS	448.11
BB_09	OCH ₃		77	164-165	C ₂₄ H ₂₂ N ₄ OS	414.15
BB_10	OCH ₃		63	226-227	C ₂₅ H ₂₄ N ₄ O ₂ S	444.16
BB_11	OCH ₃		69	151-152	C ₂₄ H ₂₁ N ₅ O ₃ S	459.14
BB_12	H		71	189-190	C ₂₃ H ₁₉ FN ₄ O	386.15
BB_13	H		76	160-161	C ₂₃ H ₁₉ ClN ₄ O	402.12
BB_14	H		81	215-216	C ₂₃ H ₂₀ N ₄ O	368.16

Conti....

Comp	R	R ₁	Yield (%)	Melting point (°C)	Molecular formula	Molecular weight
BB_15	H		76	243-245	C ₂₄ H ₂₂ N ₄ O ₂	398.17
BB_16	H		69	197-198	C ₂₃ H ₁₉ N ₅ O ₃	413.15
BB_17	OCH ₃		80	180-181	C ₂₄ H ₂₁ FN ₄ O ₂	416.16
BB_18	OCH ₃		71	155-156	C ₂₄ H ₂₁ ClN ₄ O ₂	432.14
BB_19	OCH ₃		78	266-267	C ₂₄ H ₂₂ N ₄ O ₂	398.17
BB_20	OCH ₃		69	237-238	C ₂₅ H ₂₄ N ₄ O ₃	428.18
BB_21	OCH ₃		74	214-216	C ₂₄ H ₂₁ N ₅ O ₄	443.16

5.2.3 Characterization of synthesized compounds

N¹-(2-Methylquinolin-4-yl)benzene-1,4-diamine (BB_01a): Pale yellow solid; Yield 78%; m.p: 298-299 °C; ESI-MS was found at m/z 250.61 (M+H)⁺. ¹H NMR (DMSO-d₆-300 MHz) δ_H. 7.92-7.46 (m, 4H), 6.46 (d, *J* = 8.1 Hz, 2H), 6.39 (d, *J* = 8.2 Hz, 2H), 2.62 (s, 3H).

N¹-(6-Methoxy-2-methylquinolin-4-yl)benzene-1,4-diamine (BB_01b): Pale brown solid; Yield 77%; m.p: 282-283 °C; ESI-MS was found at m/z 280.41 (M+H)⁺. ¹H NMR (DMSO-d₆-300 MHz) δ_H. 7.87-7.44 (m, 4H), 6.44 (d, *J* = 8.2 Hz, 2H), 6.39 (d, *J* = 7.9 Hz, 2H), 3.91 (s, 3H), 2.62 (s, 3H).

1-(4-(2-Methylquinolin-4-ylamino)phenyl)-3-phenylthiourea (BB_02): Off-white solid; Yield: 76%, m.p. 220-221 °C; ¹H NMR (DMSO-d₆): δ_H. 11.53 (s, 2H), 8.20-7.19 (m, 2H), 7.90-7.20 (m, 7H), 6.47 (d, *J* = 7.1 Hz, 2H), 6.68 (s, 1H), 6.58 (s, 1H), 6.31 (d, *J* = 6.9 Hz, 2H), 2.54 (s, 3H). ¹³C NMR (DMSO-d₆): δ_C. 180.4, 160.5, 149.8, 148.9, 142.3, 139.6, 130.5, 130.1 (2C), 129.2 (3C), 127.4 (2C), 126.9 (2C), 125.2, 124.3, 119.1, 118.5 (2C), 106.6, 19.7. EI-MS m/z (Calcd. for C₂₃H₂₀N₄S: 384.14);

Found: 383.11 (M-H)⁻. Anal Calcd. for C₂₃H₂₀N₄S: C, 71.85; H, 5.24; N, 14.57; Found: C, 71.91; H, 5.18; N, 14.63.

1-(4-Fluorophenyl)-3-(4-(2-methylquinolin-4-ylamino)phenyl)thiourea (BB_03):

Off-white solid; Yield: 80%, m.p. 203-204 °C; ¹H NMR (DMSO-d₆): δ_H. 11.51 (s, 2H), 8.28-7.57 (m, 4H), 7.12 (m, 2H), 6.68 (s, 1H), 6.59 (s, 1H), 6.53 (d, *J* = 8.9 Hz, 2H), 6.41 (d, *J* = 7.9 Hz, 2H), 6.28 (d, *J* = 8.0 Hz, 2H), 2.53 (s, 3H). ¹³C NMR (DMSO-d₆): δ_C. 180.5, 164.3, 159.9, 149.5, 149.0, 142.4, 134.7, 131.3 (2C), 129.8, 129.1 (2C), 127.6 (2C), 125.2, 124.5, 119.9, 118.4 (2C), 114.7 (2C), 106.9, 20.5. EI-MS *m/z* (Calcd. for C₂₃H₁₉FN₄S: 402.13); Found: 403.41 (M+H)⁺. Anal Calcd. for C₂₃H₁₉FN₄S: C, 68.63; H, 4.76; N, 13.92; Found: C, 68.55; H, 4.82; N, 13.99.

1-(4-Chlorophenyl)-3-(4-(2-methylquinolin-4-ylamino)phenyl)thiourea (BB_04):

Off-white solid; Yield: 73%, m.p. 208-209 °C; ¹H NMR (DMSO-d₆): δ_H. 11.54 (s, 2H), 8.31-7.58 (m, 4H), 7.27 (d, *J* = 8.2 Hz, 2H), 6.68 (s, 1H), 6.58 (s, 1H), 6.52 (d, *J* = 6.8 Hz, 2H), 6.38 (d, *J* = 6.9 Hz, 2H), 6.31 (d, *J* = 7.0 Hz, 2H), 2.51 (s, 3H). ¹³C NMR (DMSO-d₆): δ_C. 181.1, 159.7, 149.9, 149.2, 142.1, 137.4, 134.3, 131.9 (2C), 129.7, 129.4 (2C), 128.9, 128.7, 27.5 (2C), 125.1, 124.3, 119.7, 118.6 (2C), 105.9, 20.9. EI-MS *m/z* (Calcd. for C₂₃H₁₉ClN₄S: 418.10); Found: 419.56 (M+H)⁺. Anal Calcd. for C₂₃H₁₉ClN₄S: C, 65.94; H, 4.57; N, 13.37; Found: C, 66.03; H, 4.51; N, 13.31.

1-(4-(2-Methylquinolin-4-ylamino)phenyl)-3-(4-nitrophenyl)thiourea (BB_05):

Pale yellow solid; Yield: 71%, m.p. 238-239 °C; ¹H NMR (DMSO-d₆): δ_H. 11.56 (s, 2H), 8.13 (d, *J* = 8.4 Hz, 2H), 8.01-7.56 (m, 4H), 6.78 (s, 1H), 6.59 (d, *J* = 7.9 Hz, 2H), 6.54 (s, 1H), 6.42 (d, *J* = 6.9 Hz, 2H), 6.21 (d, *J* = 7.0 Hz, 2H), 2.51 (3H). ¹³C NMR (DMSO-d₆): δ_C. 180.2, 159.7, 149.9, 149.5, 145.3, 144.5, 142.8, 129.6, 129.0 (2C), 127.9 (2C), 125.5 (2C), 124.9, 124.5 (2C), 123.9, 120.3, 118.3 (2C), 106.7, 20.2. EI-MS *m/z* (Calcd. for C₂₃H₁₉N₅O₂S: 429.13); Found: 428.09 (M-H)⁻. Anal Calcd. for C₂₃H₁₉N₅O₂S: C, 64.32; H, 4.46; N, 16.31; Found: C, 64.29; H, 4.51; N, 16.35.

1-(4-Methoxyphenyl)-3-(4-(2-methylquinolin-4-ylamino)phenyl)thiourea

(BB_06): Pale brown solid; Yield: 69%, m.p. 136-137 °C; ¹H NMR (DMSO-d₆): δ_H. 11.53 (s, 2H), 8.23-7.55 (m, 4H), 6.79 (d, *J* = 8.1 Hz, 2H), 6.68 (s, 1H), 6.56 (s, 1H), 6.42 (d, *J* = 7.2 Hz, 2H), 6.34 (d, *J* = 8.0 Hz, 2H), 6.23 (d, *J* = 7.1 Hz, 2H), 3.83 (s,

3H), 2.53 (s, 3H). ^{13}C NMR (DMSO- d_6): δ_{C} . 179.4, 160.3, 159.9, 149.7, 149.1, 142.5, 131.2, 129.9, 128.7 (2C), 128.1 (2C), 127.6 (2C), 125.6, 124.1, 119.9, 118.5 (2C), 114.8 (2C), 106.9, 56.5, 19.9. EI-MS m/z (Calcd. for $\text{C}_{24}\text{H}_{22}\text{N}_4\text{OS}$: 414.15); Found: 415.29 (M+H) $^+$. Anal Calcd. for $\text{C}_{24}\text{H}_{22}\text{N}_4\text{OS}$: C, 69.54; H, 5.35; N, 13.52; Found: C, 69.45; H, 5.29; N, 13.47.

1-(4-(6-Methoxy-2-methylquinolin-4-ylamino)phenyl)-3-phenylthiourea (BB_07): Off-white solid; Yield: 70%, m.p. 169-170 °C; ^1H NMR (DMSO- d_6): δ_{H} . 11.52 (s, 2H), 8.24-7.26 (m, 7H), 6.82 (m, 1H), 6.69 (s, 1H), 6.59 (s, 1H), 6.42 (d, $J = 7.4$ Hz, 2H), 6.19 (d, $J = 7.2$ Hz, 2H), 3.83 (s, 3H), 2.51 (s, 3H). ^{13}C NMR (DMSO- d_6): δ_{C} . 179.4, 156.1, 155.6, 148.4, 145.5, 141.3, 139.5, 130.9, 129.7 (2C), 129.1 (2C), 128.0 (2C), 127.1 (2C), 122.2, 121.4, 117.2 (2C), 107.4, 101.7, 56.1, 19.9. EI-MS m/z (Calcd. for $\text{C}_{24}\text{H}_{22}\text{N}_4\text{OS}$: 414.15); Found: 413.03 (M-H) $^-$. Anal Calcd. for $\text{C}_{24}\text{H}_{22}\text{N}_4\text{OS}$: C, 69.54; H, 5.35; N, 13.52; Found: C, 69.61; H, 5.29; N, 13.57.

1-(4-Fluorophenyl)-3-(4-(6-methoxy-2-methylquinolin-4-ylamino) phenyl) thiourea (BB_08): Off-white solid; Yield: 75%, m.p. 170-171 °C; ^1H NMR (DMSO- d_6): δ_{H} . 11.56 (s, 2H), 8.13-7.30 (m, 3H), 7.12-6.21 (m, 8H), 6.68 (s, 1H), 6.56 (s, 1H), 3.84 (s, 3H), 2.54 (s, 3H). ^{13}C NMR (DMSO- d_6): δ_{C} . 181.1, 163.9, 157.5, 155.8, 148.4, 145.7, 142.5, 134.9, 131.8 (2C), 130.6, 129.5, 127.9 (2C), 122.5, 121.6, 117.3 (2C), 116.5 (2C), 107.2, 101.8, 56.0, 20.7. EI-MS m/z (Calcd. for $\text{C}_{24}\text{H}_{21}\text{FN}_4\text{OS}$: 432.14); Found: 433.55 (M+H) $^+$. Anal Calcd. for $\text{C}_{24}\text{H}_{21}\text{FN}_4\text{OS}$: C, 66.65; H, 4.89; F, 4.39; N, 12.95; Found: C, 66.58; H, 4.92; N, 13.01.

1-(4-Chlorophenyl)-3-(4-(6-methoxy-2-methylquinolin-4-ylamino) phenyl) thiourea (BB_09): Pale yellow solid; Yield: 77%, m.p. 164-165 °C; ^1H NMR (DMSO- d_6): δ_{H} . 11.51 (s, 2H), 8.17-7.28 (m, 5H), 6.70 (s, 1H), 6.61 (d, $J = 7.8$ Hz, 2H), 6.57 (s, 1H), 6.45 (d, $J = 7.9$ Hz, 2H), 6.22 (d, $J = 7.4$ Hz, 2H), 3.82 (s, 3H), 2.53 (s, 3H). ^{13}C NMR (DMSO- d_6): δ_{C} . 180.7, 157.8, 155.4, 148.2, 145.8, 142.5, 137.6, 134.5, 132.1 (2C), 130.7, 129.9 (2C), 129.4, 127.8 (2C), 122.3, 121.6, 118.4 (2C), 107.5, 101.9, 56.6, 20.8. EI-MS m/z (Calcd. for $\text{C}_{24}\text{H}_{21}\text{ClN}_4\text{OS}$: 448.11); Found: 449.56 (M+H) $^+$. Anal Calcd. for $\text{C}_{24}\text{H}_{21}\text{ClN}_4\text{OS}$: C, 64.20; H, 4.71; N, 12.48; Found: C, 64.15; H, 4.76; N, 12.43.

1-(4-(6-Methoxy-2-methylquinolin-4-ylamino)phenyl)-3-(4-nitrophenyl)thiourea (BB_10): Pale yellow solid; Yield: 63%, m.p. 226-227 °C; ^1H NMR (DMSO- d_6): δ_{H} .

11.57 (s, 2H), 8.35-7.31 (m, 5H), 6.74 (d, $J = 7.8$ Hz, 2H), 6.67 (s, 1H), 6.58 (s, 1H), 6.44 (d, $J = 6.9$ Hz, 2H), 6.30 (d, $J = 7.6$ Hz, 2H), 3.83 (s, 3H), 2.51 (s, 3H). ^{13}C NMR (DMSO- d_6): δ_{C} . 179.1, 157.5, 155.7, 148.4, 145.9, 145.2, 144.6, 142.3, 130.7, 128.1, 126.8 (2C), 125.3 (2C), 124.9 (2C), 122.1, 121.3, 118.1 (2C), 107.5, 101.8, 55.9, 20.9. EI-MS m/z (Calcd. for $\text{C}_{24}\text{H}_{21}\text{N}_5\text{O}_3\text{S}$: 459.14); Found: 460.19 ($\text{M}+\text{H}$) $^+$. Anal Calcd. for $\text{C}_{24}\text{H}_{21}\text{N}_5\text{O}_3\text{S}$: C, 62.73; H, 4.61; N, 15.24; Found: C, 62.75; H, 4.59; N, 15.18.

1-(4-(6-Methoxy-2-methylquinolin-4-ylamino)phenyl)-3-(4-methoxyphenyl)

thiourea (BB_11): Off-white solid; Yield: 69%, m.p. 151-152 °C; ^1H NMR (DMSO- d_6): δ_{H} . 11.53 (s, 2H), 8.25-7.26 (m, 3H), 6.91 (d, $J = 7.2$ Hz, 2H), 6.69 (s, 1H), 6.59 (s, 1H), 6.45 (d, $J = 6.9$ Hz, 2H), 6.34 (d, $J = 6.8$ Hz, 2H), 6.24 (d, $J = 7.1$ Hz, 2H), 3.89 (s, 3H), 3.84 (s, 3H), 2.53 (s, 3H). ^{13}C NMR (DMSO- d_6): δ_{C} . 180.5, 160.3, 157.3, 155.1, 148.1, 145.7, 142.9, 131.5, 130.9, 129.1, 128.4 (2C), 127.9 (2C), 122.8, 121.6, 118.5 (2C), 115.2 (2C), 106.1, 101.9, 55.2 (2C), 20.6. EI-MS m/z (Calcd. for $\text{C}_{25}\text{H}_{24}\text{N}_4\text{O}_2\text{S}$: 444.16); Found: 445.09 ($\text{M}+\text{H}$) $^+$. Anal Calcd. for $\text{C}_{25}\text{H}_{24}\text{N}_4\text{O}_2\text{S}$: C, 67.54; H, 5.44; N, 12.60; Found: C, 67.59; H, 5.41; N, 12.64.

1-(4-(2-Methylquinolin-4-ylamino)phenyl)-3-phenylurea (BB_12): Off-white solid; Yield: 71%, m.p. 189-190 °C; ^1H NMR (DMSO- d_6): δ_{H} . 11.54 (s, 2H), 8.26-7.21 (m, 9H), 7.41 (d, $J = 7.8$ Hz, 2H), 6.69 (s, 1H), 6.66 (d, $J = 7.9$ Hz, 2H), 6.56 (s, 1H), 2.53 (s, 3H). ^{13}C NMR (DMSO- d_6): δ_{C} . 158.7, 153.5, 149.5, 148.9, 141.7, 139.9, 129.5 (2C), 128.8 (2C), 128.5, 128.3, 124.6, 123.9, 122.5 (2C), 121.4 (2C), 119.7, 117.5 (2C), 106.7, 20.1. EI-MS m/z (Calcd. for $\text{C}_{23}\text{H}_{20}\text{N}_4\text{O}$: 368.16); Found: 367.03 ($\text{M}-\text{H}$) $^-$. Anal Calcd. for $\text{C}_{23}\text{H}_{20}\text{N}_4\text{O}$: C, 74.98; H, 5.47; N, 15.21; Found: C, 75.02; H, 5.54; N, 15.27.

1-(4-fluorophenyl)-3-(4-(2-methylquinolin-4-ylamino)phenyl)urea (BB_13): Off-white solid; Yield: 76%, m.p. 160-161 °C; ^1H NMR (DMSO- d_6): δ_{H} . 11.41 (s, 2H), 8.24-7.55 (m, 6H), 7.47 (d, $J = 6.9$ Hz, 2H), 7.26 (m, 2H), 6.69 (s, 1H), 6.64 (d, $J = 7.0$ Hz, 2H), 6.58 (s, 1H), 2.53 (s, 3H). ^{13}C NMR (DMSO- d_6): δ_{C} . 163.5, 159.7, 153.3, 149.6, 149.1, 141.8, 135.6, 129.9 (2C), 129.0, 125.1, 123.9, 122.7 (2C), 120.1, 119.6 (2C), 117.4 (2C), 116.3 (2C), 106.9, 20.5. EI-MS m/z (Calcd. for $\text{C}_{23}\text{H}_{19}\text{FN}_4\text{O}$: 386.15); Found: 387.29 ($\text{M}+\text{H}$) $^+$. Anal Calcd. for $\text{C}_{23}\text{H}_{19}\text{FN}_4\text{O}$: C, 71.49; H, 4.96; N, 14.50; Found: C, 71.43; H, 5.05; N, 14.61.

1-(4-Chlorophenyl)-3-(4-(2-methylquinolin-4-ylamino)phenyl)urea (BB_14): Pale brown solid; Yield: 81%, m.p. 215-216 °C; ¹H NMR (DMSO-d₆): δ_H. 11.24 (s, 2H), 8.31-7.60 (m, 4H), 7.79 (d, *J* = 8.1 Hz, 2H), 7.51 (d, *J* = 7.9 Hz, 2H), 7.42 (d, *J* = 6.9 Hz, 2H), 6.71 (s, 1H), 6.65 (d, *J* = 7.0 Hz, 2H), 6.59 (s, 1H), 2.52 (s, 3H). ¹³C NMR (DMSO-d₆): δ_C. 159.5, 153.2, 149.7, 149.0, 141.5, 137.9, 133.6, 129.8 (2C), 129.0 (2C), 128.2, 124.9, 123.3, 122.6 (2C), 120.8 (2C), 119.7, 117.4 (2C), 106.3, 20.4. EI-MS *m/z* (Calcd. for C₂₃H₁₉ClN₄O: 402.12); Found: 403.39 (M+H)⁺. Anal Calcd. for C₂₃H₁₉ClN₄O: C, 68.57; H, 4.75; N, 13.91; Found: C, 68.44; H, 4.82; N, 13.95.

1-(4-(2-Methylquinolin-4-ylamino)phenyl)-3-(4-nitrophenyl)urea (BB_15): Pale yellow solid; Yield: 76%, m.p. 243-244 °C; ¹H NMR (DMSO-d₆): δ_H. 11.52 (s, 2H), 8.44 (d, *J* = 8.2 Hz, 2H), 8.25-7.55 (m, 4H), 7.88 (d, *J* = 8.0 Hz, 2H), 7.42 (d, *J* = 7.0 Hz, 2H), 6.69 (s, 1H), 6.64 (d, *J* = 6.9 Hz, 2H), 6.53 (s, 1H), 2.51 (3H). ¹³C NMR (DMSO-d₆): δ_C. 159.5, 153.1, 150.1, 149.7, 145.9, 143.7, 141.0, 130.0 (2C), 128.9, 124.9, 124.5 (2C), 123.3, 122.7 (2C), 120.5 (2C), 120.1, 118.4 (2C), 106.6, 20.5. EI-MS *m/z* (Calcd. for C₂₃H₁₉N₅O₃: 413.15); Found: 414.42 (M+H)⁺. Anal Calcd. for C₂₃H₁₉N₅O₃: C, 66.82; H, 4.63; N, 16.94; Found: C, 66.79; H, 4.68; N, 16.96.

1-(4-Methoxyphenyl)-3-(4-(2-methylquinolin-4-ylamino)phenyl)urea (BB_16): Pale brown solid; Yield: 69%, m.p. 197-198 °C; ¹H NMR (DMSO-d₆): δ_H. 11.53 (s, 2H), 8.22-7.58 (m, 4H), 7.56 (d, *J* = 8.0 Hz, 2H), 7.45 (d, *J* = 6.9 Hz, 2H), 6.98 (d, *J* = 7.1 Hz, 2H), 6.68 (s, 1H), 6.64 (d, *J* = 7.8 Hz, 2H), 6.54 (s, 1H), 3.86 (s, 3H), 2.54 (s, 3H). ¹³C NMR (DMSO-d₆): δ_C. 159.7, 159.3, 153.6, 150.1, 149.5, 141.9, 132.3, 129.8 (2C), 129.1, 124.9, 124.2, 122.7 (2C), 120.9 (2C), 120.6, 118.3 (2C), 115.1 (2C), 106.8, 59.5, 19.9. EI-MS *m/z* (Calcd. for C₂₄H₂₂N₄O₂: 398.17); Found: 399.33 (M+H)⁺. Anal Calcd. for C₂₄H₂₂N₄O₂: C, 72.34; H, 5.57; N, 14.06; Found: C, 72.29; H, 5.63; N, 13.95.

1-(4-(6-Methoxy-2-methylquinolin-4-ylamino)phenyl)-3-phenylurea (BB_17): Off-white solid; Yield: 80%, m.p. 180-181 °C; ¹H NMR (DMSO-d₆): δ_H. 11.55 (s, 2H), 7.79-7.28 (m, 10H), 6.69 (s, 1H), 6.63 (d, *J* = 7.2 Hz, 2H), 6.54 (s, 1H), 3.84 (s, 3H), 2.51 (s, 3H). ¹³C NMR (DMSO-d₆): δ_C. 157.5, 155.2, 153.6, 148.1, 145.4, 141.9, 139.7, 130.5, 129.9, 129.3 (2C), 128.5, 122.7 (2C), 122.3, 121.9 (2C), 120.7, 118.5 (2C), 107.3, 101.6, 56.3, 20.1. EI-MS *m/z* (Calcd. for C₂₄H₂₂N₄O₂: 398.17); Found:

399.46 (M+H)⁺. Anal Calcd. for C₂₄H₂₂N₄O₂: C, 72.34; H, 5.57; N, 14.06; Found: C, 72.39; H, 5.51; N, 14.17.

1-(4-Fluorophenyl)-3-(4-(6-methoxy-2-methylquinolin-4-ylamino)phenyl)urea

(BB_18): Off-white solid; Yield: 71%, m.p. 155-156 °C; ¹H NMR (DMSO-d₆): δ_H. 11.51 (s, 2H), 8.19-7.22 (m, 5H), 7.69 (d, *J* = 7.9 Hz, 2H), 7.46 (d, *J* = 8.0 Hz, 2H), 6.79 (s, 1H), 6.62 (d, *J* = 6.9 Hz, 2H), 6.54 (s, 1H), 3.82 (s, 3H), 2.50 (s, 3H). ¹³C NMR (DMSO-d₆): δ_C. 163.7, 157.3, 155.6, 153.2, 147.4, 145.8, 141.9, 135.5, 130.8, 129.9, 122.7 (2C), 122.3, 120.9, 119.7 (2C), 118.1 (2C), 115.9 (2C), 107.4, 101.2, 56.7, 20.1. EI-MS *m/z* (Calcd. for C₂₄H₂₁FN₄O₂: 416.16); Found: 415.02 (M-H)⁻. Anal Calcd. for C₂₄H₂₁FN₄O₂: C, 69.22; H, 5.08; N, 13.45; Found: C, 69.15; H, 5.13; N, 13.49.

1-(4-Chlorophenyl)-3-(4-(6-methoxy-2-methylquinolin-4-ylamino)phenyl)urea

(BB_19): Pale yellow solid; Yield: 78%, m.p. 266-267 °C; ¹H NMR (DMSO-d₆): δ_H. 11.52 (s, 2H), 8.01 (d, *J* = 8.0 Hz, 2), 7.71-7.41 (m, 5H), 7.51 (d, *J* = 7.9 Hz, 2H), 6.69 (s, 1H), 6.63 (d, *J* = 7.4 Hz, 2H), 6.55 (s, 1H), 3.83 (s, 3H), 2.53 (s, 3H). ¹³C NMR (DMSO-d₆): δ_C. 157.7, 155.1, 153.5, 148.4, 145.7, 142.3, 137.8, 133.6, 130.9, 130.0, 129.9 (2C), 122.8 (2C), 122.3, 121.7 (2C), 121.0, 118.5 (2C), 106.3, 101.6, 55.5, 19.9. EI-MS *m/z* (Calcd. for C₂₄H₂₁ClN₄O₂: 432.14); Found: 433.55 (M+H)⁺. Anal Calcd. for C₂₄H₂₁ClN₄O₂: C, 66.59; H, 4.89; N, 12.94; Found: C, 66.65; H, 4.77; N, 13.01.

1-(4-(6-Methoxy-2-methylquinolin-4-ylamino)phenyl)-3-(4-nitrophenyl)urea

(BB_20): Pale yellow solid; Yield: 69%, m.p. 237-238 °C; ¹H NMR (DMSO-d₆): δ_H. 11.53 (s, 2H), 8.41 (d, *J* = 8.2 Hz, 2H), 7.88 (d, *J* = 8.0 Hz, 2H), 7.75-7.30 (m, 5H), 6.70 (s, 1H), 6.65 (d, *J* = 7.8 Hz, 2H), 6.54 (s, 1H), 3.82 (s, 3H), 2.53 (s, 3H). ¹³C NMR (DMSO-d₆): δ_C. 157.5, 155.9, 152.3, 148.1, 146.4, 145.9, 143.7, 142.2, 130.9, 130.0, 124.7 (2C), 122.9 (2C), 122.5, 121.2, 119.4 (2C), 117.7 (2C), 107.4, 101.9, 56.3, 20.2. EI-MS *m/z* (Calcd. for C₂₄H₂₁N₅O₄: 443.16); Found: 444.39 (M+H)⁺. Anal Calcd. for C₂₄H₂₁N₅O₄: C, 65.00; H, 4.77; N, 15.79; Found: C, 64.92; H, 4.85; N, 15.71.

1-(4-(6-Methoxy-2-methylquinolin-4-ylamino)phenyl)-3-(4-methoxyphenyl)urea

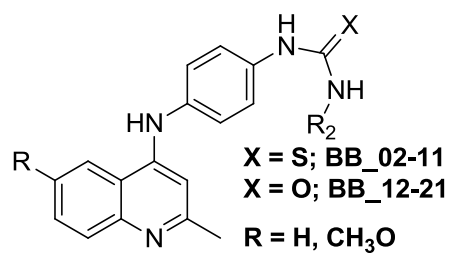
(BB_21): Off-white solid; Yield: 74%, m.p. 214-216 °C; ¹H NMR (DMSO-d₆): δ_H. 11.51 (s, 2H), 8.04-7.31 (m, 5H), 7.57 (d, *J* = 7.2 Hz, 2H), 7.01 (d, *J* = 7.9 Hz, 2H),

6.72 (s, 1H), 6.68 (d, $J = 7.8$ Hz, 2H), 6.54 (s, 1H), 3.88 (s, 3H), 3.81 (s, 3H), 2.54 (s, 3H). ^{13}C NMR (DMSO- d_6): δ_{C} . 159.5, 157.7, 155.4, 153.7, 148.3, 145.6, 141.9, 132.1, 130.5, 129.7, 122.9 (2C), 122.5, 121.3, 120.5 (2C), 118.1 (2C), 115.5 (2C), 107.6, 101.8, 55.1 (2C), 20.4. EI-MS m/z (Calcd. for $\text{C}_{25}\text{H}_{24}\text{N}_4\text{O}_3$: 428.18); Found: 427.12(M-H) $^-$. Anal Calcd. for $\text{C}_{25}\text{H}_{24}\text{N}_4\text{O}_3$: C, 70.08; H, 5.65; N, 13.08; Found: C, 69.97; H, 5.69; N, 13.11.

5.2.4 *In vitro* Msm Gyr B assay, supercoiling assay, antimycobacterial potency and cytotoxicity studies of the synthesized molecules


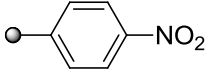
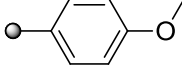
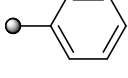
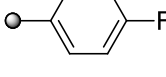
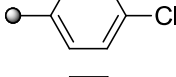
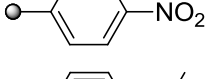
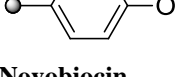
All the synthesized derivatives were evaluated for their *in vitro* Msm Gyr B assay and supercoiling assay for the derivation of SAR and lead optimization. The compounds were further subjected to a whole cell screening against *Mtb* H₃₇Rv strain to understand their bactericidal potency using the agar dilution method and later the safety profile of these molecules were evaluated by checking the *in vitro* cytotoxicity against RAW 264.7 cell line (mouse macrophage) at 50 μM concentration by MTT assay, and the results are shown in **Table 5.4**.

Table 5.4 *In vitro* biological evaluation of the synthesized derivatives **BB_02** – **BB_11** and **BB_12** – **BB_21**.



Comp	R	R ₁	<i>Msm</i> Gyr B assay (IC ₅₀)	<i>Mtb</i> Supercoiling assay (IC ₅₀)	<i>Mtb</i> MIC (μM)	Cytotoxicity at 50 μM (% Inhib.)
BB_02	H		20.31±0.52	11.95±0.2	16.26	49.12
BB_03	H		35.97±1.34	21.94±0.34	>50	39.92
BB_04	H		20.35±2.7	14.42±0.52	3.72	32.55
BB_05	H		7.21±0.71	3.62±0.42	14.56	23.70
BB_06	H		9.06±0.44	3.22±0.2	7.54	38.86
BB_07	OCH ₃		9.2±0.48	5.97±0.32	15.07	44.82
BB_08	OCH ₃		8.53±0.34	4.77±0.42	28.9	51.93
BB_09	OCH ₃		7.13±0.39	3.96±0.25	3.48	42.94
BB_10	OCH ₃		5.23±0.22	2.85±0.15	>50	56.20
BB_11	OCH ₃		8.11±0.73	4.89±0.16	14.06	48.29
BB_12	H		1.48±0.15	9.95±0.32	16.96	33.33
BB_13	H		4.42±0.65	1.27±0.13	4.03	47.01

Conti...

Comp	R	R ₁	<i>Msm</i> Gyr B assay (IC ₅₀)	<i>Mtb</i> Supercoiling assay (IC ₅₀)	<i>Mtb</i> MIC (μM)	Cytotoxicity at 50 μM (% Inhib.)
BB_14	H		13.09±0.59	0.92±0.15	>50	37.89
BB_15	H		0.92±0.16	5.92±0.16	>50	37.32
BB_16	H		15.15±1.32	0.61±0.02	7.84	32.18
BB_17	OCH ₃		0.40±0.11	0.16±0.32	15.66	48.07
BB_18	OCH ₃		0.78±0.17	0.52±0.39	>50	42.44
BB_19	OCH ₃		0.39±0.14	0.29±0.31	1.78	48.12
BB_20	OCH ₃		6.23±0.72	4.13±0.51	>50	48.12
BB_21	OCH ₃		9.69±1.2	5.21±0.33	7.84	25.98
		Novobiocin	180±3.9 nM	46±10 nM	>200	NT
		Moxifloxacin	>50	11.2±0.36	1.26	NT

IC₅₀, 50% inhibitory concentration; *Mtb*, *Mycobacterium tuberculosis*; MIC, minimum inhibitory concentration; NT, not tested; nM, nanomolar
Msm Gyr B, *Mycobacterium smegmatis* Gyr B inhibition assay
Mtb DNA gyrase supercoiling enzyme inhibition activity
In vitro activity against *Mtb* H₃₇Rv, Against RAW 264.7 cells

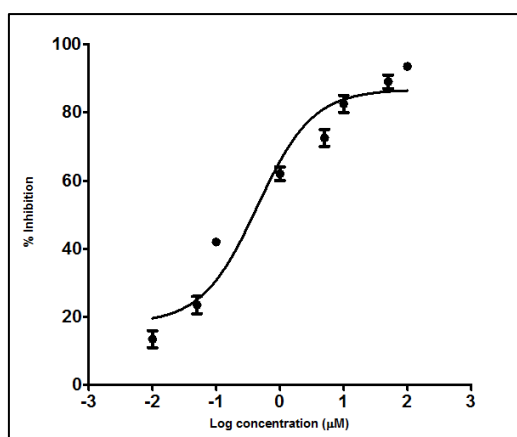


Figure 5.20: Dose response curve of compound **BA_19** with *Msm* DNA Gyr B ATPase assay at six various concentrations

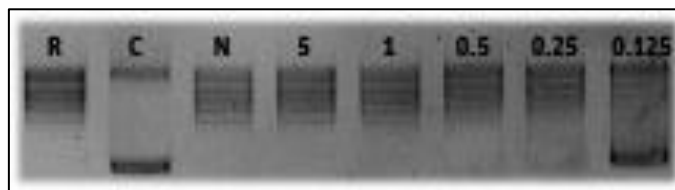


Figure 5.21: Picture depicting the supercoiling assay of most active compound **BB_19** at five different concentrations of 5, 1, 0.5, 0.25 and 0.125 μM ; R-Relaxed DNA (substrate + DMSO); C-Control (Relaxed DNA substrate + DNA Gyrase + DMSO); N-Novobiocin.

5.2.5 Evaluation of protein interaction and stability using biophysical characterization experiment (DSF)

The most potent compound from this series of molecules was further investigated using a biophysical technique, differential scanning fluorimetry (DSF). The ability of the compounds to stabilize the catalytic domain of the *Msm* Gyr B protein was assessed utilizing the DSF technique by which the thermal stability of the catalytic domain of *Msm* Gyr B native protein and of the protein bound with the ligand was measured. In our study, compound **BB_19** showed significant positive T_m shift of 2.9 $^{\circ}\text{C}$ confirming the stability of the protein-ligand complex as shown in **Figure 5.22** which depicts the curves obtained in the DSF experiment for the *Msm* Gyr B protein (red) and protein-compound **BB_19** complex (green).

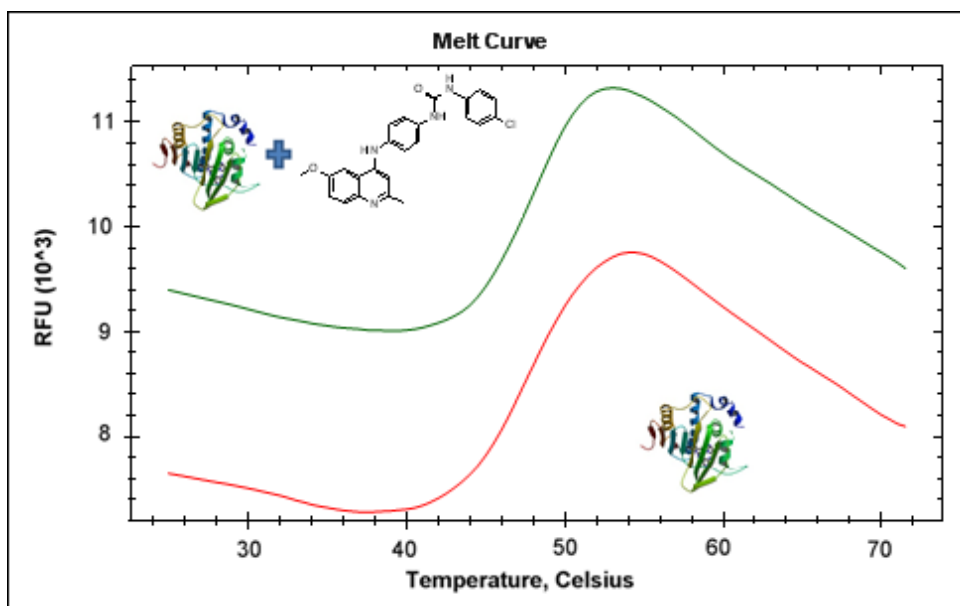


Figure 5.22: DSF experiment for compound **BB_19** showing an increase in thermal stability between the native *Msm* DNA Gyr B protein (red) and *Msm* DNA Gyr B protein-compound **BB_19** complex (green). The native protein T_m is 45.30 °C and protein with ligand T_m is 48.20 °C, a positive shift of 2.9 °C of T_m .

5.2.6 Evaluation of zERG channel inhibition in a zebra fish model

Since the previously reported N-linked aminopiperidine DNA Gyrase inhibitors showed hERG toxicity, to ensure the newly designed molecules did not suffer from similar drawbacks because they possessed a similar architecture having *p*-phenylenediamine derivatives (**BB_02-21**). The most potent compound **BB_19** was examined for hERG channel inhibition by assessing arrhythmogenic potential on Zebrafish ether-a-go-go-related gene (zERG) which is orthologous to the human ether-a-go-go-related gene (hERG) the result have been depicted in graphs below (**Figure 5.23a & 5.23b**).

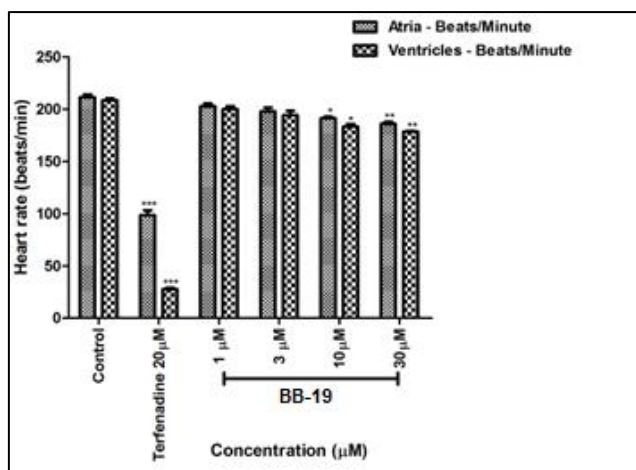


Figure 5.23a: The Mean (\pm S.E.M.) of the heart rates of atria and ventricles of most potent compound **BB_19**. (* p <0.05, ** p <0.01 and *** p <0.001). Statistical significance was analyzed comparing control group vs. treated groups.

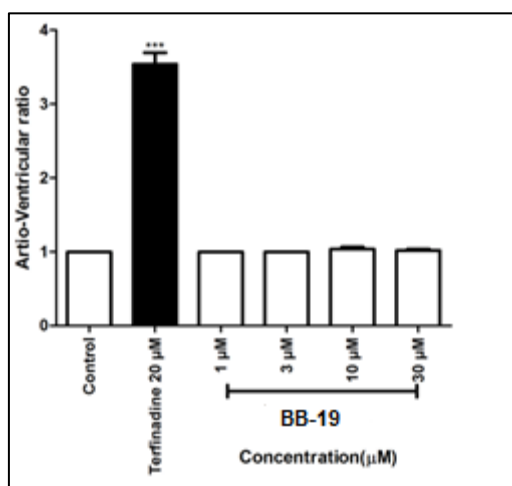


Figure 5.23b: Mean (\pm S. E. M.) score of atrio ventricular ratio of most potent compound **BB_19**. (* p <0. 05, ** p <0. 01 and *** p <0. 001). Statistical significance was analyzed comparing control group vs. all groups.

5.2.7 Discussion

In this series initially we have synthesized 20 quinoline- *p*- phenylenediamine derivatives to check the effect of linker substitution and how it influences the biological activity towards *Mtb* DNA gyrase enzyme. In the lead optimization process the R position was substituted with simple and methoxy at six position of quinoline ring as left hand side modification. On the other side the modifications were restricted to substituted aryl systems as used previously in the Scheme-1 as

simple/F/Cl/NO₂/CH₃O at R₁ position. In this series ten derivatives of thiourea and ten derivatives of urea derivatives synthesized and screened for their biological activity towards *Msm* Gyr B inhibition, *Mtb* DNA gyrase supercoiling assay, their MIC's against *Mtb* H₃₇Rv strain and their safety profile by *in vitro* MTT assay in RAW 264.7 cell lines. Attempt was done to correlate the activity of these compounds with respect to their structure in order to study their SAR. Among 20 derivatives, the methoxy substitution at R position favours than the simple phenyl substitution. In both cases i.e., thiourea and urea derivatives increase of aryl ring deactivating group in RHS side like -NO₂ favours more than the aryl ring activating groups but in case of methoxy at R position, the urea derivatives with moderately aryl ring deactivating group like -Cl substitution favours more. The urea derivatives (**BB_12-21**) were showed good IC₅₀ values of *Msm* Gyr B and DNA gyrase supercoiling assay (0.39±0.14 to 15.15±1.32 μM, 0.16±0.32 to 9.95±0.32 μM respectively). This might be probably accounted for the high electron affinity nature of oxygen which might readily takes part in hydrogen bonding at the active site of Gyr B. The thiourea derivatives (**BB_02-11**) were showed IC₅₀ values of *Msm* Gyr B and DNA gyrase supercoiling assay (5.23±0.22 to 35.97±1.34 μM, 2.85±0.15 to 21.94±0.34 μM respectively). Among all 1-(4-chlorophenyl)-3-(4-((6-methoxy-2-methylquinolin-4-yl)amino)phenyl)urea (**BB_19**) was emerged as most potent molecule with *Msm* Gyr B IC₅₀ 0.39±0.14 μM and *Mtb* DNA gyrase supercoiling IC₅₀ 0.29±0.31 μM with *Mtb* MIC 14.71 μM has less cytotoxic effect at 50 μM of RAW 264.7 cell lines. In this series synthesized derivatives showed promising *in vitro* DNA gyrase supercoiling and *Msm* Gyr B inhibition but failed in MIC's against *Mtb* H₃₇Rv strain screening by agar dilution method.

Further, the most potent compound **BB_19** was further examined for zERG channel inhibition by elucidating arrhythmogenic potential on Zebrafish (Chaudhari, Girish Hari, *et al.*, 2013). This method has significant advantages over current conventional animal models include ethical issues, low compound requirement and cost of experiment. Compound **BB_19** was treated starting from 1μM to 30μM concentrations with 0.1% DMSO as a vehicle. Both compounds were analyzed for the heart rate variations and AV ratio. The compound **BB_19** was found to be safe when compared to positive control (20 μM terfenadine), not showing any significant cardiotoxicity until 30 μM (**Figure 5.23a, 5.23b**). Significant changes in the heart rate

as well as AV ratio were also not observed, compared to control group making them relatively safe. It was a breakthrough we identified new quinoline-*p*-phenylenediamine derivatives were found to be safer than the present aminopiperidine based DNA gyrase inhibitors besides no significant cardiotoxicity.

5.2.8 Highlights of the study

In our continuous efforts to discover novel antimicrobial compounds with anti-gyrase activity, we have described the discovery of novel quinoline - *p*-phenylenediamine derivatives as gyrase inhibitors with good selection of *Mtb* DNA gyrase supercoiling, *Msm* Gyr B inhibition, less cytotoxic effect and mostly devoid of zERG toxicity than the previous aminopiperidine based antitubercular agents even at higher doses. Among 20 compounds, compound **BB_19** showed supercoiling IC₅₀ of 0.29 ± 0.31 μM, *Msm* Gyr B IC₅₀ of 0.39 ± 0.14 and MIC of 1.78 μM against *Mtb*. The compound was also found to less cytotoxic against RAW 264.7 mouse macro phage cell lines. But these synthesized derivatives failed to show effective inhibition of *in vitro Mtb* H₃₇Rv strain screening may be due to efflux mechanism and less permeability across cell membrane.

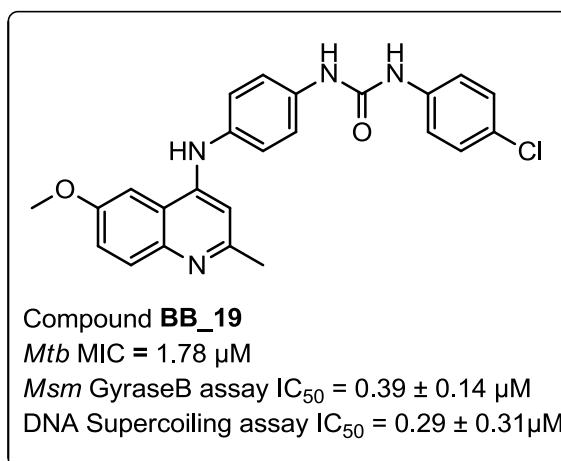


Figure 5.24: Structure and activity of most active compound **BB_19**

5.3 Development of acridine derivatives as selective *Mtb* DNA gyrase inhibitors

In the quest for developing new DNA gyrase inhibitors, we have synthesized 36 new acridine derivatives in this series to develop SAR and the importance of increase in hydrophobicity by substituting tricyclic acridine system to bicyclic quinoline nucleus for designing new mycobacterial DNA gyrase inhibitors as well as to study the effect of zERG toxicity by replacing with aminopiperidine to *p*-phenylenediamine linker. The chemical structures of NBTIs (Novel bacterial topoisomerase inhibitors) comprise a bicyclic hetero aromatic left-hand side (LHS) ring, a mono- or bicyclic hydrophobic right-hand side (RHS) ring and a middle aminopiperidine linker part. As per literature, it is reported that aminopiperidines having a bicyclic aromatic moiety, generally show potent broad-spectrum antibacterial activity, but usually suffer from potent zERG inhibition leading to zERG or cardiotoxicity toxicity (Hameed P. S., *et al.*, 2015, Reck F., *et al.*, 2011) In order to overcome this toxicity issues, we have made an attempt to synthesize tricyclic hetero aromatic acridine as LHS with *p*-phenylenediamine based linker replacing the aminopiperidine as shown in **Figure 5.28** and check its efficacy and cardiotoxicity profile.

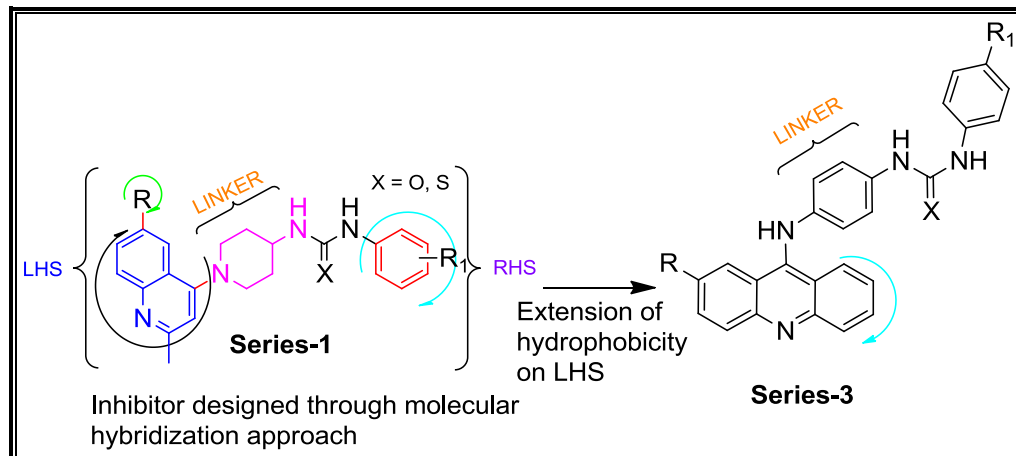


Figure 5.25: Scheme-3, further modifications of constructed hybrid/inhibitor through molecular hopping.

5.3.1 Chemical synthesis and characterization

The titled compounds were synthesized by a series of reactions that has been shown in **Figure 4.3**. Starting with commercially available 2-chlorobenzoic acid it was reacted with different *p*-substituted anilines using modified stille coupling conditions i.e.

Copper, DMF (*N,N* Dimethylformamide) heating the reactants at 140 °C for 6 h resulting in formation of 2-(*p*-tolyl/4-chlorophenyl /phenylamino)benzoic acid derivatives (**BC_01a-c**). Further these **BC_01a-c** intermediates were cyclized intramolecularly in refluxing phosphorousoxychloride (POCl₃) for 6 h to get corresponding 9-chloro-2-substituted acridine derivatives (**BC_02a-c**). The formed acridine intermediates (**BC_02a-c**) were reacted with *p*-phenylenediamine using microwave conditions at 130 °C, PTSA (*p*-toluenesulphonic acid) as catalyst in methanol for 1 h resulting in formation of *N*¹-(2-methyl/2-chloro/simple acridin-9-yl)benzene-1,4-diamine derivatives (**BC_03a-c**). These amine intermediates were further reacted with different substituted aryl sulfonylchlorides and aryl isothio/isocyanates to get desired final sulfonamide (**BC_04-15**) and thiourea/urea (**BC_16-39**) derivatives in good yields and purity. All the reactions were monitored by thin layer chromatography.

5.3.2 Experimental protocol followed for synthesis

General procedure for the synthesis of 2-(*p*-tolylamino)/ 2-((4-chlorophenyl)amino)/ 2-(phenylamino)benzoic acid intermediates (BC_01a-c):

To a stirred solution of 2-chlorobenzoic acid (5g, 32 mmol) in 20 mL of DMF (*N,N*-dimethylformamide) potassium carbonate (7.51g, 54.4 mmol) corresponding aniline (38.4 mmol) and copper powder (0.81g, 12.8 mmol) were added and heated up to 140 °C for 6 h. Progress of reaction was monitored by thin layer chromatography after completion of the reaction, reaction mass was filtered through celite, celite bed was washed with ethyl acetate. The combined organic layer was evaporated under reduced pressure; obtained crude was purified by flash column chromatography using 5-20 % ethyl acetate: hexane as eluent in 100-200 mesh silica gel to get the corresponding phenylamino benzoic acid derivatives in good yield. The intermediates (**BC_01a-c**) were confirmed by mass analysis (ESI mode) and proceed to next step.

Preparation of 9-chloroacridine derivatives from substituted phenylamino benzoic acid intermediates (BC_02a-c):

The phenyl amino benzoic acid derivatives (47 mmol) (**BC_01a-c**) were cyclized intramolecularly to 9-chloroacridine derivatives (**BC_02a-c**) by refluxing them in 60 mL of POCl₃ for 4 h and the reaction was monitored by TLC. After completion, the excess POCl₃ was removed by Rota evaporator under reduced pressure to the crude reaction mass crushed ice was added,

p^H was adjusted ~7 by adding saturated bicarbonate solution. The solid separated was filtered, dried and purified by flash column chromatography using 5-10% ethyl acetate: hexane as eluent in 60-120 mesh silica gel to get the corresponding 9-chloroacridine derivatives in good yield. These intermediates were confirmed by mass analysis (ESI mode) and proceed to next step.

Preparation of N¹-(2-methyl/2-chloro/acridin-9-yl) benzene-1,4-diamine intermediates (BC_03a-c): The 9-chloroacridine derivatives (BC_02a-c) (10 mmol) were further reacted with *p*-phenylenediamine (1.8g, 10.7 mmol) under microwave conditions in methanol using PTSA (*p*-toluene sulphonic acid) as a catalyst (5-10 mg) at 130 °C for 1 h, reaction was monitored by TLC. After completion of reaction, methanol was evaporated under vacuum the crude was dissolved in ethyl acetate, washed with saturated bicarbonate solution. The organic layer was dried over anhydrous sodium sulphate and evaporated under reduced pressure obtained crude was further purified by flash column chromatography in 60-120 silica gel using 10-35% ethyl acetate: hexane as eluent to get an orange to yellow solid in moderate yields.

Preparation of N-(3-methoxy-4-((acridine/2-methylacridin-9-yl) amino) phenyl) methane/ substituted benzene sulphonamide derivatives (BC_04-15): For the preparation of desired sulphonamide derivatives (BC_04-15) corresponding acridine amine derivatives (BC_03a-c) (0.6 mmol) were taken in (3 mL) DMF to this triethylamine (1.38 mmol) and corresponding substituted alkyl/ aryl sulphonyl chlorides (0.6 mmol) were added at 0 °C and allowed to stir at room temperature for 3 h. After completion of reaction crushed ice was added to the crude reaction mass the solid precipitated was filtered, dried and further purified by flash column chromatography in 100-200 mesh silica gel using 5-10 % methanol: dichloromethane as eluent to get desired sulphonamide derivatives in good yields.

Preparation of 1-(3-methoxy-4-((acridine/2-methylacridin-9-yl) amino)phenyl)-3-phenylthiourea/ urea derivatives (BC_16-39 and BC_28-39): For the preparation of desired thiourea (BC_16-27) and urea (BC_28-39) derivatives corresponding acridine amine derivative (BC_03a-c) (0.6 mmol), triethylamine (1.38 mmol) (Et₃N) and substituted phenyl isothiocyanate/isocyanate (0.6 mmol) were dissolved in ethanol and heated up to 80 °C for 8 h reaction was monitored by TLC, after

completion of the reaction the solid precipitated was filtered, dried and recrystallized from ethanol to get the desired corresponding thiourea and urea derivatives. Physicochemical properties of synthesized derivatives as shown in **Table 5.5**

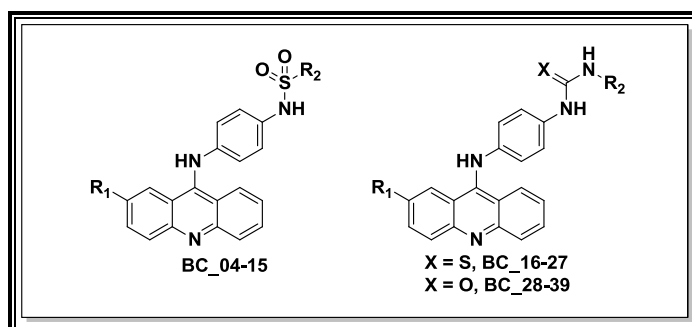
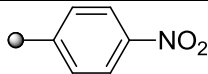
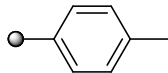
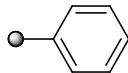

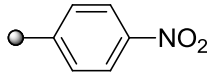
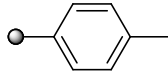
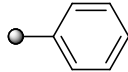

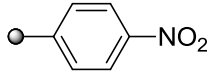
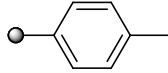
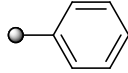
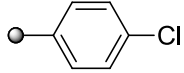
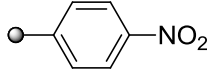
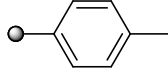
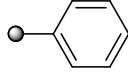

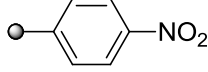
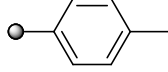


Figure 5.26: General structures of synthesized derivatives **BC_04-BC_39**

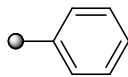
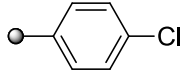
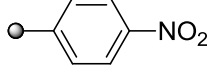
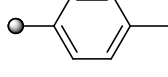
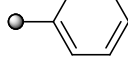
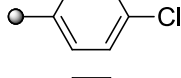
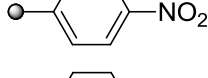
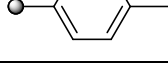
Table 5.5 Physicochemical properties of synthesized acridine derivatives **BC_04-39**

Comp	R ₁	R ₂	Yield (%)	Melting point (°C)	Molecular formula	Molecular weight
BC_04	CH ₃		68	236-238	C ₂₆ H ₂₁ N ₃ O ₂ S	439.14
BC_05	CH ₃		71	245-247	C ₂₆ H ₂₀ ClN ₃ O ₂ S	473.10
BC_06	CH ₃		69	---	C ₂₆ H ₂₀ N ₄ O ₄ S	484.12
BC_07	CH ₃		66	252-254	C ₂₇ H ₂₃ N ₃ O ₂ S	453.15
BC_08	Cl		63	181-183	C ₂₅ H ₁₈ ClN ₃ O ₂ S	459.08
BC_09	Cl		71	189-191	C ₂₅ H ₁₇ Cl ₂ N ₃ O ₂ S	493.04
BC_10	Cl		67	---	C ₂₅ H ₁₇ ClN ₄ O ₄ S	504.07
BC_11	Cl		69	214-216	C ₂₆ H ₂₀ ClN ₃ O ₂ S	473.1
BC_12	H		72	187-189	C ₂₅ H ₁₉ N ₃ O ₂ S	425.12
BC_13	H		77	220-222	C ₂₅ H ₁₈ ClN ₃ O ₂ S	459.08

Conti....

Comp	R ₁	R ₂	Yield (%)	Melting point (°C)	Molecular formula	Molecular weight
BC_14	H		68	187-189	C ₂₅ H ₁₈ N ₄ O ₄ S	470.10
BC_15	H		75	206-208	C ₂₆ H ₂₁ N ₃ O ₂ S	439.14
BC_16	CH ₃		67	120-122	C ₂₇ H ₂₂ N ₄ S	434.16
BC_17	CH ₃		68	138-140	C ₂₇ H ₂₁ ClN ₄ S	468.12
BC_18	CH ₃		65	131-133	C ₂₇ H ₂₁ N ₅ O ₂ S	479.14
BC_19	CH ₃		63	138-140	C ₂₈ H ₂₄ N ₄ S	448.17
BC_20	Cl		66	108-110	C ₂₆ H ₁₉ ClN ₄ S	454.10
BC_21	Cl		66	135-137	C ₂₆ H ₁₈ Cl ₂ N ₄ S	488.06
BC_22	Cl		68	142-144	C ₂₆ H ₁₈ ClN ₅ O ₂ S	499.09
BC_23	Cl		70	149-153	C ₂₇ H ₂₁ ClN ₄ S	468.12
BC_24	H		67	156-158	C ₂₆ H ₂₀ N ₄ S	420.14
BC_25	H		65	147-149	C ₂₆ H ₁₉ ClN ₄ S	454.10
BC_26	H		67	159-161	C ₂₆ H ₁₉ N ₅ O ₂ S	465.13
BC_27	H		64	190-192	C ₂₇ H ₂₂ N ₄ S	434.16
BC_28	CH ₃		69	---	C ₂₇ H ₂₂ N ₄ O	418.18
BC_29	CH ₃		66	163-165	C ₂₇ H ₂₁ ClN ₄ O	452.14
BC_30	CH ₃		61	---	C ₂₇ H ₂₁ N ₅ O ₃	463.16
BC_31	CH ₃		67	---	C ₂₈ H ₂₄ N ₄ O	432.20

Conti....

Comp	R ₁	R ₂	Yield (%)	Melting point (°C)	Molecular formula	Molecular weight
BC_32	Cl		68	168-170	C ₂₆ H ₁₉ ClN ₄ O	438.12
BC_33	Cl		69	234-236	C ₂₆ H ₁₈ Cl ₂ N ₄ O	472.09
BC_34	Cl		68	---	C ₂₆ H ₁₈ ClN ₅ O ₃	483.11
BC_35	Cl		62	253-255	C ₂₇ H ₂₁ ClN ₄ O	452.14
BC_36	H		65	162-164	C ₂₆ H ₂₀ N ₄ O	404.16
BC_37	H		68	241-243	C ₂₆ H ₁₉ ClN ₄ O	438.12
BC_38	H		62	252-254	C ₂₆ H ₁₉ N ₅ O ₃	449.15
BC_39	H		64	---	C ₂₇ H ₂₂ N ₄ O	418.18

5.3.3 Characterization of synthesized compounds

2-(*p*-Tolylamino) benzoic acid (BC_01a): Pale brown solid; Yield 77%; ESI-MS was found at 228.47 (M+H)⁺.

2-((4-Chlorophenyl) amino) benzoic acid (BC_01b): Off-white solid; Yield 78%; ESI-MS was found at 248.78 (M+H)⁺.

2-(Phenylamino) benzoic acid (BC_01c): Off-white solid; Yield 75%; ESI-MS was found at 212.32 (M-H)⁻.

9-Chloro-2-methylacridine (BC_02a): Pale brown solid; Yield 71%; ESI-MS was found at 228.64 (M+H)⁺.

2,9-Dichloroacridine (BC_02b): Pale brown solid; Yield 74%; ESI-MS was found at 249.34 (M+H)⁺.

9-Chloroacridine (BC_02c): Pale orange solid; Yield 69%; ESI-MS was found at 228.47 (M+H)⁺.

N¹-(2-methylacridin-9-yl)benzene-1,4-diamine (BC_03a): Brown solid; Yield 69%; ESI-MS was found at 300.38 (M+H)⁺.

***N*¹-(2-chloroacridin-9-yl)benzene-1,4-diamine (BC_03b)**: Pale brown solid; Yield 68%; ESI-MS was found at 318.89 (M-H)⁻.

***N*¹-(2-chloroacridin-9-yl)benzene-1,4-diamine (BC_03c)** : Pale brown solid; Yield 70%; ESI-MS was found at 286.42 (M+H)⁺.

***N*-(4-((2-Methylacridin-9-yl)amino)phenyl)benzene sulphonamide (BC_04)**: Yellow solid; Yield 68%; mp 236-238 °C; ¹H NMR (DMSO-d₆): δ_H. 2.35 (s, 3H), 6.41 (m, 4H), 7.52-7.83 (m, 10H), 8.01-8.19 (m, 2H), 10.69 (s, 1H), 10.96 (s, 1H). ¹³C NMR (DMSO-d₆): δ_C. 149.9, 142.7, 140.4(2C), 136.6(2C), 132.7(3C), 130.5, 129.6(3C), 128.5, 128.0(3C), 122.2, 121.4, 119.8, 118.9(2C), 117.7(2C), 108.5, 22.4. EI-MS m/z (Calcd. for C₂₆H₂₁N₃O₂S: 439.14); Found: 440.19 (M+H)⁺. Anal Calcd. for C₂₆H₂₁N₃O₂S: C, 71.25; H, 4.82; N, 9.56; Found: C, 71.19; H, 4.79; N, 9.54.

4-Chloro-*N*-(4-((2-methylacridin-9-yl)amino)phenyl)benzenesulfonamide (BC_05): Pale yellow solid; Yield 71%; mp 245-247 °C; ¹H NMR (DMSO-d₆): δ_H. 2.32 (s, 3H), 6.36 (m, 4H), 7.53-7.87 (m, 9H), 8.02-8.22 (m, 2H), 10.68 (s, 1H), 10.94 (s, 1H). ¹³C NMR (DMSO-d₆): δ_C. 150.0, 142.8, 140.2, 138.5(2C), 136.7(2C), 132.2(2C), 130.6, 130.0(3C), 129.4(2C), 128.5(2C), 122.1, 121.4, 119.8, 118.9(2C), 118.7(2C), 108.3, 22.3. EI-MS m/z (Calcd. for C₂₆H₂₀ClN₃O₂S: 473.10); Found: 472.14 (M-H)⁻. Anal Calcd. for C₂₆H₂₀ClN₃O₂S: C, 65.89; H, 4.25; N, 8.87; Found: C, 66.05; H, 4.27; N, 8.85.

***N*-(4-((2-Methylacridin-9-yl)amino)phenyl)-4-nitrobenzenesulfonamide (BC_06)**: Brown gammy; Yield 69%; ¹H NMR (DMSO-d₆): δ_H. 2.36 (s, 3H), 6.42 (m, 4H), 7.53-7.97 (m, 6H), 8.14-8.41 (m, 5H), 10.67 (s, 1H), 10.88 (s, 1H). ¹³C NMR (DMSO-d₆): δ_C. 151.9, 149.7, 146.3, 142.6, 140.1, 139.5(2C), 132.0(2C), 130.3(2C), 128.8(2C), 128.0(2C), 124.9(2C), 122.2, 121.5, 120.0, 119.2(2C), 117.9(2C), 108.4, 22.6. EI-MS m/z (Calcd. for C₂₆H₂₀N₄O₄S: 484.12); Found: 485.31 (M+H)⁺. Anal Calcd. for C₂₆H₂₀N₄O₄S: C, 64.45; H, 4.16; N, 11.56; Found: C, 64.54; H, 4.18; N, 11.54.

4-Methyl-*N*-(4-((2-methylacridin-9-yl)amino)phenyl)benzenesulfonamide (BC_07): Yellow solid; Yield 66%; mp 252-254 °C; ¹H NMR (DMSO-d₆): δ_H. 2.32 (s, 6H), 6.37 (m, 4H), 7.39-7.83 (m, 9H), 8.01-8.23 (m, 2H), 10.67 (s, 1H), 10.93 (s, 1H). ¹³C NMR (DMSO-d₆): δ_C. 149.9, 142.7, 140.1, 138.3, 137.2, 136.4(2C), 132.6(2C), 130.7(2C), 130.1(2C), 129.0(2C), 128.5(2C), 121.9(2C), 119.8, 118.9(2C), 117.7(2C), 108.3, 22.6(2C). EI-MS m/z (Calcd. for C₂₇H₂₃N₃O₂S: 453.15); Found:

454.32 (M+H)⁺. Anal Calcd. for C₂₇H₂₃N₃O₂S: C, 71.50; H, 5.11; N, 9.26; Found: C, 71.72; H, 5.09; N, 9.23.

N-(4-((2-Chloroacridin-9-yl)amino)phenyl)benzenesulfonamide (BC_08): Orange solid; Yield 63%; mp 181-183 °C; ¹H NMR (DMSO-d₆): δ_H. 6.41 (m, 4H), 7.61-7.79 (m, 9H), 7.99-8.17 (m, 3H), 10.71 (s, 1H), 10.90 (s, 1H). ¹³C NMR (DMSO-d₆): δ_C. 149.3, 143.8, 140.4(2C), 136.6, 132.3, 131.9(2C), 131.3(2C), 130.7, 129.8(2C), 128.3, 127.9(3C), 122.7, 121.4, 119.2(3C), 117.8(2C), 109.9. EI-MS m/z (Calcd. for C₂₅H₁₈ClN₃O₂S: 459.08); Found: 458.11 (M-H)⁻. Anal Calcd. for C₂₅H₁₈ClN₃O₂S: C, 65.28; H, 3.94; N, 9.14; Found: C, 65.45; H, 3.92; N, 9.16.

4-Chloro-N-(4-((2-chloroacridin-9-yl)amino)phenyl)benzenesulfonamide

(BC_09): Yellow solid; Yield 71%; mp 189-191 °C; ¹H NMR (DMSO-d₆): δ_H. 6.39 (m, 4H), 7.59-7.81 (m, 8H), 8.01-8.22 (m, 3H), 10.67 (s, 1H), 10.89 (s, 1H). ¹³C NMR (DMSO-d₆): δ_C. 149.2, 143.9, 140.2, 138.4(2C), 136.7, 132.0(2C), 131.7(2C), 130.4, 129.8(2C), 129.4(2C), 128.2(2C), 122.9, 121.6, 119.3(3C), 117.9(2C), 109.7. EI-MS m/z (Calcd. for C₂₅H₁₇Cl₂N₃O₂S: 493.04); Found: 494.25 (M+H)⁺. Anal Calcd. for C₂₅H₁₇Cl₂N₃O₂S: C, 60.73; H, 3.47; N, 8.50; Found: C, 60.92; H, 3.46; N, 8.53.

N-(4-((2-Chloroacridin-9-yl)amino)phenyl)-4-nitrobenzenesulfonamide (BC_10): Brown gammy; Yield 67%; ¹H NMR (DMSO-d₆): δ_H. 6.43 (m, 4H), 7.63-7.97 (m, 5H), 8.07-8.41 (m, 6H), 10.57 (s, 1H), 10.92 (s, 1H). ¹³C NMR (DMSO-d₆): δ_C. 152.8, 149.3, 146.5, 143.9, 140.3, 136.7, 132.2(2C), 131.5(2C), 130.5, 129.0(2C), 128.4(2C), 124.8(2C), 122.9, 121.5, 119.1(3C), 117.7(2C), 109.9. EI-MS m/z (Calcd. for C₂₅H₁₇ClN₄O₄S: 504.07); Found: 505.31 (M+H)⁺. Anal Calcd. for C₂₅H₁₇ClN₄O₄S: C, 59.47; H, 3.39; N, 11.10; Found: C, 59.62; H, 3.40; N, 11.12.

N-(4-((2-Chloroacridin-9-yl)amino)phenyl)-4-methylbenzenesulfonamide

(BC_11): Yellow solid; Yield 69%; mp 214-216 °C; ¹H NMR (DMSO-d₆): δ_H. 2.35 (s, 3H), 6.41 (m, 4H), 7.39-7.78 (m, 8H), 7.99-8.19 (m, 3H), 10.49 (s, 1H), 10.91 (s, 1H). ¹³C NMR (DMSO-d₆): δ_C. 149.5, 143.8, 140.4, 128.3, 137.5, 136.8, 132.3(2C), 131.7(2C), 130.4, 129.9(2C), 128.7(2C), 128.0(2C), 122.8, 121.4, 119.3(3C), 117.6(2C), 109.7, 22.0. EI-MS m/z (Calcd. for C₂₆H₂₀ClN₃O₂S: 473.10); Found: 472.05 (M-H)⁻. Anal Calcd. for C₂₆H₂₀ClN₃O₂S: C, 65.89; H, 4.25; N, 8.87; Found: C, 65.61; H, 4.27; N, 8.85.

N-(4-(Acridin-9-ylamino)phenyl)benzenesulfonamide (BC_12): Orange solid; Yield 72%; mp 187-189 °C; ¹H NMR (DMSO-d₆): δ_H. 6.36 (m, 4H), 7.56-7.94 (m,

11H), 8,19 (m, 2H), 10.56 (s, 1H), 10.89 (s, 1H). ¹³C NMR (DMSO-d₆): δ_C. 150.4, 142.9(2C), 140.3, 136.5, 132.2, 130.6(2C), 129.8(2C), 128.5(3C), 127.8(2C), 126.9(2C), 121.5(2C), 118.8(2C), 117.6(2C), 115.4(2C). EI-MS m/z (Calcd. for C₂₅H₁₉N₃O₂S: 425.12); Found: 426.29 (M+H)⁺. Anal Calcd. for C₂₅H₁₉N₃O₂S: C, 70.57; H, 4.50; N, 9.88; Found: C, 70.76; H, 4.48; N, 9.85.

***N*-(4-(Acridin-9-ylamino)phenyl)-4-chlorobenzenesulfonamide (BC_13):** Pale yellow solid; Yield 77%; mp 220-222 °C; ¹H NMR (DMSO-d₆): δ_H. 6.42 (m, 4H), 7.61-7.96 (m, 10H), 8.15 (m, 2H), 10.53 (s, 1H), 10.91 (s, 1H). ¹³C NMR (DMSO-d₆): δ_C. 150.2, 142.8(2C), 138.4(2C), 136.3, 130.5(2C), 129.7(2C), 129.4(2C), 128.6(3C), 126.9(2C), 121.4(2C), 119.0(2C), 117.8(2C), 115.5(2C). EI-MS m/z (Calcd. for C₂₅H₁₈ClN₃O₂S: 459.08); Found: 460.15 (M+H)⁺. Anal Calcd. for C₂₅H₁₈ClN₃O₂S: C, 65.28; H, 3.94; N, 9.14; Found: C, 65.46; H, 3.96; N, 9.11.

***N*-(4-(Acridin-9-ylamino)phenyl)-4-nitrobenzenesulfonamide (BC_14):** Brown solid; Yield 68%; mp 187-189 °C; ¹H NMR (DMSO-d₆): δ_H. 6.39 (m, 4H), 7.57-7.93 (m, 6H), 8.10-8.41 (m, 6H), 10.49 (s, 1H), 10.87 (s, 1H). ¹³C NMR (DMSO-d₆): δ_C. 152.7, 150.5, 146.2, 142.9(2C), 136.6, 130.4(2C), 128.8(2C), 128.2(3C), 127.0(2C), 124.7(2C), 121.5(2C), 119.1(2C), 117.9(2C), 115.3(2C). EI-MS m/z (Calcd. for C₂₅H₁₈N₄O₄S: 470.10); Found: 469.08 (M-H)⁻. Anal Calcd. for C₂₅H₁₈N₄O₄S: C, 63.82; H, 3.86; N, 11.91; Found: C, 63.65; H, 3.88; N, 11.94.

***N*-(4-(Acridin-9-ylamino)phenyl)-4-methylbenzenesulfonamide (BC_15):** Brown solid; Yield 75%; mp 206-208 °C; ¹H NMR (DMSO-d₆): δ_H. 2.36 (s, 3H), 6.41 (m, 4H), 7.43-7.92 (m, 10H), 8.21 (m, 2H), 10.53 (s, 1H), 10.97 (s, 1H). ¹³C NMR (DMSO-d₆): δ_C. 150.4, 142.8(2C), 138.3, 137.5, 136.8, 130.5(2C), 129.9(2C), 129.0(2C), 128.6(3C), 127.0(2C), 121.4(2C), 119.1(2C), 117.8(2C), 115.4(2C), 22.0. EI-MS m/z (Calcd. for C₂₆H₂₁N₃O₂S: 439.14); Found: 440.31 (M+H)⁺. Anal Calcd. for C₂₆H₂₁N₃O₂S: C, 71.05; H, 4.82; N, 9.56; Found: C, 71.24; H, 4.84; N, 9.52.

1-(4-((2-Methylacridin-9-yl)amino)phenyl)-3-phenylthiourea (BC_16): Orange solid; Yield 67%; mp 120-122 °C; ¹H NMR (DMSO-d₆): δ_H. 2.36(s, 3H), 6.24-6.79(m, 5H), 7.21-7.81(m, 9H), 8.01-8.19(m, 2H), 8.67 (s, 2H), 10.54 (s, 1H). ¹³C NMR (DMSO-d₆): δ_C. 180.3, 149.7, 142.4(2C), 139.9, 138.8, 135.6, 131.7(2C), 130.1(2C), 129.5(2C), 128.9(2C), 127.7(3C), 126.8(2C), 122.0, 121.2, 119.7, 118.3(2C), 108.5, 22.2. EI-MS m/z (Calcd. For C₂₇H₂₂N₄S: 434.16); Found: 435.09 (M+H)⁺. Anal Calcd. for C₂₇H₂₂N₄S: C, 74.63; H, 5.10; N, 12.89. Found: C, 74.81; H, 5.08; N, 12.85.

1-(4-Chlorophenyl)-3-(4-((2-methylacridin-9-yl)amino)phenyl)thiourea (BC_17):

Yellow solid; Yield 68%; mp 138-140 °C; ¹H NMR (DMSO-d₆): δ_H. 2.32(s, 3H), 6.19-6.56(m, 6H), 7.25-7.84(m, 7H), 8.0-8.17(m, 2H), 8.71 (s, 2H), 10.61 (s, 1H). ¹³C NMR (DMSO-d₆): δ_C. 180.1, 149.8, 142.5(2C), 140.0, 137.2, 135.7, 134.1, 132.0(2C), 131.5(2C), 130.1(2C), 129.8(2C), 128.8, 127.9(3C), 121.9, 121.0, 120.2, 118.4(2C), 108.3, 22.1. EI-MS m/z (Calcd. for C₂₇H₂₁ClN₄S: 468.12); Found: 469.01 (M+H)⁺. Anal Calcd. for C₂₇H₂₁ClN₄S: C, 69.14; H, 4.51; N, 11.95; Found: C, 69.28; H, 4.55; N, 11.97.

1-(4-((2-Methylacridin-9-yl)amino)phenyl)-3-(4-nitrophenyl)thiourea (BC_18):

Pale orange solid; Yield 65%; mp 131-133 °C; ¹H NMR (DMSO-d₆): δ_H. 2.35 (s, 3H), 6.23-6.67 (m, 6H), 7.58-7.89 (m, 6H), 8.03-8.18 (m, 3H), 8.57 (s, 2H), 10.61 (s, 1H). ¹³C NMR (DMSO-d₆): δ_C. 180.3, 150.1, 145.0, 144.4(2C), 142.1(2C), 136.7, 131.9, 130.2(2C), 128.9, 127.8(2C), 127.0, 126.3, 125.6(2C), 124.9(2C), 124.5, 122.0, 121.7, 118.4(2C), 1.8.8, 22.3. EI-MS m/z (Calcd. for C₂₇H₂₁N₅O₂S: 479.14; Found: 478.25 (M-H)⁻. Anal Calcd. for C₂₇H₂₁N₅O₂S: C, 67.62; H, 4.41; N, 14.60; Found: C, 67.43; H, 4.39; N, 14.56.

1-(4-((2-Methylacridin-9-yl)amino)phenyl)-3-(p-tolyl)thiourea (BC_19):

Orange solid; Yield 63%; mp 138-140 °C; ¹H NMR (DMSO-d₆): δ_H. 2.36 (s, 6H), 6.26-6.94 (m, 8H), 7.51-7.95 (m, 6H), 8.16 (m, 1H), 8.59 (s, 2H), 10.63 (s, 1H). ¹³C NMR (DMSO-d₆): δ_C. 180.0, 149.8, 142.3(2C), 140.1, 137.7, 135.9(2C), 132.2(2C), 130.5 (2C), 129.8(2C), 129.0, 127.9(2C), 126.8(2C), 121.7, 121.3(2C), 119.6, 118.2(2C), 108.4, 22.5(2C). EI-MS m/z (Calcd. for C₂₈H₂₄N₄S: 448.17); Found: 449.19 (M+H)⁺. Anal Calcd. for C₂₈H₂₄N₄S: C, 74.97; H, 5.39; N, 12.49; Found: C, 75.18; H, 5.37; N, 12.45.

1-(4-((2-Chloroacridin-9-yl)amino)phenyl)-3-phenylthiourea (BC_20):

Orange solid; Yield 66%; mp 108-110 °C; ¹H NMR (DMSO-d₆): δ_H. 6.22-6.35 (m, 4H), 6.85-7.18 (m, 3H), 7.62-7.97 (m, 7H), 8.07-8.21 (m, 2H), 8.55 (s, 2H), 10.48 (s, 1H). ¹³C NMR (DMSO-d₆): δ_C. 180.1, 149.3, 143.7, 142.4, 140.2, 139.0, 132.3(2C), 131.9(2C), 130.5, 129.7(2C), 129.2(2C), 128.0(2C), 127.7, 127.1(2C), 122.8, 121.4, 119.2, 118.5(2C), 109.7. EI-MS m/z (Calcd. for C₂₆H₁₉ClN₄S: 454.10); Found: 453.01 (M-H)⁻. Anal Calcd. for C₂₆H₁₉ClN₄S: C, 68.64; H, 4.21; N, 12.31; Found: C, 68.82; H, 4.19; N, 12.34.

1-(4-((2-Chloroacridin-9-yl)amino)phenyl)-3-(4-chlorophenyl)thiourea (BC_21):

Brown solid; Yield 66%; mp 135-137 °C; ¹H NMR (DMSO-d₆): δ_H. 6.19-6.55 (m,

6H), 7.21-7.75 (m, 6H), 8.01-8.19 (m, 3H), 8.76 (s, 2H), 10.57 (s, 1H). ¹³C NMR (DMSO-d₆): δ_C. 180.5, 149.1, 143.9, 142.3, 140.0, 137.2, 134.4, 132.0(2C), 131.8(2C), 131.4(2C), 130.1, 129.6(2C), 128.9, 127.7(2C), 127.3, 122.8, 121.2, 118.9, 118.4(2C), 109.9. EI-MS m/z (Calcd. for C₂₆H₁₈C₁₂N₄S:488.06); Found: 489.12 (M+H)⁺. Anal Calcd. for C₂₆H₁₈C₁₂N₄S: C, 63.81; H, 3.71; N, 11.45; Found: C, 63.62; H, 3.73; N, 11.49.

1-(4-((2-Chloroacridin-9-yl)amino)phenyl)-3-(4-nitrophenyl)thiourea (BC_22): Orange solid; Yield 68%; mp 142-144 °C; ¹H NMR (DMSO-d₆): δ_H. 6.22-6.67 (m, 6H), 7.61-7.89 (m, 5H), 8.02-8.18 (m, 4H), 8.56 (s, 2H), 10.64 (s, 1H). ¹³C NMR (DMSO-d₆): δ_C. 180.3, 150.1, 145.3, 144.5(2C), 142.3(2C), 132.9, 132.0, 130.8, 130.1, 129.2, 127.9(2C), 126.4(2C), 125.2(2C), 124.8(2C), 124.5, 122.0(2C), 118.4(2C), 108.7. EI-MS m/z (Calcd. for C₂₆H₁₈ClN₅O₂S: 499.09); Found: 500.21 (M+H)⁺. Anal Calcd. for C₂₆H₁₈ClN₅O₂S: C, 62.46; H, 3.63; N, 14.01; Found: C, 62.64; H, 3.61; N, 14.05.

1-(4-((2-Chloroacridin-9-yl)amino)phenyl)-3-(p-tolyl)thiourea (BC_23): Pale orange solid; Yield 70%; mp 149-153 °C; ¹H NMR (DMSO-d₆): δ_H. 2.36 (s, 3H), 6.23-6.95 (m, 8H), 7.65-8.14 (m, 7H), 8.63 (s, 2H), 10.71 (s, 1H). ¹³C NMR (DMSO-d₆): δ_C. 180.5, 149.2, 143.9, 142.5, 140.3, 237.8, 136.2, 132.0(2C), 131.5(2C), 130.5, 129.9(2C), 129.2, 127.8(2C), 127.4, 126.9(2C), 122.7, 121.4, 118.9, 118.3(2C), 109.7, 21.8. EI-MS m/z (Calcd. for C₂₇H₂₁ClN₄S: 468.12); Found: 467.05 (M-H)⁻. Anal Calcd. for C₂₇H₂₁ClN₄S: C, 69.14; H, 4.51; N, 11.95; Found: C, 69.33; H, 4.49; N, 11.92.

1-(4-(Acridin-9-ylamino)phenyl)-3-phenylthiourea (BC_24): Brown solid; Yield 67%; mp 156-158 °C; ¹H NMR (DMSO-d₆): δ_H. 6.25-6.78 (m, 5H), 7.23-7.71 (m, 8H), 7.97-8.15 (m, 4H), 8.69 (s, 2H), 10.71 (s, 1H). ¹³C NMR (DMSO-d₆): δ_C. 180.2, 150.4, 143.0(2C), 142.5, 139.1, 130.3(2C), 129.7(2C), 129.0(2C), 128.4(2C), 127.9(2C), 127.0(2C), 126.8(2C), 121.4(2C), 118.6(2C), 115.3(2C). EI-MS m/z (Calcd. for C₂₆H₂₀N₄S: 420.14); Found: 421.28 (M+H)⁺. Anal Calcd. for C₂₆H₂₀N₄S: C, 74.26; H, 4.79; N, 13.32; Found: C, 74.04; H, 4.83; N, 13.34.

1-(4-(Acridin-9-ylamino)phenyl)-3-(4-chlorophenyl)thiourea (BC_25): Orange solid; Yield 65%; mp 147-149 °C; ¹H NMR (DMSO-d₆): δ_H. 6.19-6.56 (m, 6H), 7.27-7.774 (m, 6H), 7.99-8.18 (m, 4H), 8.82 (s, 2H), 10.61 (s, 1H). ¹³C NMR (DMSO-d₆): δ_C. 180.4, 150.5, 142.9(2C), 142.5, 137.3, 134.2, 131.8(2C), 130.4(2C), 129.7(2C), 129.1, 128.5(2C), 127.9(2C), 126.7(2C), 121.4(2C), 118.3(2C), 115.5(2C). EI-MS

m/z (Calcd. for C₂₆H₁₉ClN₄S: 454.10); Found: 455.03(M+H)⁺. Anal Calcd. for C₂₆H₁₉ClN₄S: C, 68.64; H, 4.21; N, 12.31; Found: C, 68.83; H, 4.23; N, 12.28.

1-(4-(Acridin-9-ylamino)phenyl)-3-(4-nitrophenyl)thiourea (BC_26): Orange solid; Yield 67%; mp 159-161 °C; ¹H NMR (DMSO-d₆): δ_H. 6.22-6.65 (m, 6H), 7.61-7.92 (m, 6H), 8.04-8.19 (m, 4H), 8.78 (s, 2H), 10.73 (s, 1H). ¹³C NMR (DMSO-d₆): δ_C. 180.2, 150.4, 145.0, 144.5, 142.9(2C), 142.6, 130.4(2C), 129.1, 128.3(2C), 127.9(2C), 127.0(2C), 125.3(2C), 124.9(2C), 121.5(2C), 118.2(2C), 115.6(2C). EI-MS m/z (Calcd. for C₂₆H₁₉N₅O₂S: 465.13); Found: 466.21 (M+H)⁺. Anal Calcd. for C₂₆H₁₉N₅O₂S: C, 67.08; H, 4.11; N, 15.04; Found: C, 67.26; H, 4.13; N, 15.08.

1-(4-(Acridin-9-ylamino)phenyl)-3-(p-tolyl)thiourea (BC_27): Brown solid; Yield 64%; mp 190-192 °C; ¹H NMR (DMSO-d₆): δ_H. 2.36 (s, 3H), 6.23-6.95 (m, 8H), 7.62-7.91 (m, 6H), 8.21 (m, 2H), 8.79 (s, 2H), 10.66 (s, 1H). ¹³C NMR (DMSO-d₆): δ_C. 180.3, 150.4, 142.6(3C), 137.7, 136.2, 130.6(2C), 129.8(2C), 128.9, 128.2(2C), 127.6(2C), 126.9(2C), 126.7(2C), 121.5(2C), 118.3(2C), 115.5(2C), 21.7. EI-MS m/z (Calcd. for C₂₇H₂₂N₄S: 434.16); Found: 435.19 (M+H)⁺. Anal Calcd. for C₂₇H₂₂N₄S: C, 74.63; H, 5.10; N, 12.89; Found: C, 74.85; H, 5.08; N, 12.92.

1-(4-((2-Methylacridin-9-yl)amino)phenyl)-3-phenylurea (BC_28): Brown gummy; Yield 69%; ¹H NMR (DMSO-d₆): δ_H. 2.31 (s, 3H), 6.65 (m, 2H), 7.22-7.95 (m, 13H), 8.19 (d, *J* = 8.1 Hz, 1H), 8.79 (s, 2H), 10.58 (s, 1H). ¹³C NMR (DMSO-d₆): δ_C. 153.5, 149.7, 142.3(2C), 140.1(2C), 135.6, 132.0(2C), 130.4, 129.9(2C), 129.3(2C), 128.6, 127.4, 122.9(2C), 122.2(2C), 122.0, 121.3, 119.9, 118.4(2C), 108.6, 22.3. EI-MS m/z (Calcd. For C₂₇H₂₂N₄O: 418.18); Found: 417.06 (M-H)⁻. Anal Calcd. For C₂₇H₂₂N₄O: C, 77.49; H, 5.30; N, 13.39; Found: C, 77.25; H, 5.32; N, 13.35.

1-(4-Chlorophenyl)-3-(4-((2-methylacridin-9-yl)amino)phenyl)urea (BC_29): Pale yellow solid; Yield 66%; mp 163-165 °C; ¹H NMR (DMSO-d₆): δ_H. 2.35 (s, 3H), 6.59 (m, 2H), 7.41-7.96 (m, 12H), 8.21 (d, *J* = 7.8 Hz, 1H), 8.84 (s, 2H), 10.58 (s, 1H). ¹³C NMR (DMSO-d₆): δ_C. 153.6, 149.7, 142.3(2C), 140.1, 138.3, 135.8, 133.9, 132.1(2C), 130.5, 130.0(2C), 129.7(2C), 127.5, 122.9(2C), 122.1, 121.4(2C), 121.3, 119.8, 118.6(2C), 108.3, 22.5. EI-MS m/z (Calcd. for C₂₇H₂₁ClN₄O: 452.14); Found: 453.23 (M+H)⁺. Anal Calcd. for C₂₇H₂₁ClN₄O: C, 71.60; H, 4.67; N, 12.37; Found: C, 71.79; H, 4.65; N, 12.41.

1-(4-((2-Methylacridin-9-yl)amino)phenyl)-3-(4-nitrophenyl)urea (BC_30): Brown gummy; Yield 61%; ¹H NMR (DMSO-d₆): δ_H. 2.32 (s, 3H), 6.62 (m, 2H), 7.42-7.89 (m, 10H), 8.19-8.27 (m, 3H), 8.79 (s, 2H), 10.61 (s, 1H). ¹³C NMR (DMSO-

d₆): δ_C. 153.4, 149.8, 146.1, 144.3(2C), 142.0(2C), 136.9, 131.8, 130.5(3C), 127.3, 126.1, 124.7(3C), 122.9(2C), 122.2, 121.6, 120.3(2C), 118.5(2C), 108.7, 22.2. EI-MS m/z (Calcd. for C₂₇H₂₁N₅O₃: 463.16); Found: 462.14 (M-H)⁻. Anal Calcd. For C₂₇H₂₁N₅O₃: C, 69.97; H, 4.57; N, 15.11; Found: C, 70.16; H, 4.55; N, 15.08.

1-(4-((2-Methylacridin-9-yl)amino)phenyl)-3-(p-tolyl)urea (BC_31): Pale orange gummy; Yield 67%; ¹H NMR (DMSO-d₆): δ_H. 2.32 (s, 6H), 6.64 (m, 2H), 7.23-7.61 (m, 9H), 7.80-8.21 (m, 4H), 8.78 (s, 2H), 10.68 (s, 1H). ¹³C NMR (DMSO-d₆): δ_C. 153.6, 149.7, 142.3(2C), 140.1, 137.3(2C), 135.8, 132.0(2C), 130.7, 130.1(2C), 129.6(2C), 127.8, 123.0(2C), 122.1(3C), 121.3, 119.8, 118.4(2C), 108.3 22.5(2C). EI-MS m/z (Calcd. for C₂₈H₂₄N₄O: 432.20); Found: 433.12 (M+H)⁺. Anal Calcd. for C₂₈H₂₄N₄O: C, 77.75; H, 5.59; N, 12.95; Found: C, 77.51; H, 5.61; N, 12.99.

1-(4-((2-Chloroacridin-9-yl)amino)phenyl)-3-phenylurea (BC_32): Brown solid; Yield 68%; mp 168-170 °C; ¹H NMR (DMSO-d₆): δ_H. 6.62 (m, 2H), 7.23-7.62 (m, 9H), 7.81-8.22 (m, 5H), 8.68 (s, 2H), 10.71 (s, 1H). ¹³C NMR (DMSO-d₆): δ_C. 153.4, 149.3, 143.9, 142.1, 140.4(2C), 132.2(2C), 131.8(2C), 130.5, 129.9, 129.3(3C), 127.7, 122.9(3C), 122.3(2C), 121.4, 119.0, 118.5(2C), 109.8. EI-MS m/z (Calcd. for C₂₆H₁₉ClN₄O: 438.12); Found: 439.25 (M+H)⁺. Anal Calcd. for C₂₆H₁₉ClN₄O: C, 71.15; H, 4.36; N, 12.77; Found: C, 70.98; H, 4.34; N, 12.81.

1-(4-((2-Chloroacridin-9-yl)amino)phenyl)-3-(4-chlorophenyl)urea (BC_33): Brown solid; Yield 69%; mp 234-236 °C; ¹H NMR (DMSO-d₆): δ_H. 6.59 (m, 2H), 7.41-7.79 (m, 10H), 9.01-8.23 (m, 3H), 8.65 (s, 2H), 10.59 (s, 1H). ¹³C NMR (DMSO-d₆): δ_C. 153.5, 149.1, 143.8, 142.0, 140.1, 138.3, 133.9, 132.3(2C), 131.7(2C), 130.3(2C), 129.4(2C), 127.5, 122.9(3C), 121.6(3C), 119.1, 118.4(2C), 109.8. EI-MS m/z (Calcd. for C₂₆H₁₈Cl₂N₄O: 472.09); Found: 473.17 (M+H)⁺. Anal Calcd. for C₂₆H₁₈Cl₂N₄O: C, 65.97; H, 3.83; N, 11.84; Found: C, 66.19; H, 3.81; N, 11.86.

1-(4-((2-Chloroacridin-9-yl)amino)phenyl)-3-(4-nitrophenyl)urea (BC_34): Brown gummy; Yield 68%; ¹H NMR (DMSO-d₆): δ_H. 6.64 (m, 2H), 7.43-7.89 (m, 9H), 8.13-8.26 (m, 4H), 8.76 (s, 2H), 10.67 (s, 1H). ¹³C NMR (DMSO-d₆): δ_C. 153.7, 150.5, 146.1, 144.0(2C), 142.3(2C), 132.8, 132.0, 140.9, 130.3(2C), 126.7(2C), 124.9(3C), 123.0(2C), 12.3(2C), 120.5(2C), 118.3(2C), 108.8. EI-MS m/z (Calcd. for C₂₆H₁₈ClN₅O₃: 483.11); Found: 482.05 (M-H)⁻. Anal Calcd. for C₂₆H₁₈ClN₅O₃: C, 64.53; H, 3.75; N, 14.47; Found: C, 64.71; H, 3.73; N, 14.44.

1-(4-((2-Chloroacridin-9-yl)amino)phenyl)-3-(p-tolyl)urea (BC_35): Yellow solid; Yield 62%; mp 253-255 °C; ¹H NMR (DMSO-d₆): δ_H. 2.25 (s, 3H), 6.62 (m, 2H),

7.23-7.59 (m, 8H), 7.81-8.15 (m, 5H), 8.79 (s, 2H), 10.68 (s, 1H). ¹³C NMR (DMSO-d₆): δ_C. 153.6, 149.2, 144.1, 142.3, 140.5, 137.4(2C), 132.2(3C), 131.1, 130.3(2C), 129.8(2C), 127.7, 123.0(3C), 122.2(2C), 121.3, 119.0, 118.5(2C), 109.9, 21.7. EI-MS m/z (Calcd. for C₂₇H₂₁ClN₄O: 452.14); Found: 453.45 (M+H)⁺. Anal Calcd. for C₂₇H₂₁ClN₄O: C, 71.60; H, 4.67; N, 12.37; Found: C, 71.58; H, 4.65; N, 12.41.

1-(4-(Acridin-9-ylamino)phenyl)-3-phenylurea (BC_36): Orange solid; Yield 65%; mp 162-164 °C; ¹H NMR (DMSO-d₆): δ_H. 6.65 (m, 2H), 7.19-7.59 (m, 9H), 7.81-8.15 (m, 6H), 8.79 (s, 2H), 10.51 (s, 1H). ¹³C NMR (DMSO-d₆): δ_C. 153.4, 150.2, 142.9(2C), 142.0, 139.8, 130.3(3C), 120.5(3C), 128.3(2C), 127.0(2C), 123.2(2C), 122.1(2C), 121.5(2C), 118.1(2C), 115.4(2C). EI-MS m/z (Calcd. for C₂₆H₂₀N₄O: 404.16); Found: 405.29 (M+H)⁺. Anal Calcd. for C₂₆H₂₀N₄O: C, 77.21; H, 4.98; N, 13.85; Found: C, 77.45; H, 5.01; N, 13.82.

1-(4-(Acridin-9-ylamino)phenyl)-3-(4-chlorophenyl)urea (BC_37): Brown solid; Yield 68%; mp 241-243 °C; ¹H NMR (DMSO-d₆): δ_H. 6.59 (m, 2H), 7.41-7.92 (m, 12H), 8.19 (m, 2H). ¹³C NMR (DMSO-d₆): δ_C. 153.6, 150.4, 143.1(2C), 141.9, 138.2, 133.8, 130.5(3C), 129.5(2C), 128.2(2C), 127.0(2C), 122.9(2C), 121.4(2C), 121.0(2C), 118.3(2C), 115.5(2C). EI-MS m/z (Calcd. for C₂₆H₁₉ClN₄O: 438.12); Found: 437.01 (M-H)⁻. Anal Calcd. for C₂₆H₁₉ClN₄O: C, 71.15; H, 4.36; N, 12.77; Found: C, 70.95; H, 4.38; N, 12.74.

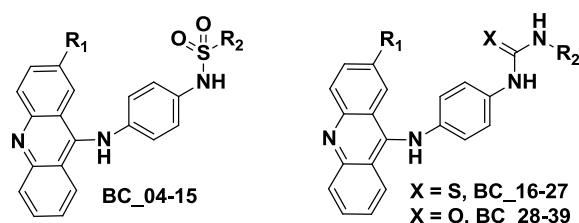
1-(4-(Acridin-9-ylamino)phenyl)-3-(4-nitrophenyl)urea (BC_38): Brown solid; Yield 62%; mp 252-254 °C; ¹H NMR (DMSO-d₆): δ_H. 6.62 (m, 2H), 7.43-7.94 (m, 10H), 8.15-8.27 (m, 4H), 8.73 (s, 2H), 10.77 (s, 1H). ¹³C NMR (DMSO-d₆): δ_C. 153.5, 150.3, 146.1, 144.3, 142.9(2C), 141.7, 130.5(3C), 128.3(2C), 127.0(2C), 124.8(2C), 123.1(2C), 121.6(2C), 120.4(2C), 118.5(2C), 115.3(2C). EI-MS m/z (Calcd. for C₂₆H₁₉N₅O₃: 449.15); Found: 450.45 (M+H)⁺. Anal Calcd. for C₂₆H₁₉N₅O₃: C, 69.48; H, 4.26; N, 15.58; Found: C, 69.68; H, 4.27; N, 15.53.

1-(4-(Acridin-9-ylamino)phenyl)-3-(p-tolyl)urea (BC_39): Brown gummy; Yield 64%; ¹H NMR (DMSO-d₆): δ_H. 2.31 (s, 3H), 6.64 (m, 2H), 7.19-7.74 (m, 10H), 7.98-8.15 (m, 4H), 8.67 (s, 2H), 10.59 (s, 1H). ¹³C NMR (DMSO-d₆): δ_C. 153.4, 150.2, 142.9(2C), 142.1, 137.3(2C), 130.5(2C), 129.9(3C), 128.3(2C), 127.0(2C), 122.8(2C), 122.1(2C), 121.6(2C), 118.3(2C), 115.6(2C), 21.9. EI-MS m/z (Calcd. for C₂₇H₂₂N₄O: 418.18); Found: 419.27 (M+H)⁺. Anal Calcd. for C₂₇H₂₂N₄O: C, 77.49; H, 5.30; N, 13.39; Found: C, 77.25; H, 5.32; N, 13.43.

5.3.4 *In vitro* supercoiling assay, antimycobacterial potency and cytotoxicity studies of the synthesized molecules (BC_04-BC_39)

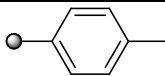
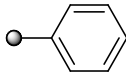
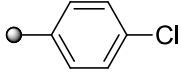
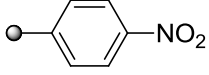
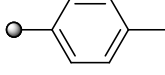
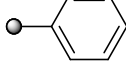
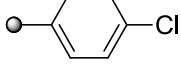
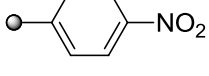
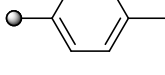
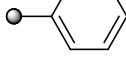
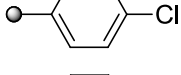
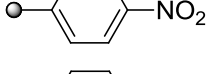
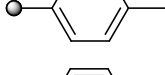
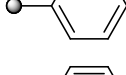
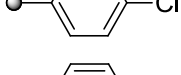
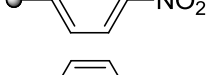
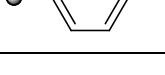
All the synthesized derivatives were evaluated for their *in vitro* supercoiling assay for the derivation of SAR and lead optimization. The compounds were further subjected to a whole cell screening against *Mtb* H₃₇Rv strain to understand their bactericidal potency using the agar dilution method and later the safety profile of these molecules were evaluated by checking the *in vitro* cytotoxicity against RAW 264.7 cell line (mouse macrophage) at 50 μ M concentration by MTT assay, and the results are shown in **Table 5.6**.

Table 5.6 *In vitro* biological evaluation of the synthesized derivatives **BC_04** – **BC_15** and **BC_16** – **BB_39**.

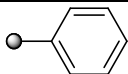
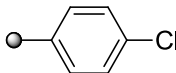
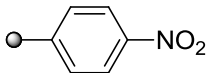
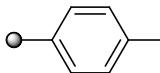
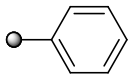

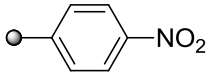
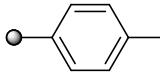
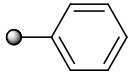

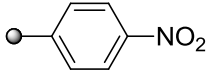
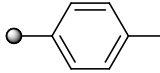


Compd.	R ₁	R ₂	<i>Mtb</i> Supercoiling assay (IC ₅₀ in μ M)	<i>Mtb</i> MIC (μ M)	Cytotoxicity at 50 μ M (% Inhib.)
BC_04	CH ₃		5.86±0.35	28.44	39.57
BC_05	CH ₃		5.21±0.51	6.59	11.78
BC_06	CH ₃		8.34±0.59	12.90	26.98
BC_07	CH ₃		9.8±0.33	27.56	27.81
BC_08	Cl		9.2±0.28	27.17	14.46
BC_09	Cl		12.4±0.66	25.08	14.19
BC_10	Cl		8.1±0.61	24.75	30.39

Conti....

Compd.	R ₁	R ₂	<i>Mtb</i> Supercoiling assay (IC ₅₀ in μM)	<i>Mtb</i> MIC (μM)	Cytotoxicity at 50 μM (% Inhib.)
BC_11	Cl		22.8±0.42	>52.75	38.54
BC_12	H		15.1±0.59	14.69	42.06
BC_13	H		23.8±1.24	27.18	34.21
BC_14	H		22.4±0.29	24.64	34.12
BC_15	H		9.3±0.65	28.44	28.44
BC_16	CH ₃		6.3±0.58	7.20	10.81
BC_17	CH ₃		11.2±0.83	26.70	26.00
BC_18	CH ₃		24.8±0.29	>52.13	28.83
BC_19	CH ₃		26.9±0.48	55.73	34.99
BC_20	Cl		29.3±0.34	27.47	11.69
BC_21	Cl		31.5±0.81	>51.08	6.70
BC_22	Cl		28.8±1.94	>50.00	30.37
BC_23	Cl		33.9±1.44	>53.30	25.51
BC_24	H		8.2±0.29	14.86	29.24
BC_25	H		8.4±0.44	13.74	12.54
BC_26	H		13.1±0.59	13.43	20.80
BC_27	H		31.1±0.54	>57.53	27.41

Conti....

Compd.	R ₁	R ₂	<i>Mtb</i> Supercoiling assay (IC ₅₀ in μM)	<i>Mtb</i> MIC (μM)	Cytotoxicity at 50 μM (% Inhib.)
BC_28	CH ₃		22.1±0.82	29.87	24.78
BC_29	CH ₃		11.4±0.64	27.60	25.86
BC_30	CH ₃		7.4±0.29	13.48	33.94
BC_31	CH ₃		29.6±0.55	57.80	43.11
BC_32	Cl		23.6±1.82	28.48	27.67
BC_33	Cl		11.8±0.34	13.20	17.12
BC_34	Cl		7.3±0.43	6.46	45.88
BC_35	Cl		12.5±0.59	13.80	29.20
BC_36	H		32.6±0.61	>61.81	30.45
BC_37	H		10.4±0.46	28.48	26.25
BC_38	H		26.8±1.59	27.81	19.25
BC_39	H		13.1±0.88	14.93	18.37
		Novobiocin	46±10 nM	>50	NT
		Isoniazid	>50	0.66	NT
		Rifampicin	>50	0.23	NT
		Moxifloxacin	11.2±0.36	1.26	1.26

IC₅₀, 50% inhibitory concentration; *Mtb*, *Mycobacterium tuberculosis*; MIC, minimum inhibitory concentration; NT, not tested; nM, nanomolar

Mtb DNA gyrase supercoiling enzyme inhibition activity

In vitro activity against *Mtb* H₃₇Rv

Cytotoxicity against RAW 264.7 cells (mouse macrophage cell line)

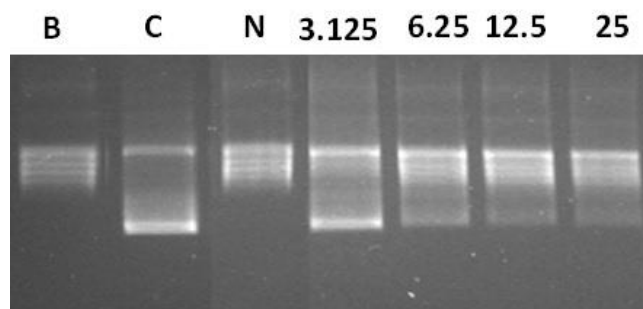


Figure 5.27: Picture depicting the *Mtb* DNA gyrase supercoiling assay of compound **BC_05**. B- Relaxed DNA; C-Relaxed DNA + Enzyme; N-Relaxed DNA + Enzyme + Novobiocin; 25, 12.5, 6.25, 3.125 - Relaxed DNA + Enzyme + comp **BC_05** at different concentrations

5.3.5 Evaluation of zERG channel inhibition in a zebra fish model

The most potent compound **BC_05** was examined for hERG channel inhibition by assessing arrhythmogenic potential on Zebrafish ether-a-go-go-related gene (zERG) which is orthologous to the human ether-a-go-go-related gene (hERG) the result have been depicted in graphs below (**Figure 5.28a & 5.28b**).

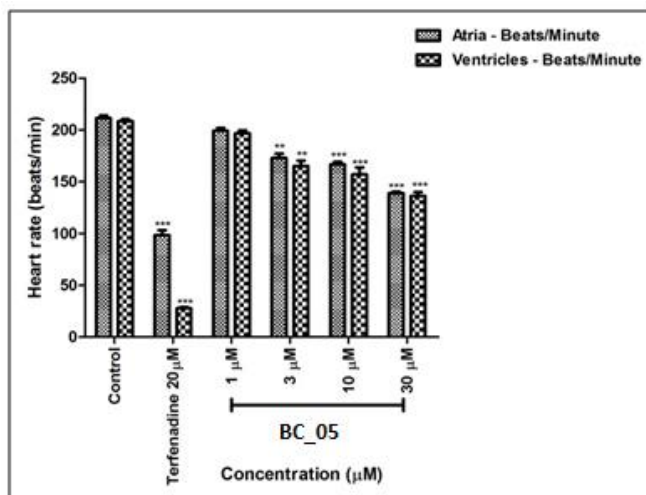


Figure 5.28a Mean (\pm S.E.M.) of the heart rates of atria and ventricles of most potent Compound **BC_05** treatment groups. (* $p < 0.05$, ** $p < 0.01$ and *** $p < 0.001$). Statistical significance was analyzed comparing control group vs. treated groups.

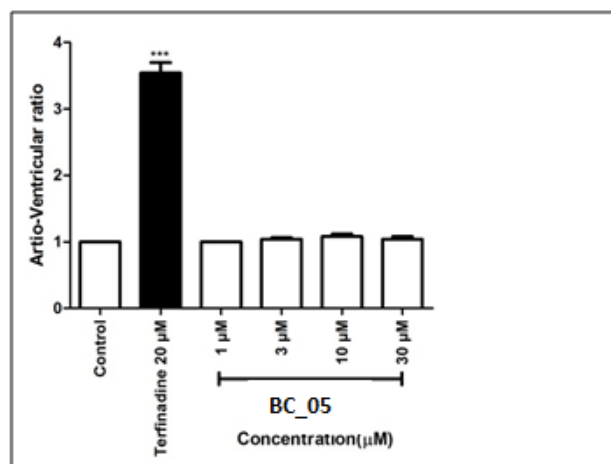


Figure 5.28b Mean (\pm S.E.M.) score of atrio ventricular ratio of most potent Compound **BC_05** treatment groups (* $p < 0.05$, ** $p < 0.01$ and *** $p < 0.001$). Statistical significance was analyzed comparing control group vs. all groups.

5.3.6 Discussion

All the thirty six synthesized derivatives were subjected to initial screening for their biological inhibition studies using *Mtb* DNA gyrase supercoiling assay using Inspiralis kit, UK. Among the compounds tested, among all synthesized derivatives, twenty six compounds showed IC_{50} value of $< 25 \mu\text{M}$, ten compounds showed IC_{50} value of $\leq 10 \mu\text{M}$. Compound 4-Chloro-N-(4-((2-methylacridin-9-yl) amino) phenyl) benzenesulfonamide (**BC_05**) emerged as more potent inhibitor of *Mtb* DNA gyrase super coiling IC_{50} of $5.21 \pm 0.51 \mu\text{M}$ (**Figure 5.27**); and was ~ 2 times more potent than standard antitubercular DNA gyrase inhibitor Moxifloxacin (IC_{50} of $11.2 \pm 0.36 \mu\text{M}$). Further we tested these compounds for their *in vitro* activity using *Msm* Gyr B ATPase assay as ATPase activity of Gyr B protein from *Mtb* was found to be very low when compared to *Msm*. None of the compounds were shown any appreciable inhibition in Gyr B assay indicates that these molecules specifically interact with Gyr A subunit of DNA gyrase like other reported NBTIs. These molecules were more also selective towards *Mtb* DNA gyrase only and did not inhibit DNA supercoiling activity of *Staphylococcus aureus*, *Escherichia coli* and *Pseudomonas aeruginosa* DNA gyrases. These molecules structurally similar to m-Amsacrine (**Figure 5.29**), an acridine derivative, originally designed as an intercalating agent has been shown to act as a eukaryotic topoisomerase II poison (Ketrone A. C., *et al.*, 2012) was reported as *Mtb* topoisomerase I inhibitor with IC_{50} of $10 \mu\text{M}$ (Godbole A. A., *et al.*, 2014). As

synthesized molecules were structurally similar to m-Amsacrine we also tested our compounds *Mtb* topoisomerase I relaxation assay (Sridevi J. P., *et al.*, 2015) and none of the compounds showed any inhibition at 50 μM . This result indicates the importance of methoxy group present in the phenyl ring linker of m-Amsacrine.

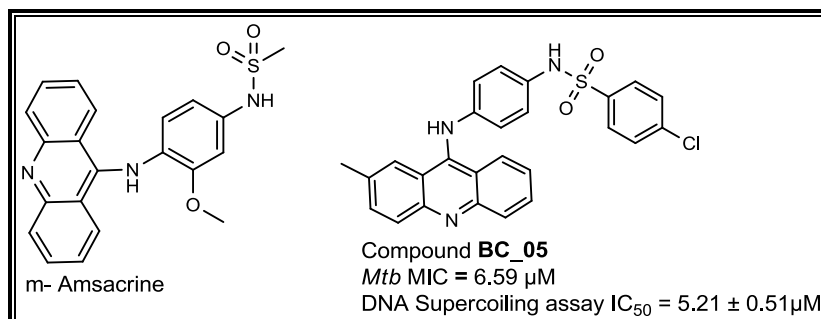


Figure 5.29: Structure of m-Amsacrine, most active compound **BC_05**

With respect to structure activity relationship, we have prepared twelve sulphonamides, thiourea and urea and in general order of activity sulphonamides (**BC_04-15**) > thiourea (**BC_16-27**) > urea (**BC_28-39**). Among sulphonamides derivatives, we prepare three derivatives with H, Cl, and CH_3 groups at 2nd position of acridine moiety (LHS). Among them methyl derivatives (**BC_04-07**) showed better activity (IC_{50} ranges from 5.21 ± 0.51 to 9.88 ± 0.33 μM) followed by chloro derivatives (**BC_08-11**) with IC_{50} ranges from 8.1 ± 0.61 to 22.8 ± 0.42 μM and then unsubstituted acridine derivatives (**BC_12-15**) with IC_{50} ranges from 9.3 ± 0.65 to $23.8.8 \pm 1.24$ μM . Among compounds **BC_04-15** we also prepared H, Cl, NO_2 , CH_3 groups in the phenyl ring of RHS; among them the order of activity $\text{H} > \text{NO}_2 > \text{CH}_3$ and Cl groups at the 4th position of RHS phenyl ring.

The compounds were further screened for their *in vitro* antimycobacterial activity against *M. tuberculosis* H₃₇Rv by microplate alamar blue assay method. Isoniazid, Rifampicin and Moxifloxacin were used as a positive control and for comparison. The minimum inhibitory concentration (MIC) was determined for each compound which was measured as the minimum concentration of compound required to completely inhibit the bacterial growth. In general a good correlation was observed between the *Mtb* DNA gyrase super coiling assay IC_{50} and *in vitro* *Mtb* MIC (**Table 5.6**). Among thirty six compounds tested twelve compounds showed MIC < 20 μM and three compounds (**BC_05**, **BC_16**, and **BC_34**) showed *Mtb* MIC of < 10 μM . Few compounds (**BC_04** and **BC_07**) MIC's were ~ 3 times more than that of DNA gyrase super coiling IC_{50} ; this might be because of less penetration of these molecules

towards the *Mtb* cell wall or efflux pump present in the cytoplasmic membrane of *Mtb* may pump out these compounds efficiently.

The safety profile of the synthesized compounds were also accessed by testing their *in vitro* cytotoxicity against RAW 264.7 cells at 50 μM concentration using (4,5-dimethylthiazol-2-yl)-2,5-diphenyltetrazolium bromide (MTT) assay. Selection of mouse macrophage cell line RAW 264.6 is based to check the toxicity in macrophages; as *Mtb* resides in its. Percentage inhibitions of cells are reported in **Table 5.6**. Most of the tested compounds demonstrated good safety profile with very low inhibitory potential (< 50%).

The most potent compound **BC_05** was further examined for zERG channel inhibition by elucidating arrhythmogenic potential on Zebrafish (Chaudhari G. H., *et al.*, 2013). This method has significant advantages over current conventional animal models include ethical issues, low compound requirement and cost of experiment. Compound was treated starting from 1 μM to 30 μM concentrations with 0.1% DMSO as a vehicle. The compound was analyzed for the heart rate variations and AV ratio. The compound was found to be safe when compared to positive control (20 μM terfenadine), not showing any significant cardiotoxicity until 30 μM (**Figure 5.28a, 5.28b**). Significant changes in the heart rate as well as AV ratio were also not observed, compared to control group making them relatively safe. In our earlier study with aminopiperidine based *Mtb* DNA gyrase molecules (Medapi B., *et al.*, 2015) at 30 μM was toxic to fish and died. To conclude replacement of aminopiperidine linker with *p*-phenylenediamine linker reduces cardiac toxicity.

5.3.7 Highlights of the study

In our continuous efforts to discover novel antimicrobial compounds with anti-gyrase activity, we have described the discovery of novel acridine - *p*-phenylenediamine derivatives as gyrase inhibitors with good selection of *Mtb* DNA gyrase supercoiling, less cytotoxic effect and devoid of cardiotoxicity than the previously reported aminopiperidine based DNA gyrase inhibitors. Among 36 compounds, compound **BC_05** shows DNA gyrase supercoiling IC_{50} of $5.21 \pm 0.51 \mu\text{M}$, and MIC of 6.59 μM against *Mtb*. The compound was also found to less cytotoxic against RAW 264.7 mouse macro phage cell lines and with good cardio safety profile among the acridine

based DNA gyrase inhibitors, would be interesting as potential leads for further development.

5.4 Development of ethyl 4-((4-Amino/Hydroxyphenyl)amino)quinoline-3-carboxylate derivatives as potential *Mtb* DNA gyrase B inhibitors

Several compounds have been reported as DNA Gyr B inhibitors which include benzimidazole ureas (Charifson P. S., *et al.*, 2008), pyrazinamides (Shirude P. S., *et al.*, 2013) and triazolopyridine ureas (Kale M. G., *et al.*, 2013). In the present study, structural optimization of the reported lead, aminopyrazinamide derivative from AstraZeneca, by using structural derivatization approach we carried out substituting at suitable positions and were synthetically derivatized to a series of 46 compounds. These compounds were subjected to *in vitro* *Msm* Gyr B inhibition and *Mtb* DNA supercoiling assay so as to study their inhibitory profile. Structure activity relationship of the compounds was build up relating their Gyr B activity and *in silico* docking pattern. Further, the compounds were tested over *in vitro* drug sensitive *Mtb* cultures using microplate alamar blue assay (MABA) and their cytotoxicity studies were carried out using macrophage cell line from mouse.

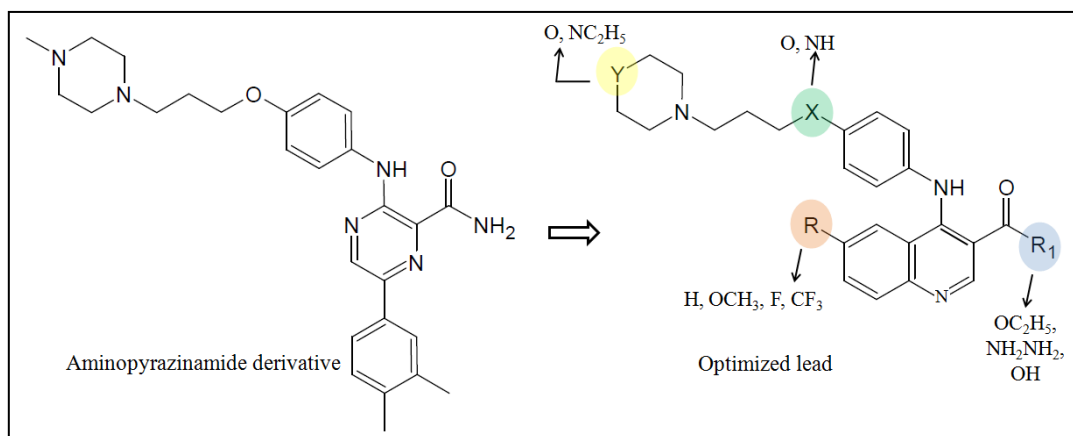


Figure 5.30: The design process of lead optimization with substituents at the respective positions, Scheme-4

5.4.1 Chemical synthesis and characterization

The titled compounds were synthesized by following multi-step synthesis protocol. Initially, we synthesized the amine derivatives (**BD_04a-b** and **BD_08a-b**) starting with simple 1,4-phenylene diamine and 4-aminophenol which were selectively

alkylated with 1,3-dibromo propane using K_2CO_3 in DMF heating at 110 °C for 3 h. This was followed by reacting them with morpholine and N-ethyl piperazine under similar conditions, subsequent de-protection of BOC to get the amine derivatives (**BD_04a-b** and **BD_08a-b**). The reaction sequences were showed in **Scheme 4.4.1** in **Section 4**. These amine derivatives were alkylated with different substituted 4-chloro quinoline analogues (**BD_11a-d**) using *p*-tolulene sulfonic acid (PTSA) as catalyst in methanol in a Biotage microwave vial by irradiating at 120 °C for 45 min to get substituted ethyl phenyl aminoquinoline-3-carboxylates (**BD_12-27**) (Höglund I. P., *et al.*, 2006). These were further converted to their corresponding hydrazide (**BD_28-43**) and acid derivatives (**BD_44-57**). The substituted 4-chloro quinoline analogues (**BD_11a-d**) were prepared by a three step synthesis process according to the reported procedure (Eswaran S., *et al.*, 2010; Thomas K. D., *et al.*, 2011) starting with different substituted anilines were converted to diethyl phenyl amino methylidene propanedioate derivatives (**BD_09a-d**) by condensing with diethyl ethoxy methylene malonate. These (**BD_09a-d**) were cyclized intramolecularly to 4-hydroxy quinoline 3-carboxylate derivatives (**BD_10a-d**) by heating them at 75 °C for 12 h in polyphosphoric acid and phosphorous oxy chloride (catalytic). In this method, the yield (89-92%) was improved much better than the reported procedure using Dowtherm and subsequent refluxing in phosphorous oxy chloride yielded the 4-chloroquinoline 3-carboxylate derivatives (**BD_11a-d**).

5.4.2 Experimental protocol followed for synthesis

General procedure for the synthesis of tert-butyl (4-aminophenyl)carbamate (BD_01) & tert-butyl (4-hydroxyphenyl)carbamate (BD_05): To a stirred solution of *p*-phenylenediamine/ 4 aminophenol (100 mmol) and triethylamine (Et_3N) (216 mmol) in *N,N*- dimethyl formamide (DMF) (150 mL) Boc-anhydride (130 mmol) was added slowly at 0 °C allowed to stir for 3 h at room temperature (rt). The reaction was monitored by TLC, after completion DMF was removed by high vacuum pump and diluted with ethylacetate (300 mL) and the organic layer was washed with brine (150 mL). The organic layer was evaporated under reduce pressure to get crude brown solid which was further purified by flash column chromatography by 230-400 mesh silica gel using ethylacetate: hexane as eluent to afford brown solid.

General synthetic procedure for the preparation of intermediates BD_02 and BD_06; General procedure A: To a stirred solution of compound **BD_01** or **BD_05** (65.0 mmol), potassium carbonate (K_2CO_3) (97.5 mmol) and 1,3-dibromopropane (78.0 mmol) in DMF (100 ml) was heated to 110 °C for 3h. After completion of the reaction (monitored by TLC), DMF was removed by under vacuo. To the crude reaction mixture crushed ice was added and diluted with ethylacetate (150 mL). The organic layer was washed with brine (100 mL), separated and dried over anhydrous sodium sulphate (anhy. Na_2SO_4) and evaporated under reduced pressure to get crude product which was further purified by flash column chromatography by 230-400 silica gel using ethylacetate: hexane as eluent to afford corresponding bromo derivative (**BD_02** & **BD_06** as a solid).

General synthetic procedure for the preparation of intermediate BD_04a-b and BD_08a-b; General procedure B: To a stirred solution of intermediate **BD_03a-b** (20 mmol) or **BD_07a-b** (20 mmol), potassium carbonate (30 mmol) (K_2CO_3) and 1.1 equivalent of morpholine/1-ethylpiperazine in DMF was heated to 110 °C for 3 h. TLC analysis indicated that the reaction was complete. DMF was removed by high vacuum pump. To the crude reaction mixture crushed ice was added and diluted with ethylacetate (150 mL). The organic layer was washed with brine (100 mL), separated, dried over anhydrous Na_2SO_4 and evaporated to get crude product which was further purified by flash column chromatography by 230-400 silica gel using ethylacetate: hexane as eluent to afford desired compounds (3a-b, 7a-b), followed by Boc deprotection of 3a-3b & 7a-b with trifluoro acetic acid (TFA) 10 eq (~10 mL) in 15 mL of DCM at 0 °C to room temperature for 4 h gives the corresponding amine (**BD_04a-b** & **BD_08a-b**) derivatives in good yields.

General procedure for synthesis of diethyl 2-((phenyl/4-methoxy/4-fluoro/4-trifluoromethylphenylamino)methylene)malonate; General procedure C (BD_09a-d): To a stirred solution of substituted anilines (50 mmol), diethyl 2-(ethoxymethylene)malonate (55 mmol) in ethanol (EtOH) (250 mL) was refluxed for 3 h. TLC analysis indicated that the reaction was complete. After cooling the reaction mixture solid was separated. The separated solid was filtered and washed with 3% ethyl acetate: hexane for further purification to afford desired compound as an off-white solid in good yield (89-92%).

General procedure for synthesis of ethyl 6-unsubstituted / methoxy/ fluoro / trifluoromethyl-4-hydroxyquinoline-3-carboxylate (BD_10a-d): Polyphosphoric acid (PPA) (2 eq by weight) was added to corresponding intermediate **BD_09a-d** (40 mmol) to this phosphorus oxychloride (POCl₃) (10mmol) was added. The reaction mixture was heated to 75 °C for 8 h, monitored by TLC, after completion of the reaction. The reaction mixture was quenched slowly with 10% sodium hydroxide solution by keeping it in an ice bath and the PH was adjusted to a pH~7, the solid separated was filtered, dried and washed with diethyl ether (3*20 mL) to afford desired compound in good yield.

General procedure for synthesis of ethyl 6-unsubstituted / methoxy / fluoro / trifluoromethyl-4-chloroquinoline-3-carboxylate (BD_11a-d): To the corresponding intermediate **BD_10a-d** (25 mmol), POCl₃ (125 mmol) was added slowly and refluxed for 3 h at 105 °C. TLC analysis indicated that the reaction was completed. Excess POCl₃ was removed under reduced pressure and the crude reaction mass was quenched with crushed ice then neutralized with saturated sodium bicarbonate solution (100 mL) and extracted with ethylacetate (3*100 mL). The organic layer was dried over anhy.Na₂SO₄, filtered and evaporated under reduced pressure to get corresponding desired chloro intermediate.

General procedure for the preparation of titled phenyl-amino-quinoline ethyl ester derivatives (BD_12-27): The alkylation of amine intermediates (**BD_04a-b** & **BD_08a-b**) was carried in a Biotage microwave vial. Compound **BD_11** (4.5 mmol) (1 equiv), **BD_4** or **BD_8** (1.2 equiv) and *p*-toluenesulfonic acid (PTSA) 5-6 mg catalytic amount in 15 ml methanol and then subjected to microwave irradiation at 120 °C for 45 min. The reaction mixture was concentrated under vacuo. The residue was dissolved in water to this saturated NaHCO₃ solution was added to make alkaline, and extracted thrice with 5% MeOH: DCM solution. Combined organic layers were dried over anhydrous Na₂SO₄ and evaporated under vacuo, purification of the resultant product in silica gel by flash column chromatography using 5-10 % MeOH: DCM as eluent to get final ethyl ester derivatives.

General procedure for the preparation of titled phenyl-amino-quinoline acidhydrazide derivatives (BD_28-43): The corresponding ethyl ester derivatives (**BD_12-27**) (0.5 mmol) were converted to acid hydrazide derivatives by refluxing

them with hydrazine hydrate (1.5 mmol) in ethanol for 6h to get corresponding acid hydrazide derivative (**BD_28-43**) which were further purified by recrystallization from ethanol.

General procedure for the preparation of titled phenyl-amino-quinoline acid derivatives (BD_44-57): The corresponding ethyl ester derivatives (0.5 mmol) (**BD_12-27**) were hydrolyzed by lithium hydroxide monohydrate (1.25 mmol) in 6mL of 1:1:1 ratio of methanol; tetrahydrofuran; distilled water as a solvent and acidified with 2N HCl to maintain pH near 5-6. The solid precipitated was filtered, dried and diethyl ether, ethyl acetate washings were given for further purification to get the corresponding acid derivatives in moderate yield. The physicochemical properties of synthesized derivatives were depicted in **Table 5.7** as shown below

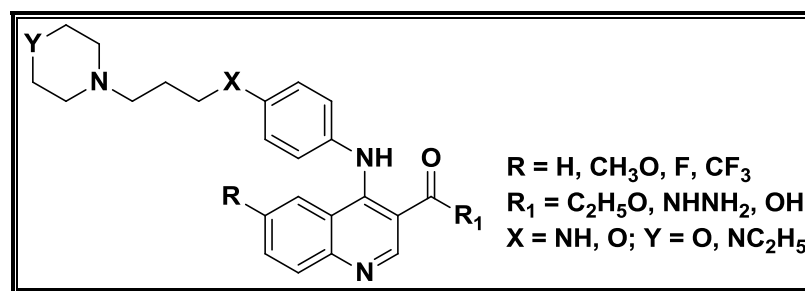
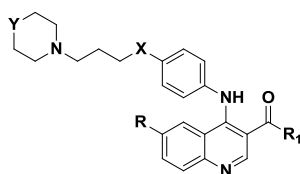


Figure 5.31 General structures of synthesized derivatives **BD_12-57**

Table 5.7 Physicochemical properties of synthesized derivatives **BD_12-57**



Comp	R	R ₁	X	Y	Yield (%)	Melting point (°C)	Molecular formula	Molecular weight
BD_12	H	OC ₂ H ₅	O	O	60	-	C ₂₅ H ₂₉ N ₃ O ₄	435.22
BD_13	OCH ₃	OC ₂ H ₅	O	O	58	170-172	C ₂₆ H ₃₁ N ₃ O ₅	465.23
BD_14	F	OC ₂ H ₅	O	O	57	93-95	C ₂₅ H ₂₈ FN ₃ O ₄	453.21
BD_15	CF ₃	OC ₂ H ₅	O	O	58	98-100	C ₂₆ H ₂₈ F ₃ N ₃ O ₄	503.20
BD_16	H	OC ₂ H ₅	NH	O	59	240-242	C ₂₅ H ₃₀ N ₄ O ₃	434.23
BD_17	OCH ₃	OC ₂ H ₅	NH	O	60	138-140	C ₂₆ H ₃₂ N ₄ O ₄	464.24
BD_18	F	OC ₂ H ₅	NH	O	59	116-188	C ₂₅ H ₂₉ FN ₄ O ₃	452.22
BD_19	CF ₃	OC ₂ H ₅	NH	O	56	101-103	C ₂₆ H ₂₉ F ₃ N ₄ O ₃	502.22
BD_20	H	OC ₂ H ₅	O	NC ₂ H ₅	59	110-112	C ₂₇ H ₃₄ N ₄ O ₃	462.58
BD_21	OCH ₃	OC ₂ H ₅	O	NC ₂ H ₅	60	-	C ₂₈ H ₃₆ N ₄ O ₄	492.27
BD_22	F	OC ₂ H ₅	O	NC ₂ H ₅	59	99-101	C ₂₇ H ₃₃ FN ₄ O ₃	480.25
BD_23	CF ₃	OC ₂ H ₅	O	NC ₂ H ₅	54	240-241	C ₂₈ H ₃₃ F ₃ N ₄ O ₃	530.25
BD_24	H	OC ₂ H ₅	NH	NC ₂ H ₅	57	90-92	C ₂₇ H ₃₅ N ₅ O ₂	461.28
BD_25	OCH ₃	OC ₂ H ₅	NH	NC ₂ H ₅	55	-	C ₂₈ H ₃₇ N ₅ O ₃	491.29
BD_26	F	OC ₂ H ₅	NH	NC ₂ H ₅	59	106-108	C ₂₇ H ₃₄ FN ₅ O ₂	479.27
BD_27	CF ₃	OC ₂ H ₅	NH	NC ₂ H ₅	54	98-100	C ₂₈ H ₃₄ F ₃ N ₅ O ₂	529.27
BD_28	H	NHNH ₂	O	O	60	289-291	C ₂₃ H ₂₇ N ₅ O ₃	421.21
BD_29	OCH ₃	NHNH ₂	O	O	58	298-300	C ₂₄ H ₂₉ N ₅ O ₄	451.22
BD_30	F	NHNH ₂	O	O	57	290-292	C ₂₃ H ₂₆ FN ₅ O ₃	439.20
BD_31	CF ₃	NHNH ₂	O	O	59	281-283	C ₂₄ H ₂₆ F ₃ N ₅ O ₃	489.20
BD_32	H	NHNH ₂	NH	O	61	310-312	C ₂₃ H ₂₈ N ₆ O ₂	420.23
BD_33	OCH ₃	NHNH ₂	NH	O	56	291-293	C ₂₄ H ₃₀ N ₆ O ₃	450.24
BD_34	F	NHNH ₂	NH	O	58	289-291	C ₂₃ H ₂₇ FN ₆ O ₂	438.22
BD_35	CF ₃	NHNH ₂	NH	O	57	302-304	C ₂₄ H ₂₇ F ₃ N ₆ O ₂	488.21
BD_36	H	NHNH ₂	O	NC ₂ H ₅	60	320-322	C ₂₅ H ₃₂ N ₆ O ₂	448.26
BD_37	OCH ₃	NHNH ₂	O	NC ₂ H ₅	59	302-304	C ₂₆ H ₃₄ N ₆ O ₃	478.27
BD_38	F	NHNH ₂	O	NC ₂ H ₅	55	320-322	C ₂₅ H ₃₁ FN ₆ O ₂	466.25

Conti....

Comp	R	R ₁	X	Y	Yield (%)	Melting point (°C)	Molecular formula	Molecular weight
BD_39	CF ₃	NHNH ₂	O	NC ₂ H ₅	60	300-302	C ₂₆ H ₃₁ F ₃ N ₆ O ₂	516.25
BD_40	H	NHNH ₂	NH	NC ₂ H ₅	57	310-312	C ₂₅ H ₃₃ N ₇ O	447.27
BD_41	OCH ₃	NHNH ₂	NH	NC ₂ H ₅	55	306-308	C ₂₆ H ₃₅ N ₇ O ₂	477.29
BD_42	F	NHNH ₂	NH	NC ₂ H ₅	56	298-300	C ₂₅ H ₃₂ FN ₇ O	465.27
BD_43	CF ₃	NHNH ₂	NH	NC ₂ H ₅	54	268-270	C ₂₆ H ₃₂ F ₃ N ₇ O	515.26
BD_44	H	OH	O	O	55	-	C ₂₃ H ₂₅ N ₃ O ₄	407.18
BD_45	OCH ₃	OH	O	O	53	239-241	C ₂₄ H ₂₇ N ₃ O ₅	437.20
BD_46	F	OH	O	O	56	199-201	C ₂₃ H ₂₄ FN ₃ O ₄	425.18
BD_47	CF ₃	OH	O	O	61	248-250	C ₂₄ H ₂₄ F ₃ N ₃ O ₄	475.17
BD_48	H	OH	NH	O	58	187-189	C ₂₃ H ₂₆ N ₄ O ₃	406.20
BD_49	OCH ₃	OH	NH	O	59	199-201	C ₂₄ H ₂₈ N ₄ O ₄	436.21
BD_50	F	OH	NH	O	56	216-218	C ₂₃ H ₂₅ FN ₄ O ₃	424.19
BD_51	CF ₃	OH	NH	O	60	223-224	C ₂₄ H ₂₅ F ₃ N ₄ O ₃	474.19
BD_52	H	OH	O	NC ₂ H ₅	59	-	C ₂₅ H ₃₀ N ₄ O ₃	434.23
BD_53	OCH ₃	OH	O	NC ₂ H ₅	57	282-284	C ₂₆ H ₃₂ N ₄ O ₄	464.24
BD_54	F	OH	O	NC ₂ H ₅	61	-	C ₂₅ H ₂₉ FN ₄ O ₃	452.22
BD_55	CF ₃	OH	O	NC ₂ H ₅	56	153-155	C ₂₆ H ₂₉ F ₃ N ₄ O ₃	502.22
BD_56	H	OH	NH	NC ₂ H ₅	59	188-190	C ₂₅ H ₃₁ N ₅ O ₂	433.25
BD_57	OCH ₃	OH	NH	NC ₂ H ₅	60	-	C ₂₆ H ₃₃ N ₅ O ₃	463.26

5.4.3 Characterization of synthesized compounds

***Tert*-butyl (4-aminophenyl) carbamate (BD_01):** Brown solid (15 g, 75%); mp: 112-114 °C. ESI-MS was found at m/z 209.43 (M+H)⁺. ¹H NMR (300 MHz, CDCl₃, TMS): δ = 9.68 (s, 1H), 7.56 (d, J = 7.6 Hz, 2H), 6.79 (d, J = 7.8 Hz, 2H), 5.89 (s, 2H), 1.36 (s, 9H).

***Tert*-butyl (4-hydroxyphenyl) carbamate (BD_05):** Brown solid (15 g, 75%); mp: 144-145 °C. ESI-MS was found at m/z 210.23 (M+H)⁺. ¹H NMR (300 MHz, CDCl₃, TMS): δ = 9.78 (s, 1H), 7.56 (d, J = 7.8 Hz, 2H), 6.79 (d, J = 8.0 Hz, 2H), 6.68 (brs, 1H), 1.36 (s, 9H).

Tert-butyl (4-((3-bromopropyl) amino) phenyl) carbamate (BD_02): Off-white solid (12.8g, 60%); m.p: 113-115 °C; ESI-MS was found at m/z 330.43 (M+H)⁺. ¹H NMR (300 MHz, CDCl₃, TMS):δ = 9.98 (s, 1H), 7.53 (d, *J* = 7.4 Hz, 2H), 6.72 (d, *J* = 8.1Hz, 2H), 5.68 (s, 1H), 3.56 (t, *J* = 7.0 Hz, 2H), 3.31 (t, *J* = 6.9 Hz, 2H), 2.01 (m, 2H), 1.39 (s, 9H).

Tert-butyl (4-(3-bromopropoxy)phenyl)carbamate (BD_06): Brown solid (10.4 g, 70%); m.p: 100-102 °C; ESI-MS was found at m/z 331.36 (M+H)⁺. ¹H NMR (300 MHz, CDCl₃, TMS):δ = 9.76 (s, 1H), 6.78 (d, *J* = 7.8 Hz, 2H), 6.68 (d, *J* = 7.6 Hz, 2H), 4.08 (t, *J* = 6.8 Hz, 2H), 3.58 (t, *J* = 7.0 Hz, 2H), 1.98 (m, 2H), 1.29 (s, 9H).

Tert-butyl (4-((3-morpholinopropyl)amino)phenyl)carbamate (BD_03a): Off-white solid (4.75 g, 71%); m.p: 66-68 °C; ESI-MS was found at m/z 336.48 (M+H)⁺. ¹H NMR (300 MHz, CDCl₃, TMS):δ = 9.98 (s, 1H), 7.57 (d, *J* = 7.1 Hz, 2H), 6.73 (d, *J* = 7.6 Hz, 2H), 5.49 (s, 1H), 3.40 (t, *J* = 6.8 Hz, 4H), 2.41 (m, 2H), 2.36 (t, *J* = 6.4 Hz, 4H), 2.34 (s, 6H), 1.67 (m, 2H), 1.32 (s, 9H).

Tert-butyl (4-((3-(4-ethylpiperazin-1-yl)propyl)amino)phenyl) carbamate (BD_03b): Pale brown solid (5g, 70%); mp: 97-98 °C; ESI-MS was found at m/z 363.56 (M+H)⁺. ¹H NMR (300 MHz, CDCl₃, TMS):δ = 10.02 (s, 1H), 7.60 (d, *J* = 7.3 Hz, 2H), 6.68 (d, *J* = 7.7 Hz, 2H), 5.38 (s, 1H), 3.38 (t, *J* = 7.0 Hz, 2H), 2.40 (m, 2H), 2.37 (t, *J* = 6.8 Hz, 4H), 2.31 (s, 6H), 1.69 (m, 2H), 1.21 (s, 9H), 1.02 (t, *J* = 6.8 Hz, 3H).

N1-(3-Morpholinopropyl)benzene-1,4-diamine (BD_04a): Pale brown liquid (2.52 g, 90%); ESI-MS was found at m/z 236.50 (M+H)⁺. ¹H NMR (300 MHz, CDCl₃, TMS):δ = 6.74 (d, *J* = 7.6 Hz, 2H), 6.56 (d, *J* = 7.2 Hz, 2H), 6.02-5.49 (bs, 3H), 3.58 (t, *J* = 7.0 Hz, 4H), 3.31 (t, *J* = 6.8 Hz, 2H), 2.29 (s, 6H), 1.62 (m, 2H).

N1-(3-(4-Ethylpiperazin-1-yl)propyl)benzene-1,4-diamine (BD_04b): Pale brown liquid (3.14g, Yield 87%); ESI-MS was found at m/z 263.55 (M+H)⁺. ¹H NMR (300 MHz, CDCl₃, TMS):δ = 6.57 (d, *J* = 7.7 Hz, 2H), 6.36 (d, *J* = 7.4 Hz, 2H), 5.56 (bs, 3H), 3.35 (t, *J* = 7.0 Hz, 2H), 2.42 (m, 2H), 2.39 (t, *J* = 6.8 Hz, 4H), 2.28 (s, 6H), 1.26 (m, 2H), 1.04 (t, *J* = 7.0 Hz, 3H).

4-(3-Morpholinopropoxy)aniline (BD_08a): Pale brown liquid (2.8 g, 85%); ESI-MS was found at m/z 237.20 (M+H)⁺. ¹H NMR (300 MHz, CDCl₃, TMS): δ = 6.76 (d, J = 7.1 Hz, 2H), 6.62 (d, J = 7.5 Hz, 2H), 6.02 (bs, 2H), 4.03 (t, J = 6.8 Hz, 2H), 3.64 (t, J = 7.0 Hz, 4H), 2.30 (s, 6H), 1.71 (m, 2H).

4-(3-(4-Ethylpiperazin-1-yl)propoxy)aniline (BD_08b): Pale brown liquid (3.2g, 87%); ESI-MS was found at m/z 264.73 (M+H)⁺. ¹H NMR (300 MHz, CDCl₃, TMS): δ = 6.74 (d, J = 7.6 Hz, 2H), 6.65 (d, J = 7.4 Hz, 2H), 6.03 (bs, 2H), 4.03 (t, J = 7.0 Hz, 2H), 2.41 (q, J = 7.2 Hz, 2H), 2.34 (t, J = 6.8 Hz, 4H), 2.29 (s, 6H), 1.77 (m, 2H), 1.05 (t, J = 7.0 Hz, 3H).

Diethyl 2-((phenylamino)methylene)malonate (BD_09a): Off-white solid (11.83 g, 90%); m.p: 94-96 °C; ESI-MS was found at m/z 264.23 (M+H)⁺. ¹H NMR (300 MHz, CDCl₃, TMS): δ = 8.46 (s, 1H), 7.32-6.84 (m, 5H), 6.62 (s, 1H), 4.35 (q, J = 7.0 Hz, 4H), 1.32 (t, J = 6.8 Hz, 6H).

Diethyl 2-(((4-methoxyphenyl)amino)methylene)malonate (BD_09b): Off-white solid (13.1 g, 89%); m.p: 40-42 °C; ESI-MS was found at m/z 294.42 (M+H)⁺. ¹H NMR (300 MHz, CDCl₃, TMS): δ = 8.43 (s, 1H), 7.46 (d, J = 6.3Hz, 2H), 6.81 (d, J = 6.5Hz, 2H), 6.68 (s, 1H), 4.37 (q, J = 7.0 Hz, 4H), 3.81 (s, 3H), 1.36 (t, J = 6.8 Hz, 6H).

Diethyl 2-(((4-fluorophenyl)amino)methylene)malonate (BD_09c): Off white solid (12.68 g, 91%) ; m.p: 74-76 °C; ESI-MS was found at m/z 282.31 (M+H)⁺. ¹H NMR (300 MHz, CDCl₃, TMS): δ = 8.47 (s, 1H), 7.11 (d, J = 7.2 Hz, 2H), 6.43 (d, J = 7.1Hz, 2H), 6.72 (s, 1H), 4.36 (q, J = 7.0 Hz, 4H), 1.35 (t, J = 7.0 Hz, 6H).

Diethyl 2-(((4-(trifluoromethyl)phenyl)amino)methylene)malonate (BD_09d): Off white solid (14.8 g, 91%); m.p: 95-97 °C; ESI-MS was found at m/z 332.32 (M+H)⁺. ¹H NMR (300 MHz, CDCl₃, TMS): δ = 8.45 (s, 1H), 7.46 (d, J = 6.8Hz, 2H), 6.46 (d, J = 6.7Hz, 2H), 6.70 (s, 1H), 4.37 (q, J = 7.0 Hz, 4H), 1.33 (t, J = 6.8 Hz, 6H).

Ethyl 4-hydroxyquinoline-3-carboxylate (BD_10a): Pale yellow solid (5.64 g, 65%); m.p: 276-278 °C; ESI-MS was found at m/z 218.32 (M+H)⁺. ¹H NMR (300 MHz, DMSO-d₆, TMS): δ = 10.72 (brs, 1H), 8.91 (s, 1H), 8.46 -7.78 (m, 4H), 4.29 (q, J = 7.1 Hz, 2H), 1.29 (t, J = 7.1Hz, 3H).

Ethyl 4-hydroxy-6-methoxyquinoline-3-carboxylate (BD_10b): Yellow solid (6.51 g, 66%); m.p: 274-276 °C; ESI-MS was found at m/z 248.32 (M+H)⁺. ¹H NMR (300 MHz, DMSO-d₆, TMS): δ = 10.67 (brs, 1H), 8.82 (s, 1H), 8.14 (d, *J* = 9.0 Hz, 1H), 7.73 (d, *J* = 7.2 Hz, 1H), 7.14 (s, 1H), 4.27 (q, *J* = 7.2 Hz, 2H), 1.29 (t, *J* = 7.0 Hz, 3H).

Ethyl 6-fluoro-4-hydroxyquinoline-3-carboxylate (BD_10c): Pale yellow solid (6.58 g, 70%); m.p: 288-290 °C; ESI-MS was found at m/z 236.22 (M+H)⁺. ¹H NMR (300 MHz, DMSO-d₆, TMS): δ = 10.45 (brs, 1H), 8.86 (s, 1H), 8.16 (d, *J* = 7.7 Hz, 1H), 7.81 (s, 1H), 7.34 (d, *J* = 7.4 Hz, 1H), 4.23 (q, *J* = 6.8 Hz, 2H), 1.29 (t, *J* = 6.8 Hz, 3H).

Ethyl 4-hydroxy-6-(trifluoromethyl)quinoline-3-carboxylate (BD_10d): Pale brown solid (7.75 g, 68%); m.p: 290-292 °C; ESI-MS was found at m/z 286.34 (M+H)⁺. ¹H NMR (300 MHz, DMSO-d₆, TMS): δ = 10.52 (brs, 1H), 8.91 (s, 1H), 8.61 (d, *J* = 7.8 Hz, 1H), 8.37 (s, 1H), 8.11 (d, *J* = 7.6 Hz, 1H), 4.27 (q, *J* = 7.0 Hz, 2H), 1.28 (t, *J* = 6.8 Hz, 3H).

Ethyl 4-chloroquinoline-3-carboxylate (BD_11a): Yellow solid (4.74 g, 81%); m.p: 43-45 °C; ESI-MS was found at m/z 236.67 (M+H)⁺. ¹H NMR (300 MHz, CDCl₃, TMS): δ = 8.92 (s, 1H), 8.46-7.78 (m, 4H), 4.28 (q, *J* = 6.8 Hz, 2H), 1.27 (t, *J* = 7.3 Hz, 3H).

Ethyl 4-chloro-6-methoxyquinoline-3-carboxylate (BD_11b): Pale yellow solid (5.44 g, 82%); m.p: 79-81 °C; ESI-MS was found at m/z 266.68 (M+H)⁺. ¹H NMR (300 MHz, CDCl₃, TMS): δ = 8.84 (s, 1H), 8.13 (d, *J* = 9.1 Hz, 1H), 7.72 (d, *J* = 7.2 Hz, 1H), 7.15 (s, 1H), 4.26 (q, *J* = 7.0 Hz, 2H), 1.28 (t, *J* = 6.8 Hz, 3H).

Ethyl 4-chloro-6-fluoroquinoline-3-carboxylate (BD_11c): Yellow solid (5.64 g, 89%); m.p: 62-64 °C; ESI-MS was found at m/z 254.60 (M+H)⁺. ¹H NMR (300 MHz, CDCl₃, TMS): δ = 8.87 (s, 1H), 8.17 (d, *J* = 7.5 Hz, 1H), 7.83 (s, 1H), 7.36 (d, *J* = 7.6 Hz, 1H), 4.22 (q, *J* = 7.0 Hz, 2H), 1.29 (t, *J* = 7.0 Hz, 3H).

Ethyl 4-chloro-6-(trifluoromethyl)quinoline-3-carboxylate (BD_11d): Pale yellow solid (6.5 g, 86%); m.p: 90-92 °C; ESI-MS was found at m/z 304.64 (M+H)⁺. ¹H

NMR (300 MHz, CDCl₃, TMS): δ = 8.95 (s, 1H), 8.62 (d, J = 7.7 Hz, 1H), 8.38 (s, 1H), 8.13 (d, J = 7.8 Hz, 1H), 4.28 (q, J = 7.1 Hz, 2H), 1.29 (t, J = 7.0 Hz, 3H).

Ethyl 4-((4-(3-morpholinopropoxy)phenyl)amino) quinoline-3-carboxylate (BD_12): Pale yellow gammy (1.10 g, 60%); ¹H NMR (300 MHz, DMSO-d₆, TMS): δ = 10.21 (s, 1H), 9.31 (s, 1H), 8.36 (d, J = 8.8 Hz, 1H), 7.99 (m, 3H), 7.52 (d, J = 8.2 Hz, 2H), 6.97 (d, J = 8.4 Hz, 2H), 4.32 (q, J = 7.0 Hz, 2H), 4.02 (t, J = 6.8 Hz, 2H), 3.67 (t, J = 7.0 Hz, 4H), 2.37 (s, 6H), 1.79 (m, 2H), 1.28 (t, J = 7.0 Hz, 3H). ¹³C NMR (75 MHz, DMSO-d₆, TMS): δ = 168.5, 153.0, 152.2, 149.9, 141.3, 132.8(2C), 129.7, 127.4, 126.0, 121.7(2C), 120.9, 115.8(2C), 113.6, 73.4, 67.1(2C), 63.4(2C), 61.6, 59.1, 28.3, 14.6. ESI-MS m/z (Calcd. for C₂₅H₂₉N₃O₄: 435.22); Found: 436.29 (M+H)⁺. Anal calcd. for C₂₅H₂₉N₃O₄: C, 68.95; H, 6.71; N, 9.65; Found: C, 68.91; H, 6.67; N, 9.62.

Ethyl 6-methoxy-4-((4-(3-morpholinopropoxy)phenyl)amino) quinoline-3-carboxylate (BD_13): Brown solid (1.2 g, 58%); m.p: 170-172 °C; ¹H NMR (300 MHz, DMSO-d₆, TMS): δ = 10.01 (s, 1H), 8.91 (s, 1H), 8.31 (d, J = 8.6 Hz, 1H), 8.01-7.53 (m, 4H), 6.98 (d, J = 8.2 Hz, 2H), 4.33 (q, J = 7.0 Hz, 2H), 4.03 (t, J = 6.8 Hz, 2H), 3.81 (s, 3H), 3.65 (t, J = 7.1 Hz, 4H), 2.41 (s, 6H), 1.80 (m, 2H), 1.29 (t, J = 7.0 Hz, 3H). ¹³C NMR (75 MHz, DMSO-d₆, TMS): δ = 168.5, 157.3, 152.0, 150.2(2C), 136.9, 132.7, 131.4, 124.8, 122.3(3C), 115.9(2C), 114.2, 103.7, 73.5, 67.2(2C), 63.6(2C), 61.3, 59.0, 56.4, 28.5, 14.8. ESI-MS m/z (Calcd. for C₂₆H₃₁N₃O₅: 465.23); Found: 464.05 (M-H)⁻. Anal calcd. for C₂₆H₃₁N₃O₅: C, 67.08; H, 6.71; N, 9.03; Found: C, 67.11; H, 6.74; N, 9.01.

Ethyl 6-fluoro-4-((4-(3-morpholinopropoxy)phenyl)amino) quinoline-3-carboxylate (BD_14): Off-white solid (1.16 g, 57%); m.p: 93-95 °C; ¹H NMR (300 MHz, DMSO-d₆, TMS): δ = 9.89 (s, 1H), 9.01 (s, 1H), 8.32 (d, J = 8.8 Hz, 1H), 7.96-7.49 (m, 4H), 6.98 (d, J = 8.1 Hz, 2H), 4.33 (q, J = 7.1 Hz, 2H), 4.03 (t, J = 6.8 Hz, 2H), 3.59 (t, J = 6.9 Hz, 4H), 2.36 (s, 6H), 1.80 (m, 2H), 1.26 (t, J = 7.0 Hz, 3H). ¹³C NMR (75 MHz, DMSO-d₆, TMS): δ = 168.3, 160.8, 153.0, 151.9, 149.7, 138.3, 133.0, 130.5, 124.2, 121.8(3C), 116.0(2C), 114.7, 104.5, 73.8, 67.5(2C), 63.2(2C), 61.4, 59.0, 28.6, 14.9. ESI-MS m/z (Calcd. for C₂₅H₂₈FN₃O₄: 453.21); Found: 452.21 (M-H)⁻. Anal calcd. for C₂₅H₂₈FN₃O₄: C, 66.21; H, 6.22; N, 9.27; Found: C, 66.19; H, 6.25; N, 9.24.

Ethyl 4-((4-(3-morpholinopropoxy)phenyl)amino)-6-(trifluoromethyl) quinoline-3-carboxylate (BD_15): Pale yellow solid (1.3 g, 58%); m.p: 98-100 °C; ¹H NMR (300 MHz, DMSO-d₆, TMS): δ = 10.20 (s, 1H), 8.87 (s, 1H), 8.37 (d, *J* = 8.1 Hz, 1H), 7.96 (m, 2H), 7.51 (d, *J* = 8.4 Hz, 2H), 6.98 (d, *J* = 8.2 Hz, 2H), 4.30 (q, *J* = 7.0 Hz, 2H), 4.04 (t, *J* = 6.8 Hz, 2H), 3.68 (t, *J* = 6.8 Hz, 4H), 2.37 (s, 6H), 1.80 (m, 2H), 1.29 (t, *J* = 6.4 Hz, 3H). ¹³C NMR (75 MHz, DMSO-d₆, TMS): δ = 168.5, 155.0, 154.3, 149.9, 142.5, 132.8, 131.6, 129.1, 127.9, 125.0, 121.8(2C), 120.5(2C), 116.2(2C), 115.4, 73.7, 67.3(2C), 63.5(2C), 61.8, 59.2, 28.5, 14.7. ESI-MS *m/z* (Calcd. for C₂₆H₂₈F₃N₃O₄: 503.20); Found: 502.02 (M-H)⁻. Anal calcd. for C₂₆H₂₈F₃N₃O₄: C, 62.02; H, 5.61; N, 8.35; Found: C, 62.04; H, 5.58; N, 8.32.

Ethyl 4-((4-((3-morpholinopropyl)amino)phenyl)amino)quinoline-3-carboxylate (BD_16): Pale yellow solid (1.15 g, 59%); m.p: 240-242 °C; ¹H NMR (300 MHz, DMSO-d₆, TMS): δ = 9.99 (s, 1H), 8.89 (s, 1H), 7.99-7.48 (m, 4H), 6.85 (d, *J* = 8.1 Hz, 2H), 6.73 (d, *J* = 8.2 Hz, 2H), 5.51 (brs, 1H), 4.30 (q, *J* = 7.4 Hz, 2H), 3.68 (t, *J* = 7.0 Hz, 4H), 3.35 (t, *J* = 6.8 Hz, 2H), 2.39 (s, 6H), 1.69 (m, 2H), 1.26 (t, *J* = 7.0 Hz, 3H). ¹³C NMR (75 MHz, DMSO-d₆, TMS): δ = 168.3, 153.1, 152.4, 140.9, 138.2, 134.9, 132.7, 129.5, 127.0, 126.2, 121.5, 119.0(2C), 118.8(2C), 113.6, 67.3(2C), 63.5(2C), 61.2, 52.7, 41.5, 27.8, 14.6. ESI-MS *m/z* (Calcd. for C₂₅H₃₀N₄O₃: 434.23); Found: 435.25 (M+H)⁺. Anal calcd. for C₂₅H₃₀N₄O₃: C, 69.10; H, 6.96; N, 12.89; Found: C, 69.13; H, 6.94; N, 12.87.

Ethyl 6-methoxy-4-((4-((3-morpholinopropyl)amino)phenyl)amino) quinoline-3-carboxylate (BD_17): Brown solid (1.2 g, 60%); m.p: 138-140 °C; ¹H NMR (300 MHz, DMSO-d₆, TMS): δ = 10.01 (s, 1H), 8.89 (s, 1H), 8.30 (d, *J* = 8.8 Hz, 1H), 8.04-7.55 (m, 2H), 6.61 (d, *J* = 9.1 Hz, 2H), 6.59 (d, *J* = 8.4 Hz, 2H), 5.53 (brs, 1H), 4.31 (q, *J* = 7.2 Hz, 2H), 3.66 (t, *J* = 7.0 Hz, 4H), 3.82 (s, 3H), 3.43 (t, *J* = 6.8 Hz, 2H), 2.41 (s, 6H), 1.81 (m, 2H), 1.26 (t, *J* = 7.4 Hz, 3H). ¹³C NMR (75 MHz, DMSO-d₆, TMS): δ = 168.5, 157.3, 152.0, 150.2, 138.0, 136.9, 135.1, 131.3, 125.0, 122.2, 119.4(2C), 119.0(2C), 114.3, 103.9, 67.4(2C), 63.6(2C), 61.3, 56.0, 52.8, 41.6, 27.9, 14.5. ESI-MS *m/z* (Calcd. for C₂₆H₃₂N₄O₄: 464.24); Found: 465.31 (M+H)⁺. Anal calcd. for C₂₆H₃₂N₄O₄: C, 67.22; H, 6.94; N, 12.06; Found: C, 67.24; H, 6.91; N, 12.03.

Ethyl 6-fluoro-4-((4-((3-morpholinopropyl)amino)phenyl)amino) quinoline-3-carboxylate (BD_18): Pale green solid (1.2 g, 59%); m.p: 116-118 °C; ¹H NMR (300 MHz, DMSO-d₆, TMS): δ = 9.96 (s, 1H), 8.82 (s, 1H), 7.76-6.98 (m, 3H), 6.63 (d, *J* = 8.4 Hz, 2H), 6.59 (d, *J* = 8.2 Hz, 2H), 5.52 (brs, 1H), 4.35 (q, *J* = 7.1 Hz, 2H), 3.57 (t, *J* = 6.8 Hz, 4H), 3.42 (t, *J* = 7.1 Hz, 2H), 2.35 (s, 6H), 1.81 (m, 2H), 1.23 (t, *J* = 7.2 Hz, 3H). ¹³C NMR (75 MHz, DMSO-d₆, TMS): δ = 168.3, 160.9, 152.7, 151.6, 138.3(2C), 134.9, 130.4, 124.2, 121.8, 119.3(2C), 119.0(2C), 114.9, 104.7, 67.4(2C), 63.5(2C), 61.7, 52.8, 41.6, 27.4, 14.7. ESI-MS m/z (Calcd. for C₂₅H₂₉FN₄O₃: 452.22); Found: 451.09 (M-H)⁻. Anal calcd. for C₂₅H₂₉FN₄O₃: C, 66.35; H, 6.46; N, 12.38; Found: C, 66.33; H, 6.48; N, 12.41.

Ethyl 4-((4-((3-morpholinopropyl)amino)phenyl)amino)-6-(trifluoro methyl) quinoline-3-carboxylate (BD_19): Brown solid (1.25 g, 56%); m.p: 101-103 °C; ¹H NMR (300 MHz, DMSO-d₆, TMS): δ = 10.01 (s, 1H), 8.83 (s, 1H), 7.96-7.01 (m, 3H), 6.54 (d, *J* = 8.0 Hz, 2H), 6.49 (d, *J* = 8.1 Hz, 2H), 5.51 (brs, 1H), 4.32 (q, *J* = 7.0 Hz, 2H), 3.64 (t, *J* = 7.2 Hz, 4H), 3.52 (t, *J* = 6.7 Hz, 2H), 2.40 (s, 6H), 1.81 (m, 2H), 1.27 (t, *J* = 7.1 Hz, 3H). ¹³C NMR (75 MHz, DMSO-d₆, TMS): δ = 168.5, 154.9, 154.3, 142.6, 138.1, 134.8, 131.6, 129.0, 127.8, 125.1, 120.5(2C), 119.4(2C), 118.9(2C), 115.2, 67.2(2C), 63.4(2C), 61.7, 52.6, 41.8, 27.5, 14.7. ESI-MS m/z (Calcd. for C₂₆H₂₉F₃N₄O₃: 502.22); Found: 503.21 (M+H)⁺. Anal calcd. for C₂₆H₂₉F₃N₄O₃: C, 62.14; H, 5.82; N, 11.15; Found: C, 62.08; H, 5.85; N, 11.12.

Ethyl 4-((4-((3-(4-ethylpiperazin-1-yl)propoxy)phenyl)amino)quinoline-3-carboxylate (BD_20): Brown solid (1.2 g, 59%); m.p: 110-112 °C; ¹H NMR (300 MHz, DMSO-d₆, TMS): δ = 9.82 (s, 1H), 8.87 (s, 1H), 8.43-7.73 (m, 4H), 7.48 (d, *J* = 8.2 Hz, 2H), 6.58 (d, *J* = 8.2 Hz, 2H), 4.23 (q, *J* = 7.0 Hz, 2H), 4.02 (m, 2H), 2.47-2.32 (m, 12H), 1.83 (m, 2H), 1.29 (t, *J* = 7.0 Hz, 3H), 1.04 (t, *J* = 7.1 Hz, 3H). ¹³C NMR (75 MHz, DMSO-d₆, TMS): δ = 167.3, 152.5, 151.7, 150.1, 139.2, 132.3(2C), 129.1, 126.5, 125.2, 122.3 (3C), 115.2(2C), 113.3, 73.5, 61.1, 58.1(3C), 57.5(2C), 49.8, 27.8, 14.3, 13.4. ESI-MS m/z (Calcd. for C₂₇H₃₄N₄O₃: 462.58); Found: 463.34 (M+H)⁺. Anal calcd. for C₂₇H₃₄N₄O₃: C, 70.10; H, 7.41; N, 12.11; Found: C, 70.09; H, 7.43; N, 12.24.

Ethyl 4-((4-((3-(4-ethylpiperazin-1-yl)propoxy)phenyl)amino)-6-methoxy quinoline-3-carboxylate (BD_21): Brown gammy (1.32 g, 60%); ¹H NMR (300

MHz, DMSO-d₆, TMS): δ = 9.92 (s, 1H), 8.86 (s, 1H), 7.81-7.45 (m, 3H), 7.43 (d, J = 8.4 Hz, 2H), 6.57 (d, J = 8.1 Hz, 2H), 4.19 (q, J = 7.0 Hz, 2H), 4.01 (t, J = 6.8 Hz, 2H), 3.54 (s, 3H), 2.48-2.31 (m, 12H), 1.82 (m, 2H), 1.31 (q, J = 7.1 Hz, 3H), 1.03 (t, J = 6.7 Hz, 3H). ¹³C NMR (75 MHz, DMSO-d₆, TMS): δ = 168.3, 157.5, 156.2, 150.4(2C), 136.9, 133.0, 131.3, 125.1, 122.4(3C), 115.9(2C), 114.3, 103.7, 73.8, 61.4, 59.1(3C), 58.5(2C), 56.3, 50.1, 28.4, 14.7, 13.9. ESI-MS m/z (Calcd. for C₂₈H₃₆N₄O₄: 492.27); Found: 493.52 (M+H)⁺. Anal calcd. for C₂₈H₃₆N₄O₄: C, 68.27; H, 7.37; N, 11.37; Found: C, 68.25; H, 7.33; N, 11.35.

Ethyl 4-((4-(3-(4-ethylpiperazin-1-yl)propoxy)phenyl)amino)-6-fluoroquinoline-3-carboxylate (BD_22): Pale yellow solid (1.27 g, 59%); m.p: 99-101 °C; ¹H NMR (300 MHz, DMSO-d₆, TMS): δ = 9.94 (s, 1H), 8.87 (s, 1H), 8.01 (d, J = 8.8 Hz, 1H), 7.73 (d, J = 8.1 Hz, 1H), 7.63 (dd, J = 8.1 Hz, 2.7 Hz, 1H), 6.92 (d, J = 8.6 Hz, 2H), 6.58 (d, J = 8.0 Hz, 2H), 4.28 (q, J = 6.8 Hz, 2H), 3.98 (t, J = 7.0 Hz, 2H), 2.49-2.32 (m, 12H), 1.83 (m, 2H), 1.32 (t, J = 6.8 Hz, 3H), 1.03 (t, J = 7.2 Hz, 3H). ¹³C NMR (75 MHz, DMSO-d₆, TMS): δ = 168.6, 160.5, 152.7, 151.9, 150.2, 138.0, 132.8, 130.5, 124.2, 121.9(3C), 115.7(2C), 114.8, 104.5, 73.7, 61.4, 59.4(3C), 58.6(2C), 50.2, 28.2, 14.5, 13.8. ESI-MS m/z (Calcd. for C₂₇H₃₃FN₄O₃: 480.25); Found: 479.16 (M-H)⁻. Anal calcd. for C₂₇H₃₃FN₄O₃: C, 67.48; H, 6.92; N, 11.66; Found: C, 67.51; H, 6.64; N, 11.67.

Ethyl 4-((4-(3-(4-ethylpiperazin-1-yl)propoxy)phenyl)amino)-6-(trifluoromethyl)quinoline-3-carboxylate (BD_23): Pale yellow gammy (1.3 g, 54%); m.p: 240 °C; ¹H NMR (300 MHz, DMSO-d₆, TMS): δ = 10.01 (s, 1H), 8.89 (s, 1H), 8.47 (d, J = 2.6 Hz, 1H), 8.29 (dd, J = 8.4 Hz, 2.4 Hz, 1H), 7.81 (d, J = 8.4 Hz, 1H), 7.43 (d, J = 8.6 Hz, 2H), 6.59 (d, J = 8.2 Hz, 2H), 4.16 (q, J = 7.0 Hz, 2H), 3.99 (t, J = 7.1 Hz, 2H), 2.47-2.35 (m, 12H), 1.82 (m, 2H), 1.31 (t, J = 6.8 Hz, 3H), 1.03 (t, J = 7.0 Hz, 3H). ¹³C NMR (75 MHz, DMSO-d₆, TMS): δ = 168.5, 154.8(2C), 150.1, 142.6, 132.9, 131.6, 129.1, 127.8, 125.0, 121.8(2C), 120.9(2C), 115.7(3C), 73.5, 70.3, 59.0(3C), 58.5(2C), 50.2, 28.4, 14.6, 13.7. ESI-MS m/z (Calcd. for C₂₈H₃₃F₃N₄O₃: 530.25); Found: 529.11 (M-H)⁻. Anal calcd. for C₂₈H₃₃F₃N₄O₃: C, 63.38; H, 6.27; N, 10.56; Found: C, 63.35; H, 6.24; N, 10.58.

Ethyl 4-((4-((3-(4-ethylpiperazin-1-yl)propyl)amino)phenyl)amino) quinoline-3-carboxylate (BD_24): Pale yellow solid (1.2 g, 57%); m.p: 90-92 °C; ¹H NMR (300

MHz, DMSO-d₆, TMS): δ = 9.97 (s, 1H), 8.81 (s, 1H), 8.39-7.71 (m, 4H), 6.57 (d, J = 8.0 Hz, 2H), 6.45 (d, J = 8.2 Hz, 2H), 5.54 (brs, 1H), 4.19 (q, J = 7.0 Hz, 2H), 3.41 (t, J = 6.8 Hz, 2H), 2.48-2.32 (m, 12H), 1.82 (m, 2H), 1.36 (t, J = 7.0 Hz, 3H), 1.02 (t, J = 6.8 Hz, 3H). ¹³C NMR (75 MHz, DMSO-d₆, TMS): δ = 168.3, 153.5, 152.4, 141.0, 138.2, 134.9, 132.6, 129.7, 127.3, 126.1, 121.4, 119.3(2C), 119.0(2C), 113.8, 61.5, 58.9(2C), 38.1(2C), 52.4, 50.2, 41.7, 27.5, 14.8, 13.9. ESI-MS m/z (Calcd. for C₂₇H₃₅N₅O₂: 461.28); Found: 462.41 (M+H)⁺. Anal calcd. for C₂₇H₃₅N₅O₂: C, 70.25; H, 7.64; N, 15.17; Found: C, 70.27; H, 7.61; N, 15.19.

Ethyl 4-((4-((3-(4-ethylpiperazin-1-yl)propyl)amino)phenyl)amino)-6-methoxyquinoline-3-carboxylate (BD_25): Yellow gummy (1.2 g, 55%); ¹H NMR (300 MHz, DMSO-d₆, TMS): δ = 9.97 (s, 1H), 8.87 (s, 1H), 7.78 (d, J = 8.6 Hz, 1H), 7.65 (d, J = 2.2 Hz, 1H), 7.39 (dd, J = 8.2 Hz, 2.4 Hz, 1H), 6.60 (d, J = 8.2 Hz, 2H), 6.54 (d, J = 8.1 Hz, 2H), 5.52 (brs, 1H), 4.21 (q, J = 7.0 Hz, 2H), 3.58 (s, 3H), 3.42 (t, J = 6.8 Hz, 2H), 2.47-2.30 (m, 12H), 1.83 (m, 2H), 1.35 (t, J = 7.0 Hz, 3H), 1.02 (t, J = 6.7 Hz, 3H). ¹³C NMR (75 MHz, DMSO-d₆, TMS): δ = 168.5, 157.3, 152.0, 150.2, 138.4, 136.9, 135.1, 131.2, 124.9, 122.2, 119.3(2C), 118.9(2C), 114.4, 103.7, 61.5, 59.1(2C), 58.4(2C), 56.3, 52.5, 50.2, 41.7, 27.9, 14.5, 13.8. ESI-MS m/z (Calcd. for C₂₈H₃₇N₅O₃: 491.29); Found: 490.18 (M-H)⁻. Anal calcd. for C₂₈H₃₇N₅O₃: C, 68.41; H, 7.59; N, 14.25; Found: C, 68.43; H, 7.61; N, 14.27.

Ethyl 4-((4-((3-(4-ethylpiperazin-1-yl)propyl)amino)phenyl)amino)-6-fluoroquinoline-3-carboxylate (BD_26): Pale yellow solid (1.27 g, 59%); m.p: 106-108 °C; ¹H NMR (300 MHz, DMSO-d₆, TMS): δ = 9.97 (s, 1H), 8.88 (s, 1H), 7.78 (d, J = 8.2 Hz, 1H), 7.60 (d, J = 2.2 Hz, 1H), 7.49 (dd, J = 8.6 Hz, 2.4 Hz, 1H), 6.91 (d, J = 8.1 Hz, 2H), 6.59 (d, J = 8.2 Hz, 2H), 5.51 (brs, 1H), 4.20 (q, J = 7.0 Hz, 2H), 3.54 (t, J = 6.7 Hz, 2H), 2.47-2.31 (m, 12H), 1.84 (m, 2H), 1.33 (t, J = 7.1 Hz, 3H), 1.01 (t, J = 6.7 Hz, 3H). ¹³C NMR (75 MHz, DMSO-d₆, TMS): δ = 168.3, 160.7, 152.5, 151.8, 138.3(2C), 134.9, 130.4, 124.2, 121.9, 119.1(2C), 118.8(2C), 115.0, 104.7, 61.4, 59.2(2C), 58.6(2C), 52.4, 50.2, 41.7, 27.9, 14.5, 13.7. ESI-MS m/z (Calcd. for C₂₇H₃₄FN₅O₂: 479.27); Found: 480.11 (M+H)⁺. Anal calcd. for C₂₇H₃₄FN₅O₂: C, 67.62; H, 7.15; N, 14.60; Found: C, 67.65; H, 7.13; N, 14.57.

Ethyl 4-((4-((3-(4-ethylpiperazin-1-yl)propyl)amino)phenyl)amino)-6-(trifluoromethyl)quinoline-3-carboxylate (BD_27): Yellow solid (1.28 g, 54%); m.p: 98-100

°C; ¹H NMR (300 MHz, DMSO-d₆, TMS): δ = 9.99 (s, 1H), 8.87 (s, 1H), 8.51 (d, *J* = 2.2 Hz, 1H), 8.29 (dd, *J* = 8.6 Hz, 2.4 Hz, 1H), 8.09 (d, *J* = 8.4 Hz, 1H), 6.56 (d, *J* = 8.4 Hz, 2H), 6.48 (d, *J* = 8.1 Hz, 2H), 5.51 (brs, 1H), 4.18 (q, *J* = 7.1 Hz, 2H), 3.51 (t, *J* = 6.7 Hz, 2H), 2.48-2.34 (m, 12H), 1.83 (m, 2H), 1.36 (t, *J* = 7.0 Hz, 3H), 1.03 (t, *J* = 6.9 Hz, 3H). ¹³C NMR (75 MHz, DMSO-d₆, TMS): δ = 168.6, 155.0, 154.5, 142.7, 138.2, 134.9, 131.8, 129.0, 127.9, 125.2, 120.6, 119.8, 118.9(2C), 118.7(2C), 115.4, 61.6, 59.1(2C), 58.5(2C), 52.7, 50.3, 41.7, 27.5, 14.9, 13.8. ESI-MS *m/z* (Calcd. for C₂₈H₃₄F₃N₅O₂: 529.27); Found: 530.29 (M+H)⁺. Anal calcd. for C₂₈H₃₄F₃N₅O₂: C, 63.50; H, 6.47; N, 13.22; Found: C, 63.48; H, 6.44; N, 13.26.

4-((4-(3-Morpholinopropoxy)phenyl)amino)quinoline-3-carbohydrazide

(BD_28): Yellow solid (0.126 g, 60%); m.p: 289-291 °C; ¹H NMR (300 MHz, DMSO-d₆, TMS): δ = 10.03 (s, 1H), 9.29 (s, 1H), 8.82 (s, 1H), 8.30 (d, *J* = 8.8 Hz, 1H), 8.01 (m, 3H), 7.52 (d, *J* = 8.2 Hz, 2H), 6.95 (d, *J* = 8.5 Hz, 2H), 4.01 (t, *J* = 7.1 Hz, 2H), 3.68 (t, *J* = 6.8 Hz, 4H), 2.46 (s, 6H), 2.21 (brs, 2H), 1.98 (m, 2H). ¹³C NMR (75 MHz, DMSO-d₆, TMS): δ = 165.5, 152.2, 150.0, 146.9, 138.1, 133.0, 132.6, 129.4, 127.1, 126.3, 123.9, 121.7(2C), 115.9(2C), 113.4, 73.6, 67.4(2C), 63.7(2C), 59.1, 28.4. ESI-MS *m/z* (Calcd. for C₂₃H₂₇N₅O₃: 421.21); Found: 422.19 (M+H)⁺. Anal calcd. for C₂₃H₂₇N₅O₃: C, 65.54; H, 6.46; N, 16.62; Found: C, 65.51; H, 6.48; N, 16.64.

6-Methoxy-4-((4-(3-morpholinopropoxy)phenyl)amino)quinoline-3-

carbohydrazide (BD_29): Yellow solid (0.13 g, 58%); m.p: 298-300 °C; ¹H NMR (300 MHz, DMSO-d₆, TMS): δ = 10.02 (s, 1H), 8.93 (s, 1H), 8.84 (s, 1H), 8.12 (d, *J* = 8.6 Hz, 1H), 7.61 (d, *J* = 8.8 Hz, 2H), 7.54 (d, *J* = 8.4 Hz, 2H), 7.39 (d, *J* = 2.3 Hz, 1H), 7.28 (dd, *J* = 8.6 Hz, 2.4 Hz, 1H), 6.96 (d, *J* = 8.4 Hz, 2H), 4.04 (t, *J* = 7.1 Hz, 2H), 3.82 (s, 3H), 3.64 (t, *J* = 6.8 Hz, 4H), 2.31 (s, 6H), 2.19 (brs, 2H), 1.81 (m, 2H). ¹³C NMR (75 MHz, DMSO-d₆, TMS): δ = 163.3, 157.5, 151.2, 150.0, 144.5, 133.7, 132.9, 131.1, 124.8(2C), 122.0(2C), 115.7(2C), 113.9, 103.6, 73.8, 67.3(2C), 63.5(2C), 59.1, 56.3, 28.5. ESI-MS *m/z* (Calcd. for C₂₄H₂₉N₅O₄: 451.22); Found: 452.45 (M+H)⁺. Anal calcd. for C₂₄H₂₉N₅O₄: C, 63.84; H, 6.47; N, 15.51; Found: C, 63.87; H, 6.45; N, 15.56.

6-Fluoro-4-((4-(3-morpholinopropoxy)phenyl)amino)quinoline-3-carbohydrazide

(BD_30): Brown solid (0.124 g, 57%); m.p: 290-292 °C; ¹H NMR (300 MHz,

DMSO-d₆, TMS): δ = 9.90 (s, 1H), 9.02 (s, 1H), 8.87(s, 1H), 7.99 (d, J = 8.8 Hz, 1H), 7.57 (d, J = 8.2 Hz, 2H), 7.46 (d, J = 2.4 Hz, 1H), 7.28 (dd, J = 8.6 Hz, 2.5 Hz, 1H), 6.86 (d, J = 8.3 Hz, 2H), 4.02 (t, J = 7.0 Hz, 2H), 3.57 (t, J = 7.1 Hz, 4H), 2.34 (s, 6H), 2.20 (brs, 2H), 1.84 (m, 2H). ¹³C NMR (75 MHz, DMSO-d₆, TMS): δ = 165.4, 160.6, 151.9, 150.0, 145.8, 135.2, 132.7, 130.1, 124.6, 123.9, 122.2(2C), 115.8(2C), 114.4, 104.5, 73.8, 67.5(2C), 63.7(2C), 59.1, 28.3. ESI-MS m/z (Calcd. for C₂₃H₂₆FN₅O₃: 439.20); Found: 440.51 (M+H)⁺. Anal calcd.for C₂₃H₂₆FN₅O₃: C, 62.86; H, 5.96; N, 15.94; Found: C, 68.84; H, 5.93; N, 15.89.

4-((4-(3-Morpholinopropoxy)phenyl)amino)-6-(trifluoromethyl) quinoline-3-carbohydrazide (BD_31): Yellow solid (0.143 g, 59%); m.p: 281-283 °C; ¹H NMR (300 MHz, DMSO-d₆, TMS): δ = 10.09 (s, 1H), 8.99 (s,1H), 8.87 (s, 1H), 8.51 (d, J = 2.1 Hz, 1H), 8.19 (dd, J = 8.6 Hz, 2.3 Hz, 1H), 8.14 (d, J = 8.2 Hz, 1H), 7.43 (d, J = 8.4 Hz, 2H), 7.01 (d, J = 8.5 Hz, 2H), 4.03 (t, J = 7.0 Hz, 2H), 3.69 (t, J = 6.7 Hz, 4H), 2.33 (s, 6H), 2.03 (brs, 2H), 1.82 (m, 2H). ¹³C NMR (75 MHz, DMSO-d₆, TMS): δ = 165.3, 153.1, 149.9, 148.8, 139.2, 132.7, 131.4, 128.8, 127.6, 125.2, 122.9(3C), 120.7, 116.1(2C), 114.6, 73.8, 67.3(2C), 63.5(2C), 59.1, 28.4. ESI-MS m/z (Calcd. for C₂₄H₂₆F₃N₅O₃: 489.20); Found: 490.25 (M+H)⁺. Anal calcd.for C₂₄H₂₆F₃N₅O₃: C, 58.89; H, 5.35; N, 14.31; Found: C, 58.91; H, 5.33; N, 14.28.

4-((4-((3-Morpholinopropyl)amino)phenyl)amino)quinoline-3-carbohydrazide (BD_32): Pale green solid (0.128 g, 61%); m.p: 310-312 °C; ¹H NMR (300 MHz, DMSO-d₆, TMS): δ = 10.01 (s, 1H), 8.90 (s, 1H), 8.88 (s, 1H), 8.20-7.46 (m, 4H), 6.86 (d, J = 8.4 Hz, 2H), 6.41 (d, J = 8.6 Hz, 2H), 5.52 (brs, 1H), 3.65 (t, J = 6.8 Hz, 4H), 3.36 (t, J = 7.0 Hz, 2H), 2.35 (s, 6H), 2.02 (s, 2H), 1.78 (m, 2H). ¹³C NMR (75 MHz, DMSO-d₆, TMS): δ = 165.3, 152.0, 146.7, 138.2(2C), 134.9, 132.5, 129.3, 127.0, 126.2, 123.9, 119.1(2C), 118.7(2C), 113.2, 67.5(2C), 63.3(2C), 52.9, 41.6, 27.8. ESI-MS m/z (Calcd. for C₂₃H₂₈N₆O₂: 420.23); Found: 419.05 (M-H)⁻. Anal calcd.for C₂₃H₂₈N₆O₂: C, 65.69; H, 6.71; N, 19.99; Found: C, 65.64; H, 6.73; N, 19.96.

6-Methoxy-4-((4-((3-morpholinopropyl)amino)phenyl)amino)quinoline-3-carbohydrazide (BD_33): Yellow solid (0.126 g, 56%); m.p: 291-293 °C; ¹H NMR (300 MHz, DMSO-d₆, TMS): δ = 9.98 (s, 1H), 8.90 (s, 1H), 8.79 (s, 1H), 8.05 (d, J = 8.6 Hz, 1H), 7.52 (d, J = 2.4 Hz, 1H), 7.31 (dd, J = 8.2 Hz, 2.3 Hz, 1H), 6.61 (d, J =

7.8 Hz, 2H), 6.42 (d, $J = 8.4$ Hz, 2H), 5.52 (brs, 1H), 3.83 (s, 3H), 3.65 (m, 4H), 3.44 (t, $J = 7.0$ Hz, 2H), 2.36 (s, 6H), 2.04 (brs, 2H), 1.85 (m, 2H). ^{13}C NMR (75 MHz, DMSO- d_6 , TMS): $\delta = 165.4, 157.1, 150.9, 144.3, 138.5, 134.8, 133.6, 130.9, 125.0(2\text{C}), 119.2(2\text{C}), 118.9(2\text{C}), 113.7, 103.5, 67.5(2\text{C}), 63.7(2\text{C}), 56.3, 52.8, 41.9, 27.6$. ESI-MS m/z (Calcd. for $\text{C}_{24}\text{H}_{30}\text{N}_6\text{O}_3$: 450.24); Found: 451.26 (M+H) $^+$. Anal calcd.for $\text{C}_{24}\text{H}_{30}\text{N}_6\text{O}_3$: C, 63.98; H, 6.71; N, 18.65; Found: C, 63.95; H, 6.73; N, 18.67.

6-Fluoro-4-((4-((3-morpholinopropyl)amino)phenyl)amino)quinoline-3-

carbohydrazide (BD_34): Brown solid (0.127 g, 58%); m.p: 289-291 °C; ^1H NMR (300 MHz, DMSO- d_6 , TMS): $\delta = 9.99$ (s, 1H), 9.21 (s, 1H), 8.85 (s,1H), 7.78 (d, $J = 8.4$ Hz, 1H), 7.41 (d, $J = 2.4$ Hz, 1H), 7.29 (dd, $J = 8.6$ Hz, 2.5 Hz, 1H), 6.58 (d, $J = 8.2$ Hz, 2H), 6.40 (d, $J = 8.4$ Hz, 2H), 5.51 (brs, 1H), 3.58 (t, $J = 7.0$ Hz, 4H), 3.44 (t, $J = 6.8$ Hz, 2H), 2.33 (s, 6H), 2.03 (s, 2H), 1.81 (m, 2H). ^{13}C NMR (75 MHz, DMSO- d_6 , TMS): $\delta = 165.3, 160.5, 151.8, 146.0, 138.2, 135.1(2\text{C}), 130.3, 124.9(2\text{C}), 119.1(2\text{C}), 118.8(2\text{C}), 114.2, 104.7, 67.3(2\text{C}), 63.6(2\text{C}), 52.9, 41.6, 27.8$. ESI-MS m/z (Calcd. for $\text{C}_{23}\text{H}_{27}\text{FN}_6\text{O}_2$: 438.22); Found: 437.11 (M-H) $^-$. Anal calcd.for $\text{C}_{23}\text{H}_{27}\text{FN}_6\text{O}_2$: C, 63.00; H, 6.21; N, 19.17; Found: C, 63.04; H, 6.22; N, 19.15.

4-((4-((3-Morpholinopropyl)amino)phenyl)amino)-6-(trifluoromethyl)quinoline-

3-carbohydrazide (BD_35): Brown solid (0.14 g, 57%); m.p: 302-304 °C; ^1H NMR (300 MHz, DMSO- d_6 , TMS): $\delta = 9.98$ (s, 1H), 9.38 (s, 1H), 8.81 (s,1H), 8.28 (d, $J = 2.4$ Hz, 1H), 8.18 (dd, $J = 8.8$ Hz, 2.2 Hz, 1H), 8.14 (d, $J = 8.1$ Hz, 1H), 6.55 (d, $J = 8.4$ Hz, 2H), 6.38 (d, $J = 8.2$ Hz, 2H), 5.52 (brs, 1H), 3.66 (t, $J = 7.0$ Hz, 4H), 3.54 (t, $J = 6.7$ Hz, 2H), 2.31 (s, 6H), 2.06 (s, 2H), 1.86 (m, 2H). ^{13}C NMR (75 MHz, DMSO- d_6 , TMS): $\delta = 165.3, 153.1, 148.9, 139.2, 138.4, 134.8, 131.5, 128.9, 127.7, 125.0, 122.8, 120.6, 119.2(2\text{C}), 118.8(2\text{C}), 114.7, 67.3(2\text{C}), 63.5(2\text{C}), 52.7, 41.4, 27.6$. ESI-MS m/z (Calcd. for $\text{C}_{24}\text{H}_{27}\text{F}_3\text{N}_6\text{O}_2$: 488.21); Found: 487.05 (M-H) $^-$. Anal calcd.for $\text{C}_{24}\text{H}_{27}\text{F}_3\text{N}_6\text{O}_2$: C, 59.01; H, 5.57; N, 17.20; Found: C, 59.05; H, 5.61; N, 17.15.

4-((4-(3-(4-Ethylpiperazin-1-yl)propoxy)phenyl)amino)quinoline-3-

carbohydrazide (BD_36): Brown solid (0.134 g, 60%); m.p: 320-322 °C; ^1H NMR (300 MHz, DMSO- d_6 , TMS): $\delta = 9.86$ (s, 1H), 8.90 (s, 1H), 8.86 (s, 1H), 8.34-7.59 (m, 4H), 7.56 (d, $J = 8.6$ Hz, 2H), 6.59 (d, $J = 8.4$ Hz, 2H), 4.03 (t, $J = 7.0$ Hz, 2H), 2.49-2.31 (m, 12H), 2.11 (s, 2H), 1.86 (m, 2H), 1.05 (t, $J = 6.8$ Hz, 3H). ^{13}C NMR (75

MHz, DMSO-d₆, TMS): δ = 165.2, 152.0, 149.9, 146.6, 137.8, 132.7(2C), 129.3, 127.1, 126.3, 123.8, 122.0(2C), 115.9(2C), 113.3, 73.7, 59.1(3C), 58.3(2C), 50.4, 28.3, 14.0. ESI-MS *m/z* (Calcd. for C₂₅H₃₂N₆O₂: 448.26); Found: 449.46 (M+H)⁺. Anal calcd. for C₂₅H₃₂N₆O₂: C, 66.94; H, 7.19; N, 18.74; Found: C, 66.97; H, 7.21; N, 18.69.

4-((4-(3-(4-Ethylpiperazin-1-yl)propoxy)phenyl)amino)-6-methoxy quinoline-3-carbohydrazide (BD_37): Yellow solid (0.14 g, 59%); m.p: 302-304 °C; ¹H NMR (300 MHz, DMSO-d₆, TMS): δ = 9.97 (s, 1H), 8.97 (s, 1H), 8.74 (s, 1H), 7.82 (d, *J* = 8.4 Hz, 1H), 7.60 (d, *J* = 8.8 Hz, 2H), 7.43 (d, *J* = 2.4 Hz, 1H), 7.28 (dd, *J* = 8.4 Hz, 2.5 Hz, 1H), 6.78 (d, *J* = 8.2 Hz, 2H), 4.04 (t, *J* = 7.0 Hz, 2H), 3.55 (s, 3H), 2.49-2.30 (m, 12H), 2.02 (s, 2H), 1.79 (m, 2H), 1.04 (t, *J* = 7.1 Hz, 3H). ¹³C NMR (75 MHz, DMSO-d₆, TMS): δ = 165.3, 157.1, 150.9, 149.7, 144.5, 133.8(2C), 130.8, 125.1(2C), 121.9(2C), 115.7(2C), 113.4, 103.6, 73.4, 59.2(3C), 58.5(2C), 56.1, 50.3, 28.1, 13.9. ESI-MS *m/z* (Calcd. for C₂₆H₃₄N₆O₃: 478.27); Found: 477.04 (M-H)⁻. Anal calcd. for C₂₆H₃₄N₆O₃: C, 65.25; H, 7.16; N, 17.56; Found: C, 66.28; H, 7.11; N, 17.52.

4-((4-(3-(4-Ethylpiperazin-1-yl)propoxy)phenyl)amino)-6-fluoro quinoline-3-carbohydrazide (BD_38): Brown solid (0.128 g, 55%); m.p: 320-322 °C; ¹H NMR (300 MHz, DMSO-d₆, TMS): δ = 9.96 (s, 1H), 9.34 (s, 1H), 8.89 (s, 1H), 7.88 (d, *J* = 8.6 Hz, 1H), 7.64 (d, *J* = 8.8 Hz, 2H), 7.39 (d, *J* = 2.5 Hz, 1H), 7.31 (dd, *J* = 8.4 Hz, 2.2 Hz, 1H), 6.57 (d, *J* = 8.2 Hz, 2H), 3.99 (t, *J* = 7.1 Hz, 2H), 2.48-2.30 (m, 12H), 2.05 (s, 2H), 1.86 (m, 2H), 1.03 (t, *J* = 6.8 Hz, 3H). ¹³C NMR (75 MHz, DMSO-d₆, TMS): δ = 165.4, 160.6, 151.9, 150.1, 145.8, 135.0, 132.7, 130.2, 124.5(2C), 121.9(2C), 115.7(2C), 114.3, 104.5, 73.8, 59.5(3C), 58.3(2C), 50.2, 28.4, 13.9. ESI-MS *m/z* (Calcd. for C₂₅H₃₁FN₆O₂: 466.25); Found: 467.48 (M+H)⁺. Anal calcd. for C₂₅H₃₁FN₆O₂: C, 64.36; H, 6.70; N, 18.01; Found: C, 64.39; H, 6.72; N, 17.98.

4-((4-(3-(4-Ethylpiperazin-1-yl)propoxy)phenyl)amino)-6-(trifluoromethyl) quinoline-3-carbohydrazide (BD_39): Yellow solid (0.154 g, 60%); m.p: 300-302 °C; ¹H NMR (300 MHz, DMSO-d₆, TMS): δ = 9.99 (s, 1H), 9.48 (s, 1H), 8.90 (s, 1H), 8.38 (d, *J* = 2.5 Hz, 1H), 8.20 (dd, *J* = 8.6 Hz, 2.4 Hz, 1H), 8.14 (d, *J* = 8.8 Hz, 1H), 7.64 (d, *J* = 8.4 Hz, 2H), 6.61 (d, *J* = 8.2 Hz, 2H), 4.01 (t, *J* = 6.8 Hz, 2H), 2.49-2.33 (m, 12H), 2.10 (brs, 2H), 1.86 (m, 2H), 1.02 (t, *J* = 7.0 Hz, 3H). ¹³C NMR (75 MHz, DMSO-d₆, TMS): δ = 165.4, 153.1, 150.0, 149.2, 139.4, 132.9, 131.5, 128.7, 127.6,

125.1, 122.8, 121.6(2C), 120.4, 115.8(2C), 114.6, 73.4, 59.0(3C), 58.5(2C), 50.2, 28.6, 14.0. ESI-MS m/z (Calcd. for $C_{26}H_{31}F_3N_6O_2$: 516.25); Found: 517.29 (M+H)⁺. Anal calcd. for $C_{26}H_{31}F_3N_6O_2$: C, 60.45; H, 6.05; N, 16.27; Found: C, 60.47; H, 6.01; N, 16.29.

4-((4-((3-(4-Ethylpiperazin-1-yl)propyl)amino)phenyl)amino)quinoline-3-

carbohydrazide (BD_40): Yellow solid (0.127 g, 57%); m.p: 310-312 °C; ¹H NMR (300 MHz, DMSO-d₆, TMS): δ = 9.98 (s, 1H), 9.39 (s, 1H), 8.86 (s, 1H), 7.54 (m, 4H), 6.73 (d, J = 8.4 Hz, 2H), 6.58 (d, J = 8.2 Hz, 2H), 5.52 (brs, 1H), 3.42 (t, J = 7.0 Hz, 2H), 2.50-2.33 (m, 12H), 2.06 (brs, 2H), 1.71 (m, 2H), 1.01 (t, J = 6.8 Hz, 3H). ¹³C NMR (75 MHz, DMSO-d₆, TMS): δ = 165.4, 152.1, 146.6, 138.3, 137.9, 134.7, 132.5, 129.3, 126.8, 125.9, 123.7, 119.1(2C), 118.8(2C), 113.4, 59.0(2C), 58.6(2C), 52.4, 50.2, 41.8, 27.5, 14.0. ESI-MS m/z (Calcd. for $C_{25}H_{33}N_7O$: 447.27); Found: 448.15 (M+H)⁺. Anal Calcd. for $C_{25}H_{33}N_7O$: C, 67.09; H, 7.43; N, 21.91; Found: C, 67.12; H, 7.39; N, 21.93.

4-((4-((3-(4-Ethylpiperazin-1-yl)propyl)amino)phenyl)amino)-6-methoxy

quinoline-3-carbohydrazide (BD_41): Yellow solid (0.13 g, 55%); m.p: 306-308 °C; ¹H NMR (300 MHz, DMSO-d₆, TMS): δ = 10.01 (s, 1H), 9.16 (s, 1H), 8.89 (s, 1H), 7.81 (d, J = 8.8 Hz, 1H), 7.46 (d, J = 2.4 Hz, 1H), 7.29 (dd, J = 8.4 Hz, 2.5 Hz, 1H), 6.56 (d, J = 8.2 Hz, 2H), 6.51 (d, J = 8.4 Hz, 2H), 5.52 (brs, 1H), 3.58 (s, 3H), 3.46 (t, J = 6.8 Hz, 2H), 2.49-2.29 (m, 12H), 2.08 (s, 2H), 1.70 9m, 2H), 1.01 (t, J = 7.0 Hz, 3H). ¹³C NMR (75 MHz, DMSO-d₆, TMS): δ = 165.4, 157.2, 150.9, 144.5, 138.3, 135.0, 133.6, 130.9, 125.1(2C), 119.4(2C), 119.0(2C), 113.7, 103.5, 59.0(2C), 58.4(2C), 56.2, 52.5, 50.1, 41.8, 27.5, 13.9. ESI-MS m/z (Calcd. for $C_{26}H_{35}N_7O_2$: 477.29); Found: 478.36 (M+H)⁺. Anal calcd. for $C_{26}H_{35}N_7O_2$: C, 65.38; H, 7.39; N, 20.53; Found: C, 65.41; H, 7.37; N, 20.55.

4-((4-((3-(4-Ethylpiperazin-1-yl)propyl)amino)phenyl)amino)-6-fluoroquinoline-

3-carbohydrazide (BD_42): Yellow solid (0.13 g, 56%); m.p: 298-300 °C; ¹H NMR (300 MHz, DMSO-d₆, TMS): δ = 10.02 (s, 1H), 9.28 (s, 1H), 8.67 (s, 1H), 7.91 (d, J = 8.6 Hz, 1H), 7.42 (d, J = 2.5 Hz, 1H), 7.31(dd, J = 8.8 Hz, 2.4 Hz, 1H), 6.61 (d, J = 8.2 Hz, 2H), 6.39 (d, J = 8.4 Hz, 2H), 5.52(brs, 1H), 3.55 (t, J = 6.8 Hz, 2H), 2.50-2.30 (m, 12H), 2.09 (s, 2H), 1.71 (m, 2H), 1.02 (t, J = 7.0 Hz, 3H). ¹³C NMR (75 MHz, DMSO-d₆, TMS): δ = 165.5, 160.6, 151.8, 146.0, 138.2, 135.1(2C), 130.3,

124.9(2C), 119.3(2C), 119.0(2C), 114.3, 104.9, 59.0(2C), 58.7(2C), 52.4, 50.2, 41.5, 27.8, 14.2. ESI-MS m/z (Calcd. for $C_{25}H_{32}FN_7O$: 465.27); Found: 466.42 (M+H)⁺. Anal calcd. for $C_{25}H_{32}FN_7O$: C, 64.50; H, 6.93; N, 21.06; Found: C, 64.53; H, 6.95; N, 21.01.

4-((4-((3-(4-Ethylpiperazin-1-yl)propyl)amino)phenyl)amino)-6-(trifluoromethyl)quinoline-3-carbohydrazide (BD_43): Yellow solid (0.138 g, 54%); m.p: 268-270 °C; ¹H NMR (300 MHz, DMSO-d₆, TMS): δ = 9.98 (s, 1H), 9.45 (s, 1H), 8.43 (s, 1H), 8.40 (d, $J = 2.5$ Hz, 1H), 8.21 (dd, $J = 8.6$ Hz, 2.5 Hz, 1H), 6.59 (d, $J = 8.4$ Hz, 2H), 6.44 (d, $J = 8.2$ Hz, 2H), 5.50 (brs, 1H), 3.52 (t, $J = 6.8$ Hz, 2H), 2.49-2.33 (m, 12H), 2.11 (s, 2H), 1.73 (m, 2H), 1.01 (t, $J = 7.0$ Hz, 3H). ¹³C NMR (75 MHz, DMSO-d₆, TMS): δ = 165.4, 153.2, 149.0, 139.5, 138.3, 134.9, 131.4, 128.7, 127.8, 125.3, 122.6, 120.8, 119.4(2C), 118.9(2C), 114.5, 59.1(2C), 58.4(2C), 52.6, 50.3, 41.6, 27.8, 14.0. ESI-MS m/z (Calcd. for $C_{26}H_{32}F_3N_7O$: 515.26); Found: 516.31 (M+H)⁺. Anal calcd. for $C_{26}H_{32}F_3N_7O$: C, 60.57; H, 6.26; N, 19.02; Found: C, 60.54; H, 6.29; N, 19.04.

4-((4-(3-Morpholinopropoxy)phenyl)amino)quinoline-3-carboxylic acid (BD_44): Yellow gammy (0.11 g, 55%); ¹H NMR (300 MHz, DMSO-d₆, TMS): δ = 11.51 (s, 1H), 9.86 (s, 1H), 9.34 (s, 1H), 8.18 (dd, $J = 8.6$ Hz, $J = 2.4$ Hz, 1H), 7.83 (dd, $J = 8.8$ Hz, $J = 2.5$ Hz, 1H), 7.76-7.60 (m, 2H), 7.49 (d, $J = 8.4$ Hz, 2H), 6.98 (d, $J = 8.2$ Hz, 2H), 4.03 (t, $J = 7.0$ Hz, 2H), 3.66 (t, $J = 6.8$ Hz, 4H), 2.34 (s, 6H), 1.79 (m, 2H). ¹³C NMR (75 MHz, DMSO-d₆, TMS): δ = 170.0, 153.2, 152.4, 149.8, 140.7, 132.5(2C), 129.3, 127.0, 126.2, 121.9(3C), 115.8(2C), 114.3, 73.6, 67.4(2C), 63.6(2C), 59.2, 28.5. ESI-MS m/z (Calcd. for $C_{23}H_{25}N_3O_4$: 407.18); Found: 408.25 (M+H)⁺. Anal calcd. for $C_{23}H_{25}N_3O_4$: C, 67.80; H, 6.18; N, 10.31; Found: C, 67.76; H, 6.21; N, 10.33.

6-Methoxy-4-((4-(3-morpholinopropoxy)phenyl)amino)quinoline-3-carboxylic acid (BD_45): Pale yellow solid (0.11 g, 53%); m.p: 239-241 °C; ¹H NMR (300 MHz, DMSO-d₆, TMS): δ = 11.65 (brs, 1H), 9.92 (s, 1H), 8.94 (s, 1H), 7.84 (d, $J = 8.6$ Hz, 1H), 7.63 (d, $J = 8.2$ Hz, 2H), 7.43 (d, $J = 2.5$ Hz, 1H), 7.28 (dd, $J = 8.4$ Hz, 2.5 Hz, 1H), 6.86 (d, $J = 8.0$ Hz, 2H), 4.01 (t, $J = 7.1$ Hz, 2H), 3.82 (s, 3H), 3.66 (t, $J = 6.8$ Hz, 4H), 2.36 (s, 6H), 1.80 (m, 2H). ¹³C NMR (75 MHz, DMSO-d₆, TMS): δ = 169.9, 157.3, 151.8, 150.2(2C), 136.4, 132.7, 130.9, 125.0, 121.8(3C), 116.1(2C),

114.9, 103.5, 73.7, 67.4(2C), 63.5(2C), 59.2, 56.4, 28.6. ESI-MS m/z (Calcd. for $C_{24}H_{27}N_3O_5$: 437.20); Found: 436.11 (M-H)⁻. Anal calcd.for $C_{24}H_{27}N_3O_5$: C, 65.89; H, 6.22; N, 9.60; Found: C, 65.87; H, 6.25; N, 9.61.

6-Fluoro-4-((4-(3-morpholinopropoxy)phenyl)amino)quinoline-3-carboxylic acid (BD_46): Off-white solid (0.11 g, 56%); m.p: 199-201 °C; ¹H NMR (300 MHz, DMSO-d₆, TMS): δ = 11.69 (brs, 1H), 9.93 (s, 1H), 8.92 (s, 1H), 7.90 (d, J = 8.8 Hz, 1H), 7.63 (d, J = 8.4 Hz, 2H), 7.45 (d, J = 2.4 Hz, 1H), 7.36 (dd, J = 8.6 Hz, 2.5 Hz, 1H), 6.98 (d, J = 8.1 Hz, 2H), 4.02 (t, J = 6.9 Hz, 2H), 3.61 (t, J = 7.0 Hz, 4H), 2.35 (s, 6H), 1.81 (m, 2H). ¹³C NMR (75 MHz, DMSO-d₆, TMS): δ = 170.1, 160.8, 152.4, 151.6, 149.9, 137.7, 133.0, 130.4, 124.1, 121.9(3C), 116.0(2C), 115.3, 104.5, 73.7, 67.3(2C), 63.6(2C), 59.1, 28.4. ESI-MS m/z (Calcd. for $C_{23}H_{24}FN_3O_4$: 425.18); Found: 426.35 (M+H)⁺. Anal calcd.for $C_{23}H_{24}FN_3O_4$: C, 64.93; H, 5.69; N, 9.88; Found: C, 64.95; H, 5.66; N, 9.91.

4-((4-(3-Morpholinopropoxy)phenyl)amino)-6-(trifluoromethyl) quinoline-3-carboxylic acid (BD_47): Pale green solid (0.144 g, 61%); m.p: 248-250 °C; ¹H NMR (300 MHz, DMSO-d₆, TMS): δ = 11.72 (brs, 1H), 9.91 (s, 1H), 8.87 (s, 1H), 8.31 (d, J = 2.5 Hz, 1H), 8.24 (dd, J = 8.8 Hz, 2.4 Hz, 1H), 8.18 (d, J = 8.6 Hz, 1H), 7.56 (d, J = 8.4 Hz, 2H), 6.96 (d, J = 8.0 Hz, 2H), 3.99 (t, J = 7.0 Hz, 2H), 3.60 (t, J = 6.8 Hz, 4H), 2.31 (s, 6H), 1.82 (m, 2H). ¹³C NMR (75 MHz, DMSO-d₆, TMS): δ = 169.9, 154.6(2C), 149.8, 142.2, 132.7, 131.5, 129.0, 127.8, 125.3, 122.1(2C), 119.9(2C), 115.7(3C), 73.5, 67.2(2C), 63.6(2C), 59.1, 28.3. ESI-MS m/z (Calcd. for $C_{24}H_{24}F_3N_3O_4$: 475.17); Found: 476.38 (M+H)⁺. Anal calcd.for $C_{24}H_{24}F_3N_3O_4$: C, 60.63; H, 5.09; N, 8.84; Found: C, 60.68; H, 5.06; N, 8.81.

4-((4-((3-Morpholinopropyl)amino)phenyl)amino)quinoline-3-carboxylic acid (BD_48): Brown solid (0.118 g, 58%); m.p: 187-189 °C; ¹H NMR (300 MHz, DMSO-d₆, TMS): δ = 11.67 (brs, 1H), 9.94 (s, 1H), 8.87 (s, 1H), 8.21 (d, J = 2.5 Hz, 1H), 7.92 (d, J = d, J = 8.4 Hz, 1H), 7.81-7.61 (m, 2H), 6.71 (d, J = 8.2 Hz, 2H), 6.40 (d, J = 8.2 Hz, 2H), 5.51 (brs, 1H), 3.64 (t, J = 7.0 Hz, 4H), 3.34 (t, J = 6.8 Hz, 2H), 2.30 (s, 6H), 1.69 (m, 2H). ¹³C NMR (75 MHz, DMSO-d₆, TMS): δ = 170.1, 153.3, 152.0, 140.9, 138.2, 134.8, 132.6, 129.3, 127.0, 125.9, 120.7, 119.2(2C), 118.6(2C), 114.2, 67.1(2C), 63.6(2C), 52.9, 41.6, 27.5. ESI-MS m/z (Calcd. for $C_{23}H_{26}N_4O_3$:

406.20); Found: 407.19 (M+H)⁺. Anal calcd. for C₂₃H₂₆N₄O₃: C, 67.96; H, 6.45; N, 13.78; Found: C, 67.94; H, 6.47; N, 13.81.

6-Methoxy-4-((4-((3-morpholinopropyl)amino)phenyl)amino)quinoline-3-carboxylic acid (BD_49): Brown solid (0.128 g, 59%); m.p: 199-201 °C; ¹H NMR (300 MHz, DMSO-d₆, TMS): δ = 11.52 (brs, 1H), 9.93 (s, 1H), 8.88 (s, 1H), 8.34 (m, 1H), 8.02 (d, *J* = 8.4 Hz, 1H), 7.54 (d, *J* = 2.5 Hz, 1H), 7.31 (d, *J* = 8.2 Hz, 2.4 Hz, 1H), 6.54 (d, *J* = 8.2 Hz, 2H), 6.40 (d, *J* = 8.0 Hz, 2H), 5.51 (brs, 1H), 3.84 (s, 3H), 3.64 (t, *J* = 6.8 Hz, 4H), 3.45 (t, *J* = 7.0 Hz, 2H), 2.36 (s, 6H), 1.82 (m, 2H). ¹³C NMR (75 MHz, DMSO-d₆, TMS): δ = 170.2, 157.5, 151.8, 150.2, 138.3, 136.7, 134.9, 131.0, 125.2, 121.8, 119.0(2C), 118.7(2C), 114.9, 103.6, 67.3(2C), 63.4(2C), 56.0, 52.9, 41.7, 27.5. ESI-MS *m/z* (Calcd. for C₂₄H₂₈N₄O₄: 436.21); Found: 437.17 (M+H)⁺. Anal calcd. for C₂₄H₂₈N₄O₄: C, 66.04; H, 6.47; N, 12.84; Found: C, 66.07; H, 6.51; N, 12.81.

6-Fluoro-4-((4-((3-morpholinopropyl)amino)phenyl)amino)quinoline-3-carboxylic acid (BD_50): Red solid (0.118 g, 56%); m.p: 216-218 °C; ¹H NMR (300 MHz, DMSO-d₆, TMS): δ = 11.71 (brs, 1H), 9.97 (s, 1H), 8.82 (s, 1H), 7.98 (d, *J* = 8.0 Hz, 1H), 7.52 (d, *J* = 2.5 Hz, 1H), 7.34 (dd, *J* = 8.2 Hz, 2.5 Hz, 1H), 6.56 (d, *J* = 8.0 Hz, 2H), 6.40 (d, *J* = 8.2 Hz, 2H), 5.52 (brs, 1H), 3.63 (t, *J* = 7.0 Hz, 4H), 3.45 (t, *J* = 6.8 Hz, 2H), 2.34 (s, 6H), 1.81 (m, 2H). ¹³C NMR (75 MHz, DMSO-d₆, TMS): δ = 169.9, 160.7, 152.5(2C), 138.3(2C), 134.9, 130.1, 124.3, 121.8, 119.5(2C), 119.1(2C), 115.4, 104.2, 67.5(2C), 63.4(2C), 52.9, 41.5, 27.7. ESI-MS *m/z* (Calcd. for C₂₃H₂₅FN₄O₃: 424.19); Found: 425.15 (M+H)⁺. Anal calcd. for C₂₃H₂₅FN₄O₃: C, 65.08; H, 5.94; N, 13.20; Found: C, 65.09; H, 5.91; N, 13.22.

4-((4-((3-Morpholinopropyl)amino)phenyl)amino)-6-(trifluoromethyl)quinoline-3-carboxylic acid (BD_51): Brown solid (0.141 g, 60%); m.p: 223-224 °C; ¹H NMR (300 MHz, DMSO-d₆, TMS): δ = 11.89 (brs, 1H), 9.98 (s, 1H), 8.80 (s, 1H), 8.29 (d, *J* = 2.5 Hz, 1H), 8.20-8.16 (m, 2H), 6.57 (d, *J* = 8.2 Hz, 2H), 6.38 (d, *J* = 8.0 Hz, 2H), 5.53 (brs, 1H), 3.64 (t, *J* = 7.0 Hz, 4H), 3.44 (t, *J* = 6.7 Hz, 2H), 2.33 (s, 6H), 1.82 (m, 2H). ¹³C NMR (75 MHz, DMSO-d₆, TMS): δ = 169.8, 155.2, 154.0, 142.5, 138.3, 134.9, 131.6, 128.8, 127.9, 125.1, 120.3(2C), 119.0(2C), 118.7(2C), 115.8, 67.5(2C), 63.6(2C), 52.7, 41.4, 27.6. ESI-MS *m/z* (Calcd. for C₂₄H₂₅F₃N₄O₃: 474.19); Found:

475.13(M+H)⁺. Anal calcd.for C₂₄H₂₅F₃N₄O₃: C, 60.75; H, 5.31; N, 11.81; Found: C, 60.71; H, 5.28; N, 11.76.

4-((4-(3-(4-Ethylpiperazin-1-yl)propoxy)phenyl)amino)quinoline-3-carboxylic acid (BD_52): Brown gammy (0.127 g, 59%); ¹H NMR (300 MHz, DMSO-d₆, TMS): δ = 11.79 (brs, 1H), 9.86 (s, 1H), 8.85 (s, 1H), 8.20 (d, *J* = 7.8 Hz, 1H), 7.98 (d, *J* = 8.0 Hz, 1H), 7.80-7.63 (m, 2H), 7.59 (d, *J* = 8.0 Hz, 2H), 6.92 (d, *J* = 8.2 Hz, 2H), 4.01 (t, *J* = 7.0 Hz, 2H), 2.48-2.30 (m, 12H), 1.83 (m, 2H), 1.05 (t, *J* = 6.8 Hz, 3H). ¹³C NMR (75 MHz, DMSO-d₆, TMS): δ = 170.0, 152.9, 152.3, 150.1, 140.8, 132.9(2C), 128.9, 127.4, 126.2, 121.7(2C), 120.6, 115.8(2C), 114.3, 73.6, 59.2(3C), 58.6(2C), 50.2, 28.3, 14.1. ESI-MS *m/z* (Calcd. for C₂₅H₃₀N₄O₃: 434.23); Found: 433.16 (M-H)⁻. Anal calcd.for C₂₅H₃₀N₄O₃: C, 69.10; H, 6.96; N, 12.89; Found: C, 69.14; H, 6.92; N, 12.91.

4-((4-(3-(4-Ethylpiperazin-1-yl)propoxy)phenyl)amino)-6-methoxyquinoline-3-carboxylic acid (BD_53): Pale green solid (0.131 g, 57%); m.p: 282-284 °C; ¹H NMR (300 MHz, DMSO-d₆, TMS): δ = 11.72 (brs, 1H), 9.96 (s, 1H), 8.87 (s, 1H), 7.79 (d, *J* = 8.0 Hz, 1H), 7.62 (d, *J* = 8.4 Hz, 2H), 7.52 (d, *J* = 2.5 Hz, 1H), 7.31 (dd, *J* = 8.1 Hz, 2.5 Hz, 1H), 6.94 (d, *J* = 8.4 Hz, 2H), 4.03 (t, *J* = 7.0 Hz, 2H), 3.55 (s, 3H), 2.47-2.30 (m, 12H), 1.82 (m, 2H), 1.04 (t, *J* = 6.8 Hz, 3H). ¹³C NMR (75 MHz, DMSO-d₆, TMS): δ = 169.9, 157.3, 151.7, 150.2(2C), 136.4, 132.8, 131.1, 125.0, 121.9(3C), 115.7(2C), 114.9, 103.5, 73.7, 59.3(3C), 58.3(2C), 56.5, 50.1, 28.3, 14.1. ESI-MS *m/z* (Calcd. for C₂₆H₃₂N₄O₄: 464.24); Found: 465.28 (M+H)⁺. Anal calcd.for C₂₆H₃₂N₄O₄: C, 67.22; H, 6.94; N, 12.06; Found: C, 67.25; H, 6.91; N, 12.09.

4-((4-(3-(4-Ethylpiperazin-1-yl)propoxy)phenyl)amino)-6-fluoroquinoline-3-carboxylic acid (BD_54): Yellow gammy (0.137 g, 61%); ¹H NMR (300 MHz, DMSO-d₆, TMS): δ = 11.54 (brs, 1H), 9.95 (s, 1H), 8.86 (s, 1H), 7.94 (d, *J* = 8.1 Hz, 1H), 7.63 (d, *J* = 8.4 Hz, 2H), 7.46 (s, 1H), 7.31 (dd, *J* = 8.2 Hz, 2.4 Hz, 1H), 6.68 (d, *J* = 8.2 Hz, 2H), 3.99 (t, *J* = 7.0 Hz, 2H), 2.47-2.30 (m, 12H), 1.82 (m, 2H), 1.02 (t, *J* = 6.8 Hz, 3H). ¹³C NMR (75 MHz, DMSO-d₆, TMS): δ = 170.1, 160.7, 152.4, 151.5, 149.9, 137.6, 132.8, 130.3, 124.1, 122.0(3C), 115.9(3C), 104.5, 73.7, 59.2(3C), 58.4(2C), 50.1, 28.5, 14.0. ESI-MS *m/z* (Calcd. for C₂₅H₂₉FN₄O₃: 452.22); Found: 453.38 (M+H)⁺. Anal calcd.for C₂₅H₂₉FN₄O₃: C, 66.35; H, 6.46; N, 12.38; Found: C, 66.33; H, 6.42; N, 12.41.

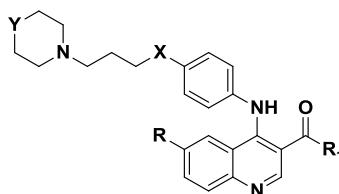
4-((4-(3-(4-Ethylpiperazin-1-yl)propoxy)phenyl)amino)-6-(trifluoromethyl)quinoline-3-carboxylic acid (BD_55): Yellow solid (0.14 g, 56%); m.p: 153-155 °C; ¹H NMR (300 MHz, DMSO-d₆, TMS): δ = 11.56 (brs, 1H), 9.97 (s, 1H), 8.88 (s, 1H), 8.36 (s, 1H), 8.21 (dd, *J* = 8.0 Hz, 2.5 Hz, 1H), 8.13 (d, *J* = 8.2 Hz, 1H), 7.82 (d, *J* = 8.6 Hz, 2H), 6.95 (d, *J* = 8.4 Hz, 2H), 3.98 (t, *J* = 7.0 Hz, 2H), 2.46-2.34 (m, 12H), 1.82 (m, 2H), 1.03 (t, *J* = 7.1 Hz, 3H). ¹³C NMR (75 MHz, DMSO-d₆, TMS): δ = 169.9, 154.7(2C), 150.1, 142.3, 132.9, 131.6, 129.2, 128.0, 125.2, 121.8(2C), 120.5(2C), 115.9(3C), 73.6, 59.1(3C), 58.3(2C), 50.0, 28.4, 14.1. ESI-MS m/z (Calcd. for C₂₆H₂₉F₃N₄O₃: 502.22); Found: 503.36 (M+H)⁺. Anal calcd. for C₂₆H₂₉F₃N₄O₃: C, 62.14; H, 5.82; N, 11.15; Found: C, 62.11; H, 5.85; N, 11.12.

4-((4-((3-(4-Ethylpiperazin-1-yl)propyl)amino)phenyl)amino)quinoline-3-carboxylic acid (BD_56): Brown solid (0.127 g, 59%); m.p: 188-190 °C; ¹H NMR (300 MHz, DMSO-d₆, TMS): δ = 11.72 (brs, 1H), 9.96 (s, 1H), 8.86 (s, 1H), 8.13-7.61 (m, 4H), 6.58 (d, *J* = 8.2 Hz, 2H), 6.34 (d, *J* = 8.0 Hz, 2H), 5.52 (brs, 1H), 3.51 (t, *J* = 7.0 Hz, 2H), 2.46-2.31 (m, 12H), 1.83 (m, 2H), 1.04 (t, *J* = 6.8 Hz, 3H). ¹³C NMR (75 MHz, DMSO-d₆, TMS): δ = 169.8, 153.0, 152.5, 140.9, 138.2, 134.8, 132.6, 129.3, 127.1, 126.2, 120.9, 119.4(2C), 118.9(2C), 114.3, 59.0(2C), 58.5(2C), 52.7, 50.2, 41.8, 27.6, 13.9. ESI-MS m/z (Calcd. for C₂₅H₃₁N₅O₂: 433.25); Found: 432.09 (M-H)⁻. Anal calcd. for C₂₅H₃₁N₅O₂: C, 69.26; H, 7.21; N, 16.15; Found: C, 69.21; H, 7.23; N, 16.18.

4-((4-((3-(4-Ethylpiperazin-1-yl)propyl)amino)phenyl)amino)-6-methoxyquinoline-3-carboxylic acid (BD_57): Yellow gummy (0.138 g, 60%); ¹H NMR (300 MHz, DMSO-d₆, TMS): δ = 11.58 (brs, 1H), 9.98 (s, 1H), 8.89 (s, 1H), 7.79 (d, *J* = 8.4 Hz, 1H), 7.51 (s, 1H), 7.34 (dd, *J* = 7.8 Hz, 2.4 Hz, 1H), 6.57 (d, *J* = 8.2 Hz, 2H), 6.46 (d, *J* = 8.0 Hz, 2H), 5.51 (s, 1H), 3.86 (s, 3H), 3.36 (t, *J* = 7.0 Hz, 2H), 2.48-2.29 (m, 12H), 1.83 (m, 2H), 1.04 (t, *J* = 6.8 Hz, 3H). ¹³C NMR (75 MHz, DMSO-d₆, TMS): δ = 170.0, 157.3, 151.9, 150.2, 138.4, 136.7, 134.8, 131.0, 124.9, 122.1, 119.2(2C), 118.7(2C), 115.2, 103.4, 59.2(2C), 58.5(2C), 56.3, 52.4, 50.1, 41.9, 27.7, 14.1. ESI-MS m/z (Calcd. For C₂₆H₃₃N₅O₃: 463.26); Found: 464.35 (M+H)⁺. Anal calcd. for C₂₆H₃₃N₅O₃: C, 67.36; H, 7.18; N, 15.11; Found: C, 67.32; H, 7.21; N, 15.07.

5.4.4 *In vitro* Msm Gyr B assay, supercoiling assay, antimycobacterial potency and cytotoxicity studies of the synthesized molecules

All the synthesized derivatives were evaluated for their *in vitro* Msm Gyr B assay and supercoiling assay for the derivation of SAR and lead optimization. Msm DNA Gyr B was used for performing the gyrase ATPase assay. The surrogate Msm Gyr B protein was used as Mtb was found to be slow growing organism (Shirude P. S., *et al.*, 2012). Moreover, the sequence similarity between the GyrB protein domains of both the organisms was found to be 87%, with most of the catalytic site being conserved which proves a higher degree of homology in their ATP binding pocket (Ali J. A., *et al.*, 1993). The compounds were further subjected to a whole cell screening against Mtb H₃₇Rv strain to understand their bactericidal potency using the agar dilution method and later the safety profile of these molecules were evaluated by checking the *in vitro* cytotoxicity against RAW 264.7 cell line (mouse macrophage) at 50 µM concentration by MTT assay, and the results are shown in **Table 5.8**.

Table 5.8 Biological evaluation of synthesized derivatives **BD_12-57**

Comp	R	R ₁	X	Y	<i>Msm</i> Gyr B assay ^a (IC ₅₀ in μM)	<i>Mtb</i> Supercoiling assay ^b (IC ₅₀ μM)	<i>Mtb</i> MIC ^c (μM)	Cytotoxicity at 50 μM ^d (% inhibition)
BD_12	H	OC ₂ H ₅	O	O	22.83±0.38	7.53±0.16	28.70	17.67
BD_13	OCH ₃	OC ₂ H ₅	O	O	14.92±0.46	13.32±0.11	13.35	21.23
BD_14	F	OC ₂ H ₅	O	O	16.87±0.31	7.63±0.18	21.72	44.06
BD_15	CF ₃	OC ₂ H ₅	O	O	38.84±0.66	16.42±0.21	43.10	20.21
BD_16	H	OC ₂ H ₅	NH	O	17.92±0.29	8.73±0.13	14.38	1.82
BD_17	OCH ₃	OC ₂ H ₅	NH	O	22.31±0.31	9.32±0.15	23.36	19.33
BD_18	F	OC ₂ H ₅	NH	O	11.34±0.51	4.61±0.19	13.45	19.61
BD_19	CF ₃	OC ₂ H ₅	NH	O	6.62±0.22	3.12±0.21	49.75	20.22
BD_20	H	OC ₂ H ₅	O	NC ₂ H ₅	>50	23.92±0.31	13.51	21.41
BD_21	OCH ₃	OC ₂ H ₅	O	NC ₂ H ₅	15.92±0.61	6.85±0.31	11.58	21.55
BD_22	F	OC ₂ H ₅	O	NC ₂ H ₅	23.61±0.38	11.83±0.51	3.25	21.61
BD_23	CF ₃	OC ₂ H ₅	O	NC ₂ H ₅	0.97±0.18	0.69±0.15	2.94	27.30
BD_24	H	OC ₂ H ₅	NH	NC ₂ H ₅	11.72±0.62	3.25±0.16	6.77	20.4
BD_25	OCH ₃	OC ₂ H ₅	NH	NC ₂ H ₅	9.55±0.44	8.52±0.18	25.43	21.41
BD_26	F	OC ₂ H ₅	NH	NC ₂ H ₅	16.92±0.39	7.99±0.16	13.03	20.22
BD_27	CF ₃	OC ₂ H ₅	NH	NC ₂ H ₅	8.82±0.64	3.77±0.11	1.47	20.15
BD_28	H	NHNH ₂	O	O	0.97±0.25	0.72±0.15	2.4	44.56
BD_29	OCH ₃	NHNH ₂	O	O	10.58±0.34	10.41±0.42	55.37	6.26
BD_30	F	NHNH ₂	O	O	20.88±0.65	21.42±0.31	28.44	13.72
BD_31	CF ₃	NHNH ₂	O	O	38.66±0.60	19.93±0.29	36.38	0.07
BD_32	H	NHNH ₂	NH	O	>50	22.87±0.51	44.86	6.48
BD_33	OCH ₃	NHNH ₂	NH	O	44.93±0.34	15.32±0.22	27.75	9.59
BD_34	F	NHNH ₂	NH	O	18.67±0.64	10.55±0.21	23.56	29.08

Conti....

Comp	R	R ₁	X	Y	<i>Msm</i> Gyr B assay ^a (IC ₅₀ in μM)	<i>Mtb</i> Supercoiling assay ^b (IC ₅₀ μM)	<i>Mtb</i> MIC ^c (μM)	Cytotoxicity at 50 μM ^d (% inhibition)
BD_35	CF ₃	NHNH ₂	NH	O	47.25±0.26	19.88±0.35	25.59	7.94
BD_36	H	NHNH ₂	O	NC ₂ H ₅	28.44±0.61	16.66±0.38	13.93	18.24
BD_37	OCH ₃	NHNH ₂	O	NC ₂ H ₅	12.63±0.31	5.89±0.25	11.63	2.72
BD_38	F	NHNH ₂	O	NC ₂ H ₅	2.92±0.16	2.96±0.21	3.34	11.95
BD_39	CF ₃	NHNH ₂	O	NC ₂ H ₅	11.88±0.52	9.33±0.16	11.51	20.14
BD_40	H	NHNH ₂	NH	NC ₂ H ₅	10.83±0.23	9.42±0.18	13.49	3.36
BD_41	OCH ₃	NHNH ₂	NH	NC ₂ H ₅	3.26±0.54	2.55±0.19	13.09	2.56
BD_42	F	NHNH ₂	NH	NC ₂ H ₅	1.15±0.16	0.82±0.15	3.3	6.11
BD_43	CF ₃	NHNH ₂	NH	NC ₂ H ₅	26.34±0.63	10.95±0.22	30.03	1.59
BD_44	H	OH	O	O	>50	21.82±0.29	30.68	11.28
BD_45	OCH ₃	OH	O	O	20.56±0.54	12.9±0.31	57.14	11.42
BD_46	F	OH	O	O	31.28±0.48	16.93±0.54	14.69	10.85
BD_47	CF ₃	OH	O	O	27.83±0.41	14.33±0.31	13.15	22.57
BD_48	H	OH	NH	O	11.33±0.61	5.56±0.61	7.69	0.55
BD_49	OCH ₃	OH	NH	O	38.92±0.71	12.55±0.55	28.64	16.07
BD_50	F	OH	NH	O	14.98±0.29	4.44±0.23	29.46	13.12
BD_51	CF ₃	OH	NH	O	7.89±0.31	3.77±0.15	6.59	19.06
BD_52	H	OH	O	NC ₂ H ₅	21.66±0.51	10.22±0.18	27.19	13.37
BD_53	OCH ₃	OH	O	NC ₂ H ₅	0.86±0.16	0.63±0.15	3.3	0.66
BD_54	F	OH	O	NC ₂ H ₅	6.82±0.32	5.96±0.22	6.91	24.16
BD_55	CF ₃	OH	O	NC ₂ H ₅	7.91±0.31	3.54±0.26	19.75	13.37
BD_56	H	OH	NH	NC ₂ H ₅	11.32±0.52	5.88±0.24	11.80	32.28
BD_57	OCH ₃	OH	NH	NC ₂ H ₅	1.32±0.21	0.93±0.21	3.48	20.10
	Novobiocin			180±3.9	46±10 nM	>200	NT	
	Moxifloxacin				>50	11.2±0.36	1.26	NT
	Isoniazid				NT	NT	0.66	NT
	Rifampicin				NT	NT	0.23	NT

IC₅₀, 50% inhibitory concentration; *Mtb*, *Mycobacterium tuberculosis*; MIC, minimum inhibitory concentration; NT, not tested; nM, nanomolar

Msm Gyr B, *Mycobacterium smegmatis* Gyr B inhibition assay

Mtb DNA gyrase supercoiling enzyme inhibition activity

In vitro activity against *Mtb* H₃₇Rv,

Against RAW 264.7 cells

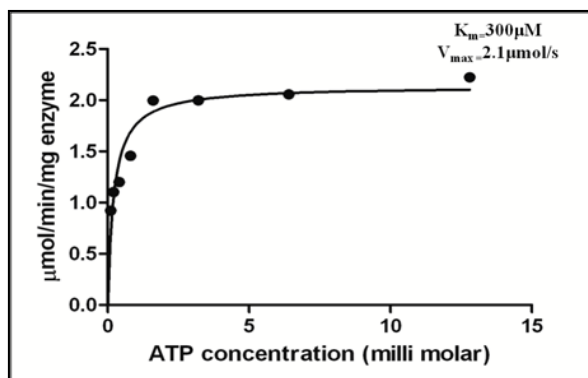


Figure 5.32: ATPase activity of *Msm* DNA Gyr B protein as a function of substrate (ATP) concentration at a constant enzyme concentration.

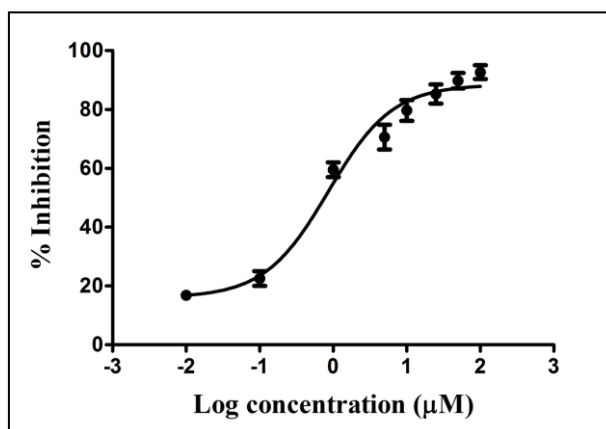


Figure 5.33: Percentage inhibition of *Msm* Gyr B by compound **BD_53** at various concentrations

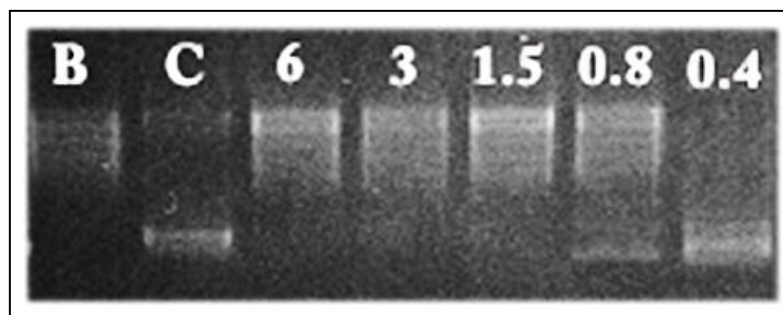


Figure 5.34: DNA supercoiling assay picture of compound **BD_53** at five different concentrations of 6 µM, 3 µM, 1.5 µM, 0.8 µM and 0.4 µM where B – relaxed DNA substrate + DMSO, C-relaxed DNA substrate with DNA gyrase enzyme + DMSO.

5.4.5 Docking studies of synthesized derivatives

In order to fully explore the structure–activity relationship associated with the *Msm* Gyr B inhibitors, compounds were docked to the Gyr B ATPase domain of *Msm* retrieved from protein data bank (PDB ID: 4B6C) using extra precision mode (XP) of Glide module. The reference ligand 6-(3,4-dimethylphenyl)-3-[[4-[3-(4-methylpiperazin-yl)propoxy]phenyl]amino]pyrazine-2-carboxamide was further re-docked with the active site residues of the *Msm* protein to validate the active site cavity. The ligand exhibited a Glide score of -6.93 kcal/mole and was placed in the active site cavity with amino acids like Asn52, Ile84, Val99, Val98, Asp97, Pro85, Arg141, Arg82, Glu56, Ala53, Asp79, Ile171, Val99, Val123, Ser126, Val128, and Glu4. Re-docking results showed that the crystal compound exhibited similar interactions as that of the original crystal structure and exhibited RMSD of 0.86Å⁰. The crystal ligand 6-(3,4-dimethylphenyl)-3-[[4-[3-(4-methylpiperazin-yl)propoxy]phenyl]amino] pyrazine-2-carboxamide exhibited two important hydrogen bonding interactions in the active site pocket, one between amino group of the carboxamide moiety and oxygen atom of Asp79 while the other was seen between the nitrogen atom of piperazine and hydrogen atom of guanidine moiety of Arg82. The molecule was stabilized by hydrophobic interaction in the hydrophobic pocket, considered to be important for bringing in specificity observed at the enzyme level as per **Figure 5.35**. In the docking studies, all the active compounds from the synthesized compounds, exhibited good docking score with significant polar and non-polar contacts, hydrogen bond interactions with the relevant amino acids and various hydrophobic interactions.

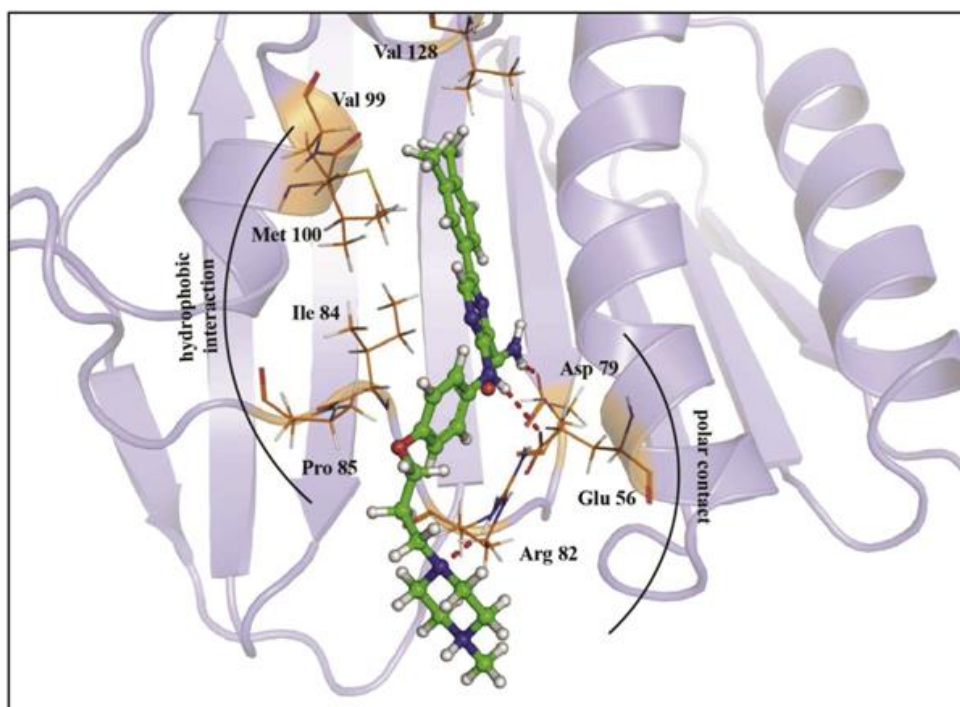


Figure 5.35: Interaction profile picture of ligand 6-(3,4-dimethylphenyl)-3-[[4-[3-(4-methylpiperazin-yl)propoxy]phenyl]amino]pyrazine-2-carboxamide in the active site of *Msm* Gyr B protein.

5.4.6 Evaluation of protein interaction and stability using biophysical characterization experiment (DSF)

The most potent compound from this series of chemical class of molecules was further investigated using a biophysical technique, differential scanning fluorimetry (DSF). The ability of the compounds to stabilize the catalytic domain of the *Msm* Gyr B protein was assessed utilizing the DSF technique by which the thermal stability of the catalytic domain of *Msm* Gyr B native protein and of the protein bound with the ligand was measured. Complex with compound **BD_53** was heated stepwise from 25 to 95 °C in steps of 0.1 °C rise in the presence of a fluorescent dye (sypro orange), whose fluorescence increased as it interacted with hydrophobic residues of the *Msm* Gyr B protein. As the protein was denatured, the amino acid residues became exposed to the dye. A right side positive shift of T_m in comparison to native protein meant higher stabilization of the protein-ligand complex, which was a consequence of the inhibitor binding. In our study, compound **BD_53** showed significant positive T_m shift of 3.3 °C confirming the stability of the protein-ligand complex as shown in **Figure**

5.36 which depicts the curves obtained in the DSF experiment for the *Msm* Gyr B protein (green) and protein-compound **BD_53** complex (red).

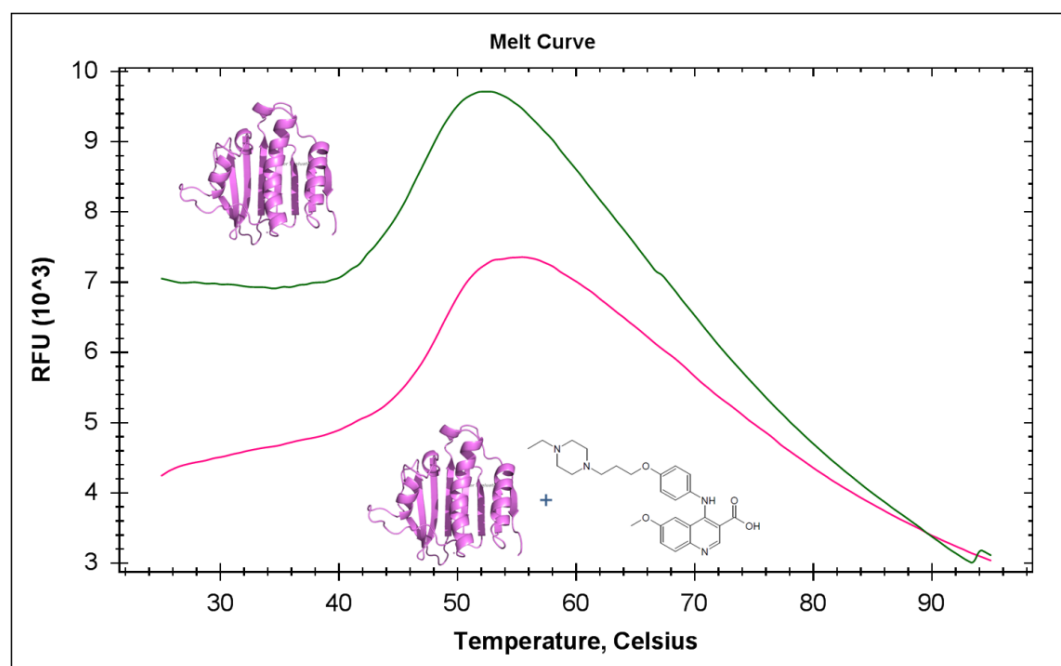


Figure 5.36: Differential scanning fluorimetry curve for Gyr B protein complexed with compound **BD_53** showed T_m of 48.60 °C (red) and native Gyr B protein 45.30 °C (green). A positive shift in T_m of about 3.3 °C was observed in protein-ligand complex when compared to native protein.

5.4.7 Discussion

The reported aminopyrazinamide compound (6-(3,4-dimethylphenyl)-3-[[4-[3-(4-methylpiperazin-1-yl)propoxy]phenyl]amino] pyrazine-2-carboxamide) was further considered for molecular reengineering by retaining the crucial groups for Gyr B activity and substituting particular sites with various suitable moieties. **Figure 5.30** demonstrates the substitutions made over the aminopyrazinamide compound ending up with a molecular lead. The 6-(3,4-dimethyl phenyl) pyrazine group which imparts for the hydrophobic interactions of the compound was replaced by quinoline moiety so as to observe the effect of fused ring system over the activity. The carboxamide group over pyrazine which was found to be crucial for activity was also modified by substituting amine group with ethoxy, hydrazine and hydroxyl moieties. The secondary amine linking the pyrazine and phenyl moiety was retained. The oxygen connecting the butyl chain with phenyl ring was retained and also substituted by

amine group. The final modification was done at the N-methyl group of piperazine by substituting with oxygen (O) and N-ethyl group.

The compounds showed *Msm* Gyr B an IC₅₀ values ranging between 0.86 to 72.48 μM and are given in **Table 5.8**. Compound **BD_53** was found to be most active with an IC₅₀ of 0.86 ± 0.42 μM against *Msm* Gyr B protein.

Subsequently, the compounds inhibiting the ATPase activity of GyrB protein should also inhibit the supercoiling activity of the gyrase holoenzyme as the Gyr A and Gyr B domains constitute the DNA gyrase. The supercoiling assay was performed in our laboratory using the DNA supercoiling assay kit (Inspiralis Pvt. limited, Norwich) as per the protocol described in the experimental section given in supporting information. All the reactions were carried on *Mtb* DNA gyrase enzyme using compounds dose dependently starting from 100 μM, 50 μM, 25 μM, 12.5 μM, 6.25 μM, 3.125 μM, 1.56 μM and 0.75 μM. The most active compound **BD_53** showed DNA supercoiling IC₅₀ of 0.63±0.19 μM as illustrated in **Table 5.8** and the agarose gel picture depicting the inhibitory activity of compound **BD_53** over DNA at various concentrations is shown in **Figure 5.34**. Compounds **BD_23**, **BD_28**, **BD_42** and **BD_57** also exhibited sub-micromolar GyrB inhibitory concentrations highlighting this series of 46 compounds as efficient inhibitors of DNA GyrB protein.

The synthesized 46 compounds were subjected to molecular docking studies in order to analyze their binding interactions and active site orientation so as to build a structure activity relationship (SAR) for the series with respect to their Gyr B activity. Among the series, compound **BD_53** was found to be exhibiting the most promising Gyr B inhibitory activity with an IC₅₀ of 0.86 μM. This compound also correlated well in terms of its supercoiling activity with 0.63 μM IC₅₀ and *Mtb* MIC of 3.3 μM. The compound's activity was well supported by its binding mode at the ATPase site of *Msm* Gyr B where it was found to be involved in two hydrogen bond interactions with Arg82 and a cation-π interaction with Arg141 as shown in the below **Figure 5.37**.

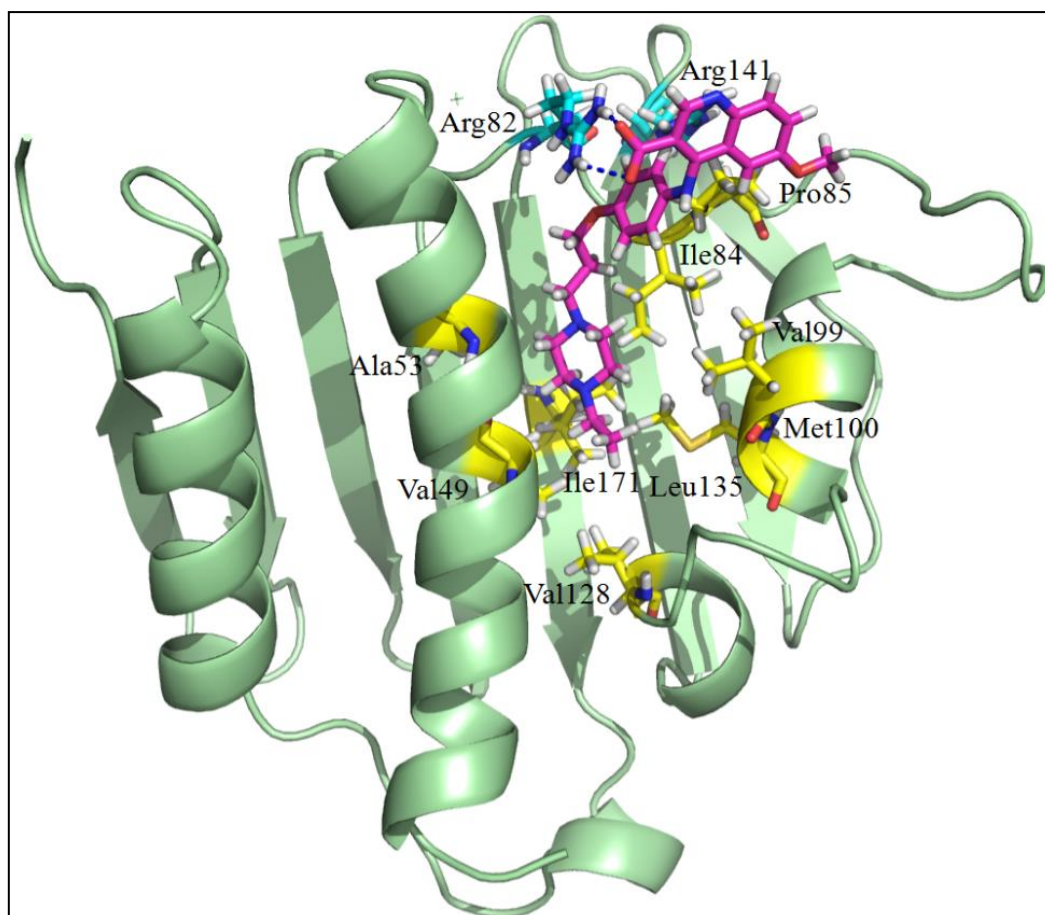


Figure 5.37: Interaction profile of compound **BD_53** (pink sticks) at the ATPase domain of *Msm* Gyr B. Residues involved in hydrogen bond and hydrophobic interactions are shown in cyan and yellow respectively. Blue dashed lines indicate hydrogen bonds.

The compound was oriented such that the quinoline moiety was directed towards the solvent accessible surface area with the carboxylic group over it involving in the hydrogen bonding. The N-ethyl piperazine was set in to the GyrB hydrophobic pocket where it was found to be stabilized by hydrophobic interactions with residues Val49, Ile84, Pro85, Val99, Met100, Val128, Leu135 and Ile171.

The compounds in the present series can be divided into three groups for convenience according to their R₁ substitutions – (i) Ester compounds **BD_12-27**, (ii) Hydrazide compounds **BD_28-43** and (iii) Acid compounds **BD_44-57**. The compounds **BD_12-27** with ethoxy substitution at R₁ position, compound **BD_23** was found to be the top active one with Gyr B inhibitory activity of 0.97 μ M and *Mtb* MIC of 2.94 μ M. The

interaction profile of the compound revealed the presence of polar contact between Arg82 and nitrogen of piperazine ring as shown in **Figure 5.38(a)**.

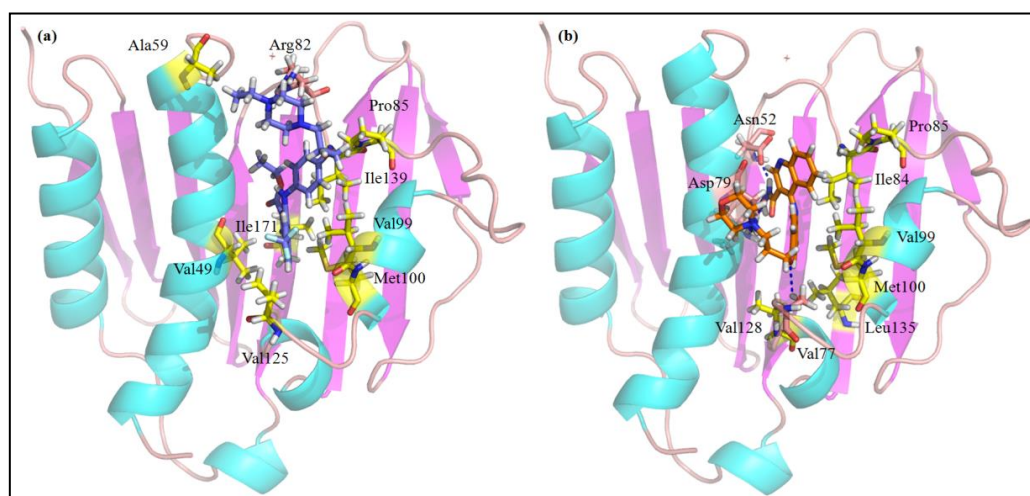


Figure 5.38: Interaction patterns of (a) compound **BD_23** and (b) compound **BD_28** at *Msm* GyrB ATPase domain.

Unlike compound **BD_53**, compound **BD_23** was oriented such that the quinoline group was embedded into the hydrophobic pocket and involved in non-polar interactions with Ile84, Pro85, Val99, Met100, Val128, and Leu135. The trifluoro methyl group over quinoline added up the hydrophobicity of the moiety making it highly stable in the pocket. Compounds **BD_12-19** with morpholine ring in place of piperazine were found to be inactive with an exception of compound **BD_19** which was found with IC_{50} of 6.62 μ M. This loss in activity can be attributed to the absence of N-ethyl substitution over Y-position for hydrogen bonding. The importance of $-NC_2H_5$ can be understood from the interaction profiles of compounds **BD_23** and **BD_15** given in **Figure 5.39**. The compounds **BD_20**, **BD_21** and **BD_22** were found to be lesser active when compared to compound **BD_23** which may be explained by the presence of trifluoro methyl group at R substitution. It was observed that with an increase in hydrophobic component at R position, as seen in compounds **BD_20**, **BD_21**, **BD_22** and **BD_23**, the activity was found to be improved starting from >50 μ M to 0.97 μ M. Replacement of oxygen at X-position in compounds **BD_20**, **BD_21** and **BD_22** by nitrogen resulted in compounds **BD_24**, **BD_25** and **BD_26** with improved Gyr B activity which can be explained by the participation of nitrogen in hydrogen bonding with residues Glu48 or Glu56 which enhanced the inhibitory activity by ~ 2 folds.

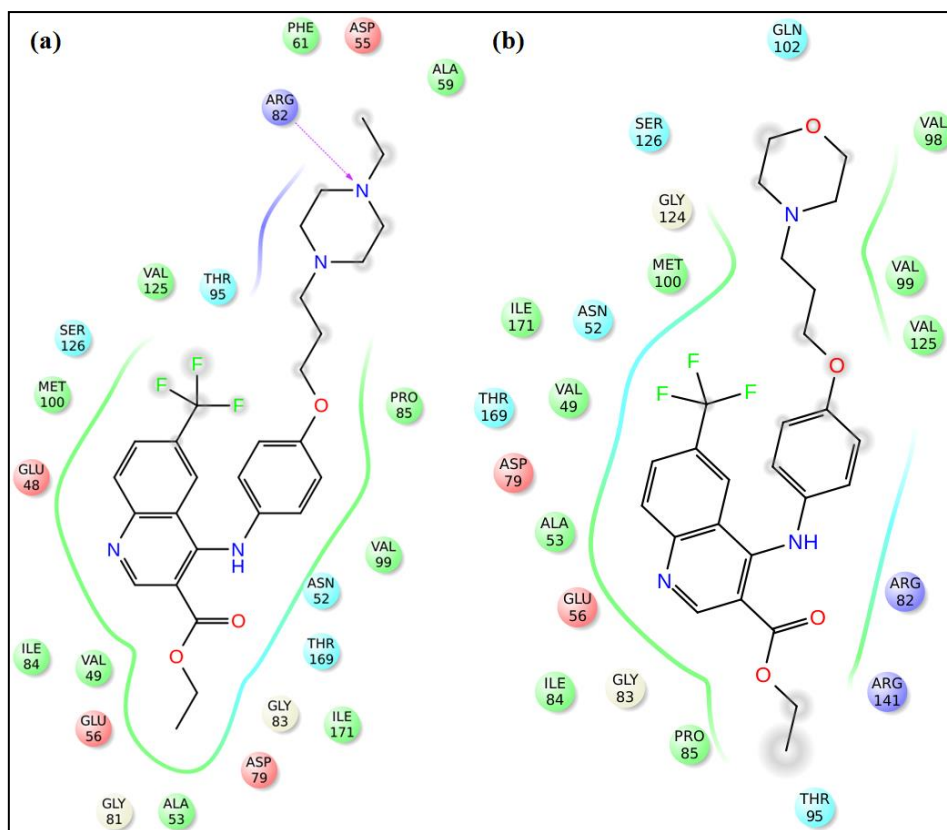


Figure 5.39: Interaction profile of (a) compound **BD_23** and (b) compound **BD_15** at *Msm* Gyr B ATPase domain active site.

Considering compounds **BD_28-43** with hydrazine at R₁ position, compound **BD_28** was found to be the best active one with Gyr B IC₅₀ of 0.97 μM and corresponding *Mtb* MIC of 2.4 μM. The compound was found interacting by hydrogen bonding with residues Asn52, Val77 and Asp79 as shown in **Figure 5.38 (b)**. Interesting point is that the hydrazine group was found to be involved in two hydrogen bonds of three orienting the compound in such a way that quinoline bound in to the hydrophobic pocket. The compound was also involved in non-polar interactions with Ile84, Pro85, Val99, Met100 and Val128. The difference in Gyr B activity of compounds **BD_12** and **BD_28** by almost 23 folds can be described by the presence of hydrazine in compound **BD_28**, as shown in **Figure 5.40**. On substitution of methoxy (compound **BD_29**), fluorine (compound **BD_30**) and trifluoro methyl (compound **BD_31**) at R position of compound **BD_28**, activity was found to be continuously decreased. This may be attributed to the steric bulk of the substitutions which made the compound orient such that hydrazine was moved away from the interacting residues thereby making them inactive. The substitution of nitrogen in place of oxygen at X-position

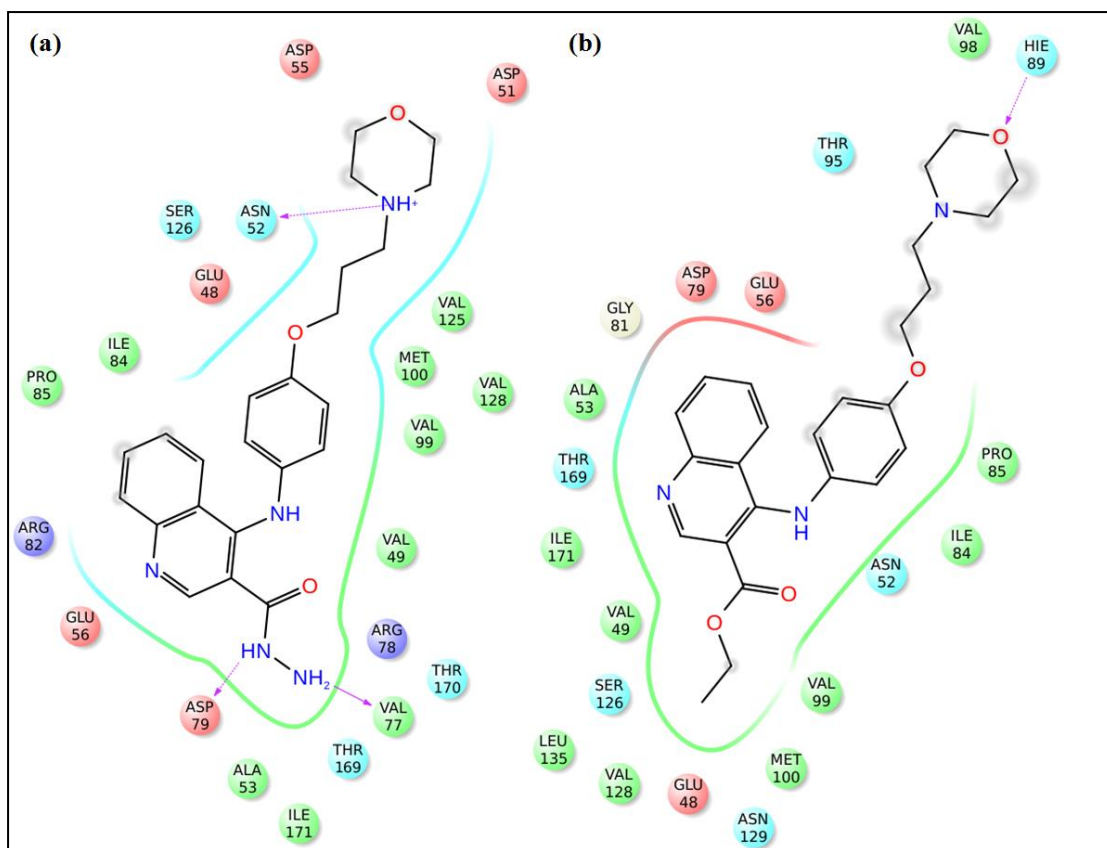


Figure 5.40: Interaction profile of (a) compound **BD_28** and (b) compound **BD_12** at *M. smegmatis* Gyr B ATPase domain active site.

resulted in complete loss of Gyr B inhibitory activity as observed in compounds **BD_32-35**. The Gyr B activity was found to be improved up on the presence of N-ethyl substitution at Y-position making the compounds active by several folds when compared to their morpholine counterparts. This might be reasoned for the addition of N-ethyl moiety over the compounds in which it was found participating in strong hydrophobic interactions. The hydrazine group facing the solvent was found to be involved in polar contacts with residues such as Asp55 (as in compounds **BD_36**, **BD_37**, **BD_38**, and **BD_41**), Asn52 (compounds **BD_38**, **BD_40**, **BD_41** and **BD_42**).

The final set of compounds includes **BD_44-57** with hydroxyl group with an IC_{50} of 7.89 μ M. The Gyr B inhibitory activity and DNA supercoiling activity was found to be improved among the compounds **BD_52-57** with N-ethyl substitution. The difference in the activity of the compounds set **BD_44-51** and **BD_52-57** can be probably explained in terms of their hydroxyl and N-ethyl substitution. In this set of **BD_44-57** compounds, the presence of hydroxyl group at the R₁ position reversed the

pose of the compounds making them orient such that the hydroxyl group facing the solvent due to its high polar nature. In compounds **BD_44-51**, the morpholine group was oriented in the pocket which was found with less non-polar interactions. Conversely, in compounds **BD_52-57** the presence of N-ethyl piperazine ring in the active site pocket was found to be highly stabilized and interacting with residues Val49, Ile84, Pro85, Val99, Met100, Val128 and Leu135.

Based on the above results, quinoline-3-carboxylic acid (-OH at R1) and quinoline-3-carbohydrazide (-NHNH₂ at R1) derivatives with ethyl piperazine (-NC₂H₅ at Y) moiety were found to be desirable substitutions resulting in compounds with efficient Gyr B inhibitory potential.

5.4.8 Highlights of the study

In our continuous efforts to discover novel antimicrobial compounds with anti-gyrase activity, we have described the discovery of novel quinoline derivatives as gyrase inhibitors with potent *Mtb* MIC and inhibitory profiles of the gyrase enzyme with well correlated structural activity relationship and less cytotoxic effect. Among 46 compounds, compound **BD_53** shows supercoiling IC₅₀ of 0.63 ± 0.15 μM, *Msm* Gyr B IC₅₀ of 0.86 ± 0.16 and well correlating MIC of 3.3 μM against *Mtb*. Compound **BD_53** as had shown a 3.3 °C positive shift in T_m than the native *Msm* Gyr B protein and also found to devoid of cytotoxicity against RAW mouse macro phage cell lines. Furthermore, we believe that this class of compounds has potential to be as novel anti-TB drug candidate.

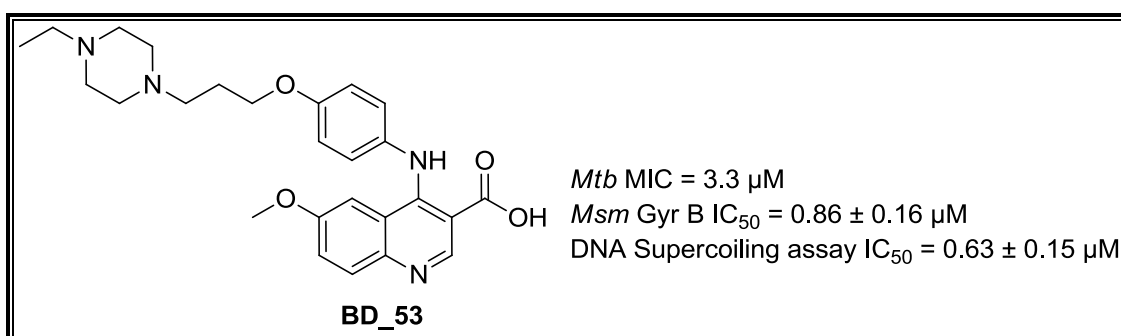


Figure 5.41: Structure and activity of most active compound **BD_53**

5.5 Development of substituted 4-((1-(3-(substituted) quinolin-4-yl)-1H-1,2,3-triazol-4-yl)methoxy)-2-phenylthiazole derivatives as potential *Mtb* DNA gyrase B inhibitors

The most important objective for discovery of new anti-TB drugs is to find new drugs/drug combinations able to effectively eradicate *in vivo* both actively replicative (aerobic) bacilli and non-replicative (microaerophilic, anaerobic and persisters) bacilli to shorten therapy of active TB below 6 months, and effectively reduce the reservoir of latently infected individuals. By keeping this objective in our mind we designed to inhibit *Mtb* DNA gyrase enzyme (Devi P. B., *et al.*, 2015).

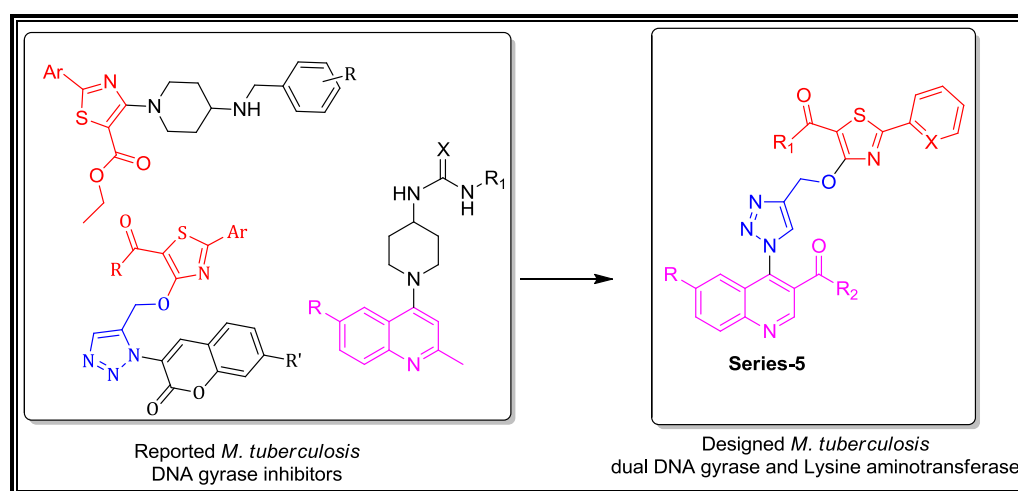


Figure 5.42 Scheme-5, Design logic and Scaffold modification and derivatization based on reported antimycobacterials

5.5.1 Chemical synthesis and characterization

The synthetic pathway utilized to achieve the target compounds has been delineated in **Figure 4.11 & Figure 4.12**. Synthesis of the target compounds, quinoline-4-1H-1,2,3 triazole 2-phenyl / pyridyl thiazole analogues (**BE_06-29**) was started with intermediate prepared in **Scheme 4B (BD_11a-c)** were used as starting material for further reactions. The intermediate (**BD_11a-c**) was then converted to corresponding substituted ethyl 4-azido-6- simple/methoxy/fluoro quinoline-3-carboxylate (**BE_01a-c**) by heating it in ethanol-water mixture at 100 °C for 1.5 h with sodium azide derivatives (**BE_01a-c**). The azide intermediates were then converted to corresponding acid derivatives (**BE_02a-c**) using LiOH. H₂O in methanol-water mixture stirring at room temperature for 2.5 h. Both these intermediates (**BE_01-02a-**

c) were reacted with thiazolopyridine and phenyl thiazole acetylene derivatives (**BE_04-05a-b**) using click chemistry conditions to get the desired final substituted 4-((1-(3-(substituted) quinolin-4-yl)-1H-1,2,3-triazol-4-yl)methoxy)-2-phenylthiazole derivatives (**BE_06-29**). The intermediates (**BE_04-05a-b**) were synthesized, starting from thiobenzamide and 2-pyridinecarbothioamide reacting with diethylbromomalonate in toluene at reflux conditions using pyridine as a base to get corresponding thiazole derivatives (**BE_04a-b**). These thiazole derivatives were o-alkylated with propargyl alcohol using Mitsunobu conditions using triphenylphosphine, diethylazodicarboxylate in THF to get corresponding thiazole acetylene derivatives (**BE_04a-b**) upon hydrolysis to get intermediates **BE_05a-b** with good yields and purity.

5.5.2 Experimental protocol followed for synthesis

General procedure for synthesis of ethyl 4-azido 6-unsubstituted/6-methoxy/6-fluoroquinoline-3-carboxylate intermediates (BE_01a-c):

To a stirred solution of **BD_11a-c** in EtOH: H₂O (mL) sodium azide was added and refluxed for 1.5 h. The reaction was monitored by TLC. After completion of reaction ethanol was evaporated and ice cold water was added and extracted with ethylacetate. The combined organic layer was dried over sodium sulphate, filtered and evaporated under reduced pressure. The crude azide derivative was recrystallized from ethanol to get the desired azide compound (**BE_01a-c**) in good yields and continued to further reactions.

General procedure for synthesis of 4-azido 6-unsubstituted/6-methoxy/6-fluoroquinoline-3-carboxylic acid intermediates (BE_02a-c):

To a solution of the corresponding ethyl 4-azido 6-unsubstituted/6-methoxy/6-fluoroquinoline-3-carboxylate intermediates (**BE_01a-c**, 1 eq) in THF: Methanol: Water (1:1:1) system, was added lot wise lithium hydroxide (2 equiv). The reaction mixture was stirred at room temperature for 3-4 h (monitored by TLC & LCMS for completion) and allowed to cool. Solvent was evaporated under vacuum, and the reaction mixture was diluted with water and acidified to P^H 2 with 1N HCl. The precipitate formed was filtered and re-crystallized from ethanol to afford the desired product in good yield.

General procedure for synthesis of Ethyl 4-hydroxy-2-(phenyl/pyridyl)-thiazole-5-carboxylate (BE_03a-b):

The synthesis followed the literature procedure (Kerdesky F. A., *et al.*, 1991). Diethyl-2-bromomalonate (1 equiv) was added drop wise to a well stirred solution of the corresponding phenyl/pyridyl thioamide (1 equiv) and pyridine (3 equiv) in toluene (60 mL) at room temperature (rt). The reaction mixture was then heated to reflux for 2-4 hours (monitored by TLC & LCMS for completion) and allowed to cool. The precipitate formed was filtered and re-crystallized from ethanol to afford the desired product in good yield.

General procedure for synthesis Ethyl 4-(prop-2-yn-1-yloxy)-2-(phenyl/pyridyl)thiazole-5-carboxylate (BE_04a-b):

To an ice cooled (0 °C) solution of Ethyl 4-hydroxy-2-(phenyl/pyridyl)-thiazole-5-carboxylate (**BE_03a-b**, 1 equiv) in dry THF (50mL) were added the propargyl alcohol (3 equiv) and triphenylphosphine (3 equiv) one after another and maintained the same temperature for 15 min. To the above mixture, diethylazodicarboxylate (3 equiv) was added drop wise and the reaction mixture was stirred at room temperature for 12 hours (monitored by TLC & LCMS for completion). The reaction mixture was evaporated under reduced pressure. The crude product was purified by column chromatography using hexane: ethylacetate as eluent to give the desired product in good yield.

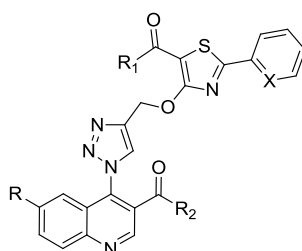
General procedure for synthesis of 4-(prop-2-yn-1-yloxy)-2-(phenyl/pyridyl)thiazole-5-carboxylic acid (BE_05a-b):

To a solution of the corresponding Ethyl 4-hydroxy-2-(phenyl/pyridyl)-thiazole-5-carboxylate (**BE_04a-b**, 1 equiv) in THF: Methanol: Water (1:1:1) system, was added lot wise lithium hydroxide (2 equiv). The reaction mixture was then heated at 60°C for 4-5 hours (monitored by TLC & LCMS for completion) and allowed to cool. Solvent was evaporated under vacuum, and the reaction mixture was diluted with water and acidified to pH 2 with 1N HCl. The precipitate formed was filtered and re-crystallized form ethanol to afford the desired product in moderate to good yield as described below.

General procedure utilized for the preparation of designed analogues (10-45):

To a mixture of the corresponding acetylene intermediate (1 equiv) and corresponding azide (1.1equiv) in THF: H₂O (1:1) system was added CuSO₄.5H₂O (0.05 equiv), sodium ascorbate (0.1equiv) at rt. The reaction was then stirred at rt for 12-15 hours (monitored by TLC & LCMS for completion). The residue was further diluted with water (2 mL) and dichloromethane (4 mL) and the layers separated. The aqueous layer was re-extracted with dichloromethane (2 x 4 mL) and the combined organic layer was washed with brine (3 mL), dried over anhydrous sodium sulphate and evaporated under reduced pressure and the residue re-crystallized from diethyl ether/ethanol to afford the desired product in good yield as described below. The physicochemical properties of synthesized derivatives were shown in **Table 5.9**.

Table 5.9 Physicochemical properties of synthesized derivatives **BE_06-BE_29**



Comp.	R	R ₁	R ₂	X	Yield (%)	Melting point (°C)	Molecular formula	Molecular weight
BE_06	H	OC ₂ H ₅	OC ₂ H ₅	H	81	113-114	C ₂₇ H ₂₃ N ₅ O ₅ S	529.57
BE_07	OCH ₃	OC ₂ H ₅	OC ₂ H ₅	H	79	175-176	C ₂₈ H ₂₅ N ₅ O ₆ S	559.59
BE_08	F	OC ₂ H ₅	OC ₂ H ₅	H	76	139-140	C ₂₇ H ₂₂ FN ₅ O ₅ S	547.56
BE_09	H	OH	OC ₂ H ₅	H	74	186-187	C ₂₅ H ₁₉ N ₅ O ₅ S	501.51
BE_10	OCH ₃	OH	OC ₂ H ₅	H	70	155-156	C ₂₆ H ₂₁ N ₅ O ₆ S	531.54
BE_11	F	OH	OC ₂ H ₅	H	80	174-175	C ₂₅ H ₁₈ FN ₅ O ₅ S	519.50
BE_12	H	OC ₂ H ₅	OC ₂ H ₅	N	78	162-163	C ₂₆ H ₂₂ N ₆ O ₅ S	530.56
BE_13	OCH ₃	OC ₂ H ₅	OC ₂ H ₅	N	71	238-239	C ₂₇ H ₂₄ N ₆ O ₆ S	560.58
BE_14	F	OC ₂ H ₅	OC ₂ H ₅	N	73	189-190	C ₂₆ H ₂₁ FN ₆ O ₅ S	548.55
BE_15	H	OH	OC ₂ H ₅	N	76	110-112	C ₂₄ H ₁₈ N ₆ O ₅ S	502.50
BE_16	OCH ₃	OH	OC ₂ H ₅	N	71	136-137	C ₂₅ H ₂₀ N ₆ O ₆ S	532.53
BE_17	F	OH	OC ₂ H ₅	N	69	196-197	C ₂₄ H ₁₇ FN ₆ O ₅ S	520.49
BE_18	H	OC ₂ H ₅	OH	H	74	137-138	C ₂₅ H ₁₉ N ₅ O ₅ S	501.51
BE_19	OCH ₃	OC ₂ H ₅	OH	H	72	205-206	C ₂₆ H ₂₁ N ₅ O ₆ S	531.54

Conti....

Comp.	R	R ₁	R ₂	X	Yield (%)	Melting point (°C)	Molecular formula	Molecular weight
BE_20	F	OC ₂ H ₅	OH	H	67	200-201	C ₂₅ H ₁₈ FN ₅ O ₅ S	519.50
BE_21	H	OH	OH	H	70	220-221	C ₂₃ H ₁₅ N ₅ O ₅ S	473.46
BE_22	OCH ₃	OH	OH	H	73	213-214	C ₂₄ H ₁₇ N ₅ O ₆ S	503.49
BE_23	F	OH	OH	H	68	185-186	C ₂₃ H ₁₄ FN ₅ O ₅ S	491.45
BE_24	H	OC ₂ H ₅	OH	N	74	256-257	C ₂₄ H ₁₈ N ₆ O ₅ S	502.50
BE_25	OCH ₃	OC ₂ H ₅	OH	N	71	189-190	C ₂₅ H ₂₀ N ₆ O ₆ S	532.53
BE_26	F	OC ₂ H ₅	OH	N	72	196-197	C ₂₄ H ₁₇ FN ₆ O ₅ S	520.49
BE_27	H	OH	OH	N	69	169-170	C ₂₂ H ₁₄ N ₆ O ₅ S	474.45
BE_28	OCH ₃	OH	OH	N	70	240-241	C ₂₃ H ₁₆ N ₆ O ₆ S	504.47
BE_29	F	OH	OH	N	74	232-234	C ₂₂ H ₁₃ FN ₆ O ₅ S	492.44

5.5.3 Characterization of synthesized compounds

Ethyl 4-azidoquinoline-3-carboxylate (BE_01a):

Pale yellow solid; Yield 72%; EI-MS m/z (Calcd. for C₁₂H₉FN₄O₂: 242.23); Found: 243.54 (M+H)⁺. Anal Calcd. for C₁₂H₉FN₄O₂: C, 59.50; H, 4.16; N, 23.13; Found: C, 60.08; H, 4.19; N, 23.22.

Ethyl 4-azido-6-methoxyquinoline-3-carboxylate (BE_01b):

Off white solid; Yield: 77%; EI-MS m/z (Calcd. for C₁₃H₁₂N₄O₃: 272.26); Found: 273.31 (M+H)⁺. Anal Calcd. for C₁₃H₁₂N₄O₃: C, 57.35; H, 4.44; N, 20.58; Found: C, 57.41; H, 4.39; N, 20.61.

Ethyl 4-azido-6-fluoroquinoline-3-carboxylate (BE_01c):

Pale yellow solid; Yield: 86%; EI-MS m/z (Calcd. for C₁₂H₉FN₄O₂: 260.22); Found: 261.21 (M+H)⁺. Anal Calcd. for C₁₂H₉FN₄O₂: C, 55.39; H, 3.49; N, 21.53; Found: C, 55.46; H, 3.51; N, 21.48.

4-Azidoquinoline-3-carboxylic acid (BE_02a):

Off white solid; Yield: 70%; EI-MS m/z (Calcd. for C₁₀H₆N₄O₂: 214.18); Found: 215.41 (M+H)⁺. Anal Calcd. for C₁₀H₆N₄O₂: C, 56.08; H, 2.82; N, 26.16; Found: C, 56.13; H, 2.76; N, 26.20.

4-Azido-6-methoxyquinoline-3-carboxylic acid (BE_02b):

Off white solid; Yield: 75%; EI-MS m/z (Calcd. for $C_{11}H_8N_4O_3$: 244.21); Found: 245.34 (M+H)⁺. Anal Calcd. for $C_{11}H_8N_4O_3$: C, 54.10; H, 3.30; N, 22.94; Found: C, 54.21; H, 3.34; N, 23.02.

4-Azido-6-fluoroquinoline-3-carboxylic acid (BE_02c):

Pale yellow solid; Yield: 71%; EI-MS m/z (Calcd. for $C_{10}H_5FN_4O_2$: 232.17); Found: 233.41 (M+H)⁺. Anal Calcd. for $C_{10}H_5FN_4O_2$: C, 51.73; H, 2.17; N, 24.13; Found: C, 51.80; H, 2.21; N, 24.19.

Ethyl 4-hydroxy-2-phenylthiazole-5-carboxylate (BE_03a):

Pale yellow solid; Yield: 86%; ¹H NMR (DMSO-d₆): δ_H 1.26 (t, $J = 7.2$ Hz, 3H), 4.23 (d, $J = 7.2$ Hz, 2H), 7.49- 7.95 (m, 5H). ¹³C NMR (DMSO-d₆): δ_C 167.3, 165.7, 161.3, 132.1, 131.6, 129.4, 126, 97.8, 60.3, 14.3. ESI-MS m/z (Calcd. for $C_{12}H_{11}NO_3S$: 249.29); Found: 250.1 (M+H)⁺. Anal Calcd for $C_{12}H_{11}NO_3S$: C, 57.82; H, 4.45; N, 5.62; Found: C, 57.79; H, 4.43; N, 5.61.

Ethyl 4-hydroxy-2-(pyridin-2-yl)thiazole-5-carboxylate (BE_03b):

Pale green solid; Yield: 80%; ¹H NMR (DMSO-d₆): δ_H 1.28 (t, $J = 7.1$ Hz, 3H), 4.24 (q, $J = 7.1$ Hz, 2H), 7.41- 8.53 (m, 4H). ¹³C NMR (DMSO-d₆): δ_C 166.6, 161.8 155.9, 149, 148.1, 142.3, 137.6, 125.3, 123.2, 60.4, 14.2. ESI-MS m/z (Calcd. for $C_{11}H_{10}N_2O_3S$: 250.27); Found: 251.1 (M+H)⁺. Anal Calcd for $C_{11}H_{10}N_2O_3S$: C, 52.79; H, 4.03; N, 11.19; Found: C, 52.8; H, 4.02; N, 11.21.

Ethyl 4-(prop-2-yn-1-yloxy)-2-phenylthiazole-5-carboxylate (BE_04a):

Off white solid; Yield: 74%; ¹H NMR (DMSO-d₆): δ_H 1.27 (t, $J = 6.9$ Hz, 3H), 3.6 (s, 1H), 4.24 (q, $J = 6.9$ Hz, 2H), 5.21 (s, 2H), 7.54- 8.01 (m, 5H). ¹³C NMR (DMSO-d₆): δ_C 167, 163.5, 160, 131.9, 131.8, 129.4, 126.4, 101.2, 78.9, 78.2, 60.6, 58, 14.2. ESI-MS m/z (Calcd. for $C_{15}H_{13}NO_3S$: 287.33); Found: 288.19 (M+H)⁺. Anal Calcd for $C_{15}H_{13}NO_3S$: C, 62.70; H, 4.56; N, 4.87; Found: C, 62.68; H, 4.55; N, 4.85.

Ethyl 4-(prop-2-yn-1-yloxy)-2-(pyridin-2-yl)thiazole-5-carboxylate (BE_04b):

Off white solid; Yield: 71%; ^1H NMR (DMSO- d_6): δ_{H} 1.27 (t, $J = 6.7$ Hz, 3H), 3.62 (s, 1H), 4.23 (q, $J = 6.7$ Hz, 2H), 5.23 (s, 2H), 7.43- 8.54 (m, 4H). ^{13}C NMR (DMSO- d_6): δ_{C} 166.8, 162.1, 157.2, 149.4, 147.8, 146.2, 137.3, 124.4, 123.8, 78.8, 77.9, 60.6, 58.3, 14.3. ESI-MS m/z (Calcd. for $\text{C}_{14}\text{H}_{12}\text{N}_2\text{O}_3\text{S}$: 288.32); Found: 289.21 (M+H) $^+$. Anal Calcd for $\text{C}_{14}\text{H}_{12}\text{N}_2\text{O}_3\text{S}$: C, 58.32; H, 4.20; N, 9.72; Found: C, 58.29; H, 4.18; N, 9.73.

4-(Prop-2-yn-1-yloxy)-2-phenylthiazole-5-carboxylic acid (BE_05a):

White solid; Yield: 88%; ^1H NMR (DMSO- d_6): δ_{H} 3.61 (s, 1H), 5.18 (s, 2H), 7.54 – 8.00 (m, 5H). ^{13}C NMR (DMSO- d_6): δ_{C} 166.4, 162.9, 161.6, 132, 131.7, 129.4, 126.1, 102.7, 79.1, 78.2, 57.9. ESI-MS m/z (Calcd. for $\text{C}_{13}\text{H}_9\text{NO}_3\text{S}$: 259.28); Found: 258.13 (M-H) $^-$. Anal Calcd for $\text{C}_{13}\text{H}_9\text{NO}_3\text{S}$: C, 60.22; H, 3.50; N, 5.40; Found: C, 60.21; H, 3.49; N, 5.38.

4-(Prop-2-yn-1-yloxy)-2-(pyridin-2-yl)thiazole-5-carboxylic acid (BE_05b):

White solid; Yield: 81%; ^1H NMR (DMSO- d_6): δ_{H} 3.62 (s, 1H), 5.22 (s, 2H), 7.39 – 8.57 (m, 4H). ^{13}C NMR (DMSO- d_6): δ_{C} 166.3, 161, 156.3, 149.2, 148.4, 143, 137.4, 124.8, 123.3, 79.1, 78, 60. ESI-MS m/z (Calcd. for $\text{C}_{12}\text{H}_8\text{N}_2\text{O}_3\text{S}$: 260.27); Found: 259.31 (M-H) $^-$. Anal Calcd for $\text{C}_{12}\text{H}_8\text{N}_2\text{O}_3\text{S}$: C, 55.38; H, 3.10; N, 10.76; Found: C, 55.35; H, 3.12; N, 10.74.

Ethyl 4-((1-(3-(ethoxycarbonyl)quinolin-4-yl)-1H-1,2,3-triazol-4-yl)methoxy)-2-phenylthiazole-5-carboxylate (BE_06):

Off-white solid; Yield 81%, m.p. 113-114 °C; ^1H NMR (DMSO- d_6): δ_{H} 9.38 (s, 1H), 8.86 (s, 1H), 8.41-8.05 (m, 4H), 7.91-7.49 (m, 5H) 5.79 (s, 2H), 4.32(q, $J = 7.1$ Hz, 2H), 4.05 (q, $J = 6.9$ Hz, 2H), 1.36 (t, $J = 7.1$ Hz, 3H), 1.02 (t, $J = 6.8$ Hz, 3H). ^{13}C NMR (DMSO- d_6): δ_{C} 169.9, 168.7, 163.5, 159.6, 150.8, 148.1, 143.9, 142.6, 138.2, 132.8, 131.5 (2C), 129.7 (2C), 129.1 (2C), 128.6 (2C), 124.8, 123.4, 119.7, 118.9, 72.6, 61.4(2C), 14.8 (2C). EI-MS m/z (Calcd. for $\text{C}_{27}\text{H}_{23}\text{N}_5\text{O}_5\text{S}$: 529.57); Found: 528.21 (M-H) $^-$. Anal Calcd. for $\text{C}_{27}\text{H}_{23}\text{N}_5\text{O}_5\text{S}$: C, 61.24; H, 4.38; N, 13.22; Found: C, 61.42; H, 4.36; N, 13.19.

Ethyl 4-((1-(3-(ethoxycarbonyl)-6-methoxyquinolin-4-yl)-1H-1,2,3-triazol-4-yl)methoxy)-2-phenylthiazole-5-carboxylate (BE_07):

Pale brown solid; Yield 79%, m.p. 175-176 °C; ¹H NMR (DMSO-d₆): δ_H. 9.39 (s, 1H), 8.91 (s, 1H), 8.11-8.05 (m, 3H), 7.89-7.35 (m, 5H), 5.89 (s, 2H), 4.31(q, *J* = 7.2 Hz, 2H), 4.04 (q, *J* = 6.9 Hz, 2H), 3.85 (s, 3H), 1.35 (t, *J* = 7.1 Hz, 3H), 1.27 (t, *J* = 6.9 Hz, 3H). ¹³C NMR (DMSO-d₆): δ_C. 169.9, 168.7, 163.5, 158.8, 155.3, 150.6, 145.6, 143.9, 142.5, 136.7, 131.4 (2C), 130.8, 129.9 (3C), 125.6 (2C), 123.8, 119.5, 118.4, 107.7, 72.5, 61.3 (2C), 56.6, 14.7 (2C). EI-MS *m/z* (Calcd. for C₂₈H₂₅N₅O₆S: 559.59); Found: 558.05 (M-H)⁻. Anal Calcd.for C₂₈H₂₅N₅O₆S: C, 60.10; H, 4.50; N, 12.52; Found: C, 60.28; H, 4.48; N, 12.56.

Ethyl4-((1-(3-(ethoxycarbonyl)-6-fluoroquinolin-4-yl)-1H-1,2,3-triazol-4-yl)methoxy)-2-phenylthiazole-5-carboxylate (BE_08):

White solid; Yield 76%, m.p. 139-140 °C; ¹H NMR (DMSO-d₆): δ_H. 9.46 (s, 1H), 8.86 (s, 1H), 8.09-8.02 (m, 3H), 7.78-7.39 (m, 5H), 5.87 (s, 2H), 4.32 (q, *J* = 7.3 Hz, 2H), 4.03 (q, *J* = 6.9 Hz, 2H), 1.34 (t, *J* = 7.3 Hz, 3H), 1.02 (t, *J* = 6.8 Hz, 3H). ¹³C NMR (DMSO-d₆): δ_C. 169.7, 168.5, 163.3, 161.8, 156.4, 150.6, 147.2, 143.9, 142.4, 137.6, 131.3 (2C), 130.0 (2C), 129.5 (2C), 125.4, 124.5 (2C), 119.4, 118.6, 111.8, 72.5, 61.3 (2C), 14.6 (2C). EI-MS *m/z* (Calcd. for C₂₇H₂₂FN₅O₅S: 547.56); Found: 548.58 (M+H)⁺. Anal Calcd.for C₂₇H₂₂FN₅O₅S: C, 59.22; H, 4.05; N, 12.79; Found: C, 59.39; H, 4.04; N, 12.74.

4-((1-(3-(Ethoxycarbonyl)quinolin-4-yl)-1H-1,2,3-triazol-4-yl)methoxy)-2-phenylthiazole-5-carboxylic acid (BE_09):

Pale green solid; Yield 74%, m.p. 186-187 °C; ¹H NMR (DMSO-d₆): δ_H. 11.03 (s, 1H), 9.47(s, 1H), 8.88 (s, 1H), 8.41-8.08 (m, 4H), 7.89-7.42 (m, 5H), 5.87 (s, 2H), 4.33 (q, *J* = 7.2 Hz, 2H), 1.31 (t, *J* = 6.8 Hz, 3H). ¹³C NMR (DMSO-d₆): δ_C. 170.0, 168.8, 163.4, 159.5, 150.7, 147.9, 143.6, 142.8, 138.3, 132.9, 131.5(2C), 129.9 (2C), 129.4 (2C), 128.7 (2C), 124.9, 123.3, 119.6, 118.7, 72.4, 61.5, 14.7. EI-MS *m/z* (Calcd. for C₂₅H₁₉N₅O₅S: 501.51); Found: 502.48 (M+H)⁺. Anal Calcd.for C₂₅H₁₉N₅O₅S: C, 59.87; H, 3.82; N, 13.96; Found: C, 59.67; H, 3.83; N, 13.92.

4-((1-(3-(Ethoxycarbonyl)-6-methoxyquinolin-4-yl)-1H-1,2,3-triazol-4-yl)methoxy)-2-phenylthiazole-5-carboxylic acid (BE_10):

Brown solid; Yield 70%, m.p. 155-156 °C; ¹H NMR (DMSO-d₆): δ_H. 11.20 (s, 1H), 8.87 (s, 1H), 8.12-8.05 (m, 3H), 7.89-7.32 (m, 6H), 5.89 (s, 2H), 4.28 (q, *J* = 7.2 Hz, 2H), 3.82 (s, 3H), 1.30 (t, *J* = 6.9 Hz, 3H). ¹³C NMR (DMSO-d₆): δ_C. 169.8, 168.5, 163.4, 158.7, 155.2, 151.0, 146.2, 143.6, 142.4, 136.9, 131.5 (3C), 129.7 (3C), 125.9, 125.2, 123.8, 119.6, 118.4, 107.7, 72.4, 61.6, 56.3, 14.5. EI-MS *m/z* (Calcd. for C₂₆H₂₁N₅O₆S: 531.54); Found: 532.51 (M+H)⁺. Anal Calcd. for C₂₆H₂₁N₅O₆S: C, 58.75; H, 3.98; N, 13.18; Found: C, 58.57; H, 3.99; N, 13.21.

4-((1-(3-(Ethoxycarbonyl)-6-fluoroquinolin-4-yl)-1H-1,2,3-triazol-4-yl)methoxy)-2-phenylthiazole-5-carboxylic acid (BE_11):

Pale brown solid; Yield 80%, m.p. 174-175 °C; ¹H NMR (DMSO-d₆): δ_H. 9.47 (s, 1H), 8.88 (s, 1H), 8.10-8.05 (m, 4H), 7.75-7.42 (m, 5H), 5.89 (s, 2H), 4.29 (q, *J* = 7.4 Hz, 2H), 1.32 (t, *J* = 7.0 Hz, 3H). ¹³C NMR (DMSO-d₆): δ_C. 169.9, 168.8, 163.6, 162.0, 156.5, 150.7, 147.3, 143.8, 142.5, 137.6, 131.4 (2C), 129.9 (3C), 129.2, 125.4, 124.6 (2C), 119.7, 118.9, 111.5, 72.3, 61.5, 14.7. EI-MS *m/z* (Calcd. for C₂₅H₁₈FN₅O₅S: 519.50); Found: 518.28 (M-H)⁻. Anal Calcd. for C₂₅H₁₈FN₅O₅S: C, 57.80; H, 3.49; N, 13.48; Found: C, 57.62; H, 3.48; N, 13.51.

Ethyl 4-((1-(3-(ethoxycarbonyl)quinolin-4-yl)-1H-1,2,3-triazol-4-yl)methoxy)-2-(pyridin-2-yl)thiazole-5-carboxylate (BE_12):

Off-white solid; Yield 78%, m.p. 162-163 °C; ¹H NMR (DMSO-d₆): δ_H. 9.49(s, 1H), 8.94 (s, 1H), 8.57-8.09 (m, 4H), 7.91-7.34 (m, 4H), 5.86 (s, 2H), 4.30 (q, *J* = 7.2 Hz, 2H), 4.09 (q, *J* = 6.9 Hz, 2 H), 1.35 (t, *J* = 7.1 Hz, 3H), 1.08 (t, *J* = 6.9 Hz, 3H). ¹³C NMR (DMSO-d₆): δ_C. 168.6, 163.4(2C), 159.7, 157.9, 148.0, 142.5, 138.3(2C), 132.8, 129.1(2C), 128.4, 124.7(2C), 124.0, 123.5, 119.3, 118.7, 72.4, 61.6(2C), 14.8(2C). EI-MS *m/z* (Calcd. for C₂₆H₂₂N₆O₅S: 530.56); Found: 531.21 (M+H)⁺. Anal Calcd. for C₂₆H₂₂N₆O₅S: C, 58.86; H, 4.18; N, 15.84; Found: C, 58.68; H, 4.20; N, 15.87.

Ethyl 4-((1-(3-(ethoxycarbonyl)-6-methoxyquinolin-4-yl)-1H-1,2,3-triazol-4-yl)methoxy)-2-(pyridin-2-yl)thiazole-5-carboxylate (BE_13):

Off-white solid; Yield 71%, m.p. 238-239 °C; ¹H NMR (DMSO-d₆): δ_H. 9.38 (s, 1H), 8.89 (s, 1H), 8.61-8.05 (m, 2H), 7.89-7.34 (m, 5H), 5.81 (s, 2H), 4.29 (q, *J* = 7.4 Hz,

2H), 4.09 (q, $J = 6.9$ Hz, 2H), 3.84 (s, 3H), 1.32 (t, $J = 7.1$ Hz, 3H), 1.04 (t, $J = 6.8$ Hz, 3H). ^{13}C NMR (DMSO- d_6): δ_{C} . 168.9, 163.5(2C), 158.7, 157.9, 155.3, 149.8(2C), 145.6, 142.4, 137.7, 136.9, 131.1, 125.7, 125.0 (2C), 124.2(2C), 119.4, 118.6, 107.8, 72.5, 61.6 (2C), 56.3, 14.5 (2C). EI-MS m/z (Calcd. for $\text{C}_{27}\text{H}_{24}\text{N}_6\text{O}_6\text{S}$: 560.58); Found: 559.17 (M-H) $^-$. Anal Calcd. for $\text{C}_{27}\text{H}_{24}\text{N}_6\text{O}_6\text{S}$: C, 57.85; H, 4.32; N, 14.99; Found: C, 58.02; H, 4.31; N, 14.94.

Ethyl 4-((1-(3-(ethoxycarbonyl)-6-fluoroquinolin-4-yl)-1H-1,2,3-triazol-4-yl)methoxy)-2-(pyridin-2-yl)thiazole-5-carboxylate (BE_14):

Off-white solid; Yield 73%, m.p. 189-190 °C; ^1H NMR (DMSO- d_6): δ_{H} . 9.48 (s, 1H), 8.95 (s, 1H), 8.61-8.02 (m, 3H), 7.37-7.88 (m, 4H), 5.79 (s, 2H), 4.31 (q, $J = 7.2$ Hz, 2H), 4.03 (q, $J = 6.9$ Hz, 2H), 1.36 (t, $J = 7.1$ Hz, 3H), 1.09 (t, $J = 6.8$ Hz, 3H). ^{13}C NMR (DMSO- d_6): δ_{C} . 168.5, 163.3 (2C), 161.9, 157.7, 156.6, 149.8 (2C), 147.4, 142.5, 137.7 (2C), 130.1, 125.4 (3C), 124.2 (2C), 119.4, 118.6, 111.9, 72.5, 61.3 (2C), 14.6 (2C). EI-MS m/z (Calcd. for $\text{C}_{26}\text{H}_{21}\text{FN}_6\text{O}_5\text{S}$: 548.55); Found: 549.45 (M+H) $^+$. Anal Calcd. for $\text{C}_{26}\text{H}_{21}\text{FN}_6\text{O}_5\text{S}$: C, 56.93; H, 3.86; N, 15.32; Found: C, 56.76; H, 3.87; N, 15.37.

4-((1-(3-(Ethoxycarbonyl)quinolin-4-yl)-1H-1,2,3-triazol-4-yl)methoxy)-2-(pyridin-2-yl)thiazole-5-carboxylic acid (BE_15):

Brown solid; Yield 76%, m.p. 110-112 °C; ^1H NMR (DMSO- d_6): δ_{H} . 11.05 (s, 1H), 9.47 (s, 1H), 8.89 (s, 1H), 8.64-8.08 (m, 4H), 8.01-7.42 (m, 4H), 5.81 (s, 2H), 4.31 (q, $J = 7.2$ Hz, 2H), 1.29 (t, $J = 6.9$ Hz, 3H). ^{13}C NMR (DMSO- d_6): δ_{C} . 168.8, 163.5, 162.9, 159.6, 157.8, 149.9(2C), 148.1, 142.5, 138.3 (2C), 132.7, 129.4(2C), 128.5, 124.8 (2C), 124.1, 123.4, 119.6, 118.8, 72.5, 61.3, 14.7. EI-MS m/z (Calcd. for $\text{C}_{24}\text{H}_{18}\text{N}_6\text{O}_5\text{S}$: 502.50); Found: 503.38 (M+H) $^+$. Anal Calcd. for $\text{C}_{24}\text{H}_{18}\text{N}_6\text{O}_5\text{S}$: C, 57.36; H, 3.61; N, 16.72; Found: C, 57.52; H, 3.59; N, 16.67.

4-((1-(3-(Ethoxycarbonyl)-6-methoxyquinolin-4-yl)-1H-1,2,3-triazol-4-yl)methoxy)-2-(pyridin-2-yl)thiazole-5-carboxylic acid (BE_16):

Brown solid; Yield 71%, m.p. 136-137 °C; ^1H NMR (DMSO- d_6): δ_{H} . 11.01 (s, 1H), 9.36 (s, 1H), 8.79 (s, 1H), 8.58-8.02 (m, 2H), 7.87-7.36 (m, 5H), 5.79 (s, 2H), 4.31 (q, $J = 7.2$ Hz, 2H), 3.82 (s, 3H), 1.28 (t, $J = 6.9$ Hz, 3H). ^{13}C NMR (DMSO- d_6): δ_{C} .

168.8, 163.6 (2C), 158.9, 158.0, 155.3, 149.9 (2C), 145.7, 142.5, 137.8, 136.9, 130.6, 125.8 (2C), 124.6, 123.9 (2C), 119.2, 118.7, 107.6, 72.8, 61.4, 56.5, 14.4. EI-MS m/z (Calcd. for $C_{25}H_{20}N_6O_6S$: 532.53); Found: 533.28 (M+H)⁺. Anal Calcd. for $C_{25}H_{20}N_6O_6S$: C, 56.39; H, 3.79; N, 15.78; Found: C, 56.58; H, 3.77; N, 15.83.

4-((1-(3-(Ethoxycarbonyl)-6-fluoroquinolin-4-yl)-1H-1,2,3-triazol-4-yl)methoxy)-2-(pyridin-2-yl)thiazole-5-carboxylic acid (BE_17):

Pale brown solid; Yield 69%, m.p. 196-197 °C; ¹H NMR (DMSO-d₆): δ_H. 11.20 (s, 1H), 9.46 (s, 1H), 8.87 (s, 1H), 8.64-8.04 (m, 3H), 7.86-7.34 (m, 4H), 5.79 (s, 2H), 4.29 (q, $J = 7.3$ Hz, 2H), 1.31 (t, $J = 6.9$ Hz, 3H). ¹³C NMR (DMSO-d₆): δ_C. 168.6, 163.4 (2C), 161.8, 157.6, 156.4, 149.7 (2C), 147.1, 142.6, 137.8 (2C), 130.0, 125.6 (2C), 124.3 (2C), 123.9, 119.5, 118.7, 111.8, 72.4, 61.6, 14.8. EI-MS m/z (Calcd. for $C_{24}H_{17}FN_6O_5S$: 520.49); Found: 519.26 (M-H)⁻. Anal Calcd. for $C_{24}H_{17}FN_6O_5S$: C, 55.38; H, 3.29; N, 16.15; Found: C, 55.54; H, 3.28; N, 16.11.

4-(4-(((5-(Ethoxycarbonyl)-2-phenylthiazol-4-yl)oxy)methyl)-1H-1,2,3-triazol-1-yl)quinoline-3-carboxylic acid (BE_18):

Pale brown solid; Yield 74%, m.p. 137-138 °C; ¹H NMR (DMSO-d₆): δ_H. 11.14 (s, 1H), 9.25 (s, 1H), 8.87 (s, 1H), 8.25-8.02 (4H), 7.97-7.39 (m, 5H), 5.89 (s, 2H), 4.12 (q, $J = 7.4$ Hz, 2H), 1.07 (t, $J = 7.0$ Hz, 3H). ¹³C NMR (DMSO-d₆): δ_C. 170.0 (2C), 168.5, 159.3, 150.7, 147.9, 143.6, 142.5, 137.7, 132.9, 131.4 (2C), 129.6 (2C), 129.1 (2C), 128.5 (2C), 124.7 (2C), 119.5, 118.8, 72.6, 61.4, 14.7. EI-MS m/z (Calcd. for $C_{25}H_{19}N_5O_5S$: 501.51); Found: 500.19 (M-H)⁻. Anal Calcd. for $C_{25}H_{19}N_5O_5S$: C, 59.87; H, 3.82; N, 13.96; Found: C, 59.68; H, 3.83; N, 13.91.

4-(4-(((5-(Ethoxycarbonyl)-2-phenylthiazol-4-yl)oxy)methyl)-1H-1,2,3-triazol-1-yl)-6-methoxyquinoline-3-carboxylic acid (BE_19):

Off-white solid; Yield 72%, m.p. 205-206 °C; ¹H NMR (DMSO-d₆): δ_H. 11.41 (s, 1H), 9.45 (s, 1H), 8.89 (s, 1H), 8.10-8.02 (m, 2H), 7.81-7.15 (m, 6H), 5.87 (s, 2H), 4.19 (q, $J = 7.2$ Hz, 2H), 3.84 (s, 3H), 1.20 (t, $J = 7.0$ Hz, 3H). ¹³C NMR (DMSO-d₆): δ_C. 169.8 (2C), 168.5, 158.7, 154.9, 150.6, 145.4, 143.8, 142.5, 136.8, 131.4 (2C), 130.6, 129.7 (2C), 129.1, 125.4(2C), 124.6, 119.8, 118.5, 107.3, 72.6, 61.4, 56.5, 14.7. EI-MS m/z (Calcd. for $C_{26}H_{21}N_5O_6S$: 531.54); Found: 532.47 (M+H)⁺. Anal

Calcd. for $C_{26}H_{21}N_5O_6S$: C, 58.75; H, 3.98; N, 13.18; Found: C, 58.92; H, 3.97; N, 13.14.

4-(4-(((5-(Ethoxycarbonyl)-2-phenylthiazol-4-yl)oxy)methyl)-1H-1,2,3-triazol-1-yl)-6-fluoroquinoline-3-carboxylic acid (BE_20):

Off-white solid; Yield 67%, m.p. 200-201 °C; 1H NMR (DMSO- d_6): δ_H . 11.41 (s, 1H), 9.46 (s, 1H), 8.90 (s, 1H), 8.12-8.02 (m, 2H), 7.80-7.39 (m, 6H), 5.90 (s, 2H), 4.21 (q, $J = 7.4$ Hz, 2H), 1.15 (t, $J = 7.0$ Hz, 3H). ^{13}C NMR (DMSO- d_6): δ_C . 169.9 (2C), 168.6, 162.0, 156.5, 150.8, 147.3, 143.7, 142.4, 137.1, 131.5 (2C), 129.9 (2C), 129.4 (2C), 125.1 (2C), 124.6, 119.3, 118.7, 111.4, 72.6, 61.5, 14.7. EI-MS m/z (Calcd. for $C_{25}H_{18}FN_5O_5S$: 519.50); Found: 520.48 (M+H) $^+$. Anal Calcd. for $C_{25}H_{18}FN_5O_5S$: C, 57.80; H, 3.49; N, 13.48; Found: C, 57.96; H, 3.47; N, 13.52.

4-(((1-(3-Carboxyquinolin-4-yl)-1H-1,2,3-triazol-4-yl)methoxy)-2-phenylthiazole-5-carboxylic acid (BE_21):

Pale brown solid; Yield 70%, m.p. 220-221 °C; 1H NMR (DMSO- d_6): δ_H . 11.27 (s, 1H), 11.04 (s, 1H), 9.36 (s, 1H), 8.87 (s, 1H), 8.23-8.04 (m, 3H), 7.97-7.42 (m, 6H), 5.87 (s, 2H). ^{13}C NMR (DMSO- d_6): δ_C . 169.9 (2C), 168.6, 159.4, 150.8, 148.0, 143.7, 142.4, 137.8, 133.1, 131.5 (2C), 129.9 (2C), 129.2 (2C), 128.4 (2C), 124.7 (2C), 119.4, 118.6, 72.3. EI-MS m/z (Calcd. for $C_{23}H_{15}N_5O_5S$: 473.46); Found: 474.28 (M+H) $^+$. Anal Calcd. for $C_{23}H_{15}N_5O_5S$: C, 58.35; H, 3.19; N, 14.79; Found: C, 58.52; H, 3.17; N, 14.83.

4-(((1-(3-Carboxy-6-methoxyquinolin-4-yl)-1H-1,2,3-triazol-4-yl)methoxy)-2-phenylthiazole-5-carboxylic acid (BE_22):

Pale brown solid; Yield 73%, m.p. 213-214 °C; 1H NMR (DMSO- d_6): δ_H . 11.41 (s, 1H), 11.06 (s, 1H), 9.48 (s, 1H), 8.91 (s, 1H), 8.14-8.01 (m, 2H), 7.78-7.16 (m, 6H), 5.87 (s, 2H), 3.84 (s, 3H). ^{13}C NMR (DMSO- d_6): δ_C . 169.7 (2C), 168.6, 158.9, 155.1, 150.8, 145.6, 143.7, 142.5, 136.8, 131.4 (2C), 130.7, 129.9 (2C), 129.3, 125.6 (2C), 124.4, 119.5, 118.7, 107.4, 72.6, 56.3. EI-MS m/z (Calcd. for $C_{24}H_{17}N_5O_6S$: 503.49); Found: 502.25 (M-H) $^-$. Anal Calcd. for $C_{24}H_{17}N_5O_6S$: C, 57.25; H, 3.40; N, 13.91; Found: C, 57.08; H, 3.42; N, 13.96.

4-((1-(3-Carboxy-6-fluoroquinolin-4-yl)-1H-1,2,3-triazol-4-yl)methoxy)-2-phenylthiazole-5-carboxylic acid (BE_23):

Brown solid; Yield 68%, m.p. 185-186 °C; ¹H NMR (DMSO-d₆): δ_H. 11.42 (s, 1H), 11.06 (s, 1H), 9.48 (s, 1H), 8.87 (s, 1H), 8.11-8.03 (m, 2H), 7.98-7.42 (m, 6H), 5.89 (s, 2H). ¹³C NMR (DMSO-d₆): δ_C. 169.7 (2C), 168.5, 161.9, 156.3, 150.6, 147.2, 143.8, 142.5, 137.3, 131.6 (2C), 129.8 (2C), 129.5 (2C), 125.2 (3C), 119.5, 118.3, 111.8, 72.4. EI-MS m/z (Calcd. for C₂₃H₁₄FN₅O₅S: 491.45); Found: 490.22 (M-H)⁻. Anal Calcd.for C₂₃H₁₄FN₅O₅S: C, 56.21; H, 2.87; N, 14.25; Found: C, 56.05; H, 2.88; N, 14.21.

4-(4-(((5-(Ethoxycarbonyl)-2-(pyridin-2-yl)thiazol-4-yl)oxy)methyl)-1H-1,2,3-triazol-1-yl)quinoline-3-carboxylic acid (BE_24):

Off-white solid; Yield 74%, m.p. 256-257 °C; ¹H NMR (DMSO-d₆): δ_H. 11.06 (s, 1H), 9.29 (s, 1H), 8.89 (s, 1H), 8.63-8.06 (m, 3H), 7.97-7.35 (m, 5H), 5.87 (s, 2H), 4.09 (q, *J* = 7.3 Hz, 2H), 1.09 (t, *J* = 6.9 Hz, 3H). ¹³C NMR (DMSO-d₆): δ_C. 169.8, 168.6, 163.2, 159.1, 157.9, 149.6 (2C), 147.8, 142.5, 137.7 (2C), 132.5, 129.1 (3C), 124.6 (2C), 123.9 (2C), 119.5, 118.3, 72.6, 61.3, 14.5. EI-MS m/z (Calcd. for C₂₄H₁₈N₆O₅S: 502.50); Found: 503.42 (M+H)⁺. Anal Calcd.for C₂₄H₁₈N₆O₅S: C, 57.36; H, 3.61; N, 16.72;; Found: C, 57.21; H, 3.63; N, 16.67.

4-(4-(((5-(Ethoxycarbonyl)-2-(pyridin-2-yl)thiazol-4-yl)oxy)methyl)-1H-1,2,3-triazol-1-yl)-6-methoxyquinoline-3-carboxylic acid (BE_25):

Brown solid; Yield 71%, m.p. 189-190 °C; ¹H NMR (DMSO-d₆): δ_H. 11.39 (s, 1H), 9.17 (s, 1H), 8.88 (s, 1H), 8.62-8.05 (m, 2H), 7.88-7.16 (m, 5H), 5.87 (s, 2H), 4.14 (q, *J* = 7.4 Hz, 2H), 3.85 (s, 3H), 1.20 (t, *J* = 6.9 Hz, 3H). ¹³C NMR (DMSO-d₆): δ_C. 169.7, 168.5, 163.1, 158.6, 157.9, 154.7, 150.0 (2C), 145.6, 142.3, 137.5, 136.7, 130.4, 125.6 (2C), 124.8, 124.3 (2C), 119.5, 118.7, 107.4, 72.6, 61.3, 56.7, 14.5. EI-MS m/z (Calcd. for C₂₅H₂₀N₆O₆S: 532.53); Found: 531.11 (M-H)⁻. Anal Calcd.for C₂₅H₂₀N₆O₆S: C, 56.39; H, 3.79; N, 15.78; Found: C, 56.23; H, 3.78; N, 15.83.

4-(4-(((5-(Ethoxycarbonyl)-2-(pyridin-2-yl)thiazol-4-yl)oxy)methyl)-1H-1,2,3-triazol-1-yl)-6-fluoroquinoline-3-carboxylic acid (BE_26):

Pale yellow solid; Yield 72%, m.p. 196-197 °C; ¹H NMR (DMSO-d₆): δ_H. 11.39 (s, 1H), 9.39 (s, 1H), 8.88 (s, 1H), 8.61-8.05 (m, 2H), 7.95-7.35 (m, 5H), 5.91 (s, 2H), 4.14 (q, *J* = 7.4 Hz, 2H), 1.18 (t, *J* = 7.0 Hz, 3H). ¹³C NMR (DMSO-d₆): δ_C. 169.9, 168.5, 163.3, 161.7, 158.0, 156.2, 149.9 (2C), 147.1, 142.6, 137.8 (2C), 129.7, 125.2 (2C), 124.7 (2C), 124.0, 119.4, 118.6, 111.7, 72.5, 61.7, 14.4. SEI-MS m/z (Calcd. for C₂₄H₁₇FN₆O₅S: 520.49); Found: 521.36 (M+H)⁺. Anal Calcd. for C₂₄H₁₇FN₆O₅S: C, 55.38; H, 3.29; N, 16.15; Found: C, 55.56; H, 3.28; N, 16.21.

4-((1-(3-Carboxyquinolin-4-yl)-1H-1,2,3-triazol-4-yl)methoxy)-2-(pyridin-2-yl)thiazole-5-carboxylic acid (BE_27):

Brown solid; Yield 69%, m.p. 169-170 °C; ¹H NMR (DMSO-d₆): δ_H. 11.41 (s, 1H), 11.02 (s, 1H), 9.26 (s, 1H), 8.85 (s, 1H), 8.64-8.05 (m, 3H), 7.95-7.35 (m, 5H), 5.91 (s, 2H). ¹³C NMR (DMSO-d₆): δ_C. 169.9, 168.7, 163.2, 159.0, 157.8, 149.6 (2C), 147.7, 142.4, 137.6 (2C), 132.8, 129.2 (2C), 128.5, 124.6 (2C), 124.0 (2C), 119.3, 118.5, 72.3. EI-MS m/z (Calcd. for C₂₂H₁₄N₆O₅S: 474.45); Found: 475.35 (M+H)⁺. Anal Calcd. for C₂₂H₁₄N₆O₅S: C, 55.69; H, 2.97; N, 17.71; Found: C, 55.86; H, 2.96; N, 17.67.

4-((1-(3-Carboxy-6-methoxyquinolin-4-yl)-1H-1,2,3-triazol-4-yl)methoxy)-2-(pyridin-2-yl)thiazole-5-carboxylic acid (BE_28):

Brown solid; Yield 70%, m.p. 240-241 °C; ¹H NMR (DMSO-d₆): δ_H. 11.39 (s, 1H), 9.28 (s, 1H), 8.89 (s, 1H), 8.58-8.01 (m, 2H), 7.85-7.18 (m, 5H), 5.87 (s, 2H), 3.82 (s, 3H). ¹³C NMR (DMSO-d₆): δ_C. 169.6, 168.8, 163.2, 158.5, 157.8, 154.9, 150.2 (2C), 145.7, 142.5, 137.8, 136.6, 130.3, 125.8 (2C), 124.5, 124.7 (2C), 119.4, 118.6, 107.5, 72.3, 56.1. EI-MS m/z (Calcd. for C₂₃H₁₆N₆O₆S: 504.47); Found: 505.42 (M+H)⁺. Anal Calcd. for C₂₃H₁₆N₆O₆S: C, 54.76; H, 3.20; N, 16.66; Found: C, 54.61; H, 3.21; N, 16.71.

4-((1-(3-Carboxy-6-fluoroquinolin-4-yl)-1H-1,2,3-triazol-4-yl)methoxy)-2-(pyridin-2-yl)thiazole-5-carboxylic acid (BE_29):

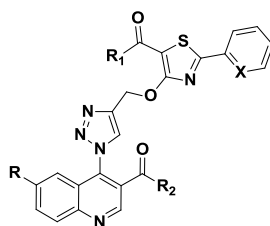
Pale Brown solid; Yield 74%, m.p. 232-234 °C; ¹H NMR (DMSO-d₆): δ_H. 11.38 (s, 1H), 11.04 (s, 1H), 9.47 (s, 1H), 8.89 (s, 1H), 8.59-8.02 (m, 2H), 7.94-7.37 (m, 5H), 5.89 (s, 2H). ¹³C NMR (DMSO-d₆): δ_C. 169.7, 168.6, 163.2, 161.8, 157.7, 156.4, 150.0

(2C), 147.2, 142.5, 137.6 (2C), 129.8, 125.3 (2C), 124.6 (2C), 124.1, 118.9, 117.7, 111.5, 72.4. EI-MS m/z (Calcd. for C₂₂H₁₃FN₆O₅S: 492.44); Found: 491.31 (M-H). Anal Calcd.for C₂₂H₁₃FN₆O₅S: C, 53.66; H, 2.66; N, 17.07; Found: C, 53.49; H, 2.67; N, 17.03.

5.5.4 *In vitro* Msm Gyr B assay, supercoiling assay, antimycobacterial potency, Mtb LAT assay and cytotoxicity studies of the synthesized molecules

All the synthesized derivatives were evaluated for their *in vitro* Msm Gyr B supercoiling assay, Mtb LAT (Lysine aminotransferase) assay for the derivation of SAR and lead optimization. But the compounds didn't show any inhibition against Msm Gyr B protein then we tested *in vitro* Mtb LAT assay based on the design logic for dual inhibition of DNA gyrase and LAT enzyme. The compounds were further subjected to a whole cell screening against Mtb H₃₇Rv strain to understand their bactericidal potency using MABA method and later the safety profile of these molecules were evaluated by checking the *in vitro* cytotoxicity against RAW 264.7 cell line (mouse macrophage) at 50 µM concentration by MTT assay, and the results are shown in **Table 5.10**.

Table 5.10 Biological screening of synthesized derivatives **BE_06-BE_29**



Comp.	R	R ₁	R ₂	X	<i>Mtb</i>			Cytotoxicity at 50 μM (% Inhibition)
					<i>Mtb</i> MIC (μM)	Supercoiling assay (% of Inhibition at 10 μM)	<i>Mtb</i> LAT IC ₅₀ in μM	
BE_06	H	OC ₂ H ₅	OC ₂ H ₅	H	>47.21	NT	NT	11.06
BE_07	OCH ₃	OC ₂ H ₅	OC ₂ H ₅	H	1.39	50	>25	24.25
BE_08	F	OC ₂ H ₅	OC ₂ H ₅	H	5.71	40	4.24±0.14	0
BE_09	H	OH	OC ₂ H ₅	H	24.92	NT	NT	28.68
BE_10	OCH ₃	OH	OC ₂ H ₅	H	5.88	55	10.92±0.17	48.28
BE_11	F	OH	OC ₂ H ₅	H	6.02	50	7.75±0.13	9.48
BE_12	H	OC ₂ H ₅	OC ₂ H ₅	N	23.56	NT	NT	0
BE_13	OCH ₃	OC ₂ H ₅	OC ₂ H ₅	N	11.15	NT	NT	0
BE_14	F	OC ₂ H ₅	OC ₂ H ₅	N	1.42	35	>25	7.82
BE_15	H	OH	OC ₂ H ₅	N	>49.75	NT	NT	0
BE_16	OCH ₃	OH	OC ₂ H ₅	N	23.47	NT	NT	18.11
BE_17	F	OH	OC ₂ H ₅	N	3.00	45	3.76±0.15	8.29
BE_18	H	OC ₂ H ₅	OH	H	6.23	50	3.37±0.18	36.59
BE_19	OCH ₃	OC ₂ H ₅	OH	H	23.52	NT	NT	0
BE_20	F	OC ₂ H ₅	OH	H	24.06	NT	NT	25.44
BE_21	H	OH	OH	H	26.40	NT	NT	69.08
BE_22	OCH ₃	OH	OH	H	6.21	35	4.07±0.14	0
BE_23	F	OH	OH	H	3.17	43	4.50±0.11	23.89
BE_24	H	OC ₂ H ₅	OH	N	6.22	40	6.33±0.13	33.19
BE_25	OCH ₃	OC ₂ H ₅	OH	N	23.5	NT	NT	8.30
BE_26	F	OC ₂ H ₅	OH	N	24.01	NT	NT	0
BE_27	H	OH	OH	N	6.59	45	7.81±0.16	20.18
BE_28	OCH ₃	OH	OH	N	12.39	NT	NT	0
BE_29	F	OH	OH	N	25.38	NT	NT	18.64
		Isoniazid			0.66			
		Rifampicin			0.23			
		Moxifloxacin			1.26			

Conti...

% inhibitory at 10 μM concentration; *Mtb*, *Mycobacterium tuberculosis*; MIC, minimum inhibitory concentration; NT, not tested;
Mtb DNA gyrase supercoiling enzyme inhibition activity
Mtb lysine aminotransferase enzyme inhibition activity
In vitro activity against *Mtb* H₃₇Rv
Against RAW 264.7 cells (Cytotoxicity)

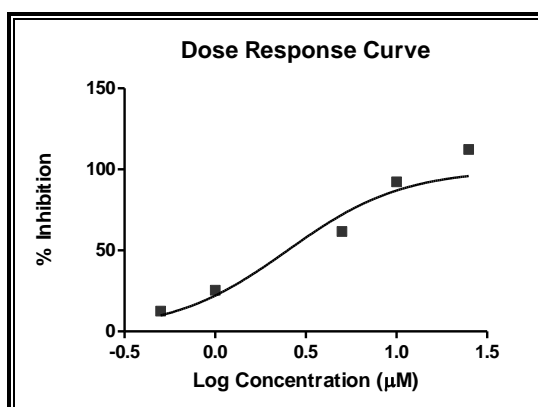


Figure 5.43: Dose response curve of compound **BE_18** with *Mtb* LAT assay at six various concentrations.

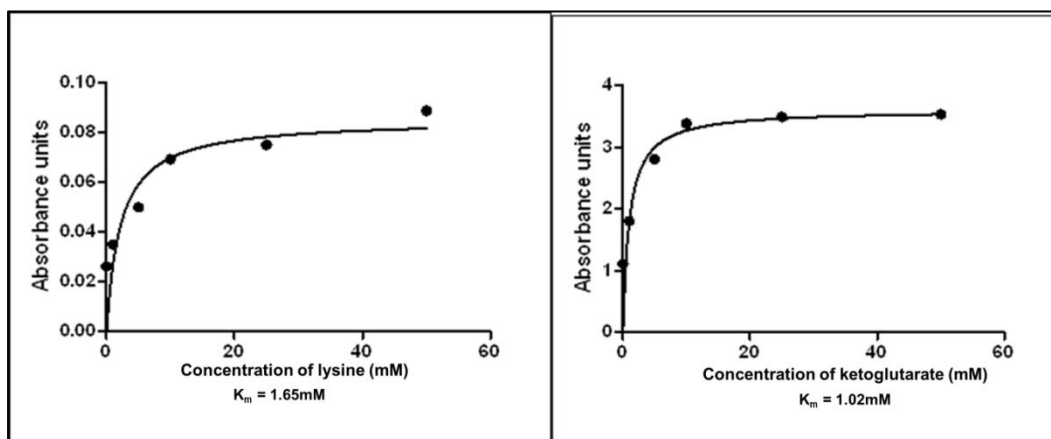


Figure 5.44: Kinetic parameters of lysine and α -ketoglutarate

5.5.5 Docking studies of selected LAT inhibitors

The active compounds among the screened against LAT enzyme in series namely-Compound **BE_18** and **BE_22** were docked into the crystal structure of LAT from *Mtb* in internal aldimine form with bound substrate of lysine (PDB code: 2CJD) with 2.00 Å resolution. The docking was done by Glide XP (extra precision) protocol

where the output gives a docking pose with XP glide score with rmsd (root mean square deviation) to crystal ligand at active site. Compound **BE_18** and **BE_22** exhibited glide scores of -5.62 and -6.40 kcal/mole respectively. Compound **BE_18** showed three hydrogen bonds with Arg 170 and Ash 271; pi stacking interaction with Phe 167. It also retained the crucial interaction with Lys 300. Compound **BE_22** exhibited four hydrogen bonds with Ala 129, Lys 300, Gly 127, Asp 337 and pi stacking interaction with Phe 167. All these interactions were crucial and found to be present in the active pocket of LAT as shown below **Figure 5.45, 5.46 & 5.47**.

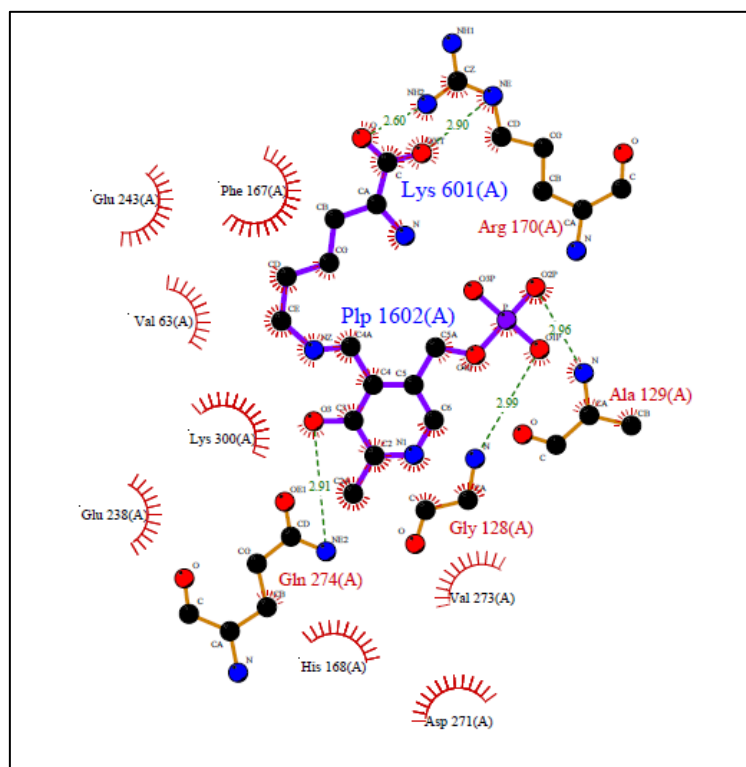


Figure 5.45: The interaction profile picture of reference ligand lysine in active site of LAT (lysine aminotransferase).

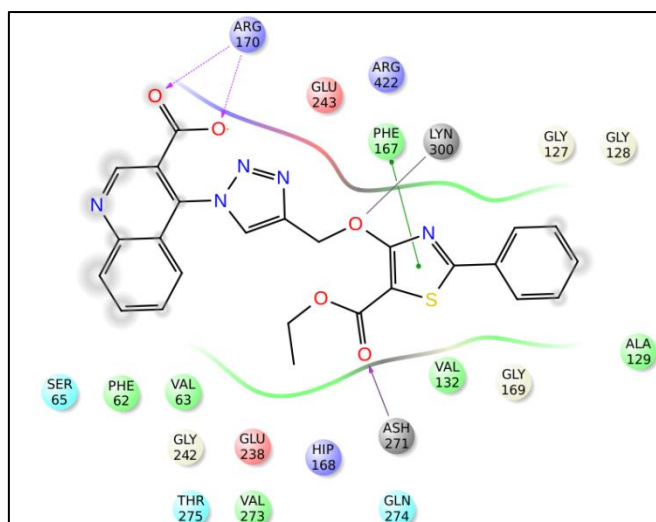


Figure 5.46: Interaction profile picture of Compound **BE_18** in *Mtb* LAT protein

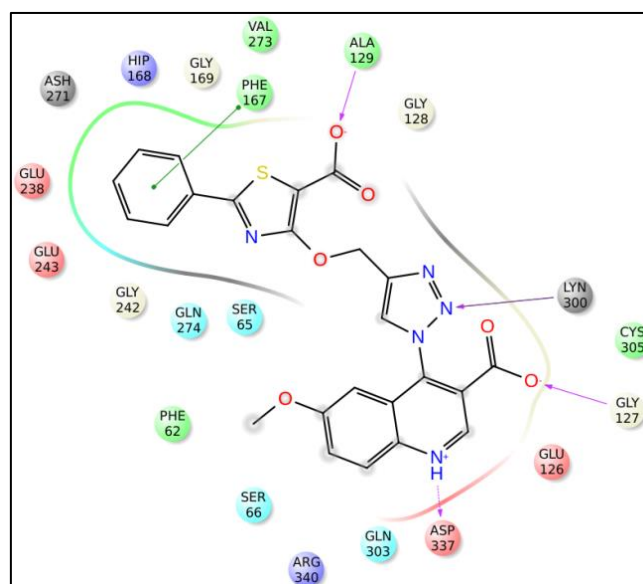


Figure 5.47: Interaction profile picture of Compound **BE_22** in *Mtb* LAT protein

5.5.6 Evaluation of protein interaction and stability using biophysical characterization experiment (DSF)

The most potent compound of LAT inhibition assay from this series was further investigated using a biophysical technique, differential scanning fluorimetry (DSF). The ability of the compounds to stabilize the catalytic domain of the *Mtb* LAT (lysine aminotransferase) protein was assessed utilizing the DSF technique by which the thermal stability of the catalytic domain of *Mtb* LAT native protein and of the protein bound with the ligand was measured. Complex with compound **BE_18** was heated

stepwise from 25 to 95 °C in steps of 0.1 °C rise in the presence of a fluorescent dye (sypro orange), whose fluorescence increased as it interacted with hydrophobic residues of the *Mtb* LAT protein. As the protein was denatured, the amino acid residues became exposed to the dye. A right side positive shift of T_m in comparison to native protein meant higher stabilization of the protein-ligand complex, which was a consequence of the inhibitor binding. In our study, compound **BE_18** showed significant positive T_m shift of 1.9 °C confirming the stability of the protein-ligand complex as shown in **Figure 5.48** which depicts the curves obtained in the DSF experiment for the *Mtb* LAT protein (green) T_m is 52.10 °C and protein-compound **BE_18** complex T_m is 54.0 °C (red).

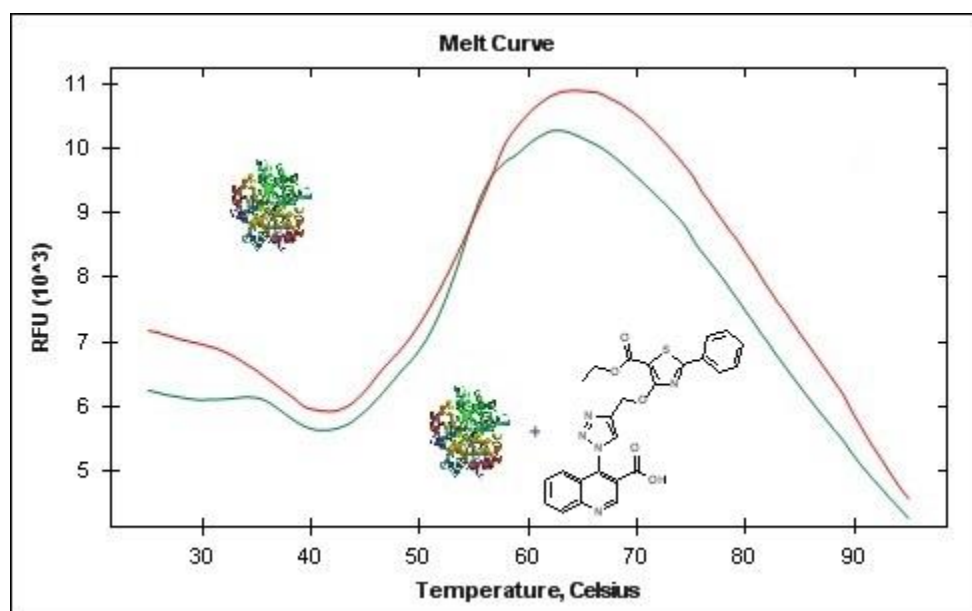


Figure 5.48: Differential scanning fluorimetry curve for *Mtb* LAT protein complexed with compound **BE_18** (red) and native *Mtb* LAT protein (green). A positive shift in T_m of about 1.9 °C was observed in protein-ligand complex when compared to native protein.

5.5.7 Discussion

Initially all the synthesized compounds were screened for their in-vitro antimycobacterial activity against *Mtb* H₃₇Rv by microplate alamar blue assay method. Isoniazid, Rifampicin and Moxifloxacin were used as a positive control and for comparison. The minimum inhibitory concentration (MIC) was determined for each compound which was measured as the minimum concentration of compound

required to completely inhibit the bacterial growth. Among twenty four compounds screened, twenty two of them inhibited *Mtb* growth with MIC ranging from 1.39 to 26.40 μM ; out of them eleven compounds showed MIC less than 1 μM . Compound ethyl 4-((1-(3-(ethoxycarbonyl)-6-methoxyquinolin-4-yl)-1H-1,2,3-triazol-4-yl)methoxy)-2-phenylthiazole-5-carboxylate (**BE_07**) emerged as the most potent one with MIC of 1.39 μM and was equivalent as of Moxifloxacin (MIC of 1.26 μM). With respect to SAR; we have prepared two sets of compounds in 3rd position of quinoline ring, with ethyl ester (**BE_06-BE_17**) and carboxylic acids (**BE_18-29**); among them ethyl esters derivatives showed better activity than carboxylic acids. We also prepared three kind of substitution (H, CH₃O, F) in 6th position of quinolone moiety; among them fluoro substitution showed better activity than methoxy group followed by unsubstituted quinolone derivatives. In the thiazole ring 2nd position we used phenyl and pyridyl ring substituents, among them phenyl ring showed slightly better *Mtb* activity than pyridyl ring. In the 5th position of thiazole ring we prepared ethyl ester and carboxylic acid derivatives; among them both were showing similar *Mtb* activity.

In the secondary level screening, eleven molecules which showed good *Mtb* MIC (< 10 μM) were selected and tested their efficacy in *Mtb* DNA gyrase and LAT enzymes. In case of DNA gyrase supercoiling assay, at 10 μM concentration all the compounds showed 35-55% inhibition. Four compounds (**BE_07**, **BE_10-11** and **BE_18**) showed $\sim\text{IC}_{50}$ of 10 μM . These results indicate that these molecules may target other enzymes of active *Mtb* as the MIC and DNA gyrase IC_{50} were not correlating. In the case of LAT enzymes, we tested at 25 μM initially and nine compounds showed more than 50% inhibition. Further, we tested them at lower concentrations we found that their IC_{50} ranging between 3.37 to 10.92 μM . LAT is a vitamin B₆-dependent enzyme and converts l-lysine to α -aminoadipate- δ -semialdehyde, which is subsequently cyclized to form Δ^1 -piperidine-6-carboxylic acid. This enzyme attracts the attention as it is reported to be highly up-regulated (41.86 times) in *in vitro* nutrient starved *Mtb* model designed to mimic the latent stage. To check the binding stability studies of most active compound **BE_18** against LAT enzyme reveals that it stabilizes with a positive T_m shift of 1.9 $^\circ\text{C}$ when compared with native *Mtb* LAT protein.

Finally to check the toxicity of compounds we have screened at 50 μM against RAW 264.7 (mouse macrophage) cells by MTT assay method. Eight compounds showed no toxicity whereas other compounds showed % inhibition ranging from 7.82 to 69.08.

5.5.8 Highlights of the study

In our continuous efforts to discover novel antimicrobial compounds with anti-gyrase activity, we have described the discovery of novel quinoline-thiazole based derivatives as dual inhibitors of DNA gyrase as well as *Mtb* LAT enzyme with potent *Mtb* MIC through molecular hopping technique and inhibitory profile of the LAT enzyme well correlated structural activity relationship and less cytotoxic effect. Among 24 compounds, compound **BE_18** shows *Mtb* LAT IC_{50} of 3.37 ± 0.14 and well correlating MIC of $6.23 \mu\text{M}$ against *Mtb*. Compound **BE_18** as had shown a 1.9°C positive shift in T_m than the native *Mtb* LAT protein and also found to devoid of cytotoxicity against RAW mouse macro phage cell lines at $50 \mu\text{M}$. Furthermore, we believe that this class of compounds has potential to be as novel anti-TB drug candidate.

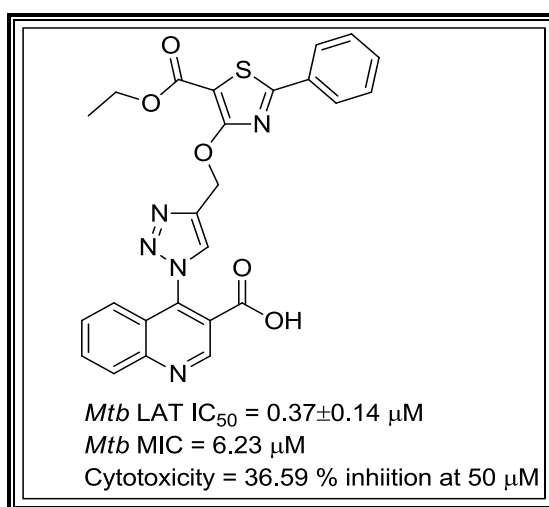


Figure 5.49: Most active compound against *Mtb* LAT inhibition **BE_18**

TB has become one of the most dangerous infectious diseases of the modern times with the epidemic of acquired immune deficiency syndrome (AIDS) in the 1980s. The emergence of drug resistant strains of *Mtb* along with some other factors has resulted in multidrug-resistant (MDR), extensively drug-resistant (XDR), or more recently, totally drug-resistant (TDR)-TB. This has rendered the presently available anti-tubercular drug regimen inadequate to address the many inherent and emerging challenges of treatment. These factors initiate the need for the development of newer, safer and more effective drugs which can reduce the TB treatment duration drastically.

Among the different targets in TB drug discovery, DNA gyrase is a well validated target. Fluoroquinolones were successful in market as they target gyrase and inhibit DNA supercoiling. But emergence of resistance to this class of antibiotics makes researchers to develop newer antibiotics which can inhibit DNA gyrase A subunit or target both A and B subunits of gyrase.

In this work we explored quinoline based new inhibitors which were known to possess antitubercular activity. By using more successful molecular hopping approach quinoline based scaffold was coupled with different linkers and five different series of compounds were synthesized. All 174 synthesized derivatives were first evaluated for their *in vitro Msm* Gyr B, *in vitro Mtb* DNA gyrase, supercoiling inhibitory potency and few molecules were screened against LAT (lysine aminotransferase) enzyme which was more expressed in latent stress conditions as step towards the derivation of structure-activity relationships and hit optimization. Also, some of the active compounds from each series of chemical class were further evaluated for protein interaction and stability using biophysical technique, differential scanning fluorimetry (DSF). The compounds were further subjected to a whole cell screening against *Mtb* H₃₇Rv strain to understand their bactericidal potency using the agar dilution method, and later the safety profile of these molecules were evaluated by checking the *in vitro* cytotoxicity against RAW 264.7 cell line (mouse macrophage) by MTT assay.

In 1-(1-(2-methylquinolin-4-yl) piperidin-4-yl) -3-phenylurea/thiourea series, compound **BA_38** (1-(4-chlorophenyl)-3-(1-(6-methoxy-2-methylquinolin-4-yl) piperidin-4-yl) thiourea) was found to be most active compound exhibiting *Msm* Gyr B IC₅₀ of 0.95±0.12 µM, *Mtb* DNA gyrase supercoiling IC₅₀ of 0.62±0.16 µM. It inhibited drug sensitive *Mtb* with MIC of 3.49 µM and was non-cytotoxic at 50 µM. Compound **BA_39** 1-(1-(6-methoxy-2-methylquinolin-4-yl) piperidin-4-yl)-3-(4-nitrophenyl) thiourea was recognised as most potent antimycobacterial compound with *Mtb* MIC of 1.72 µM. Differential scanning fluorimetry curve for *Msm* Gyr B protein complexed with compound **BA_38** has a positive shift in T_m of about 3.1 °C was observed in protein-ligand complex when compared to native protein.

In 1-(4-((6-substituted-2-methylquinolin-4-yl)amino)phenyl)-3-phenylurea/thiourea series, compound **BB_19** (1-(4-chlorophenyl)-3-(4-((6-methoxy-2-methylquinolin-4-yl)amino)phenyl)urea) was found to be the most active compound exhibiting *Msm* Gyr B IC₅₀ of 0.39±0.14 µM, *Mtb* DNA gyrase supercoiling IC₅₀ of 0.29±0.31 µM. It inhibited drug sensitive *Mtb* with MIC of 1.78 µM and was non-cytotoxic at 50 µM. Compound **BB_17** (1-(4-((6-methoxy-2-methylquinolin-4-yl)amino)phenyl)-3-phenylurea) was the most potent DNA gyrase supercoiling inhibitor with IC₅₀ 0.16±0.32 µM. Differential scanning fluorimetry curve for *Msm* Gyr B protein complexed with compound **BB_19** has a positive shift in T_m of about 2.9 °C was observed in protein-ligand complex when compared to native protein.

In N¹-(acridin-9-yl)benzene-1,4-diamine series, compound **BC_05** (4-chloro-N-(4-((2-methylacridin-9-yl)amino)phenyl)benzenesulfonamide) was found to be the potent compound showing *Mtb* DNA gyrase supercoiling inhibition IC₅₀ of 5.21±0.51 µM. It inhibited drug sensitive *Mtb* with MIC of 6.59 µM and was non-cytotoxic at 50 µM. The potent compound **BC_05** was also screened for zERG toxicity and found to be safe at 30 µM drug treatment.

In ethyl 4-((4-amino/hydroxyl phenyl)amino)quinoline-3-carboxylate series, compound **BD_53** (4-((4-(3-(4-ethylpiperazin-1-yl)propoxy)phenyl)amino)-6-methoxyquinoline-3-carboxylic acid) was found to be the most active compound exhibiting *Msm* Gyr B IC₅₀ of 0.86±0.16 µM, *Mtb* DNA gyrase supercoiling IC₅₀ of 0.63±0.15 µM. It inhibited drug sensitive *Mtb* with MIC of 3.3 µM and was non-cytotoxic at 50 µM. Differential scanning fluorimetry curve for Gyr B protein

complexed with compound **BD_53** has a positive shift in T_m of about 3.3 °C was observed in protein-ligand complex when compared to native protein.

In 4-((1-(3-quinolin-4-yl)-1H-1,2,3-triazol-4-yl)methoxy)-2-phenylthiazole series, **BE_17** (4-((1-(3-(ethoxycarbonyl)-6-fluoroquinolin-4-yl)-1H-1,2,3-triazol-4-yl)methoxy)-2-(pyridin-2-yl)thiazole-5-carboxylic acid) was the potent compound with drug sensitive *Mtb* MIC 3.00 μ M, *Mtb* LAT (lysine aminotransferase) IC_{50} of 3.76 μ M and showing *Mtb* DNA gyrase supercoiling IC_{50} of 45 μ M. Differential scanning fluorimetry curve for *Mtb* LAT protein complexed with compound **BE_17** has a positive shift in T_m of about 1.9 °C was observed in protein-ligand complex when compared to native protein.

In conclusion, the class of compounds described here besets a collection of promising lead compounds for further optimization and development to yield best novel drugs aimed to combat ever-present and ever-increasing mycobacterial infections. The study also provides the basis for further chemical optimization of these potent inhibitors as potential anti-tubercular agents.

Future perspectives

The bacterial DNA gyrase is essential for cell viability. Inhibition of DNA gyrase enzymes leads to cell death suggesting that it provides potential targets for the development of novel anti-tubercular agents. The present study focused on developing promising *Mtb* DNA gyrase inhibitors as potential anti-tubercular agents, thus offers an excellent opportunity to address the ever increasing problem of mycobacterial resistance and to develop an effective treatment for TB.

The study describes the development of five chemically diverse series of molecules as potential DNA gyrase inhibitors. The molecules reported here displayed considerable *in vitro* enzyme inhibition and potency against *Mtb* H₃₇Rv strain. Although these results are encouraging, lead optimization is still needed to build an efficient pharmacokinetic and a pharmacodynamics profile, and to achieve an adequate safety profile to ensure that the dose to humans would be in an acceptable range.

The advancement of any of the candidate molecules presented in this thesis along a drug development track will require a substantial investment in medicinal chemistry, preclinical and clinical studies.

References

World Health Organization. Global tuberculosis control. WHO 2015 report:

http://www.who.int/tb/publications/global_report/en/

World Health Organization. Global tuberculosis control. WHO 2013 report:

http://apps.who.int/iris/bitstream/10665/91355/1/9789241564656_eng.pdf

J. A. Ali, A. P. Jackson, A. J. Howells, and A. Maxwell. The 43-kilodalton N-terminal fragment of the DNA gyrase B protein hydrolyzes ATP and binds coumarin drugs. *Biochemistry*, 32(10):2717-2724, **1993**.

E. J. Alvarez-Freites, J. L. Carter, and M. H. Cynamon. *In vitro* and *in vivo* activities of gatifloxacin against *Mycobacterium tuberculosis*. *Antimicrobial Agents and Chemotherapy*, 46(4):1022-1025, **2002**.

D. D. An, N. T. H. Duyen, N. T. N. Lan, D. T. M. Ha, V. S. Kiet, N. V. V. Chau, N. H. Dung, D. N. Sy, J. Farrar, M. Caws, *et al.* Beijing genotype of *Mycobacterium tuberculosis* is significantly associated with high-level fluoroquinolone resistance in Vietnam. *Antimicrobial agents and chemotherapy*, 53(11):4835-4839, **2009**.

S. Armstrong, S. Geraldini, R. Maia, L. H. A. Raposo, C. J. Soares, and J. Yamagawa. Adhesion to tooth structure: a critical review of bond strength test methods. *Dental Materials*, 26(2):e50-e62, **2010**.

A. Assiri, A. McGeer, T. M. Perl, C. S. Price, A. A. Al Rabeah, D. A. Cummings, Z. N. Alabdullatif, M. Assad, A. Almulhim, H. Makhdoom, *et al.* Hospital outbreak of middle east respiratory syndrome coronavirus. *New England Journal of Medicine*, 369(5):407-416, **2013**.

A. Aubry, L. M. Fisher, V. Jarlier and E. Cambau. First functional characterization of a singly expressed bacterial type II topoisomerase: the enzyme from *Mycobacterium tuberculosis*. *Biochemical and Biophysical Research Communications*, 348(1):158-165, **2006**.

- R. K. Banote, S. Koutarapu, K. S. Chennubhotla, K. Chatti, and P. Kulkarni. Oral gabapentin suppresses pentylenetetrazole-induced seizure-like behavior and cephalic field potential in adult zebrafish. *Epilepsy & Behavior*, 27(1):212-219, **2013**.
- D. Barros. Recent advances in TB drug development-novel MTB DNA gyrase inhibitors. *40th Union, World Conference, on Lung Health, Cancun*, **2009**.
- B. D. Bax, P. F. Chan, D. S. Eggleston, A. Fosberry, D. R. Gentry, F. Gorrec, I. Giordano, M. M. Hann, A. Hennessy, M. Hibbs, *et al.* Type IIA topoisomerase inhibition by a new class of antibacterial agents. *Nature*, 466(7309):935-940, **2010**.
- M. T. Black, T. Stachyra, D. Platel, A.-M. Girard, M. Claudon, J.-M. Bruneau, and C. Miossec. Mechanism of action of the antibiotic NXL101, a novel nonfluoroquinolone inhibitor of bacterial type II topoisomerases. *Antimicrobial Agents and Chemotherapy*, 52(9):3339-3349, **2008**.
- P. A. Black, R. M. Warren, G. E. Louw, P. D. van Helden, T. C. Victor, and B. D. Kana. Energy metabolism and drug efflux in *Mycobacterium tuberculosis*. *Antimicrobial Agents and Chemotherapy*, 58(5):2491-2503, **2014**.
- M. K. Bolon, D. Hooper, K. B. Stevenson, M. Greenbaum, M. A. Olsen, L. Herwaldt, G. A. Noskin, V. J. Fraser, M. Climo, Y. Khan, *et al.* Improved surveillance for surgical site infections after orthopedic implantation procedures: extending applications for automated data. *Clinical Infectious Diseases*, 48(9):1223-1229, **2009**.
- L. Brino, A. Urzhumtsev, M. Mousli, C. Bronner, A. Mitschler, P. Oudet, and D. Moras. Dimerization of *Escherichia coli* DNA-gyrase B provides a structural mechanism for activating the ATPase catalytic center. *Journal of Biological Chemistry*, 275(13):9468-9475, **2000**.
- W. J. Burman, S. Goldberg, J. L. Johnson, G. Muzanye, M. Engle, A. W. Mosher, S. Choudhri, C. L. Daley, S. S. Munsiff, Z. Zhao, *et al.* Moxifloxacin versus ethambutol in the first 2 months of treatment for pulmonary tuberculosis. *American Journal of Respiratory and Critical Care Medicine*, 174(3):331-338, **2006**.
- J. J. Champoux. DNA topoisomerases: structure, function, and mechanism. *Annual Review of Biochemistry*, 70(1):369-413, **2001**.

P. Charifson, D. Deininger, A.L. Grillot, Y. Liao, S. Ronkin, D. Stamos, E. Perola, T. Wang, A. LeTiran, J. Drumm, *et al.* Gyrase inhibitors and uses thereof, Nov. 29 **2011**. US Patent 8,067,606.

P. S. Charifson, A.L. Grillot, T. H. Grossman, J. D. Parsons, M. Badia, S. Bellon, D. D. Deininger, J. E. Drumm, C. H. Gross, A. LeTiran, *et al.* Novel dual-targeting benzimidazole urea inhibitors of DNA gyrase and topoisomerase IV possessing potent antibacterial activity: Intelligent design and evolution through the judicious use of structure-guided design and structure- activity relationships. *Journal of Medicinal Chemistry*, 51(17):5243-5263, **2008**.

S. Chopra, K. Matsuyama, T. Tran, J. P. Malerich, B. Wan, S. G. Franzblau, S. Lun, H. Guo, M. C. Maiga, W. R. Bishai, *et al.* Evaluation of gyrase B as a drug target in *Mycobacterium tuberculosis*. *Journal of Antimicrobial Chemotherapy*, 67(2):415-421, **2012**.

J. E. Clark-Curtiss and S. E. Haydel. Molecular genetics of *Mycobacterium tuberculosis* pathogenesis. *Annual Reviews in Microbiology*, 57(1):517-549, **2003**.

J. Cohen. Approval of novel TB drug celebrated -with restraint. *Science*, 339(6116):130-130, **2013**.

M. B. Conde, A. Efron, C. Loreda, G. R. M. De Souza, N. P. Graqa, M. C. Cezar, M. Ram, M. A. Chaudhary, W. R. Bishai, A. L. Kritski, *et al.* Moxifloxacin versus ethambutol in the initial treatment of tuberculosis: a double-blind, randomised, controlled phase II trial. *The Lancet*, 373(9670):1183-1189, **2009**.

K. D. Corbett and J. M. Berger. Structure, molecular mechanisms, and evolutionary relationships in DNA topoisomerases. *Annu. Re.v. Biophys. Biomol. Struct.*, 33:95-118, **2004**.

K. D. Corbett, A. J. Schoeffler, N. D. Thomsen, and J. M. Berger. The structural basis for substrate specificity in DNA topoisomerase IV. *Journal of Molecular Biology*, 351(3):545-561, **2005**.

S. E. Critchlow and A. Maxwell. DNA cleavage is not required for the binding of quinolone drugs to the DNA gyrase-DNA complex. *Biochemistry*, 35(23):7387-7393,

1996.

P. B. Devi, J. P. Kakan, S. S. Saxena, V. U. Jeankumar, V. Soni, H. S. Anantharaju, P. Yogeewari, and D. Sriram. Discovery of novel lysine ϵ -aminotransferase inhibitors: An intriguing potential target for latent tuberculosis. *Tuberculosis*, 95(6):786—794,

2015

A. Diacon, R. Dawson, M. Hanekom, K. Narunsky, A. Venter, N. Hittel, L. Geiter, C. Wells, A. Paccaly, and P. Donald. Early bactericidal activity of delamanid (OPC-67683) in smear-positive pulmonary tuberculosis patients. *The International Journal of Tuberculosis and Lung Disease*, 15(7):949—954, **2011**.

J. M. Domagala. Structure-activity and structure-side-effect relationships for the quinolone antibacterials. *Journal of Antimicrobial Chemotherapy*, 33(4):685—706, 1994.

K. Drlica, M. Malik, R. J. Kerns, and X. Zhao. Quinolone-mediated bacterial death. *Antimicrobial Agents and Chemotherapy*, 52(2):385—392, **2008**.

K. Drlica and X. Zhao. DNA gyrase, topoisomerase IV, and the 4-quinolones. *Microbiology and Molecular Biology Reviews*, 61(3):377—392, **1997**.

S. Eswaran, A. V. Adhikari, N. K. Pal, and I. H. Chowdhury. Design and synthesis of some new quinoline-3-carbohydrazone derivatives as potential antimycobacterial agents. *Bioorganic & Medicinal Chemistry Letters*, 20(3):1040—1044, **2010**.

D. M. Ferraris, D. Sbardella, A. Petrera, S. Marini, B. Amstutz, M. Coletta, P. Sander, and M. Rizzi. Crystal structure of *Mycobacterium tuberculosis* zinc-dependent metalloprotease-1 (Zmp1), a metalloprotease involved in pathogenicity. *Journal of Biological Chemistry*, 286(37):32475—32482, **2011**.

J. L. Flynn and J. Chan. Tuberculosis: latency and reactivation. *Infection and Immunity*, 69(7):4195—4201, **2001**.

M. A. Forrellad, L. I. Klepp, A. Gioffre, J. Sabio y Garcia, H. R. Morbidoni, M. d. 1. P. Santangelo, A. A. Cataldi, and Bigi. Virulence factors of the *Mycobacterium tuberculosis* Complex. *Virulence*, 4(1):3—66, **2013**.

- C. A. M. Fraga. Drug hybridization strategies: before or after lead identification?. *Expert Opinion on Drug Discovery*, 46:605-609, **2009**.
- B. Geng, J. Comita-Prevoir, C. J. Eyermann, F. Reck, and S. Fisher. Exploring left-hand-side substitutions in the benzoxazinone series of 4-amino-piperidine bacterial type IIA topoisomerase inhibitors. *Bioorganic & Medicinal Chemistry Letters*, 21(18):5432—5435, **2011**.
- T. D. Gootz and K. E. Brighty. Fluoroquinolone antibacterials: SAR, mechanism of action, resistance, and clinical aspects. *Medicinal Research Reviews*, 16(5):433—486, **1996**.
- S. Hameed P, V. Patil, S. Solapure, U. Sharma, P. Madhavapeddi, A. Raichurkar, M. Chinnapattu, P. Manjrekar, Shanbhag, J. Puttur, *et al.* Novel N-linked aminopiperidine-based gyrase inhibitors with improved hERG and *in vivo* efficacy against *Mycobacterium tuberculosis*. *Journal of Medicinal Chemistry*, 57(11):4889—4905, **2014**.
- L. Heide. Genetic engineering of antibiotic biosynthesis for the generation of new aminocoumarins. *Biotechnology Advances*, 27(6):1006—1014, **2009**.
- H. Hiasa, M. E. Shea, C. M. Richardson, and M. N. Gwynn. *Staphylococcus aureus* Gyrase-Quinolone-DNA ternary complexes fail to arrest replication fork progression *in vitro* effects of salt on the DNA binding mode and the catalytic activity of *s. aureus* Gyrase. *Journal of Biological Chemistry*, 278(10):8861—8868, **2003**.
- I. P. Hoglund, S. Silver, M. T. Engstrom, H. Salo, A. Tauber, H.K. Kyyronen, P. Saarenketo, A.M. Hoffren, K. Kokko, K. Pohjanoksa, *et al.* Structure-activity relationship of quinoline derivatives as potent and selective α 2C-adrenoceptor antagonists. *Journal of Medicinal Chemistry*, 49(21):6351—6363, **2006**.
- P. K. A. Jagtap, V. Soni, N. Vithani, G. D. Jhingan, V. S. Bais, V. K. Nandicoori, and B. Prakash. Substrate-bound crystal structures reveal features unique to *Mycobacterium tuberculosis* N-acetyl-glucosamine 1-phosphate uridylyltransferase and a catalytic mechanism for acetyl transfer. *Journal of Biological Chemistry*, 287(47):39524—39537, **2012**.

- V. U. Jeankumar, J. Renuka, S. Kotagiri, S. Saxena, S. S. Kakan, J. P. Sridevi, S. Yellanki, P. Kulkarni, P. Yogeewari, and D. Sriram. Gyrase ATPase domain as an antitubercular drug discovery platform: Structure-based design and lead optimization of nitrothiazolyl carboxamide analogues. *ChemMedChem*, 9(8):1850—1859, **2014**.
- V. U. Jeankumar, J. Renuka, P. Santosh, V. Soni, J. P. Sridevi, P. Suryadevara, P. Yogeewari, and D. Sriram. Thiazole-aminopiperidine hybrid analogues: design and synthesis of novel *Mycobacterium tuberculosis* Gyr B inhibitors. *European Journal of Medicinal Chemistry*, 70:143-153, **2013**.
- M. G. Kale, A. Raichurkar, D. Waterson, D. McKinney, M. Manjunatha, U. Kranthi, K. Koushik, L. k. Jena, V. Shinde, S. Rudrapatna, et al. Thiazolopyridine ureas as novel antitubercular agents acting through inhibition of DNA gyrase B. *Journal of Medicinal Chemistry*, 56(21):8834—8848, **2013**.
- F. A. Kerdesky and A. Basha. A facile synthesis of aryl trifluoromethyl ketones. *Tetrahedron Letters*, 32(18):2003—2004, **1991**.
- A. Koul, E. Arnoult, N. Lounis, J. Guillemont, and K. Andries. The challenge of new drug discovery for tuberculosis. *Nature*, 469(7331):483—490, **2011**.
- P. Kulkarni, G. H. Chaudhari, V. Sripuram, R. K. Banote, K. T. Kirla, R. Sultana, P. Rao, S. Oruganti, and K. Chatti. Oral dosing in adult zebrafish: proof-of-concept using pharmacokinetics and pharmacological evaluation of carbamazepine. *Pharmacological Reports*, 66(1):179—183, **2014**.
- Y.S. Kwon, B.H. Jeong, and W.J. Koh. Tuberculosis: Clinical trials and new drug regimens. *Current Opinion in Pulmonary Medicine*, 20(3):280—286, **2014**.
- C. Lazar, A. Kluczyk, T. Kiyota, and Y. Konishi. Drug evolution concept in drug design: 1. Hybridization method. *Journal of Medicinal Chemistry*, 47(27):6973—6982, **2004**.
- B. Lechartier, J. Rybniker, A. Zumla, and S. T. Cole. Tuberculosis drug discovery in the post-post-genomic era. *EMBO Molecular Medicine*, 6(2):158—168, **2014**.
- M. P. Lee and T.S. Hsieh. Linker insertion mutagenesis of *Drosophila* topoisomerase

II: probing the structure of eukaryotic topoisomerase II. *Journal of Molecular Biology*, 235(2):436—447, **1994**.

G. Y. Leshner, E. J. Froelich, M. D. Gruett, J. H. Bailey, and R. P. Brundage. 1, 8-Naphthyridine derivatives. A new class of chemotherapeutic agents. *Journal of Medicinal Chemistry*, 5(5):1063—1065, **1962**.

W. Li and J. C. Wang. Foot printing of yeast DNA topoisomerase II lysyl side chains involved in substrate binding and interdomainal interactions. *Journal of Biological Chemistry*, 272(49):31190—31195, **1997**.

J. D. Lifson, J. L. Rossio, M. Piatak, T. Parks, L. Li, R. Kiser, V. Coalter, B. Fisher, B. M. Flynn, S. Czajak, *et al.* Role of CD8⁺ lymphocytes in control of simian immunodeficiency virus infection and resistance to rechallenge after transient early antiretroviral treatment. *Journal of Virology*, 75(21):10187—10199, **2001**.

Z. Ma, C. Lienhardt, H. McIlhleron, A. J. Nunn, and X. Wang. Global tuberculosis drug development pipeline: the need and the reality. *The Lancet*, 375(9731):2100—2109, **2010**.

G. A. Marriner, A. Nayyar, E. Uh, S. Y. Wong, T. Mukherjee, L. E. Via, M. Carroll, R. L. Edwards, T. D. Gruber, I. Choi, *et al.* The medicinal chemistry of tuberculosis chemotherapy. *Third World Diseases*, pages 47—124. Springer Berlin Heidelberg, **2011**.

C. Mayer and Y. L. Janin. Non-quinolone inhibitors of bacterial type IIA topoisomerases: a feat of bioisosterism. *Chemical Reviews*, 114(4):2313—2342, **2013**.

K. Mdluli and Z. Ma. *Mycobacterium tuberculosis* DNA gyrase as a target for drug discovery. *Infectious Disorders-Drug Targets (Formerly Current Drug Targets-Infectious Disorders)*, 7(2):159—168, **2007**.

L. A. Mitscher. Bacterial topoisomerase inhibitors: quinolone and pyridone antibacterial agents. *Chemical Reviews*, 105(2):559—592, **2005**.

G. Orphanides and A. Maxwell. Evidence for a conformational change in the DNA gyrase-DNA complex from hydroxyl radical footprinting. *Nucleic Acids Research*,

22(9):1567—1575, **1994**.

S. Parida, R. Axelsson-Robertson, M. Rao, N. Singh, I. Master, A. Lutckii, S. Keshavjee, J. Andersson, A. Zumla, and M. Maeurer. Totally drug-resistant tuberculosis and adjunct therapies. *Journal of Internal Medicine*, 277(4):388—405, **2015**.

S. R. Patpi, L. Pulipati, P. Yogeewari, D. Sriram, N. Jain, B. Sridhar, R. Murthy, S. V. Kalivendi, and S. Kantevari. Design, synthesis, and structure—activity correlations of novel dibenzo [b, d] furan, dibenzo [b, d] thiophene, and N-methylcarbazole clubbed 1, 2, 3-triazoles as potent inhibitors of *Mycobacterium tuberculosis*. *Journal of Medicinal Chemistry*, 55(8):3911—3922, **2012**.

B. J. Peter, J. Arsuaga, A. M. Breier, A. B. Khodursky, P. O. Brown, and N. R. Cozzarelli. Genomic transcriptional response to loss of chromosomal supercoiling in *Escherichia coli*. *Genome Biol*, 5(11):R87, **2004**.

J. Poissy, A. Aubry, C. Fernandez, M.-C. Lott, A. Chauffour, V. Jarlier, R. Farinotti, and N. Veziris. Should moxifloxacin be used for the treatment of extensively drug-resistant tuberculosis? an answer from a murine model. *Antimicrobial Agents and Chemotherapy*, 54(11):4765—4771, **2010**.

R. J. Reece, A. Maxwell, and J. C. Wang. DNA gyrase: structure and function. *Critical Reviews in Biochemistry and Molecular Biology*, 26(3-4):335—375, **1991**.

E. C. Rivers and R. L. Mancera. New anti-tuberculosis drugs in clinical trials with novel mechanisms of action. *Drug Discovery Today*, 13(23):1090—1098, **2008**.

R. K. Shandil, R. Jayaram, P. Kaur, S. Gaonkar, B. Suresh, B. Mahesh, R. Jayashree, V. Nandi, S. Bharath, and V. Balasubramanian. Moxifloxacin, ofloxacin, sparfloxacin, and ciprofloxacin against *Mycobacterium tuberculosis*: evaluation of *in vitro* and pharmacodynamic indices that best predict *in vivo* efficacy. *Antimicrobial Agents and Chemotherapy*, 51(2):576—582, **2007**.

S. K. Sharma and A. Mohan. Tuberculosis: From an incurable scourge to a curable disease-journey over a millennium. *The Indian Journal of Medical Research*, 137(3):455—493, **2013**.

P. S. Shirude and S. Hameed. 21 Nonfluoroquinolone-Based Inhibitors of Mycobacterial Type II Topoisomerase as Potential Therapeutic Agents for TB. *Annual Reports in Medicinal Chemistry*, 47:319—328, **2012**.

P. S. Shirude, P. Madhavapeddi, J. A. Tucker, K. Murugan, V. Patil, H. Basavarajappa, A. V. Raichurkar, V. Humnabadkar, S. Hussein, S. Sharma, *et al.* Aminopyrazinamides: novel and specific Gyr B inhibitors that kill replicating and nonreplicating *Mycobacterium tuberculosis*. *ACS Chemical Biology*, 8(3):519—523, **2012**.

P. S. Shirude, R. Shandil, C. Sadler, M. Naik, V. Hosagrahara, S. Hameed, V. Shinde, C. Bathula, V. Humnabadkar, N. Kumar, *et al.* Azaindoles: noncovalent DprE1 inhibitors from scaffold morphing efforts, kill *Mycobacterium tuberculosis* and are efficacious *in vivo*. *Journal of Medicinal Chemistry*, 56(23):9701—9708, **2013**.

G. Sotgiu, R. Centis, L. D'Ambrosio, J.-W. C. Alffenaar, H. A. Anger, J. A. Caminero, P. Castiglia, S. De Lorenzo, G. Ferrara, W.J. Koh, *et al.* Efficacy, safety and tolerability of linezolid containing regimens in treating MDR-TB and XDR-TB: Systematic review and meta-analysis. *European Respiratory Journal*, 40(6):1430—1442, **2012**.

J. K. Tamura and M. Gellert. Characterization of the ATP binding site on *Escherichia coli* DNA gyrase. Affinity labeling of Lys-103 and Lys-110 of the B subunit by pyridoxal 5'-diphospho-5'-adenosine. *Journal of Biological Chemistry*, 265(34):21342—21349, **1990**.

K. Thomas, A. V. Adhikari, I. H. Chowdhury, E. Sumesh, and N. K. Pal. New quinolin-4-yl-1, 2, 3-triazoles carrying amides, sulphonamides and amidopiperazines as potential antitubercular agents. *European Journal of Medicinal Chemistry*, 46(6):2503-2512, **2011**.

K. Thomas, A. V. Adhikari, S. Telkar, I. H. Chowdhury, R. Mahmood, N. K. Pal, G. Row, and E. Sumesh. Design, synthesis and docking studies of new quinoline-3-carbohydrazide derivatives as antitubercular agents. *European Journal of Medicinal Chemistry*, 46(11):5283—5292, **2011**.

A. P. Tingey and A. Maxwell. Probing the role of the ATP-operated clamp in the strand-passage reaction of DNA gyrase. *Nucleic Acids Research*, 24(24):4868—4873, **1996**.

R. S. Upadhyaya, J. K. Vandavasi, R. A. Kardile, S. V. Lahore, S. S. Dixit, H. S. Deokar, P. D. Shinde, M. P. Sarmah, and J. Chattopadhyaya. Novel quinoline and naphthalene derivatives as potent antimycobacterial agents. *European Journal of Medicinal Chemistry*, 45(5):1854—1867, **2010**.

B. Villemagne, C. Crauste, M. Flipo, A. R. Baulard, B. Deprez, and N. Willand. Tuberculosis: the drug development pipeline at a glance. *European Journal of Medicinal Chemistry*, 51:1—16, **2012**.

E. B. Wong, K. A. Cohen, and W. R. Bishai. Rising to the challenge: new therapies for tuberculosis. *Trends in Microbiology*, 21(9):493—501, **2013**.

T. Yempala, D. Sriram, P. Yogeewari, and S. Kantevvari. Molecular hybridization of bioactives: synthesis and antitubercular evaluation of novel dibenzofuran embodied homoisoflavonoids via Baylis-Hillman reaction. *Bioorganic & Medicinal Chemistry Letters*, 22(24):7426—7430, **2012**.

A. Zumla, M. Raviglione, R. Hafner, and C. F. von Reyn. Current concepts. *New England Journal of Medicine*, 368:745—55, **2013**.

A. I. Zumla, S. H. Gillespie, M. Hoelscher, P. P. Philips, S. T. Cole, I. Abubakar, T. D. McHugh, M. Schito, M. Maeurer, and A. J. Nunn. New antituberculosis drugs, regimens, and adjunct therapies: needs, advances, and future prospects. *The Lancet Infectious Diseases*, 14(4):327—340, **2014**.

Appendix

List of Publications

From Thesis work

Brahmam Medapi, Janupally Renuka, Shalini Saxena, Jonnalagadda Padma Sridevi, Raghavender Medishetti, Pushkar Kulkarni, Perumal Yogeeswari, Dharmarajan Sriram. Design and synthesis of novel quinoline-aminopiperidine hybrid analogues as *Mycobacterium tuberculosis* DNA gyrase B inhibitors. *Bioorganic & Medicinal Chemistry*. 2015, 23 (9), 2062-2078.

Brahmam Medapi, Priyanka Suryadevara, Janupally Renuka, Jonnalagadda Padma Sridevi, Perumal Yogeeswari and Dharmarajan Sriram. 4-Aminoquinoline Derivatives as Novel *Mycobacterium tuberculosis* GyrB Inhibitors: Structural Optimization, Synthesis and Biological Evaluation. *European journal of medicinal chemistry*. 2015, 103, 1-16.

Brahmam Medapi, Nikhila Meda, Pushkar Kulkarni, Perumal Yogeeswari, Dharmarajan Sriram. Development of acridine derivatives as selective *Mycobacterium tuberculosis* DNA gyrase inhibitors. *Bioorganic & Medicinal Chemistry*, 2016, 24 (4), 877-885.

List of Publications

Other publications

Variam Ullas Jeankumar, Rudraraju Reshma Srilakshmi , Renuka Janupally, **Brahmam Medapi**, Shalini Saxena, Jonnalagadda Padma Sridevi, Pushkar Kulkarni, Perumal Yogeeswari, Dharmarajan Sriram. Enabling the (3+2) cycloaddition reaction in assembling newer anti-tubercular lead acting through the inhibition of Gyrase ATPase domain: Lead optimization and structure activity profiling. *Organic & Biomolecular Chemistry*. 2015, 13 (8), 2423-2431.

Renuka Janupally, **Bhramam Medapi**, Parthiban BrindhaDevi, Priyanka Suryadevara, Pushkar Kulkarni, Perumal Yogeeswari, Dharmarajan Sriram. Design and biological evaluation of furan/thio-phen-2-carboxamide derivatives as efficient DNA gyrB inhibitors of *Staphylococcus aureus*. *Chemical Biology & Drug design*. 2015, 86 (4), 918-925.

Mary Priyanka, **Brahmam Medapi**, Indu Dhar, Audesh Bhat, Kaushik Desai, Dharmarajan Sriram, Arthi dhar. The small molecule Indirubin inhibits protein kinase R: Antiapoptotic and antioxidant effect in rat cardiac myocytes. *Pharmacology*. 2015 Nov 17; 97(1-2):25-30.

Matharasala Gangadhar, **Brahmam Medapi**, Ram Kumar Mishra, Madhu Babu Battu, Sriram Dharmarajan and Yogeeswari Perumal. Neuropathic Pain attenuation by drugs having anticonvulsive Properties-Novel Semicarbazone derivatives. (In communication)

Hasitha Shilpa Anantaraju, **Brahmam Medapi**, Prashanti malapati, Roma viswanath, Perumal Yogeeswari, Dharmarajan Sriram, Arti dhar. Anti-proliferative, Apoptotic and Cyclin dependent kinase effects of synthesized indirubin-3'-monooxime derivatives on LPS-treated cancer cell lines. (In communication).

Indian Patents

Yogeeswari, P., Sriram, D., Madhubabu, B., **Brahmam, M.**, Indian Patent Application No. 2945/DEL/2014 (15/10/2014): A Compound for treating inflammatory neuropathic pain and cancer

Yogeeswari, P., Sriram, D., Hasitha, S.A., **Brahmam, M.**, Indian Patent Application No. 1763/DEL/2014 (12/06/2015): Cathepsin D inhibitors and compositions thereof for treating breast cancer.

Papers presented at International/National Conferences

Brahmam M, Bobesh K A, Nikila Meda, Sriram D, Yogeeswari P. Development of novel 1,2,3 triazolo-quinoline analogues as *Mycobacterium tuberculosis* DNA gyrase inhibitors. Drug Discovery & Development – Global scenario – Indian Perspective at NIPER- Hyderabad, Nov. 20-21, 2015.

Brahmam M, Renuka J, Nikila M, Sridevi J P, Yogeeswari P, Sriram D. Development of novel quinolone-p-phenylenediamine hybrid analogues as mycobacterial DNA gyrase inhibitors to increase the cardio safety profile. National conference on Drug Discovery and Development in Chemistry- Applications in Pharma Industry (DDDC-2015) at S.V. University, Tirupathi, Sep. 14-15th, 2015.

Medapi Brahmam, Renuka J, V u Jean Kumar, Yogeeswari P, Sriram D. *In silico* discovery of novel phenylenediamine class of antibacterials as potential DNA Gyrase Inhibitors. 2nd UK-India Medchem Congress at ICT-Hyderabad, Hyderabad, Mar. 22-23rd, 2013.

BIOGRAPHY OF MEDAPI BRAHMAM

Mr. Medapi Brahmam completed his Master's Degree in Organic Chemistry in 2008 from Acharya Nagarjuna University, Guntur, Andhra Pradesh. He has about 4 years of Industry experience in Various CRO Industries from 2008-2012. He has been appointed as a DST Project Fellow at Birla Institute of Technology and Science, Pilani, Hyderabad campus from 2012-2016 under the supervision of Prof. P. Yogeeswari. He has published six scientific papers in well-renowned international journals (three from previous work and three from current work) and also presented papers at International/National conferences.

BIOGRAPHY OF PROF. P. YOGESWARI

Prof. P. Yogeeswari is presently working in the capacity of professor and Associate Dean (Sponsored Research and Consultancy Division), Department of Pharmacy, Birla Institute of Technology and Science, Pilani, Hyderabad Campus. She received her Ph.D. degree in the year 2001 from Banaras Hindu University; Varanasi. She has been involved in research for the last 15 years and in teaching for 14 years. APTI honoured her with Young Pharmacy Teacher Award for the year 2007. In 2010, ICMR honoured her by awarding “Shakuntala Amir Chand Award” for her excellent biomedical research. She has also been granted IASP 2014 award for “Excellence in Pain Research and Management in Developing Countries” under the basic science research category to be received at the “15th World Congress on Pain” at Argentina in October 2014. She has collaborations with various national and international organizations that include National Institute of Mental Health and Neurosciences, Bangalore, Karolinska Institute, Stockholm, Sweden, National Institute of immunology, New Delhi, India, Pastuer Institute, University of Lille, France, Bogomoletz Institute of Physiology National Academy of Science, Ukraine and Faculty of Medicine of Porto, Portugal,. She has to her credit more than 200 research publications and one Indian Patent, Application No: 1138/CHE/2009. She is an expert reviewer of many international journals like Journal of Medicinal Chemistry (ACS), Journal of Chemical Information & Modelling (ACS, USA), Bioorganic Medicinal Chemistry (Elsevier), Recent Patents on CNS Drug Discovery (Bentham), etc. She has also co-authored a textbook on organic medicinal chemistry with Prof. D. Sriram titled “Medicinal Chemistry” published by Pearson Education and one book chapter in Jan 2013 by IGI Global. She is a life time member of Association of Pharmacy Teachers of India and Indian Pharmaceutical Society. She has successively completed many sponsored projects and currently on projects sponsored by DST, DBT, INDO-BRAZIL, ICMR-INSERM, and CSIR. She has guided 14 Ph.D. students and currently 7 students are pursuing their Ph.D. work.